FINAL REPORT

Magnetotelluric Investigation of Deep Aquifers in Rub Al Khali

تحديد مكامن الخزانات المائية العميقة في الربع الخالي باستخدام التقنية الكهرومغناطيسية

Submitted To : **Deutsche Gesellschaft für Internationale Zusammenarbeit (GIZ)**

Submitted By : **Prof. Abdullah M. Alamri**

Director of Empty Quarter Chair, King Saud Univ.

Date of Submission : **May 27, 2013**

LIST OF CONTENTS

Acknowledgments

First and foremost, I would like to express my thank and gratitude to the Ministry of Water & Electricity and Deutsche Gesellschaft fur Internationale Zusammenarbeit **(GIZ)** for funding this project.

This research project would not have been possible without the support of many people. I wish to extend my sincerest thank to MT field team of the RAK for their tremendous support and help : Prof. Adam Schultz, Nordine Bouzeid (Engineer), Ali Alattas (geologist), Omar Lafouza Loni (geophysicist), Hassan Alzahrani (geophysicist), and Husam Toffaha (geologist).

Furthermore, I would also like to acknowledge with much appreciation Mr. Yahya Al-Shenawi, Director of the Deputy Ministry of Petroleum and Minerals, Dhahran, who provided us with logs and seismic profiles of **LUKSAR** and gave us the permission to use all required analyses to complete our task.

Summary

A natural source magnetotelluric investigation has been carried out in the Rub Al-Khali region of Saudi Arabia by a team lead by King Saud University, with the participation of personnel from the USA and France. The aim of the investigation was to determine the variation in electrical resistivity with depth and geographic position within an area of ~20000 km^2 in a triangular region whose boundaries were determined by the locations of three wells. A total of 80 MT stations were completed over an array of observation points designed to provide large area coverage of the survey area while also providing enhanced fine scale resolving power in the center of the array and also nearby two of the wells, which permits the integration of well-log information into the interpretation of the survey data.

Analysis of the data has resulted in a set of magnetotelluric transfer functions that show considerable heterogeneity in geoelectrical structure within the survey area. We refined these initial estimates and a set of geoelectric cross sections through the survey area was developed using 1D and 2D inverse modeling methods.

Resultant geophysical and seismological models are in good agreement and confirmed the existence of several water–bearing zones. Moreover, the most promising locations for ground water potentiality and drilling along these cross sections are determined.

Introduction

Rub Al-Khali **(RAK)** is an arid system that is relatively young, being only Neogene in age (covering a period of time 1.64 to 23.3 Mya). It was formed when the African and Arabian tectonic plates separated, and began to drift apart, and the Arabian plate and Asian plate abutted. In between formation of the basin and the current desert conditions, the area was dominated by large alluvial fans, consisting of networks of braided rivers and large sediment islands and banks. As a result of this, sedimentary deposits of lake, river and shallow marine origin dominate the geology of the Rub Al-Khali, reworked as aeolian (desert) sands (Flower and Abu Nasser, 2004).

The largest sand dunes are situated in the northeast, where they rise to a maximum height of over 250 m. To the southeast, the dunes reduce in size, giving way to salt marsh and saltpan environments. Many types of dunes are evident in the region, which is thought to be mainly due to the influence of desert winds. The two main types of dune found in the Rub al-Khali are transverse and linear dunes (Flower and Abu Nasser, 2004).

Due to the low precipitation and high evaporation rates experienced in the RAK, no major surface water sources have been identified. Seasonal precipitation is low (<10 mm per year) and the evaporation rate is very high (about 4500 mm per hour). Five groundwater aquifers underlie the RAK. They are the Neogene, Dammam, Umm erRadhuma, Wasia–Biyadh & Cretaceous, and Wajid aquifers. The total volume of groundwater stored in these aquifers is estimated to be **$1.5 \times 10^{13} m^3$**, however water quality is variable, often being highly mineralized.

The main goal of this project is the assessment and evaluation of the groundwater potential of the Rub' Al Khali deep aquifers by applying the latest geophysical techniques to a better understanding of the hydrogeological systems and their functioning. The principal aquifers to be investigated are those of the Umm ErRadhuma limestone, Aruma limestone, Wasia sandstone and Biyadh sandstone.

To meet the aforementioned objectives, we adopted the magneto telluric method (MT) with the goal to delineate the presence of deep aquifers of RAK, in the assigned areas by the prime contractor. This project addresses the issue of monitoring and controlling deep-looking EM (electromagnetic) geophysical work for the purpose of mapping deep aquifers in the RAK. Moreover, MT fieldwork has already been carried out in Saudi Arabia for hydrocarbon exploration (Stewart et al, 1996; Al-Dulaijan et al 2008) so it is an established method in the RAK environment.

MT is an electromagnetic sounding method for obtaining subsurface resistivity data, and is commonly used by the minerals and geothermal industries. MT has also been used successfully in the past to map geological basins, mineral deposits, for numerous groundwater exploration and geothermal projects for water utilities and government entities, and for regional and continental-scale geophysical mapping. The MT method typically has better lateral and vertical resolution than many other resistivity methods, particularly for targets deeper than 1 km, and is often logistically easier in complicated environments. While there are several variants of the MT method (such as audio frequency MT (AMT), radiofrequency MT (RFMT) and controlled source variants such as CSAMT), we have applied the classic passive MT/AMT method in the RAK. This involves the measurement of electromagnetic fields at an array of measurement stations on the Earth's surface that are generated by natural electromagnetic activity in the atmosphere, ionosphere and magnetosphere above. MT signals (low frequencies < 1-10 Hz) are generated by the interaction between the Earth's magnetosphere and the solar wind, sunspot activity and auroras. High frequency sources (> 1-10 Hz) in the Audio range (AMT) are generated by worldwide thunderstorms and lightning. These time-varying electric and magnetic fields induce currents to flow in the Earth and oceans.

Executing a fully 3D survey design would have been prohibitively expensive given the cost and logistic constraints, as well as the relatively shallow scale of the targets and vast size of the RAK survey area. The data were acquired on a fast production schedule, which limits the long-period responses, with the impact of reducing the depth of penetration of AMT soundings at the majority of stations. We compensated for this, to some extent, by operating a subset of AMT stations overnight, for a nominal 12-hour data acquisition period (vs. a nominal 2.5 hours elsewhere).

It must be emphasized that while the data acquisition was based on 2D geometry, there are very strong 3D effects within the RAK survey area. Also, since issuing the March, 2013 project report, we have determined that the impedance tensor data for station 1 (the central station of the array) was rotated 90 degrees east of geographic north, rather than 0 degrees. This has been corrected for the analysis described in this final report.

Generally, MT data collection in the RAK was logistically difficult due to its remoteness, lack of infrastructure, and the presence of large sand dunes. It was also technically difficult because of the high contact resistance of the loosely consolidated, arid near-surface sand. As described below, the use of specially developed buffer amplifiers helped to partially overcome the very high contact resistance.

SOURCES OF INFORMATION

This study is based on the following sources :

- Information available prior to MT field work,
- Analyzing of well–logs data and 4 Seismic refraction profiles which were carried out by LUKSAR via Deputy Ministry of Petroleum in Dhahran, and
- 60 days of MT field investigation by our team in the RAK.

Regional Structures & Seismotectonics

The Arabian Peninsula forms a single tectonic plate, the Arabian Plate. It is surrounded on all sides by active plate boundaries as evidenced by earthquake locations. Figure 1 shows a map of the Arabian Peninsula along with major tectonic features and earthquake locations. Active tectonics of the region is dominated by the collision of the Arabian Plate with the Eurasian Plate along the Zagros and Bitlis Thrust systems, rifting and seafloor spreading in the Red Sea and Gulf of Aden. Strike-slip faulting occurs along the Gulf of Aqabah and Dead Sea Transform fault systems. The great number of earthquakes in the Gulf of Aqabah pose a significant seismic hazard to Saudi Arabia. Large earthquakes in the Zagros Mountains of southern Iran may lead to long-period ground motion in eastern Saudi Arabia.

The accretionary evolution of the Arabian plate is thought to have originated and formed by amalgation of five Precambrian terranes. These are the Asir; Hijaz, and Midyan terranes from the western part of the Arabian shield, and from the eastern side of the shield are the Afif terrane and the Amar arc of the ArRayn micro-plate. The western fusion is along the BirUmq and Yanbu sutures (Loosveld et al 1996). The eastern accretion may have started by about 680-640 million years ago (Ma) when the Afif terrane collided with the western shield along the Nabitah suture. At about 670 Ma, a subduction complex formed west of Amar arc. Along this subduction zone, the Afif terrane and ArRayn microplate collided that lasted from about 640-620 Ma. (Al-Husseini 2000). The north trending Rayn anticlines and conjugate northwest and northeast fractures may have formed at this time (Figure 2).

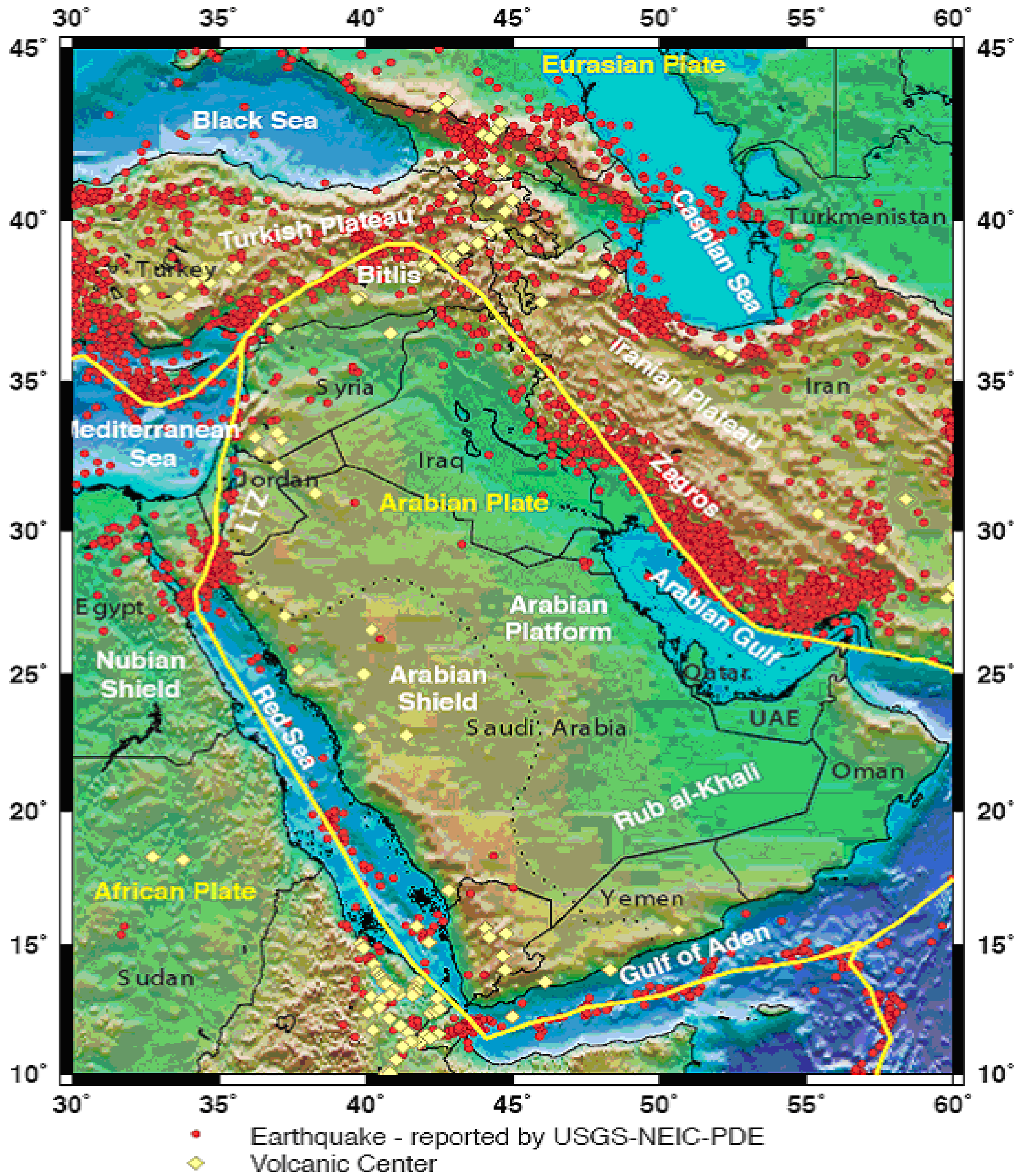

Figure 1. Seismotectonic map of the Arabian Peninsula and Arabian plate boundaries.

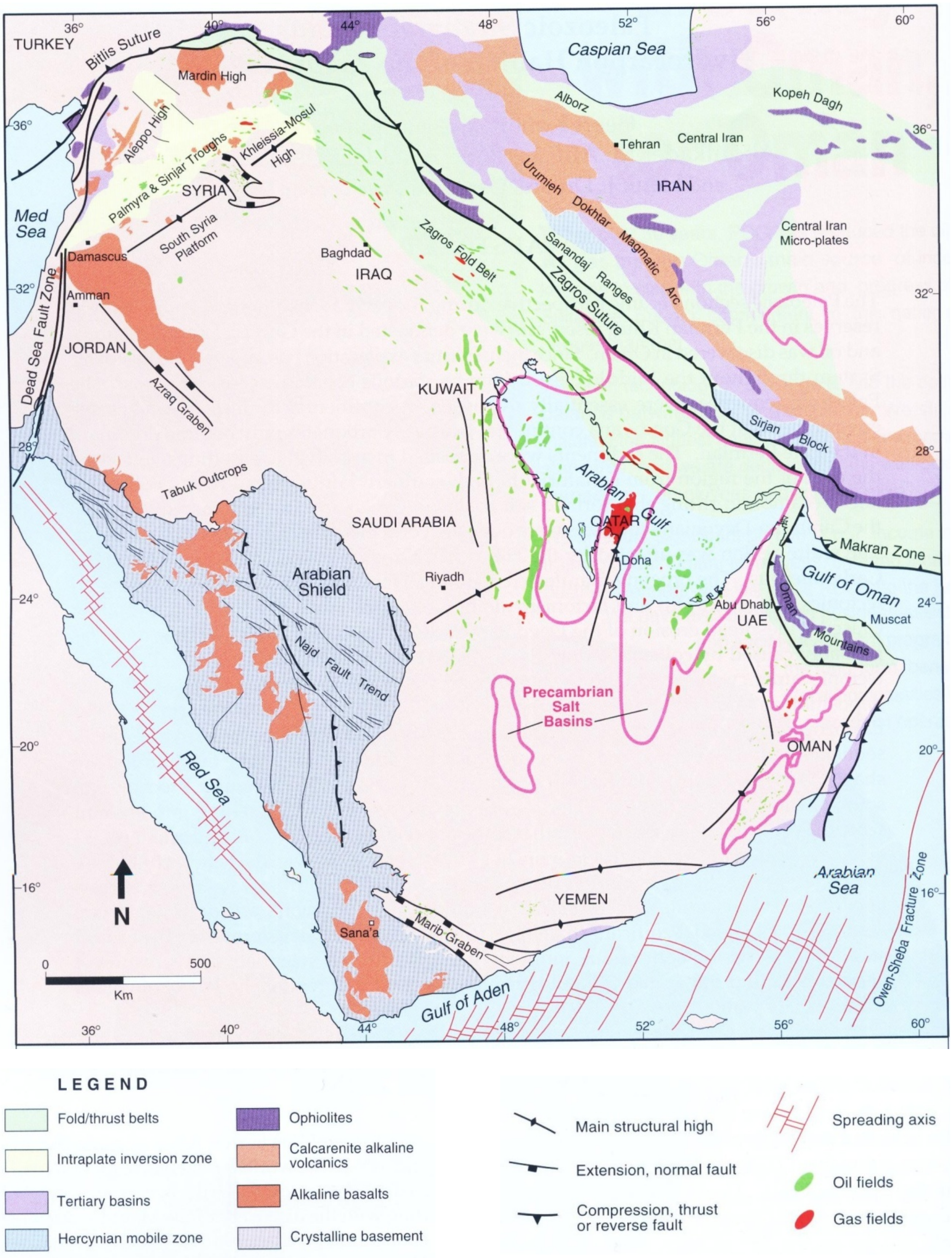

Figure 2. Location map of the Arabian Plate showing major tectonic elements of the Arabian Shield and Platform (Al-Husseini,2000).

The Arabian Shield is an ancient land mass with a trapezoidal shape and area of about 770,000 sq. km. Its slightly-arched surface is a peneplain sloping very gently toward the north, northeast, and east. The framework of the shield is composed of Precambrian rocks and metamorphosed sedimentary and intruded by granites. The fold-fault pattern of the shield, together with some stratigraphic relationships suggests that the shield have undergone two orogenic cycles.

To the first order, the Arabian shield is composed of two layers, each about 20km thick, with average velocities of about 6.3 km/s and 7 km/s respectively (Mooney et al 1985). The crust thins rapidly to less than 20 km total thickness at the western shield margin, beyond which the sediments of the Red Sea shelf and coastal plain are underlain by oceanic crust.

The platform consists of the Paleozoic and Mesozoic sedimentary rocks that unconformably overlays the shield and dip very gently and uniformly to the E-NE towards the Arabian Gulf (Powers et al., 1966). The accumulated sediments in the Arabian platform represent the southeastern part of the vast Middle east basin that extend eastward into Iran, westward into the eastern Mediterranean and northward into Jordan, Iraq and Syria.

The Arabian shield isolated the Arabian platform from the north African Tethys and played an active paleo geographic role through gentle subsidence of its northern and eastern sectors during the Phanerozoic, allowing almost 5000 m of continental and marine sediments deposited over the platform. This accumulation of sediments represents several cycles from the Cambrian onward, now forms a homocline dipping very gently away from the Arabian shield.

Several structural provinces can be identified within the Arabian platform : 1) An interior homocline in the form of a belt, about 400 km wide, in which the sedimentary rocks dip very gently away from the shield outcrops. 2) An interior platform, up to 400 km wide, within which the sedimentary rocks continue to dip regionally away from the shield at low angles. 3) Intra-shelf depressions, found mainly around the interior homocline and interior platform

Unfortunately, no locally recorded earthquake data have been used to determine the crustal characteristics of the Arabian platform. The regularly spaced north trending Summan platform, Khurais-Burgan and En Nala-Ghawar anticlines, and Qatar arch in the eastern part of the Arabian plate appear to have formed during the Precambrian Amar Collision about 640-620 million years ago (Ma). This collision occurred along the north trending Amar suture that bisects the Arabian peninsula at about 45 degrees east longitude when the Rayn microplate in the east was fused to the western part of the Arabian craton (Husseini 2000, Looseveld et al 1996). The great anticlines are bounded by the northeast trending Wadi Batin fault and northwest trending Abu Jifan fault that converge on the Amar suture. The anticlines intersected deformed metasediments that are dated as syn-collisional. The Amar collision was followed by a widespread extensional collapse of the Arabian-Nubian shield between about 620-530 Ma. The extensional collapse culminated in the regional development of the extensive Najd fault and its complimentary rift basins, Zagros suture, the northeast trending Oman salt basins, Dibba fault, and the Sinai triple junction.

The Saudi Arabian Broadband Deployment (Vernon and Berger, 1997; Al-Amri et al., 1999) provided the first broadband recordings for the Arabian Shield and Platform. This deployment consisted of 9 broadband, three-component seismic stations along a similar transect to a seismic refraction study (Mooney et al., 1985; Gettings et al., 1986; Badri, 1991). Data from this deployment resulted in several reports of crustal and upper mantle structure (Sandvol et al., 1998a; Mellors et al., 1999; Rodgers et al., 1999; Benoit et al., 2003). The crustal model of the western Arabian Platform shows a slightly higher P-velocity for the upper crust in the Arabian Shield than in the Platform. Also the crust of the Platform appears to be 3-5 km thicker than in the Shield. The Moho Discontinuity beneath the western Arabian Platform occurs at a depth of 40-45 km, and the velocity of the upper mantle is about 8.2 km/sec (Al-Amri 1998; 1999; Rodgers et al., 1999; Tkalcic et al., 2006).

Generally, the crustal thickness in the Arabian Shield varies from about 15 km in the Red Sea, to 20 km along the Red Sea coast to about 35-40 km in the in central Arabian Shield (Sandvol et al., 1998a; Tkalcic et al., 2006).Reports of large-scale seismic tomography (e.g. Debayle et al., 2001) suggest that a low-velocity anomaly in the upper mantle extends laterally beneath the Arabian Shield from the Red Sea in the west to the Shield-Platform boundary in the east. Additionally, Debayle et al. (2001) observed a narrow region of low-velocity beneath the Red Sea and the western edge of the Arabian Shield, extending to 650 km depth. Recent tomographic imaging by Park et al. (2007) using SANDSN data found low velocities extending to 400 km in the upper mantle beneath the southern Red Sea and Arabian Shield, but more normal velocities beneath the northern Red Sea, suggesting different geodynamic connections between rifting of the Red Sea and mantle upwelling in the southern and northern Red Sea.

High-frequency regional S-wave phases are quite different for paths sampling the Arabian Shield than those sampling the Arabian Platform (Mellors et al., 1999). In particular the mantle Sn phase is nearly absent for paths crossing parts of the Arabian Shield, while the crustal Lg phase has abnormally large amplitude. This may result from an elastic propagation effect or extremely high mantle attenuation and low crustal attenuation occurring simultaneously, or a combination of both. High-frequency Lg does not propagate as efficiently across the Arabian Platform compared to the Shield but Sn does propagate efficiently. This suggests that crustal attenuation is low in the higher velocity crust of the Arabian Shield, or sedimentary structure in the Arabian Platform attenuates and disrupts the crustal waveguide for Lg. These observations imply high-frequency ground motions will propagate with lower attenuation in the Arabian Shield compared to the Arabian Platform.

It is known that high-frequency regional phase behavior in the Arabian Plate is quite variable as demonstrated by Al-Damegh et al. (2004). They investigated the attenuation of *Pn*phase (Q_{Pn}) for 1–2 Hz along the Red Sea, the Dead Sea fault system, within the Arabian Shield and in the Arabian Platform. Consistent with the *Sn* attenuation, they observed low Q_{Pn} values of 22 and 15 along the western coast of the Arabian Plate and along the Dead Sea fault system, respectively, for a frequency of 1.5 Hz. Higher Q_{Pn} values of the order of 400 were observed within the Arabian Shield and Platform for the same frequency. Their results based on *Sn* and *Pn* observations along the western and northern portions of the Arabian Plate imply the presence of a major anomalously hot and thinned lithosphere in these regions that may be caused by the extensive upper mantle anomaly that appears to span most of East Africa and western Arabia.

More recently, Pasyanos et al. (2009b) applied a technique to simultaneously invert amplitudes measurements of Pn, Pg, Sn and Lg to produce P-wave and S-wave attenuation models of the crust and upper mantle. The attenuation is modeled as P-wave and S-wave attenuation surfaces for the crust, and similar set for the upper mantle. They used all of the phase amplitudes together by using the appropriate (source, geometrical-spreading, site, and attenuation) terms for each phase. Because this is a model-based inversion, the velocity structure of the region can be included to more accurately model the predicted ray paths .

Generally speaking, The most important tectonic elements in the RAK are the three known Infra Cambrian salt basins. These are the Fahud and Ghaba salt basins in the north and the south Oman salt basin. Immediately to the west of the south Oman basin is the Ghudun-Khasfah high. It shows a north trending positive linear gravity anomaly that separates the south Oman basin from a gravity low to the west. It is thought that the western gravity low in the extreme southwest represents a fourth Infracambrian basin. This new basin is called Ghudun salt basin and appears to be comparable in areal extent with the Ghaba basin and analogous with the other Oman salt basins.

The depth of the basement is estimated to be from 8-10 km. The tectonic history of the Ghaba salt basin is dominated by compressional events ranging in age from late Precambrian to Tertiary. The Ghaba salt basin is described as a push-down basin. The loading of the Oman mountains led to the development of foreland basins. Loading from the north resulted in a regional dip in that direction on which the Mesozoic carbonate section began to slide, resulting in a series of extensional faults of WNW orientation. This event allowed reactivation of the salt and many diapirs developed.

There are only 8 documented seismic events in the RAK. Two were historical and 6 are instrumental. The maximum magnitude observed for the historical is 5.6 in Aug 20, 1954 which is located the Rub Al khali basin. The observed maximum magnitude for the instrumental data is 5 in Aug 20, 1997 which is also located in the basin.

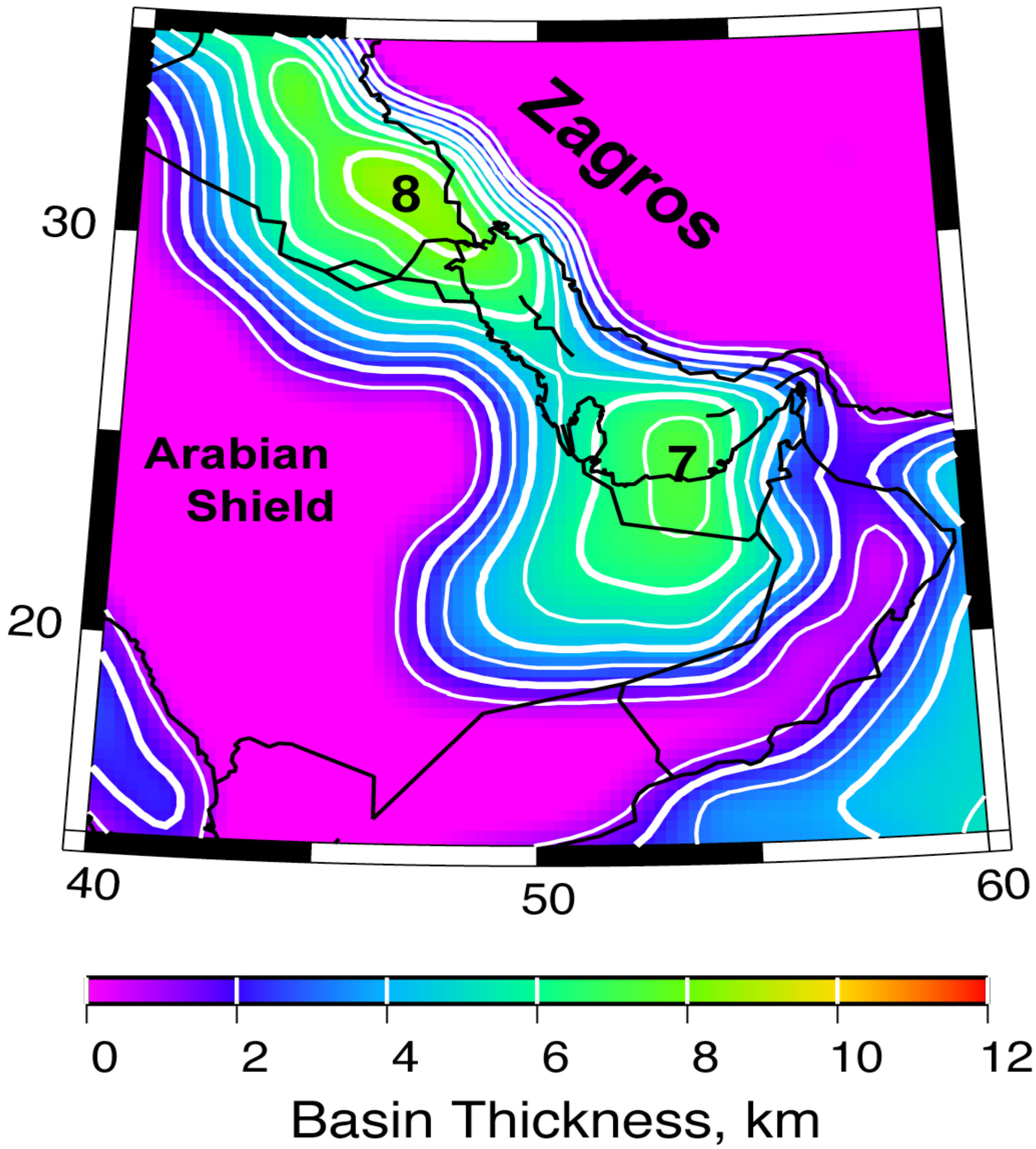

Figure 3. Map of Sedimentary thickness of the Arabian Platform

Geology of the RAK

Precambrian crystalline basement of the Arabian Shield crops out along the eastern margins of the Red Sea coastline forming the westernmost margin of the RAK terrain. The basement complex rocks are impermeable and groundwater in basement areas is found in fractures or in the alluvial aquifers within the wadi network dissecting these domains. Unconformably overlying the crystalline basement are thick sequences of sedimentary formations ranging in age from Cambrian to recent; they dip gently to the east and thicken in the same direction reaching thicknesses of up to 5 km in the vicinity of the Persian Gulf. These stratigraphic relationships are demonstrated in Fig. 4, a generalized schematic cross section along a SW to NE trending transect.

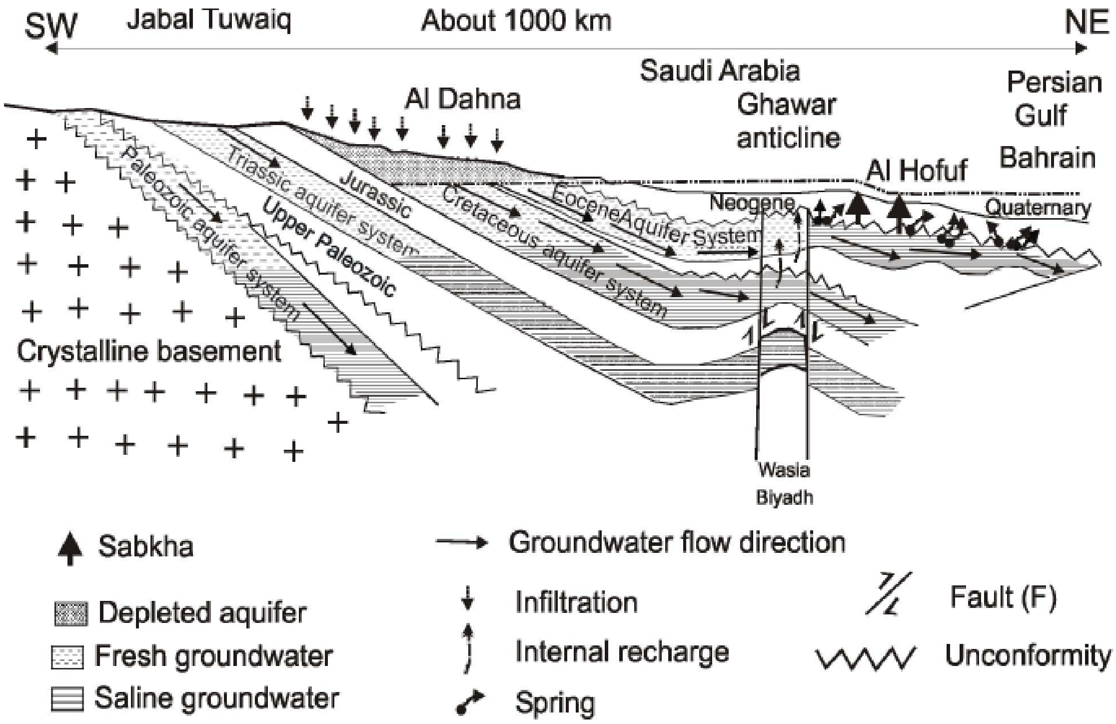

Figure 4. A SW to NE schematic cross section through the RAK modified from Beaumont (1977) and AlSharhan et al. (2001).

Groundwater in the RAK is hosted primarily in sandstone, limestone, and dolomite formations separated by interleaving confining shale units. These aquifers are here grouped in: (1) Paleozoic sandstone aquifers (e.g., Wajid aquifer: 200-900m thick) and limestone and dolomite aquifers of the Kuff formation (250-600m), (2) Mesozoic sandstone aquifer (e.g., Minjur: 400m thick; Biyadh-Wasia: 425m), and (3) Cenozoic (Eocene and Neogene) limestone and dolomite (e.g., Umm er Radhuma: 250-700m; Dammam: 250m) (Al Alawi and Abdulrazzak, 1994; 2001; Ministry for Higher Education, 2000).

Geologically, The Rub Al-Khali basin is located in southeastern Saudi Arabia, south and central Interior Oman, and the United Arab Emirates. It is a part of the Arabian Peninsula, which is a crustal plate composed of ancient sedimentary and volcanic rocks that are deformed, metamorphosed, and injected by plutonic intrusions. The Arabian Peninsula is a relatively stable region compared to the active zones of mountainous belts of Iran and Oman (Edgell, 1989).

The Rub Al-Khali basin is an arid system with an area of about 647,500 km^2 that is relatively young, originating during the late Quaternary (Alsharhan et al., 2001). It is one of the largest single arid systems acting at the present time. It is covered with more or less continuous aeolian accumulation seldom interrupted by eroded remnants of older relief (mainly near the edges) or by uncovered gravel pavements and sabkhas in some inter dune areas. (Flower and Abu Nasser, 2004).

The Rub Al-Khali basin evolved during the initial separation of the Arabo-Nubian shield along the Red Sea (when the separation and the drifting apart of the African and Arabian plates occurred) in the Neogene (1.64 to 23.3 million years ago, Ma). This period also witnessed the abutment of the Arabian plate against the Asian plate, which caused the up thrusting that resulted in the formation of the Zagros Mountain chain in Iran. The up thrust of the Zagros Mountain chain and the wet phase that prevailed in the Pliocene (1.64 to 5.2 Ma) led to the creation of the Wadi Ad-Dawaser and Wadi As Sahba river systems, which served to drain the western and central shield areas and the overlying sedimentary basins into the Rub Al-Khali basin. The

Wadi Al-Batin and Wadi ArRimah river system was also formed at this time, draining the north shield and sedimentary basins, and discharging into the Gulf (Flower and Abu Nasser, 2004; Edgell, 1989).

Due to the present aridity of the area no lakes are found in Rub Al-Khali except some scattered wet sabkhas in its eastern part. In the less arid periods of the Quaternary, more water was available and lakes were formed in the depressions. These depressions are related with the old alluvial surface or with inter dune areas. Major wet phase characterized the period between 17,000 and 36,000 years ago that coincided with the global glacial maximum in the late Pleistocene. This period was associated with lake formation, especially in the southwestern part of Rub Al-Khali (McClure1984; Edgell, 1989). Quaternary sediments of the Rub Al-Khali are basically reworked Pliocene sediments. Distribution of alluvium continued until Pleistocene aridity started (Alsharhan et al, 2001). Quaternary aeolian sand accumulations that blanket most of the Rub Al-Khali range in thickness from a few meters in areas of sand sheet cover to as much as 250 meters in areas of high dune accumulation.

Hydrogeology of the RAK

The Rub Al-Khali desert has generally been classified as arid to hyper arid area. Hence no major surface water resource is found in the area. There are several aquifers of widespread extent, that exist beneath the Rub Al-Khali desert of Saudi Arabia. The total volume of groundwater stored in these aquifers is estimated to be about **1.5×10^{13} m^3** (Foster et al, 2003). About eight aquifers of varying characteristics and importance underlie the study area. They are the Neogene, Dammam, Umm erRadhuma, Aruma, Wasia–Biyadh and Cretaceous, Juraissic, Jilh, and Khuff, aquifers. A typical lithological column section of these aquifers is shown in Figure 5.

The Neogene aquifer belongs to Miocene and Pliocene age and consists of Kharj, Hofuf, Dam and Hadrukh formations. Neogene aquifer, which is confined, extends over the large area from Wadi Dawasir northward to the Jordanian border and eastward to the Arabian Gulf covering almost the whole of the Rub al-Khali. The Neogene aquifer is a thin primary aquifer system in calcareous sandstone, with thickness varying from approximately 30 m to 85 m. The average depth above sea level of the aquifer top is 300 m in the Rub Al-Khali desert (Flower and Abu Nasser, 2004).

The yield and water quality of this aquifer vary depending on the location and amount of local recharge. Since Neogene aquifer is not consistently water bearing and the underlying aquifers are more reliable, it is not developed extensively except near Hassa Oasis, Wadi Miyah and some other locations. A large quantity of water is, however, too mineralized for use as a drinking water supply, showing high concentrations of sodium chloride and nitrate. Good quality water (TDS ranging from 3,700 to 4,000 ppm) was found in the aquifer in the Al-Hassa area and also in wedges towards the Dammam Dome and northward along the Ghawwar structure (Water Atlas of Saudi Arabia, 1984).

The Dammam aquifer is divided into five sedimentary member units, namely: Alat, Khober, Alveolina limestones, Saila Shale and Midra Shale. This confined aquifer extends over most of the northern Saudi Arabia and the Rub Al-Khali. The Dammam aquifer is a secondary aquifer system in calcareous limestone[1] that has a thickness of about 30 m (Edgell, 1997). The aquifer extends to the subsurface of the UAE and surfaces at Shishur in interior Dhofar, Oman. Both the thickness of the aquifer and its storage properties are low. Only Alat and Khober formations are water bearing yielding moderate amounts of water (Flower and Abu Nasser, 2004). Water quality in this aquifer is affected by high concentrations of sodium and chloride ions. Water samples collected from the aquifer between 1937 and 1983 showed a specific conductance range of 1,180 and 26,200 micro S/cm (Water Atlas of Saudi Arabia, 1984). Water quality deteriorates significantly towards the Arabian Gulf coast. Since the thickness of this aquifer is low and its water quality is poor, it is not, therefore, expected to be a reliable source of water for domestic or agricultural purposes. Reserve water in the aquifer is about 4.5×10^{10} m^3 and recharge water is about 2.0×10^8 m^3/year. Average TDS value varies from 2,600 to 6,000 ppm (Al-Alawi and Abdulrazzak, 1994).

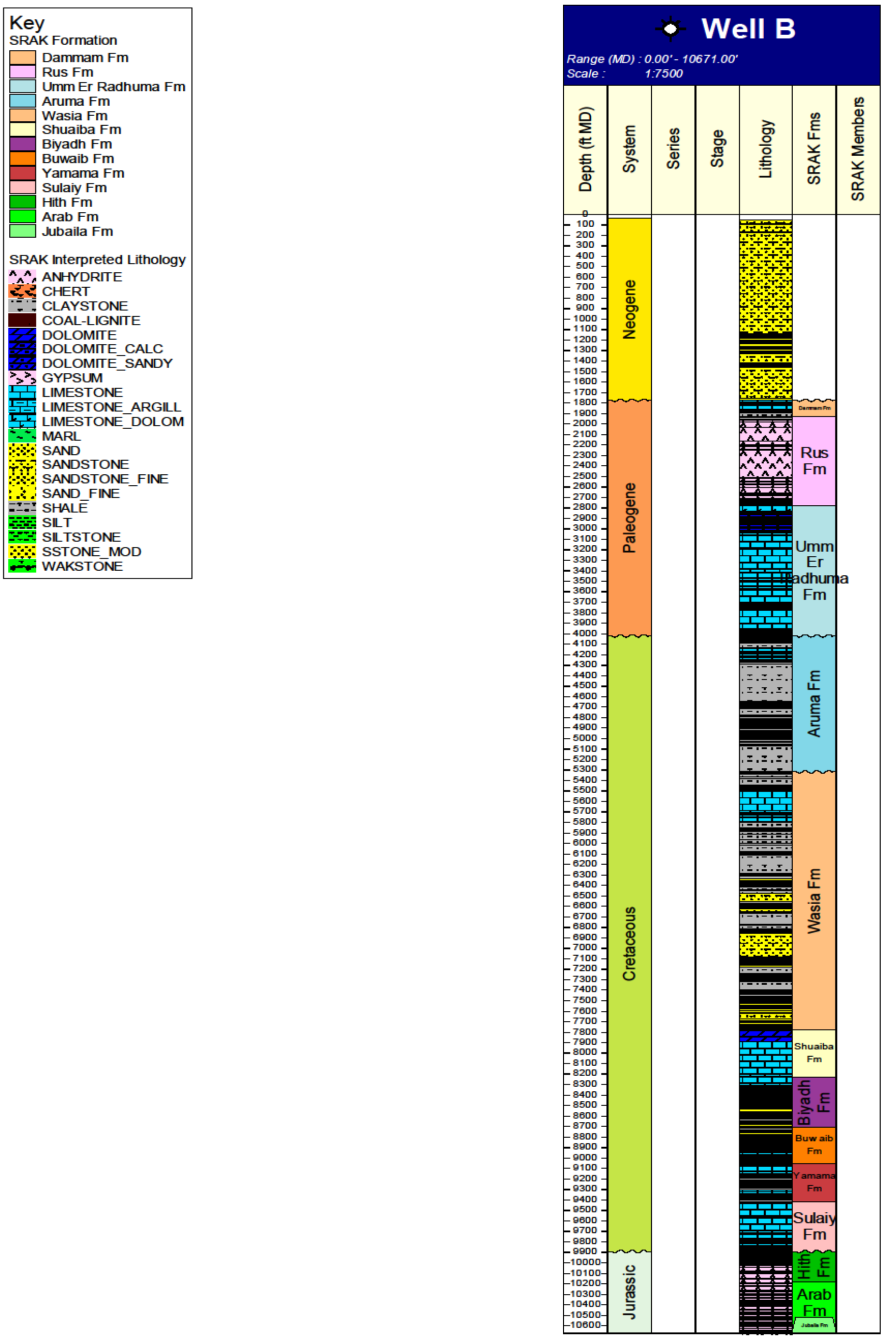

Figure 5. Lithological column section of Well B which was drilled by SRAK up to 3050 m depth. The figure delineates at least six water-bearing layers.

Umm erRadhuma (UER) is one of the Kingdom's most important and extensive aquifers. Lithologically it consists of calcareous limestone with dolomitic limestone, dolomite, minor marl, shale, and argillaceous limestones in the lower strata (Al-Alawi and Abdulrazzak, 1994). It extends from northern Hadhramaut in Yemen and western Oman, to the Saudi-Iraqi border and underlies almost all of the Rub Al-Khali. Based on the classification by origin, UER is classified as a secondary aquifer. Isotopic age determinations show that groundwater in UER aquifer system is 'fossil water', being 10,000 to 28,000 years old (Edgell 1997). UER is a major source of water for domestic and agricultural purposes in northeastern, eastern and southeastern Saudi Arabia.

UER is a single thick hydraulic unit that is water bearing throughout the Rub al-Khali. It has a thickness of approximately 250 m at its exposed reference section at Wadi Al-Batin, but its subsurface thickness varies from about 300 m to 700 m. Groundwater in UER flows to the east and northeast from the outcrop. The yield of wells ranges between 4 and 32 liters per second (ls^{-1}) (345 to 2,764 m^3/day) in most of the areas.

The transmissivity of the aquifer ranges between 3.45 m^2/day and $9.5x10^2$ m^2/day and the storage coefficient varies from $5x10^{-5}$ to $1.1x10^{-2}$. The aquifer is unconfined over an area of about 54,800 km^2 (Edgell, 1997).

The UER aquifer yields good to poor quality groundwater, providing reasonably good quality groundwater from the upper one third of the formation. The quality declines significantly in the lower part of this formation, and also north eastward (from a TDS of < 1,000 ppm to 6,000 ppm) along the coastal area. Better quality subsurface water is found at the Dammam Dome. Groundwater reserves in the aquifer are estimated at $1.90x10^{11}$ m^3 with the TDS values varying from 1,500 to 15,000 ppm (Water Atlas of Saudi Arabia, 1984).

The Aruma aquifer is upper cretaceous in age and its rock formation is mainly shallow water limestone and massive dolomites. It crops out in a west-facing escarpment[2] in central Saudi Arabia for about 1,600 km from the Wadi Dawasir north to beyond the Saudi Arabian-Iraqi border. The outcrop increases in width northward from 20 km where the unit passes under the Rub Al-Khali sands to about 200 km at the northern border. Depth to the top of Aruma formation increases eastward from the outcrop to about 600 m in the Eastern Province (Flower and Abu Nasser, 2004).

The TDS of water collected from wells in this aquifer was found to range between 1,000 ppm and 1,800 ppm, with high concentration of calcium sulfate. According to Al-Alawi and Abdulrazzak (1994), reserve of groundwater in the Aruma aquifer is about 8.5×10^{10} m^3, with quality ranging between 1,600 and 2,000 ppm. (Flower and Abu Nasser, 2004).

The Wasia-Biyadh and Cretaceous aquifer (referred as the Cretaceous aquifer) is composed of sandstones of the Wasia and Biyadh formations combined with facies of Aruma east of Wadi Dawasir. The Cretaceous succession is a primary aquifer system consisting of several hundred meters of quartz sandstone. The lower unit has inter bedded limestone, shale, marl, and sandstone, and the upper unit is coarse-grained, cross-bedded quartz sandstone with quartz pebbles. This aquifer has good permeability. The transmissivity of the aquifer varies from 4.5 x 10^3 to 8.4 x 10^3 m^2/day and the unconfined storage coefficient is around 2 x 10^{-2}. The Cretaceous aquifer contains water of good quality in the southwestern Rub Al-Khali, but becomes saline towards the north. Wells tapping the aquifer can yield water at a rate of up to 6000 m^3/day. Despite being deeper than UER aquifer, the Cretaceous aquifer is sometimes preferentially tapped due to its better quality water (Flower and Abu Nasser, 2004).

Lower Cretaceous and Upper Jurassic Aquifers (referred as Jurassic Aquifers) consist of the Tuwayq Mountain Limestone, Hanifah Formation, Jubaila limestone, Arab formation, and the Hit anhydrite. The lower cretaceous age aquifers are made up of the Sulay Formation, the Yamama Limestone, and the Buwaib Limestone (Flower and Abu Nasser, 2004).

Dissolved solids in groundwater from the Jubaila and Arab Aquifers in the Riyadh area were found to be between 2,000 and 3,000 ppm. The specific conductance of the water was between 1,200 and 1,500 micro mho/cm in the west and more than 5,000 micro mho/cm in the east. Average transmissivity was found to be $6x10^2$ m^2/day. Average unconfined storage co-efficient was $2x10^{-2}$. Good quality water is found in the south-western Rub Al-Khali.

The Jilh formation is of Middle and Upper Triassic age. The outcrop extends for about 770 km in a narrow band from Haddar to the northern edge of Shamat Akbad. The width of the outcrop ranges from 8 to 20 kilometers. The rock consists of sandstone and shale with some subordinate limestone near latitude 24°N. Reserve water found in this aquifer amounts to about $1.15x10^{11}$ m^3 and recharge water was found to be $6x10^8$ m^3/year. The yield of water east of Riyadh on average was found to be about 5,000 m^3/day. Due to poor quality of the water, its use is very limited. In the Qasim area, average TDS exceeded 6,000 ppm. In the outcrop area, west of Riyadh, specific conductance ranged from 3,000 to 20,000 micro S/cm.

Khuff aquifer crops out over a distance of 1,200 km along the Interior Homocline from Bani Khatmah in the south to near Turabah in the southeastern Nafud. It extends under almost all the Rub Al-Khali and Arabian platform, as well as under most of the Arabian Gulf. Khuff aquifer is composed of limestones and dolomites, with some anhydrites interbeds which act as aquicludes and divide it into four permeable, carbonate aquifer units with low effective porosity, termed Khuff A, B, C, and D in descending order. Its thickness is about 600 m at Wadyan Basin of Saudi-Iraqi border and about 250 m at Saudi-Kuwaiti border in the Northern Interior Homocline and the Qasim Area. Total ground water reserves are $3x10^9$ m^3 and recharge is 1.32 $x10^8$ m^3/year in the Khuff Aquifer. Estimated yield is about 1700 m^3/d. TDS value varies between 500 ppm and 1,200 ppm (Al Alawi and Abdulrazzak, 1994).

These sedimentary formations are exposed in the foothills of the Red Sea Hills providing ample opportunities for groundwater recharge for all aquifers (Cambrian to Quaternary) from rain precipitating over the Red Sea Hills and surroundings. Precipitation is concentrated over the mountain ranges and/or highlands surrounding the area from the east (Red Sea Hills), west (Oman mountains), south (e.g., Hadramount and Dhofar mountains), and north (Yabrin mountains) and is channeled by extensive E-W trending watersheds intercepting the recharge areas. These relationships are demonstrated in Figure 6a, which shows a mosaic of Landsat Thematic Mapper scenes draped over digital elevation data for the RAK and surrounding mountains and a similar drape for the major watersheds and drainage networks in the area (Fig. 6b). The precipitation over the southern and eastern highlands is less likely to recharge the aquifer sequence in its entirety since only the more recent aquifers (Cenozoic) crop out at the foothills of these mountain ranges

Radiocarbon dating of groundwater samples from a number of these reservoirs (Saq: 22,000-28,000 ka; Biyadh-Wasia: 8,000-16,000 ka; Umm er Radhuma: 10,000-28,000 ka) have lead to interpretations suggesting that these reservoirs were recharged during

previous wet climatic periods in the Quaternary (AlSharhan, 2003; Beaumont, 1977; Otkun, 1971). Although we believe that the aquifers are largely formed of fossil water, we suggest that during the intervening dry periods, as is the case now, these aquifers must receive additional recharge given the relatively high precipitation over the Red Sea Hills and the presence of a network of ephemeral streams that can channel these waters to the recharge areas at the foothills of these mountains. This has been demonstrated to be the case in similar settings in the Eastern Desert of Egypt and the Sinai Peninsula (Sultan et al., 2007; 2000).

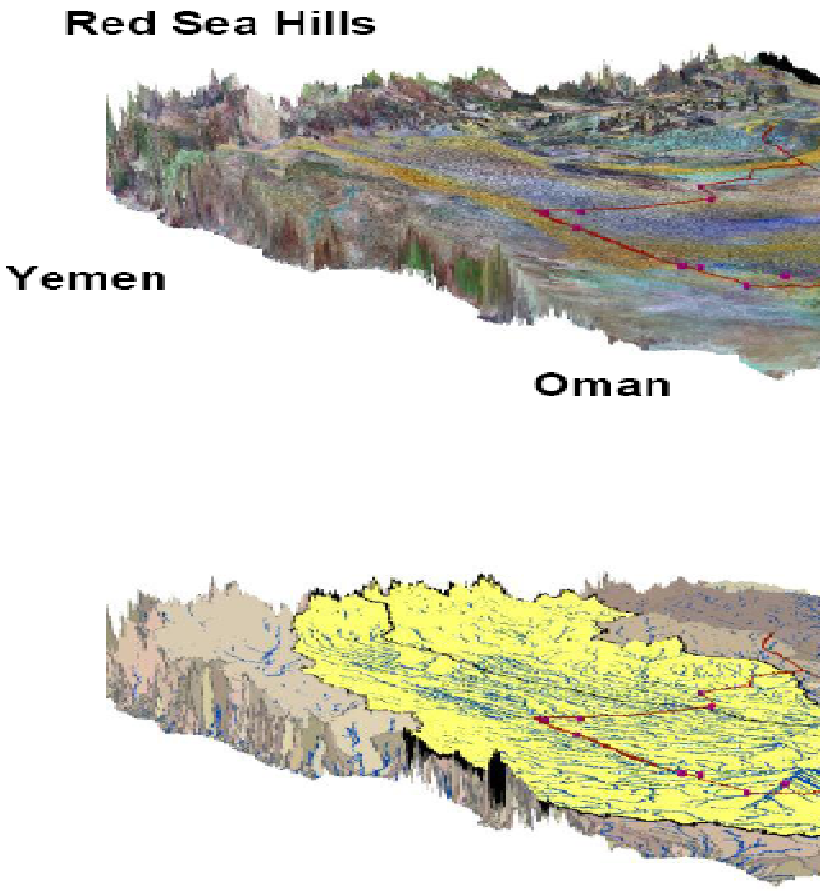

Figure 6 - representations. (a) Landsat TM false color images draped over vertically exaggerated digital elevation data (1 km SRTM). (b) Watersheds and drainage networks extracted from SRTM data draped over 1 km SRTM data.

MT Data Collection

The study area as determined by the prime contractor represents a triangle of three wells (RAK 03, RAK 04 and RAK 06). The geometry of the MT survey array and the locations of the wells are seen in Figure 7 below. The distances between the wells is as follows :RAK 06 – RAK 03 = 193 km ; RAK 06 –RAK 04 = 211 km; RAK 03 –RAK 04 = 202 km. The geographic coordinates of these wells are listed below:

WELL	LATITUDE (N)	LONGITUDE (E)	ELEVATION (m)	NOTES
RAK 6	22 07 45.4	48 32 48.2	272	
RAK 3	20 50 20.0	49 47 42.0	250	
RAK 4	20 19 19.3	47 56 11.1	367	700m depth, under construction

In the beginning, we reviewed existing relevant data, checked MWE wells and other information provided by the prime contractor under suitable terms and conditions.

Given the large survey area (~18,000 km^2), it is not feasible to undertake a full 3D MT experiment design, which would require a substantially larger number of stations, nor is it warranted given the available information about the RAK. Rather, we designed the survey to include a series of profiles radiating from a common crossing point near the center of the survey area (see Figure 7).

We used variable station spacing along the profile lines, which allowed us to cover a wide area with only 80 MT stations, while providing a distribution of lateral resolving power that, to a large extent, is determined by the spacing between adjacent stations. This approach permits us to evaluate in selected areas any finer-scale heterogeneities in near-surface resistivity structure that may be associated with the shallower aquifers, while also providing comprehensive wide-area coverage of deeper resistivity structure that may be characteristic of the deeper aquifers. Accordingly, we set up nine radial profiles of variable lengths, namely, A, D, E, B, M, H, F, K and N intersected at the center C (Figure 7).

With the exception of profiles B and H that had larger gaps in station coverage due to the logistical difficulty of traveling over nearly impassable sand dunes, the distance between any two adjacent MT stations along these profiles varies from 2, 3, 4, 5 and 10 km depending on the length of the profile and topographic obstacles. A total of 80 MT stations were completed, and the entire fieldwork was accomplished in 30 days by two teams using one wideband MT receiver system each. Six stations were completed daily following an initial 4 days setup and field crew orientation period.

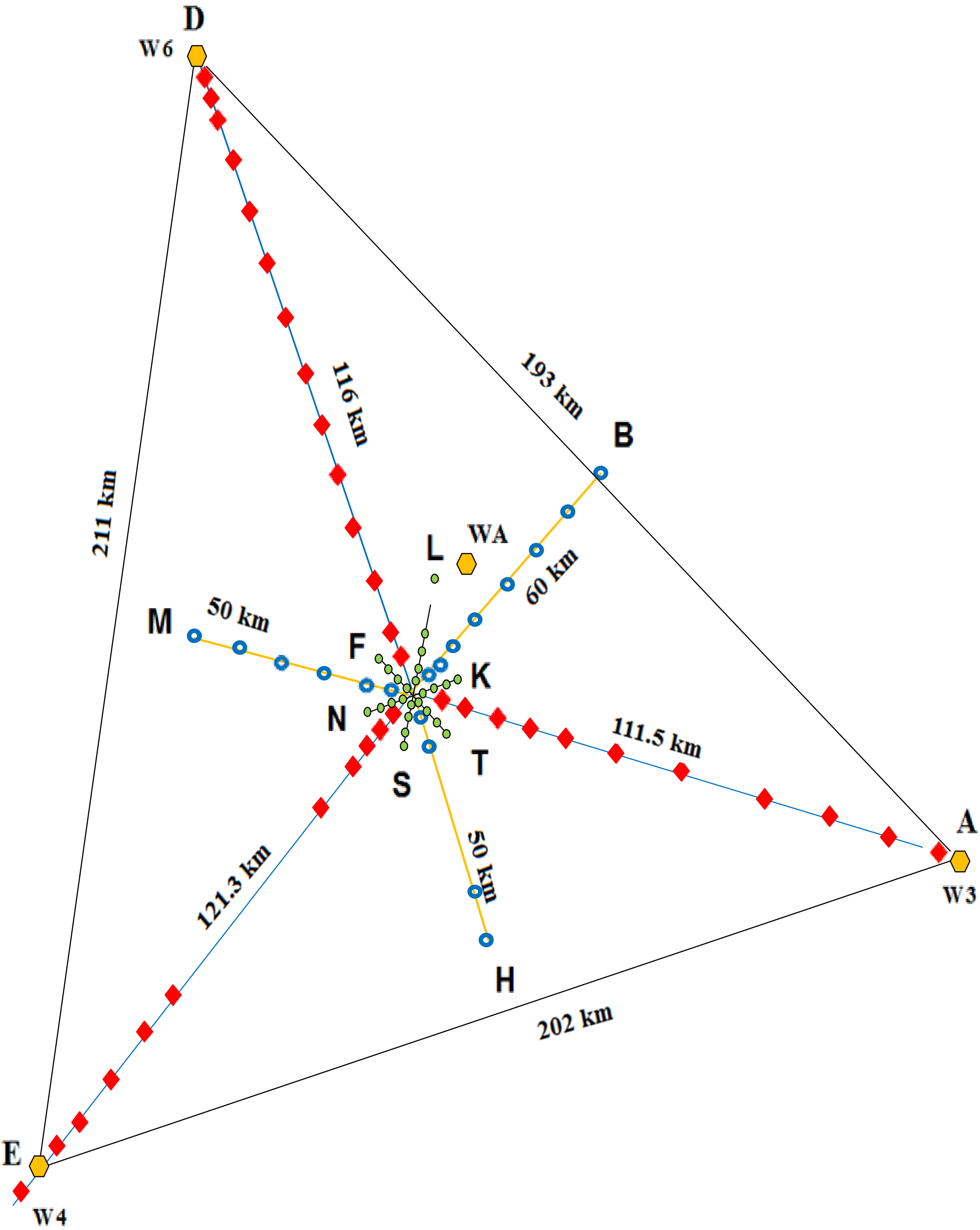

SCALE

1: 1000,000

Figure 7. Location map of the study area as determined by **GIZ**

We targeted the center of the RAK survey area for a higher density of MT stations, with a greater number of stations as we approached center point C. This point is the intersection of all 9 survey lines, enabling us to construct 2D cross-sections of resistivity structure along twelve different points of the compass from that center point. We also achieved modest densification of the survey grid close to wells W6 and W4 (see Figure 7), since resistivity well logs in these locations can be tied into our analysis and used to constrain the resistivity structure beneath the MT stations local to the wells. Such well-tie information is particularly useful as we evaluate static distortion (scattering) effects on the MT impedances that may be due to near-surface resistivity heterogeneities on arbitrarily small scales. Such distortion/scattering effects are well known for the MT method, and while there is a considerable tool chest of mathematical methods for removing these distortion methods (known collectively as *Tensor Stripping*), the use of well ties to known borehole resistivities provides the strongest possible constraints on these effects, and thus has considerable value.

Survey Challenges

Within the frequency range of the MT and AMT method, the depth of penetration of external magnetic fields into a conducting medium depends on the electrical resistivity of the medium and the harmonic frequency at which the incident magnetic field varies. For a homogeneous half space, the depth of penetration follows the well-known skin depth relationship,

$$\delta \approx 500\sqrt{\frac{\rho}{f}} \tag{1}$$

where δ, the skin depth, is the distance scale over which the incident field attenuates to $1/e$ its surface value, ρ is the electrical resistivity of the medium, and f is the frequency. Thus, for a more resistive medium, for a given frequency, penetration depths will be greater and the MT method will obtain information about a larger and deeper volume of earth beneath and surrounding a given station location. Frequency serves as a proxy for depth, so by collecting MT data over a range of frequencies, on a grid of survey locations, information on resistivity can be obtained within 2D profile cross-sections, or within a 3D volume.

The extraordinarily high resistivity of the shallow subsurface, due to the dry sand composition, suggests that the penetration depths of MT observations would tend to be very great. This is deceptive. Beneath the shallowest strata, the resistivity drops substantially, and this must be taken into account when determining survey parameters (station spacing, frequency band to acquire).

The most profound challenge to successfully acquiring MT data in the RAK is the 2 MOhm contact resistance we encountered. This was anticipated ahead of the deployment, but it was also confirmed *in situ* by a test installation near the field camp of grounded pairs of conventional Cu-$CuSO_4$ ceramic porous pot electrodes that are of the type typically used in the MT survey industry. To improve the contact resistance, we deployed pairs of such non-polarizing, wet chemistry electrodes in "Russian buckets", which comprise small impermeable plastic containers buried 30 cm beneath the sand. The bottom of each sandy hole was filled with an oversaturated NaCl-H_2O solution, which was allowed to percolate and to moisten the immediate area around each hole, providing conductive electrolyte. The plastic containers were filled with a slurry of hydrophilic bentonite and oversaturated NaCl-H_2O solution and placed in the bottom of the holes. The non-polarizing electrodes were then placed inside the containers, whose tops remained uncovered and filled with wet, electrically conductive, hydrophilic bentonite slurry. Local sandy earth was then packed on top of the containers, providing an electrically conductive path through the salty bentonite mixture, to the surrounding earth, through the annulus of slurry on the top periphery of the containers. This method is one that is used extensively for MT work around the world, and it provides near-optimal, stable conditions for good electrode coupling to the earth.

Having carried out this procedure, and after letting the electrodes stabilize for hours-to-days, we periodically measured the contact resistance between electrode pairs separated by 5 meters. These were found to stabilize in the MOhm range.

In conventional non-desert settings, typical electrode contact resistances range between hundreds of Ohms to as much as a couple of tens of kOhms range, but no higher. The key challenge to experimental design for the RAK lies in these unusually high contact resistances. If the source impedance of the electrode pairs that serve as electric field dipole sensors approaches the input impedance of the MT receiver's electric field preamplifiers, then electric currents can flow between the electrode pairs. This cannot be permitted to happen since current flow will polarize (deposit charges on) the electrodes, generating a spurious electrical potential that does not reflect the true state of the local electric field, and the MT impedance measurements will be distorted.

A method has been developed to deal with such situations. Rather than relying on conventional galvanic coupling between the electric field preamplifiers and the earth through porous pot electrodes, specially designed buffer amplifiers have been developed that take advantage of capacitive coupling. Conventional porous pot electrodes were replaces with steel rods. This is described in greater detail later in this report.

Other challenges included the high temperatures in the RAK, and also the strong temperature gradients with depth beneath the sand. When connecting copper wire to metals of different compositions such as steel rods, if a temperature gradient exists between two sets of bimetallic contacts (the two copper ends of the wires where they are joined to the two steel rods that make up the electric field dipole sensors), an electric potential is set up that is proportional to the difference in temperature between the two bimetallic junctions. This is the familiar thermocouple effect. Because of this, one must take care when installing the dipole sensor rods in the sand. Rather than inserting them vertically, where the steel rods can conduct heat in proportion to the local vertical temperature gradient, leading to different temperature profiles on the two rods making up the dipole receiver and exacerbating the differences in temperature at the point on each rod where copper wire is joined to the steel, it is best to cut a trench in the sand and to bury the rods horizontally at the same depth, so the temperatures are nearly isothermal. We discovered that by implementing this procedure, spurious drifting electric potentials ("self potentials") due to thermoelectric effects could be substantially eliminated from our measurements.

Two other significant and related challenges were encountered in implementing the survey. The first of these is the operational time available to complete each survey location. This is, in part, related to the number of MT receivers available to the survey, the number of survey crew and vehicles available, and the available operating period for the survey to be completed. To partially address this issue, we supplemented the KSU owned MT receiver with a second identical leased unit so we had two instruments available. The intent of doing this was to allow us to implement the MT Remote Reference method while collecting data simultaneously at two field locations separated by tens of km.

MT surveys can be conducted with a single instrument, with a single field crew, deploying a single station at a time. The limitation of this approach is that there are known frequency bands at which there are very low natural signal levels. These are the so-called *MT dead band* in the decade around 1 Hz, and the *AMT dead band* around 1-5 kHz. The low signal levels in these bands of frequencies lead to lower coherence levels between the electric and magnetic fields because of a lower signal-to-noise ratio than at other MT frequencies, with the result being distorted MT data with larger confidence limits than may be desired, at least within the dead bands. A well-established approach to dealing with this is to tightly synchronize the operation of two MT receivers separated by a sufficient distance that local EM noise sources will not produce coherent fields at both receivers simultaneously. Mathematical approaches have been developed that remove the effects of the incoherent noise fields, which can substantially improve the quality of data within the two dead bands.

The previous discussion of skin depth and the relationship of resistivity and frequency in that context is relevant here. For the RAK survey, it is necessary to acquire MT data over a wide frequency band that includes the MT dead band at low frequencies, and that intrudes at the highest frequencies into the AMT dead band. As a result the survey was designed to make it possible to implement the remote reference method by using two synchronized MT receivers separated by tens of km. Unfortunately, logistical considerations made this impractical to implement.

In order to complete the survey within a reasonable period of time, it was necessary for each field crew to transit to the next field station in their target grid, to install and operate that station typically only for 2 ½ hours of active data acquisition, and then to remove and relocate the equipment to the next station in the grid. Since there were two simultaneously operating field crews separated by substantial distances, and since the transit time over the sand dunes was unpredictable, this production schedule made it impractical to synchronize the two receivers. Rather, each receiver was set to record as soon as the installation was complete, and there was no way to delay the start of the 2nd receiver without direct communications between the distant field crews or without imposing an overly generous transit and installation period allowance for each crew so that fixed start and end times could be used for both instruments in the absence of communication. Adopting either of these approaches would have imposed substantial and unacceptable delays in the production schedule as the first field crew waited for the 2nd to complete the installation of their equipment or both crews waited for the predetermined time to start recording. Even maintaining reliable communications between field crews was problematic because of unreliability of the Thuraya satellite telephone system. As a consequence of these operational realities, the remote reference method was not employed.

While there are consequences of this in terms of data quality within the dead bands, it was considered likely that local-scale EM noise in the RAK, which would reasonably be attributed to man-made EM noise generation sources, would be less likely to overwhelm the lower natural signal levels in those bands because of the lack of development and infrastructure in the remote desert region. There are few sources of artificial EM energy in the survey region. The one clearly detectible local noise source was the 50 Hz and 60 Hz electric generators used in the field camp, and also used in one other Bedouin camp that was positioned nearby. For those MT sites installed within 10 km of the field camp, the generators were switched off in an effort to remove this source of EM energy. Even so, the power line frequencies are outside the dead band frequencies, so this was not considered to be a significant issue.

The rapid production schedule also impacted the width of the frequency band that was available to the survey. In order to collect low frequency data, it is necessary to operate the MT receivers for a greater period of time than required to collect higher frequency data of equivalent quality. On statistical grounds, one would ideally hope to record at least 100 realizations of the fundamental frequency of interest. For instance, to obtain 0.01 Hz data of high quality, i.e. harmonic data with a period of 100 seconds, one would ideally obtain 100 cycles or more of the 100 s period data, requiring measuring the signal for at least 10,000 s if not longer. The precise length depends on the electrical resistivity structure beneath the site, since conductive regions at various depths act to attenuate signal levels at different frequencies. Compromises can be made, and long-period data obtained with fewer than 100 cycles of the target frequency, but data quality will be diminished.

In order to improve data quality at the longest periods, once full production speed was reached, field crews left the final station installed each day to run overnight so that there were a subset of stations that would be particularly well configured to achieve low frequency, deep penetration of the deepest aquifer target (> 2.5 km). The majority of stations did not operate overnight, so their longest period data is less effective at penetrating into and through the conductive deep aquifer layers, and thus is better suited for providing wider areal characterization of mid-depth aquifers.

GEOGRAPHIC COORDINATES OF RAK MAGNETOTELLURIC STATIONS (80 MT POINTS)

No	STATION	LATITUDE (N)	LONGITUDE (E)	DIST. FROM CENTER (km)	Elev. (m)	NOTES
	W6	22 07 45.4	48 32 48.2		272	
	W3	20 50 20.0	49 47 42.0		250	
	W4	20 19 19.3	47 56 11.1		367	700m depth, under construction
	Al Ubaila	21 22 10.5	48 55 56.0		267	Drilled, 1985
1	C	21 05 54.6	48 45 32.7	0	286	
101	CAN1	21 06 35.8	48 42 45.5	5.0	292	C – CA1 (Night)
2	CA1	21 07 17.5	48 39 57.6	10	293	
3	CA2	21 08 39.9	48 34 22.4	20	296	
4	CA3	21 10 02.3	48 28 47.0	30	305	
5	CA4	21 11 24.5	48 23 11.6	40	311	
6	CA5	21 12 46.4	48 17 36.1	50	317	
81	CN2	21 07 31.4	48 47 06.6	4	285	C – CB1 (Night)
83	CN3	21 08 38.5	48 48 21.4	7	286	C – CB1 (Night)
7	CB1	21 09 44.2	48 49 38.0	10	280	
8	CB2	21 13 33.8	48 53 43.6	20	279	
9	CB3	21 17 23.2	48 57 49.3	30	273	
10	CB4	21 21 12.6	49 01 55.3	40	262	
11	CB5	21 25 01.9	49 06 01.4	50	239	
87	CB6	21 28 51.0	49 10 07.9	60	248	
89	CN7	21 03 46.3	48 45 59.3	4.0	289	C – CD1 (Night)
12	CD1	21 00 35.3	48 46 37.9	10	307	
15	CD4	20 44 37.4	48 49 53.3	40	319	
16	CD5	20 39 18.0	48 50 58.3	50	316	
84	CN4	21 08 02.4	48 45 06.7	4.0	287	C – CW 61 (Night)
17	CW61	21 11 14.0	48 44 27.3	10	284	
18	CW62	21 16 33.3	48 43 21.9	20	282	
19	CW63	21 21 52.6	48 42 16.4	30	283	
20	CW64	21 27 11.9	48 41 10.8	40	280	Night
21	CW65	21 32 31.1	48 40 31.1	50	279	
22	CW66	21 37 50.4	48 38 59.3	60	275	
23	CW67	21 43 09.6	48 37 53.5	70	273	
24	CW68	21 48 28.9	48 36 47.6	80	272	
25	CW69	21 53 48.1	48 35 41.6	90	270	
26	CW610	21 59 07.3	48 34 35.6	100	262	
27	CW611	22 04 26.6	48 33 29.5	110	265	

86	CN6	21 05 19.0	48 47 45.2	4	298	C – CW31 (Night)
28	CW31	21 04 31.7	48 51 07.7	10	297	
100	CW3011	21 03 49.5	48 53 58.2	15	288	CW31 – CW32 (Night)
29	CW32	21 03 08.7	48 56 42.6	20	287	Night
30	CW33	21 01 45.4	49 02 17.4	30	262	Shaibaniyah well is around
31	CW34	21 00 22.0	49 07 52.2	40	280	
32	CW35	20 58 58.3	49 13 26.7	50	276	
34	CW37	20 56 10.5	49 24 35.6	70	270	
36	CW39	20 53 21.9	49 35 44.0	90	264	
37	CW310	20 51 57.4	49 41 18.1	100	258	
102	CWN1	21 03 59.8	48 43 30.3	5	289	C – CW41 (Night)
39	CW41	21 02 04.9	48 41 27.6	10	295	
103	CW413	21 00 11.2	48 39 26.3	15	308	CW41-CW42
40	CW42	20 58 15.1	48 37 22.7	20	314	
41	CW43	20 54 25.1	48 33 18.0	30	309	
47	CW49	20 31 23.4	48 08 54.0	90	346	
48	CW410	20 27 32.8	48 04 50.7	100	359	
49	CW411	20 23 42.1	48 00 47.6	110	362	
50	CW412	20 18 48.7	47 55 08.7	120	369	
51	C11	21 06 55.5	48 45 57.5	2	290	
52	C12	21 07 56.2	48 46 22.4	4	286	
53	C13	21 09 27.2	48 46 59.7	7	291	
54	C14	21 10 58.2	48 47 36.4	10	281	
91	C16	21 13 30.7	48 48 38.7	15	277	
88	C15	21 21 06.4	48 5145.2	30	271	7.5 km from Ubaila Well
55	C21	21 06 11.5	48 46 39.7	2	288	
56	C22	21 06 28.2	48 47 46.6	4	301	
57	C23	21 06 53.3	48 49 27.1	7	292	
58	C24	21 07 18.3	48 51 07.6	10	298	
59	C31	21 05 09.6	48 46 22.6	2	307	
60	C32	21 04 24.5	48 47 12.5	4	303	
61	C33	21 03 16.7	48 48 27.2	7	293	
62	C34	21 02 09.0	48 49 42.1	10	300	
63	C41	21 04 54.1	48 45 07.7	2	290	
64	C42	21 03 53.5	48 44 42.7	4	302	
65	C43	21 02 22.6	48 44 05.0	7	302	
66	C44	21 00 51.6	48 43 27.6	10	310	
67	C51	21 05 38.1	48 44 25.7	2	286	
68	C52	21 05 21.4	48 43 18.7	4	297	
69	C53	21 04 56.3	48 41 38.4	7	290	
70	C54	21 04 31.4	48 39 58.0	10	293	
71	C61	21 06 39.8	48 44 42.7	2	279	
72	C62	21 07 24.9	48 43 52.7	4	284	

73	C63	21 08 32.5	48 42 37.8	7	285	
74	C64	21 09 40.2	48 41 22.9	10	287	
75	L1	22 06 41.4	48 33 01.5	2	264	Night
76	L2	22 05 37.6	48 33 14.8	4	269	
77	L3	20 50 36.9	49 46 35.2	2	257	Night
79	L5	20 20 05.4	47 56 59.5	2	365	Night
80	L6	20 20 51.6	47 57 48.1	4	365	

- W3, W4, and W6 : represent the three wells of the triangle given by GIZ
- Blue lines indicate MT stations that were left to operate overnight in order to obtain data in the lower frequency band

Methodology

The magnetotelluric (MT) method uses the time-varying Earth's electromagnetic (EM) field as its source, and depth penetration from a few hundred meters to about 200 km or even greater is generally possible depending on the range of frequencies measured. At high frequencies (about 8 Hz and higher), the EM fields penetrate typically to about mid-crustal depths. These variations are caused by distant lightning storms, perhaps half the globe away. The time variations at deep-crustal and mantle-probing depths are caused by the interaction of the solar plasma with the Earth's magnetosphere - the most visible form of this interaction is the *northern lights*. The EM energy from both of these sources is trapped within the Earth-ionosphere waveguide.

EM techniques are sensitive to electrical conductivity. In the exploration industry, conductivity is usually displayed as its reciprocal property, resistivity (1/conductivity) since this is consistent with the property obtained from DC resistivity surveys and from down hole well logs.

Most aquifers are more electrically conductive than the formations above and below the aquifers. EM techniques are characterized as either "natural source" (no man-made energy source required) or "Controlled Source" (CSEM) which require a man-made power source. The usual EM techniques applied to groundwater exploration and characterization include the controlled-source techniques VES (Vertical Electric Sounding"), dipole-dipole resistivity, TDEM (Time Domain EM), and Frequency Domain EM. However, all of these are shallow-penetrating techniques.

ES and dipole-dipole resistivity require the use of a transmitter/motor generator and fuel supply, and also, well-grounded current electrodes (which may be difficult to achieve in the extremely dry surface sands). VES and dipole-dipole resistivity (with typical multi-channel systems) have considerable difficulty seeing below the first conductive layer. VES requires very large current dipoles (expanding up to several km in length) to achieve significant depth of exploration.

TDEM and **FDEM** do not require grounded electrodes, but typical groundwater-oriented FDEM has depth of investigation of usually < 100m, and TDEM, < 300m. As well, TDEM has difficulty seeing through the first conductive layer. The depths in the RAK aquifer systems exceed the capabilities of the usual techniques described above, so to investigate the aquifer formations below the shallowest one, deep-penetrating EM technique(s) are required. The only two CSEM options are CSAMT and LoTEM. Any deep-penetrating CSEM technique requires a powerful motor generator, with ample fuel supply, and a large transmitting antenna. The logistic handicap of CSEM for RAK operations is obvious.

Therefore, the most feasible EM technique to use in this project appears to be MT, a well-known natural-source geophysical technique (invented in the 1950s) and used in exploration for hydrocarbons, geothermal systems, metallic minerals, and groundwater.

The MT signal source is natural fluctuations of Earth's magnetic field. Since no heavy motor generator / fuel supply /large antenna is needed, this greatly simplifies operations in the RAK. The MT depth of investigation is can be

>tens of km or even greater if desired, depending on the frequency bands recorded, which is more than sufficient for this project. MT equipment is relatively compact and light in weight, battery powered, with small footprint and minimal environmental disturbance; and MT provides a rich information set, with dimensionality indicators, etc.

There are five channels of data input at each MT station. These are two orthogonal horizontal components of electric field (E_x and E_y time series) and three orthogonal components of the magnetic field (H_x, H_y, and H_z time series). Note that boundary conditions require that E_z = 0, so a full three dimensional vector measurement is being made. The electric field components(E_x and E_y) are usually measured by orthogonal pairs of non-polarizable porous pot electrodes connected by cables. For the high contact impedance characteristic of the RAK, the porous pot electrodes can be substituted with steel rods or titanium plates, and a specialized buffer pre amplifer used to capacitively couple the electric dipole receivers to the earth. The magnetic field components (H_x, H_y,and H_z) are normally measured with ferrous-cored induction coils, although for long-period measurements at frequencies below the MT dead band, compact fluxgate magnetometers are also frequently used.

For an Earth whose resistivity varies in only one dimension, every E_x has an associated orthogonal H_y measurement, and every E_y has an associated H_x. For a 2D or 3D Earth, the relationship between the different field components is more complicated. Tensor MT and AMT data measure additional components (E_y andH_x) that provide information about directionality, 3D heterogeneity, and potentially anisotropy. In this more general case, the relationship between the components of the electric and magnetic fields is expressed in the form of a complex-valued, frequency domain 2 x 2 tensor impedance Z,

$$\begin{bmatrix} E_x \\ E_y \end{bmatrix} = \begin{bmatrix} Z_{xx} & Z_{xy} \\ Z_{yx} & Z_{yy} \end{bmatrix} \begin{bmatrix} H_x \\ H_y \end{bmatrix} + N$$

where E_i represents the components of the electric field, H_j are the components of the magnetic field, Z_{ij} are the elements of the impedance tensor, and N represents the incoherent noise between E and H within the given frequency band. In practical terms, the impedance tensor is obtained from time series recordings of the electric and magnetic field components. These are then Fourier transformed, and cross-powers are calculated and the impedance, which is a form of *transfer function,* is then estimated usually using statistically robust variants of least squares of other methods designed to down weight the influence of spurious data. A similar procedure is used to generate the transfer function relating vertical magnetic field components to each of the horizontal components. These are known as *induction vectors,* or *tippers, Wiese* or *Parkinsonvectors*. Induction vectors provide additional constraints for inversion of MT data and also can be used to directly indicate the presence of channeled electrical currents in the subsurface.

A schematic diagram showing a typical MT field installation appears in Figure 8.

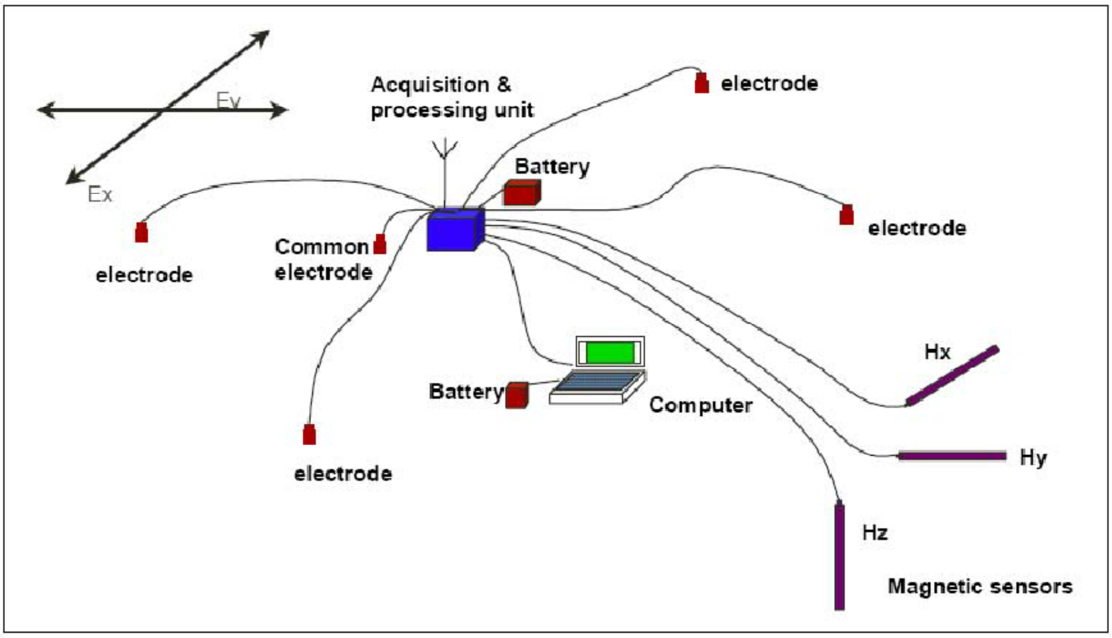

Figure 8. Typical MT station layout

At each station, electrode pairs measure the electric (E) field, and magnetometers are used to measure the magnetic (H) field in the frequency ranges of interest, typically from 0.001 Hz to10KHz. High sensitivity magnetometers and careful installation of low noise electric field sensors are required to measure extremely subtle MT signals.

The amplitude, phase, and directional relationships of the E- and H-fields on the surface depend on the electrical conductivity in the subsurface. Different array types are considered for acquiring the most beneficial data for a particular survey area.

Instrumentation

This study used Zonge's GDP-32/24 receivers system to fulfill and meet requirements of the RAK proposal. For typical MT installations, the electric field signal is measured at the receiver site using non polarizing ceramic porous-pot Cu-CuSO4 electrodes connected to the receiver with insulated 14-gauge wire.

For the Rub' al Khali survey described here, we used horizontally oriented steel rods, trenched approximately 10 cm beneath the sand surface, in lieu of conventional electrodes. By connecting the steel rods to active buffer amplifiers, we used capacitive coupling to the ground rather than more typical galvanic coupling. This was necessary since the contact resistance of the electrodes was in the hundreds of kohm to Mohm range when buried in the sand. Such high contact resistances persisted even when the porous pot electrodes were placed in "Russian buckets", i.e. plastic buckets containing approximately 2 liters of bentonite+H2O+NaCl gel, buried underground.

We typically use the Russian bucket configuration to provide a moister, more chemically stable environment for the electrodes, with improved electrical coupling between electrodes and ground. In the case of the Rub' al Khali survey, use of such porous pot electrodes is precluded because the extremely high contact resistance approaches the same order of magnitude as the input impedance of the GDP system's electric field pre amplifiers. With such an unfavorable ratio between source and amplifier input impedance, electric field measurements would be distorted, and electrodes can polarize because of current flow between connected pairs.

By using capacitive coupling, the up to 2 Mohm source impedance is well within operational limits, and at the cost of somewhat higher noise levels at long-periods than is typical for porous pot electrodes, MT measurement may be taken even at these extremely high contact resistance levels.MT magnetic field measurements in the MT frequency range (0.0005 – 1000 Hz) were made with Zonge ANT/4 antennas. A complete listing of instrument specifications is shown below:

GDP-32 Receiver

The GDP-32^{II} multifunction receiver is the fifth generation GDP and it plays a pivotal role in the Zonge system of instrumentation. It is rugged, one-man portable and environmentally sealed. The Geophysical Data Processor receivers perform broadband synchronous time or frequency domain measurements on both controlled-source (i.e. signals generated by transmitting current into grounded dipoles or wire loops) and on natural fields.

Performance advantages:

- multifunction capability
- synchronous timing
- unique multi-channel acquisition

Unique capabilities:

- Remote control operation
- Broadband time-series recording
- High-speed data transfer

Specifications

- Type: **Receiver**
- Methods: EM (Resistivity, Time/Frequency Domain IP, CR, CSAMT, Harmonic analysis CSAMT (HACSAMT), AMT, MT, TEM &NanoTEM®)
- Dimensions: 43x31x23 cm
- Weight: 13.7 kg
- Environmental: -40°c to 45°C
- Input Power: 12V rechargeable batteries
- Frequency Range: 0.015625 Hz - 8 KHz
- Impedance: 10MΩ
- Produced by: **Zonge International, Inc.** (USA)

The GDP-32" is Zonge International's most widely used multi-channel receiver for acquisition of controlled- and natural source geoelectric and EM data. The receiver allows one to perform remote control operation, record broadband time-series, as well automatically to buck outelectric field dipole self potentials (SP), and to automatically set gains, and carry out in situ calibration.

The GDP-32" receiver is most widely used multi-channel receiver for acquisition of controlled- and natural source geoelectric and EM data.

Buffer Amplifier

Numeric Resources Inc. Model HZB_01 / PWR_01 buffer amplifier. The right image shows the device as it appears just after power-on, with all LED indicators ON. The left image shows the input (white-black) and output (red-black) binding post connections (Stodt, 2005).

This buffer amplifier is designed to mitigate the effects of high electrode contact impedance when making electrical geophysical measurements. The device can be used with GDP receivers to make either single-ended or differential measurements of the electric field. The problems created by a high electrode contact impedance when making typical geophysical E-field measurements, and the effectiveness of using buffer amplifiers at the electrodes to mitigate the adverse effects are detailed in Stodt (2005).

Antennas (ANT/4 & ANT/6)

The ANT/4 and ANT/6 magnetic field sensors are extremely low noise instruments. Using feedback amplifier technology and including carefully designed mu-metal cores, these antennas are each designed with specific purposes in mind. Each antenna is designed to be a highly flexible instrument, built to withstand the difficult conditions encountered in the field environment.

The Zonge ANT/6 magnetic field sensor has a noise threshold level below typical AMT and MT natural source signal levels. With this setup it is possible to collect the most useful AMT data in the "dead band" under most conditions. Additional magnetic field sensors can be used for reference data collection.

When collecting MT data at frequencies below 3.0 Hz, the Zonge ANT/4 magnetic field sensor provides significantly better results than the ANT/6 (compare the B-field gains below 3 Hz). Operationally, for the frequencies required for the RAK survey, and given the logistic and time constraints, we exclusively deployed ANT/4 sensors, particularly since the lower frequencies are most effective at illuminating the deeper aquifer target formations.

For tensor MT coverage, two ANT/4 sensors are needed to measure H_x and H_y. For full tensor MT (including induction vectors), a third ANT/4 sensor is needed to record H_z. Remote Reference full tensor MT requires operation of two GDP units and six ANT/4 sensors.

MT Data Correction

MT time series were successfully recorded at all 80 stations installed during the survey at the locations indicated in Figure 7. MT transfer functions (impedances) have been calculated using a statistically robust processing approach described previously. These transfer function estimates are preliminary, and they will be adjusted to improve the MT receiver system's instrument response correction.

The instrument response of the GDP 32/24 is well established for conventional MT deployments using porous pot electrodes. The addition of buffer amplifiers and (primarily) capacitively coupled steel rod electric field sensors modifies the response of the electric field section of the instruments, and thus distorts the MT transfer functions. This can be corrected. Zonge geophysicist N. Bouzid worked with the buffer amplifier manufacturer Dr. Stodt to refine the instrument response correction.

A preliminary buffer amplifier response model output is displayed in the figure below, which was provided by Dr. Stodt based on the contact resistance of the RAK MT survey. This shows the output of a SPICEIV circuit model for response analysis of steel rod contact impedance and the Numeric Resources buffer amplifier.

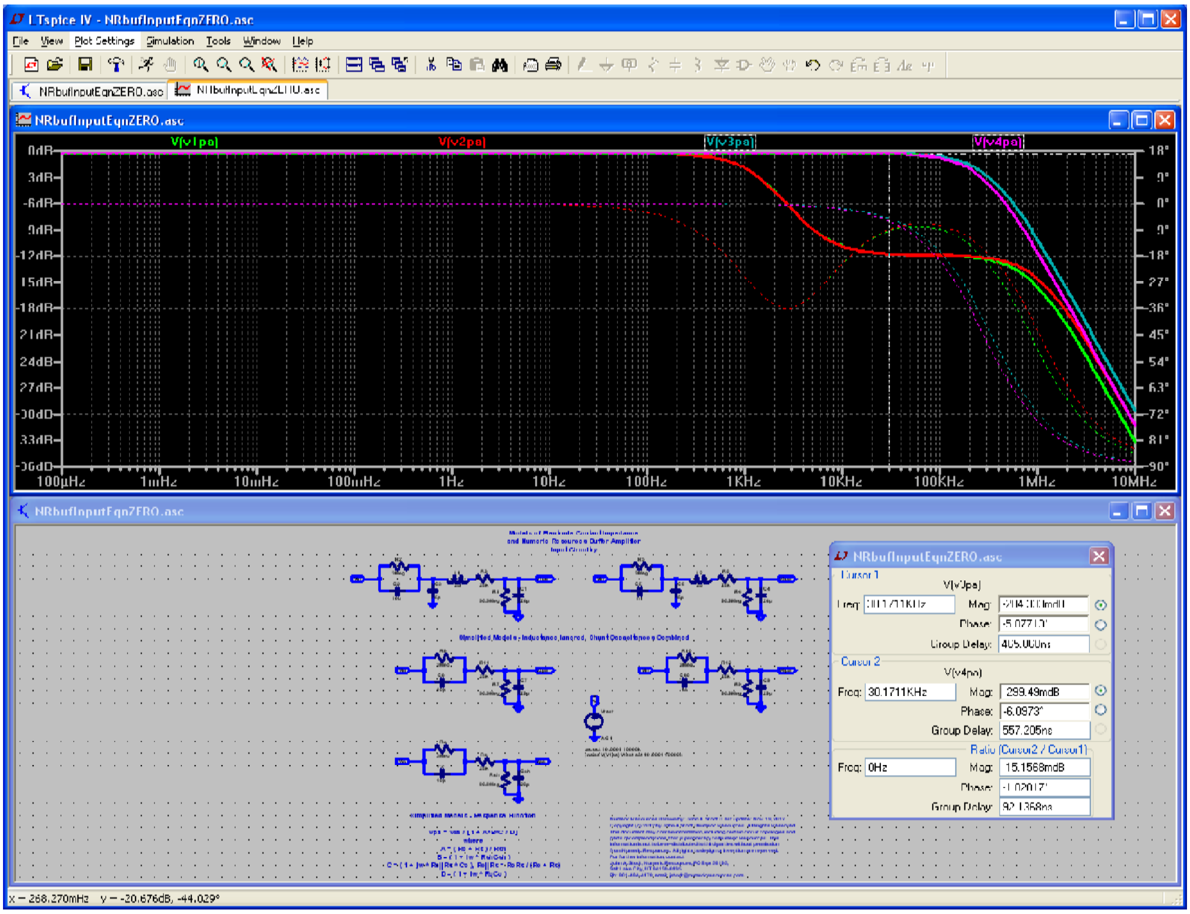

Response curves for the Numeric Resources buffer amplifier

The modeled buffer amplifier responses indicate that below 1Hz there is no impact of the buffer amplifier on the GDP response other than a small attenuation of the electric field signal attenuation of approximately 0.969*Vin. Some frequency dependence from a high pass filter effect is possible if there is parallel capacitance across the input resistance, and the input resistance is much larger than 3Mohm. This is not likely to be a concern, since contact resistances were more typically 2 Mohm rather than greater than 3 Mohm.

We anticipate that adjustments to the MT impedances will therefore be small.

Even though that may be the case, it would be premature to carry out additional interpretation such as inversion of these MT data for resistivity structure, since the residual buffer amplifier response correction, if not implemented, will distort the results and potentially lead to a static distortion effect because of unadjusted gain corrections and small frequency effects.

The apparent resistivity is merely a scaled version of the magnitude of the impedance, and the impedance phase is calculated from the arc-tan of the ratio of imaginary and real part of the impedance. For an earth with a resistivity structure that varies only with depth, the impedance tensor reduces to a simple scalar, and a single apparent resistivity and phase estimate exists at each frequency. If the earth has a 2D resistivity structure, the impedance tensor can be transformed into two sets of apparent resistivities and phases, with one set aligned parallel to geoelectric strike, and the other perpendicular to geoelectric strike. If the earth is fully 3D, no simplifications of this sort can be used.

For present purposes, we display the apparent resistivity as the *Berdichevskiy* average, which is determined by rotating the impedance tensor into a coordinate system that orients the impedance into parallel and cross-strike directions, which is appropriate for a 2D Earth. One then averages these impedance estimates, at each frequency, to get an estimate that can be inverted for 1D earth structure. This is only a rough approximation, although it is commonly used in the MT industry where surveys are conducted in large sedimentary basins that locally are predominately 1D in nature. Examples of averaged apparent resistivity and phase vs frequency for a number of the stations used in the survey, appear below.

In each graph below, we display apparent resistivity (units: Ohm-m) as a pair of red curves, and phase (units: degrees) as a pair of blue curves, with axis labels for these quantities in these respective colors. The x-axis is period in seconds (1/frequency in Hz). A log-log scale is used and a random selection of data from the 80 sites is show. The curves with error bars are the calculated data, while the curves with only dots represent the fit of a layered Earth model fit to those calculated data. For the reasons previously discussed relating to instrument response corrections, the details of those 1D models are not of interest, so your attention is drawn to the curves with error bars.

For a homogeneous half-space of constant resistivity, the apparent resistivity curves would be constant and the phase would be 45 degrees. Phases greater than 45 degrees suggest decreasing resistivity below the depths of penetration associated with those frequencies, while lower phases indicate increasing resistivity. The apparent resistivities show a similar transition with frequency, also indicative of changes in the true resistivity with depth.

While the data quality varies from site-to-site, it is already evident at this preliminary stage of the analysis that there is significant site-to-site variability in resistivity structure; that data of sufficient quality has been obtained to detect the presence of highly conductive zones; that the frequencies at which increasing phases and decreasing apparent resistivities have been detected are broadly in the range to be expected for the known and predicted depths to the mid-level aquifers, and that analysis of this large data set will involve use of 2D inversion techniques at a minimum.

Generally, the impact on data quality from the lower signal levels in the dead bands will need to be further appraised, as will the relative paucity of stations with longer-period (overnight) data coverage. There is the likelihood that at the majority of sites it will not be possible to resolve the presence and extent of the deepest target aquifer or other features at depths below 1500 m. There is a greater possibility that such features may be resolvable, or at least the depth to the top of those conductive features may be detectible, at those sites where longer-period data is available from overnight operations. This will be an area of active investigation during this period.

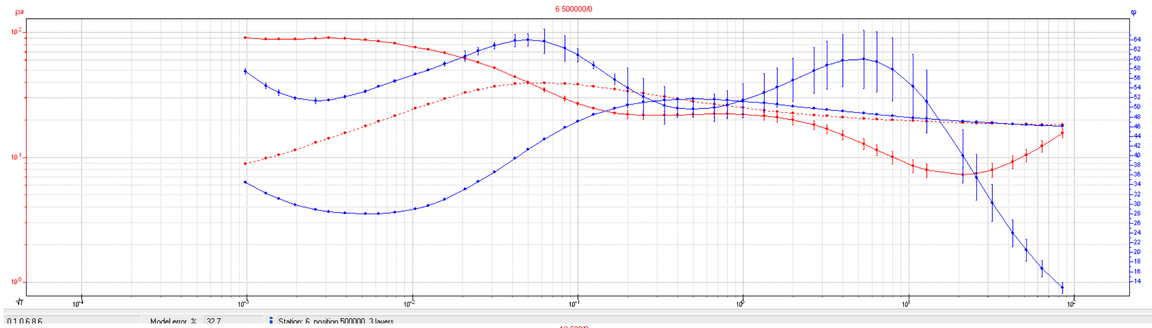
6 500000/0
0.1 0.6 8.6
Model error, %
32.7
Station: 6, position 500000, 3 layers

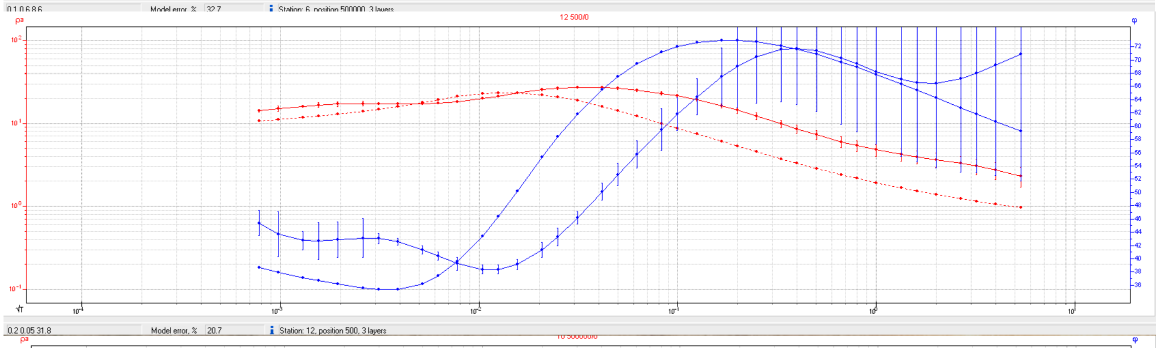
12 500/0
0.2 0.05 31.8
Model error, %
20.7
Station: 12, position 500, 3 layers

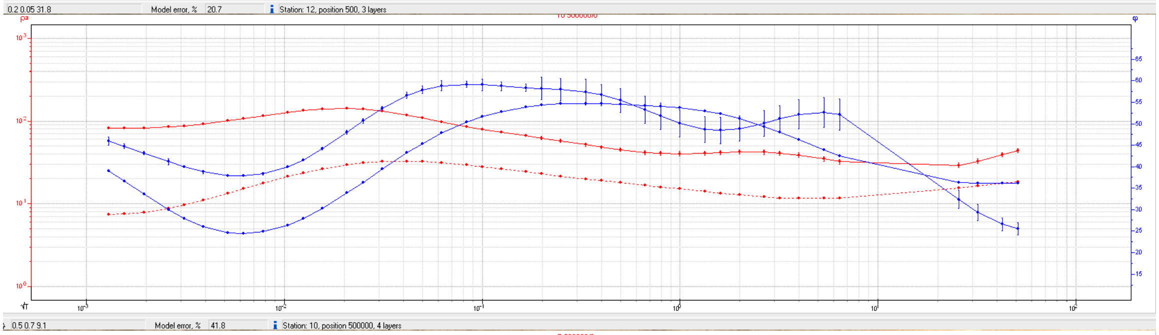
0.5 0.7 9.1
Model error, %
41.8
Station: 10, position 500000, 4 layers

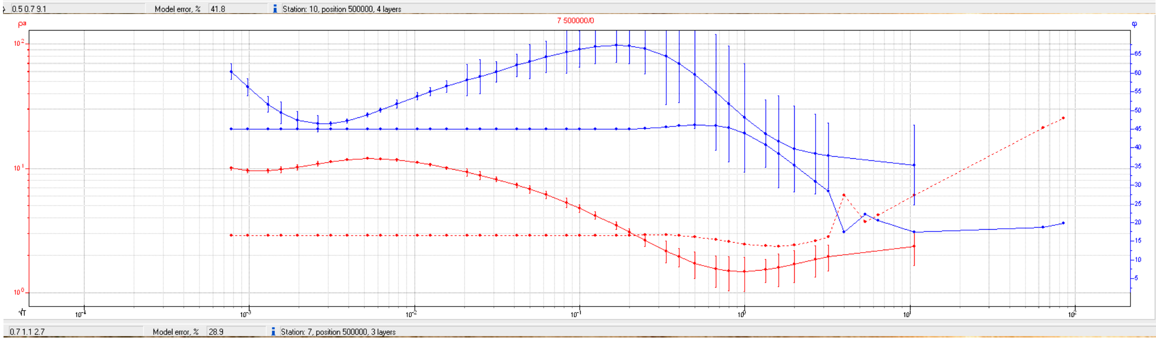
7 500000/0
0.7 1.1 2.7
Model error, %
28.9
Station: 7, position 500000, 3 layers

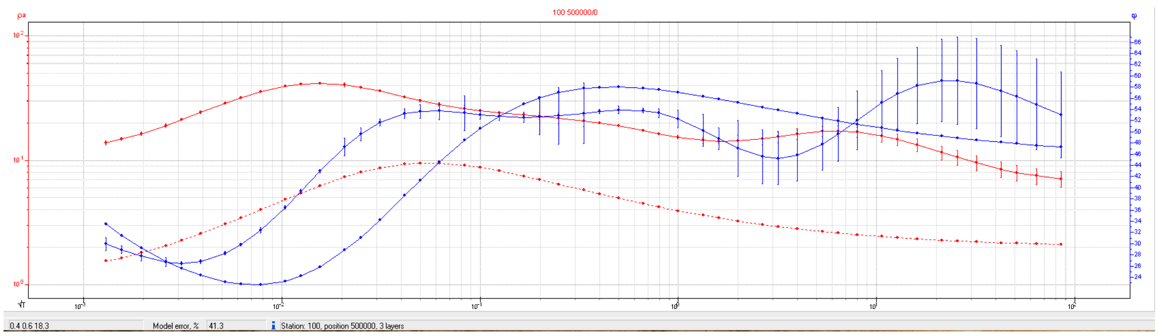
100 500000/0
0.4 0.6 18.3
Model error, %
41.3
Station: 100, position 500000, 3 layers

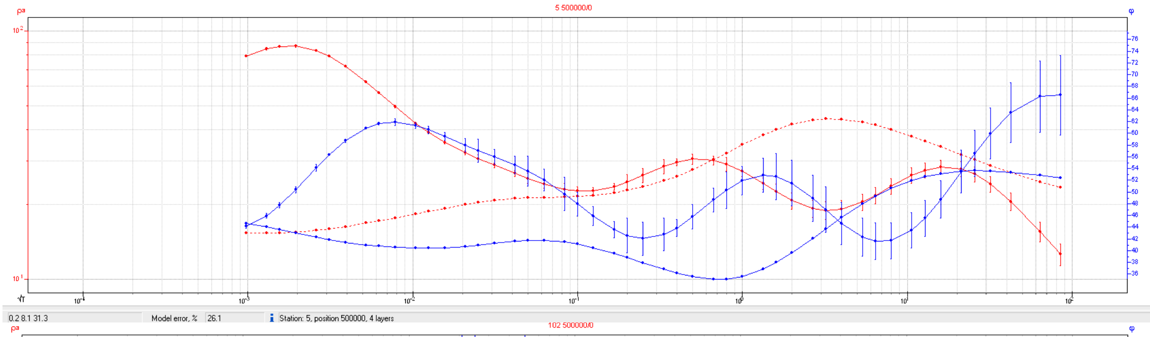
5 500000/0
0.2 8.1 31.3
Model error, % 26.1
Station: 5, position 500000, 4 layers

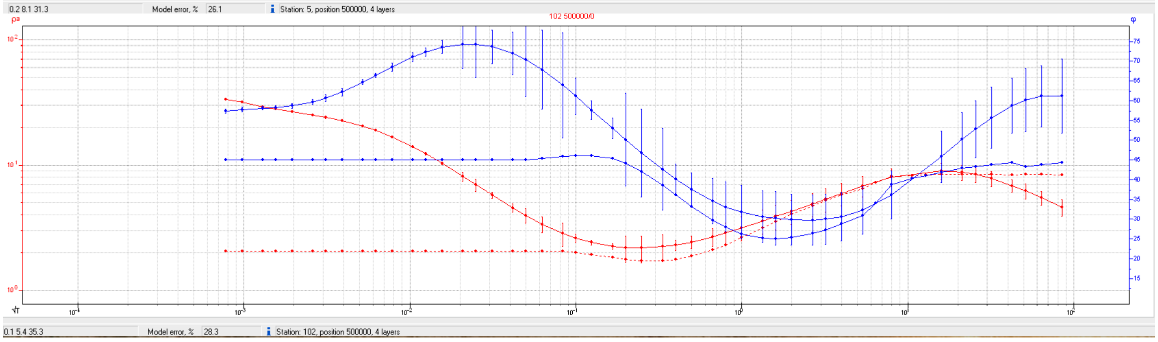
102 500000/0
0.1 5.4 35.3
Model error, % 28.3
Station: 102, position 500000, 4 layers

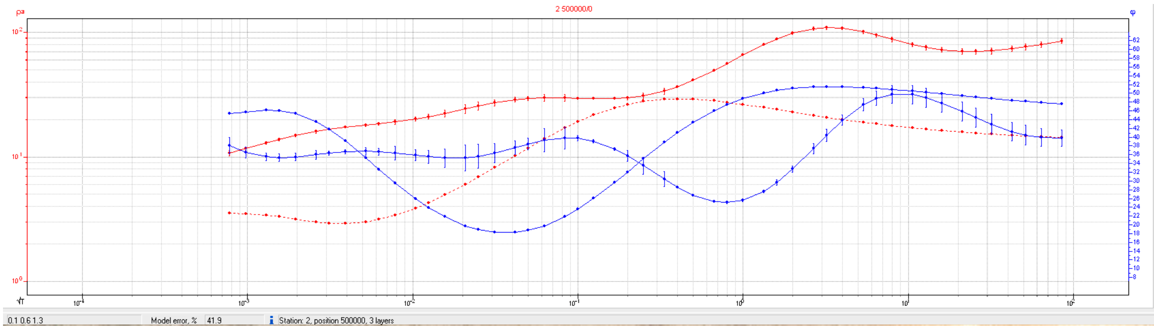
2 500000/0
0.1 0.6 1.3
Model error, % 41.9
Station: 2, position 500000, 3 layers

MT Data Analysis & Interpretation

A more detailed theoretical discussion of MT impedance tensor dimensional analysis was provided in our report of March 2013. To summarize briefly, in order to calculate the impact of higher dimensional structures such as regional geoelectric strike directions that can be used to decompose the MT impedance tensor into transverse electric (TE) and transverse magnetic (TM) modes, or to assess the degree of near surface scattering effects (i.e. static distortion) on the analysis, we employed Weaver's (*Geophysical Journal International, 141, 321-336,* 2000) dimensional parameters, a set of eight invariants that have been used to establish the consistency of an MT data set with 1D, 2D or 3D dimensional structure. We have calculated the Weaver invariants by implementing a Fortran code (**WALDIM**) distributed by the authors (Marti, Queralt and Ledo, *Computers & Geosciences*, **25**, 12, 2295-2303, 2009). The **WALDIM** approach also considers galvanic distortion of the local impedance tensors, which are caused by electromagnetic scattering by near surface heterogeneities in electrical conductivity structure that are of too small a scale to be resolved by the MT data, but that may distort the electric field at all frequencies. One may describe such surface (galvanic) scattering effects as a series of factors including changes in the effective gain of the system, and changes in the electric field at the measurement location, represented by twist, shear and anisotropy.

A variety of methods for evaluating dimensionality and accounting for galvanic, near surface scattering effects have been advanced over the years. Perhaps the most refined of these is the Phase Tensor approach of Caldwell et al (*Geophysical Journal International*, **158**, 457-469, 2004). This latter approach, while highly useful for determining regional geoelectric strike directions (if these indeed exist for a given survey region), does not in and of itself allow one to remove static distortion effects.

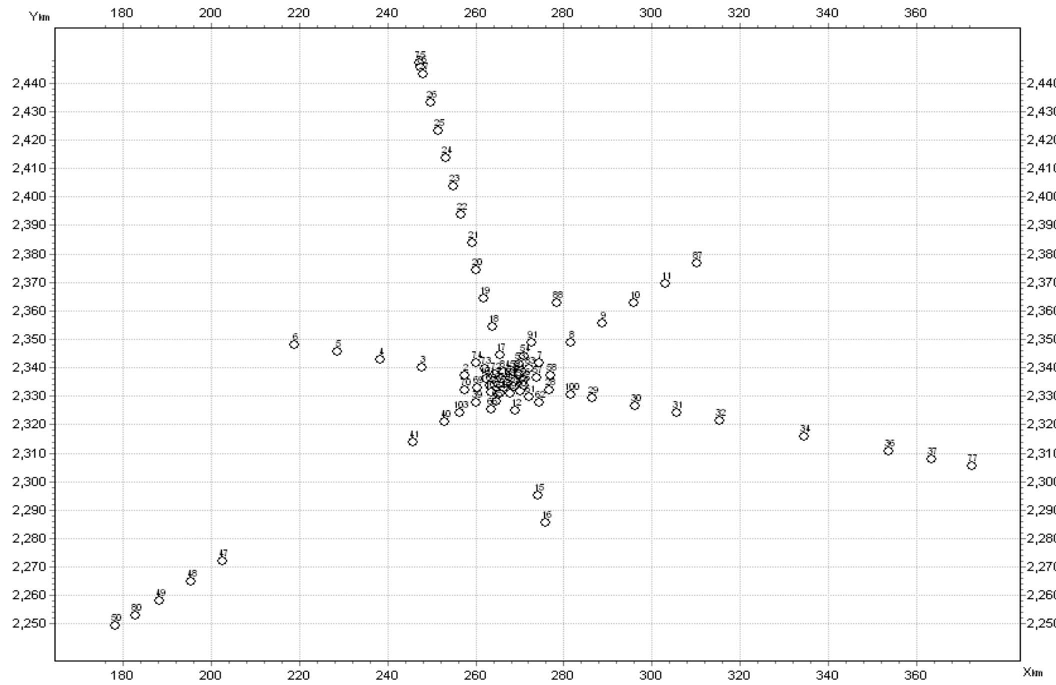

Figure 9. RAK AMT survey locations. X-axis is marked in km east, Y-axis marked in km north. The origin is arbitrary.

The **WALDIM** parameters have the useful property of addressing both recovery of regional strike directions, where these exist, and of estimating surface scattering impacts on the impedance tensors.

We have applied the **WALDIM** analysis to all 80 stations acquired in the RAK in October 2012. A map of the survey station locations is seen in Figure 9. The numbers adjacent to the survey locations (marked by open circles) represent the station identification numbers that we have used throughout our analysis.

As seen in Figure 10, the AMT survey consisted of three long 2D profile lines, meeting at a common center point (which is designated as station '1'). Three additional shorter 2D survey lines also radiate from the common center point. We presented the **WALDIM** dimensional analysis of each of these survey lines in our report of March 2013 (Appendix A).

Here we recapitulate the results in Appendix A of our March 2013 report – there is no regional geoelectric strike direction that can be determined from the RAK AMT survey data. There are strong 3D effects throughout the survey area. The survey is inconsistent with regional or local 1D interpretation, and 2D interpretation (complete decomposition of the MT impedances into TE and TM modes) is only possible in a small subset of (frequency, station) pairs within this survey.

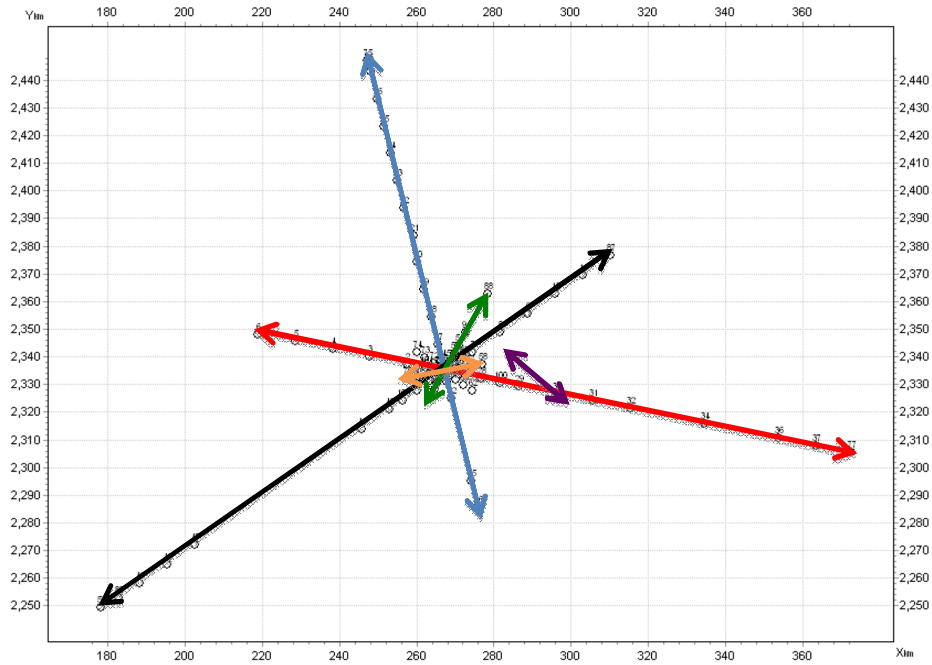

Figure 10. North-South long survey line marked by blue line. Northwest-Southeast long survey line is marked by red line. The Southwest-Northeast long survey line is marked by a black line. The Northwest-Southeast short survey line is marked by purple line. The Southwest-Northeast short survey line is marked by a mustard colored line. The South-Southwest-North-Northeast short survey line is marked by a green line.

Specifically, for a very limited range of frequencies and MT station locations, at frequencies that are not consistent between the stations, we find the average regional geoelectric strike direction, where and when it can be defined, is close to 83 degrees (geographic), or nearly west-east. It must be emphasized, however, that this strike direction is not consistent from one site to the next, and it holds only for a small majority of frequencies. This presents some limitations to the interpretation. This will be described further below.

Inversion of the RAK AMT survey lines

- **3D analysis**

In this report, we describe the systematic 2D inversion of the three long survey profiles, and the three short survey profiles, as seen in Figure 11. These survey profiles were designed for 2D interpretation. There is insufficient station density in between the long survey lines to consider useful 3D inversion and interpretation over the entire survey area.

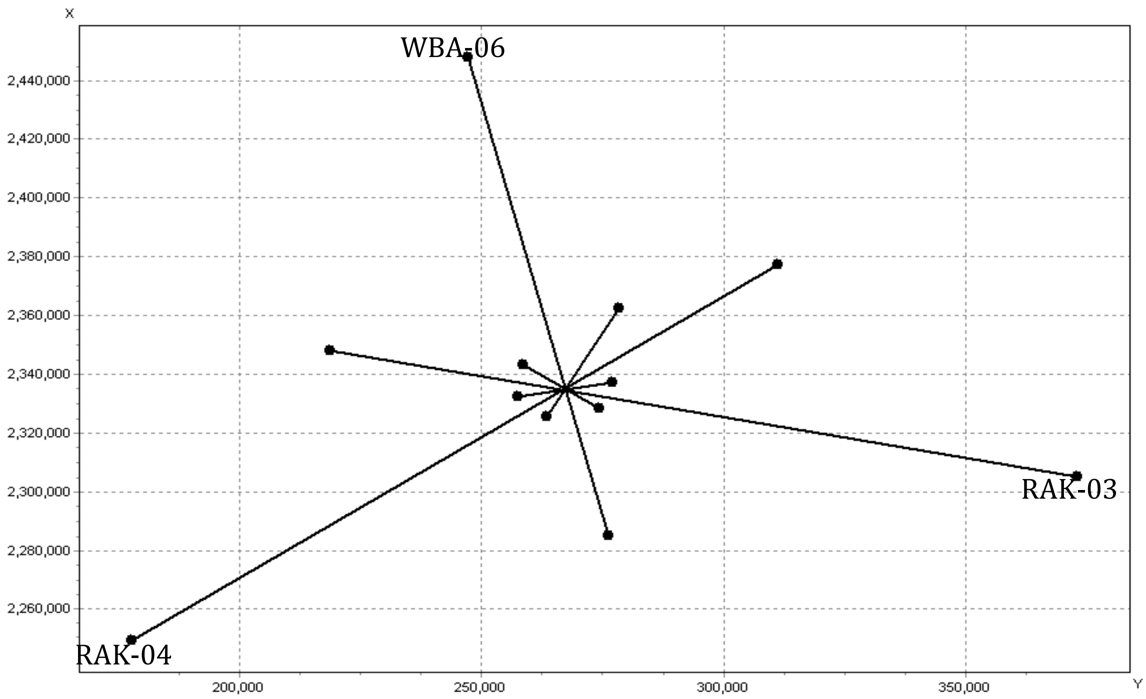

Figure 11. All six RAK survey profiles intersect at a common point. This point is designated as Station 1 in the body of this report as well as in all geoelectric cross sections below. The three wells in the area are marked as locations RAK-03, RAK-04 and WBA-06. These correspond to the end points of the three long survey profiles.

Before proceeding to a detailed discussion of the 2D results, we will briefly discuss 3D interpretation immediately below.

We have explored the possibility of localized 3D inversion and interpretation in the centermost part of the array, where the three long and three short survey profiles intersect at a common point (at Station 1, as in Figure 11). To examine the feasibility of 3D inverse modeling for the RAK data set, we have made use of the recently released ModEM – Modular EM inversion environment (Egbert, G.D. & A. Kelbert, Computational recipes for electromagnetic inverse problems, *Geophysical Journal* International, 2012, doi: 10.1111/j.1365-246X.2011.05347.x), which employs a 3D staggered grid finite difference forward solution, but (in contrast to our 2D inversion analysis) which does not allow for topographic variations of ground level. ModEM provides for a variety of inverse solvers including nonlinear conjugate gradient methods. Our 3D results to date are not yet entirely satisfactory, and are a work-in-progress. The complications stem from the array design, which permits 3D interpretation only within the central region of the RAK survey, the strong levels of heteroegeneity in electrical conductivity structure in that central region, and the large confidence limits for the MT impedance tensors that lead to a poorly conditioned system that is challenging to invert stably in 3D.

For present purposes, however, here we consider a 2D interpretation covering the entire wide area of the RAK survey region, including all six (three long and three short) intersecting survey profiles.

- **Developing a lithologically constrained 1D prior model for 2D inversion**

As indicated in the introduction, it is possible to constrain the 2D inversions by reference to known lithology/geoelectric structure. We have been given access to well log data from the locations indicated in Figure 11 that has made it possible to develop a 1D prior model to use as an optional constraint on the inversion. The well logs, and an inferred lithology derived from the preliminary stratigraphy transmitted from DGIZ's *Call for Technical Proposal: Magnetotelluric Investigations of Aquifers*, as well as supporting information, and from the LUKSAR Hydrogeology Report produced by the Research Institute of King Fahd University of Petroleum and Minerals), confirms that likely targets for investigation are the following formations:

Each putative aquifer was believed to exceed 100 m in thickness, with multiple intervening thin aquitards as thin as 50 m thick. In Table 2 we do not provide separate depths to the tops and bottoms of individual putative aquitards because the spatial resolving power of the MT method is quite limited in its ability to determine the thickness of resistive layers surrounded by conductive layers, particularly when these are fine scale structures at depth.

Formation	Depth to top at RAK-03	Depth to bottom at RAK-03	Depth to top at RAK-04	Depth to bottom at RAK-04	Depth to top at WBA-06	Depth to bottom at WBA-06
Umm er Radhuma limestone	813	1153	468	684	220	560
Aruma limestone/shale	1153	1506	684	954	560	760
Wasia sandstone/shale	1506	2180	954	1503	760	1420
Biyadh sandstone	2306	2436	1548	1773	1475	1500

Table 2. Depths to bounding tops and bottoms of stratigraphic formations at each of three wells; internal bedding and intervening aquitards not distinguished

MT is far more sensitive to conductive layers in general, and specifically to the product of conductivity and layer thickness. Consequently we do not anticipate that our survey data would be able to distinguish individual aquitards, but instead would reveal the bulk volume averaged electrical conductivity (or, equivalently, the electrical resistivity) of water-saturated formations. The MT data would be particularly sensitive to the presence of formations with interconnected films or pockets of saline fluids, or fluids with enhanced levels of total dissolved solids, since the ionic conduction within such aqueous fluids is enhanced.

In our report of March, 2013, we described carrying out 2D inversions from a prior 1D model that was not based on known lithology, but instead was determined by 1D inversion of all of the data from each of the 2D profile lines. Based on this preliminary work, as well as the known lithology, and given the relative insensitivity of the method to the presence of thin aquitards, we developed a lithologically constrained gross averaged 1D model broadly representative of the aquifer-bearing zones. This takes the form of a simple 3 layer 1D prior model, which appears in Table 3 below:

Depth (m)	Electrical Resistivity (Ohm-m)
0-600	100
600-4800	4
4800-10000	100

Table 3. 1D prior model optionally used to constrain 2D inversions

An additional control on electrical resistivity structure is provided by the common survey station shared by all six profiles (as seen in Figures 8 and 9). In the absence of 3D effects or residual static distortion, the electrical profiles beneath Station1, the point common between all survey profiles, should be similar in all of the 2D inverse models.

- **2D Inversion**

In addition to being able to compare the various 2D survey profiles at their shared common Station 1 location as a means of determining the consistency of the results following surface distortion removal and 2D inversion (to be described in more detail later in this report), we provide an additional test of the robustness of the conspicuous model features. For each survey profile we invert the data twice. First, we use a uniform half space of 60 Ohm-m resistivity as the prior model as we carry out 2D inversion. Second, we use the 1D lithologically constrained prior model of Table 3 as a constraint on a 2nd 2D inversion. By comparing the two sets of results, we can determine which features in the two models are consistent (one having started from a half space, and the other from the lithologically constrained model), and which features are inconsistent. Features that are consistent between the two models are deemed to be more robustly constrained than those that are inconsistent.

For the present survey we have selected ZONDMT2D, a very flexible package authored by A. Kaminsky and available commercially. We have worked continuously through this analysis with the author to improve the code, and it is under continuous revision as we continue to utilize it. The ZOND2DMT inversion environment provides several inversion strategies, allows one to rotate the impedance tensors into regional geoelectric strike direction, estimates and removes static (galvanic) distortion terms, permits one to use prior models and to constrain the inversion to be maximally close to the priors, and allows one to select subsets of the full impedance tensor and tipper responses (e.g. inverting full tensor with or without tipper, just apparent resistivity, just phase or just log phase alone).

For the present analysis, we have employed an Occam’s inversion strategy, which applies Tikhonov regularization to find the minimum structure model that fits the full impedance tensor, and that lies closest to the prior model (either the half space or the 1D prior derived from the lithology).

We have set an identical model grid for the inversion of all survey profiles. We have set the top most model layer to 30 m thickness. The thickness of each successively deeper model increments by a factor of 1.09 relative to its adjoining overlying layer. We have used 39 layers in total, discretizing from the Earth’s surface, to a depth of 9.6 km. The finite element forward modeling algorithm used in the inversion accounts for the topography. We have also allowed for two intermediate horizontal nodes, in between each AMT station location.

We have used this strategy in attempts to simultaneously fit both TE and TM modes for the three long MT profiles seen in Figure 11. We have found that it is not possible to simultaneously fit both modes, even with inversion for galvanic distortion terms. This is not surprising, given the strong 3D effects revealed through **WALDIM** analysis (see Appendix A in our March, 2013 report for details).

We have adopted the following approach. First we simultaneously invert for galvanic distortion terms, and also for the best TM mode decomposition of the impedance tensors to obtain 2D resistivity profiles. We then use the resulting 2D profile as a prior model, and invert jointly for TM and TE modes, to refine the model. Nearly all of the model variance is explained by the TM mode, with relatively little contribution from the TE mode. In this way we stabilize the inversion since the strong 3D effects made stable 2D joint inversion of TM and TE models otherwise impossible. The result is a model that fits the TM mode apparent resistivity and phase closely, but that has been (deliberately) more weakly constrained by the TE mode. Berdichevsky (1997) points out that the TM mode is more robust to 3D effects caused by resistive structures, but more susceptible to static distortion effects than TE mode. By removing the static distortion effects, TM mode is the best guide to reconstruct the resistivity sections for each of the 2D profiles.

- **Geoelectric strike direction**

As indicated previously, the WALDIM analysis revealed there is no consistent geoelectric strike direction, although there is an average 83 degree strike direction that applies to some stations at some limited frequency ranges. In all other respects the data are intrinsically 3D.

We have tested the robustness of our 2D inversion results to rotations of the impedance tensor by inverting the data in the original survey coordinates (i.e. aligned with geographic north-south and east-west), and also in a rotated coordinate system where we infer the approximate geoelectric strike direction to be 83 degrees east. As seen later in this report, there was no significant impact of using the rotated coordinate system. Consequently, we present results obtained from inversion in survey coordinates unless otherwise indicated.

1) Northwest-Southeast Long Profile from Stations 75 to 16

The orientation of the first 2D profile, for the Northwest-Southeast long survey profile of Figure 10 (red line in that figure) is seen in Figure 12 below.

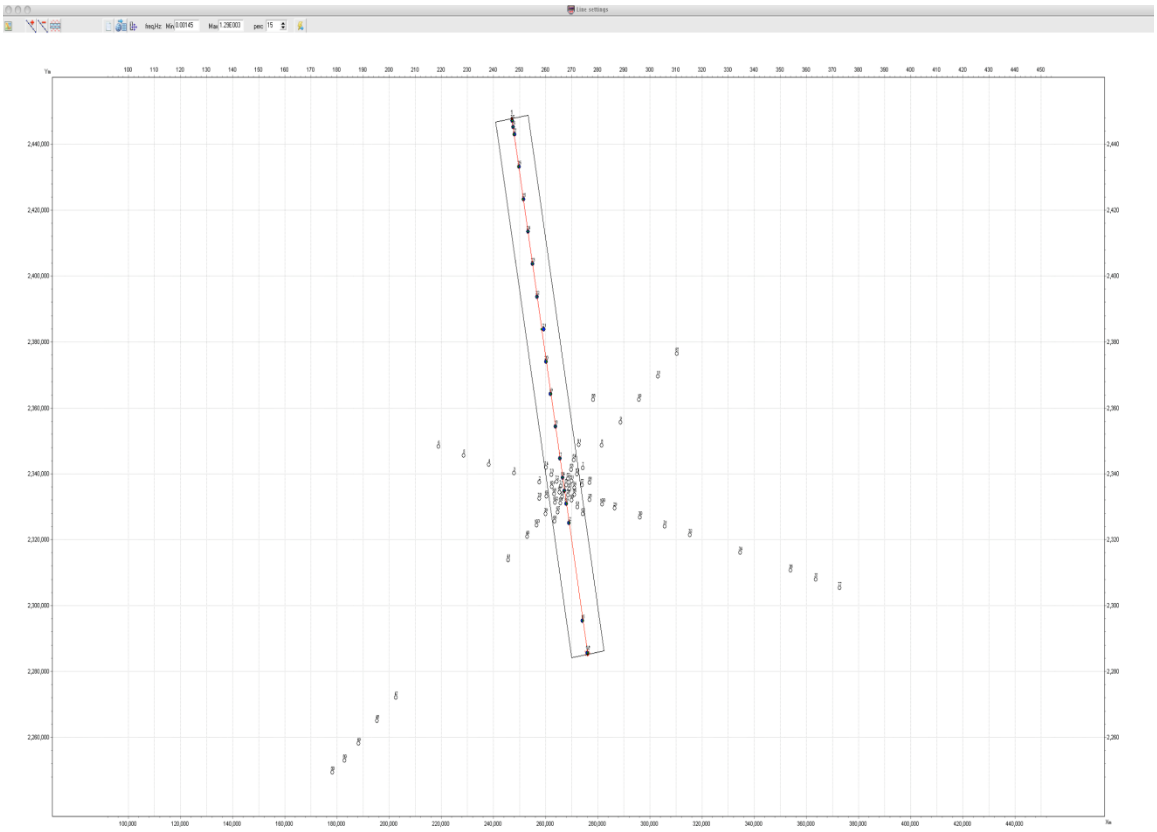

Figure 12. The orientation of long profile from stations 75 to 16. Station 1 is the central point shared by all profiles.

We present the resulting model from inversion of this profile in the figures below

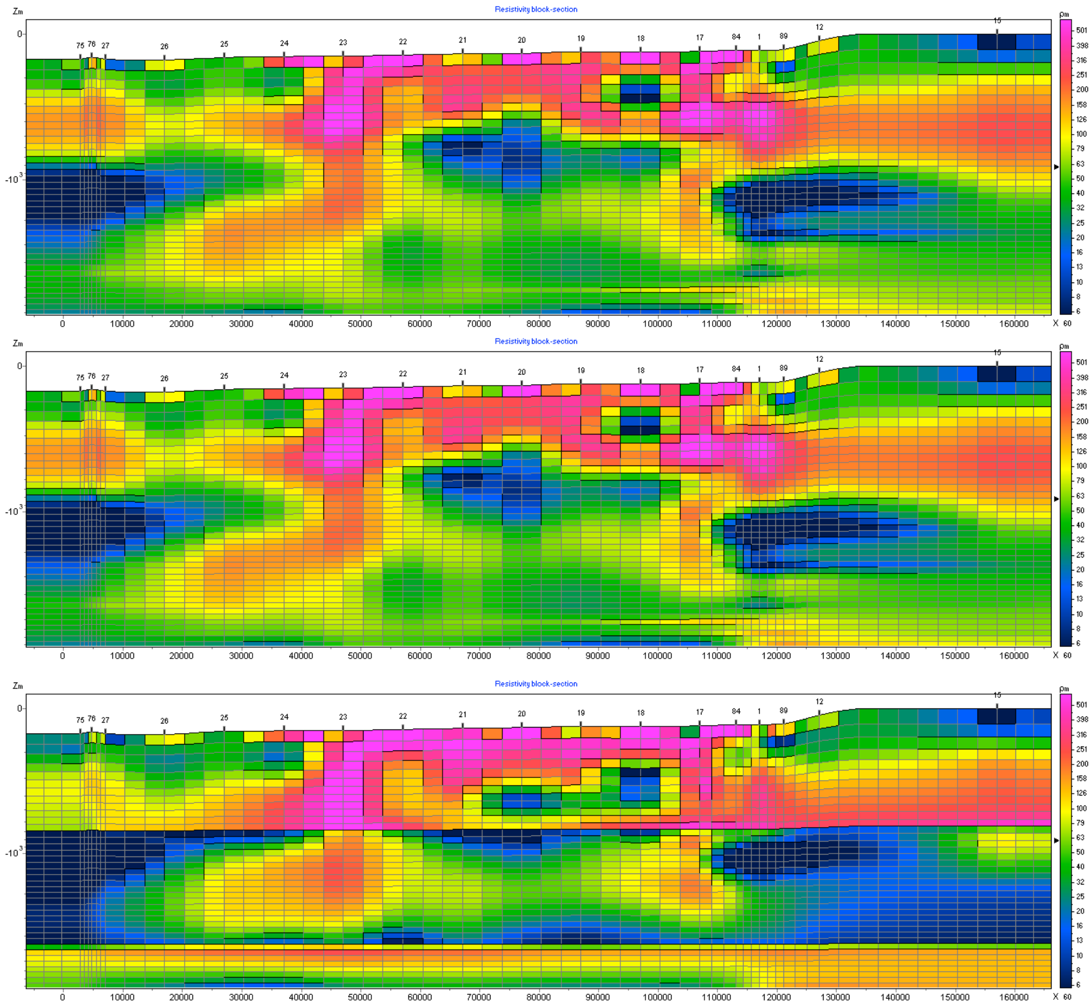

Figure 13. (top) 2D MT profile from station 75 in the north (left hand side) to station 16 in the south (right hand side). A uniform half space of 60 Ohm-m was used as the prior model. The impedance tensor was rotated to 83 degrees from N prior to inversion. Note – the depth scale is logarithmic (Log_{10}), so the depths shown range from 1 m to just over 9000 m. (center) Same as above, but MT impedance tensor was not rotated, but instead left in geographic coordinate reference frame. The two models are indistinguishable. (bottom) Same as center model, but 1D prior model was used.

The models in Figure 13 demonstrate the insensitivity of the results to rotations of the impedance tensor, and the strong similarities between resulting conductive model features regardless of the starting model used. Station 75 at the extreme left hand side of each model (please note the station numbers are located immediately above the resistivity sections at the locations of each station along the profile) is adjacent to well WBA-06 as seen in Figure 11. At this location, the top of the Aruma limestone formation is at 560 m depth, which closely corresponds to the 1d prior model's top to conductive layer of 600 m. Please note that the resistivity sections are displayed on a Log_{10} depth scale, so the sections extend from 1 m to just over 9000 m depth. This was done to expand the visibility of the shallower parts of each section.

At this location, roughly coincident with WBA-06, the 2D inverse model arising from the 1D prior (Figure 13 bottom) shows little change from the prior model itself. That is, the full thickness and original resistivity of the prior model beneath Station 75, 76 and 27 (roughly coincident with and adjacent to WBA-06) has not changed in the inversion. In the absence of other information, one might infer that the MT survey data had no sensitivity to these model depths, so there would be little confidence in the presence of the conductive layer indicated in the model. That this supposition is incorrect can be seen in Figure 13 (center) where the 2D model using a featureless uniform 60 Ohm-m half space as the prior has also placed a strong conductive layer directly beneath this location. There was no information in the prior that constrained the inversion to produce a conductive region at these depths. This was required by the MT survey data itself.

The top to this layer also begins at depths of 600-700 km (as per the model constrained by the 1D prior), but it is somewhat thinner, extending to 3000 m rather than 4800 m, as in the 1D prior. The data constrain the depth to the bottom of this conductive zone only poorly, but they do a good job of constraining the depth to the top of this layer. There was limited long-period data at these stations (this will be seen in the figures following), and the presence of such a highly conducting layer of <10 Ohm-m resistivity rapidly attenuates the MT signal as it diffuses through it.

We can say with some confidence that this survey profile has identified a conductive zone that starts at 600-700 m depth (coincident with the Aruma formation), and that it is high conductance (likely thick), but that its thickness can not be quantitatively constrained by these data.

Similarly, closer to the center of this profile, beneath stations 18 – 21, one or two shallower conductive features are shared between the two models. These appear at depths of ~300-500 m beneath station 21 in the north, shallowing to ~ 250-500 m beneath station 18 closer to the array center. At these intermediate locations, these conductive areas might be associated with the Umm er Radhuma formation, or potentially with even younger overburden layers above.

A more proncounced conductive feature is found beneath the array center (station 1) and extending a short distance to the south beneath stations 89 and 12. This conductor appears at the same range of depths as the one beneath WBA-06 at the extreme north of this profile, i.e. starting at depths coincident with the Aruma formation.

The next series of figures illustrate the fit of these models to the data. Results for both half space and 1D prior model constrained inversions are shown.

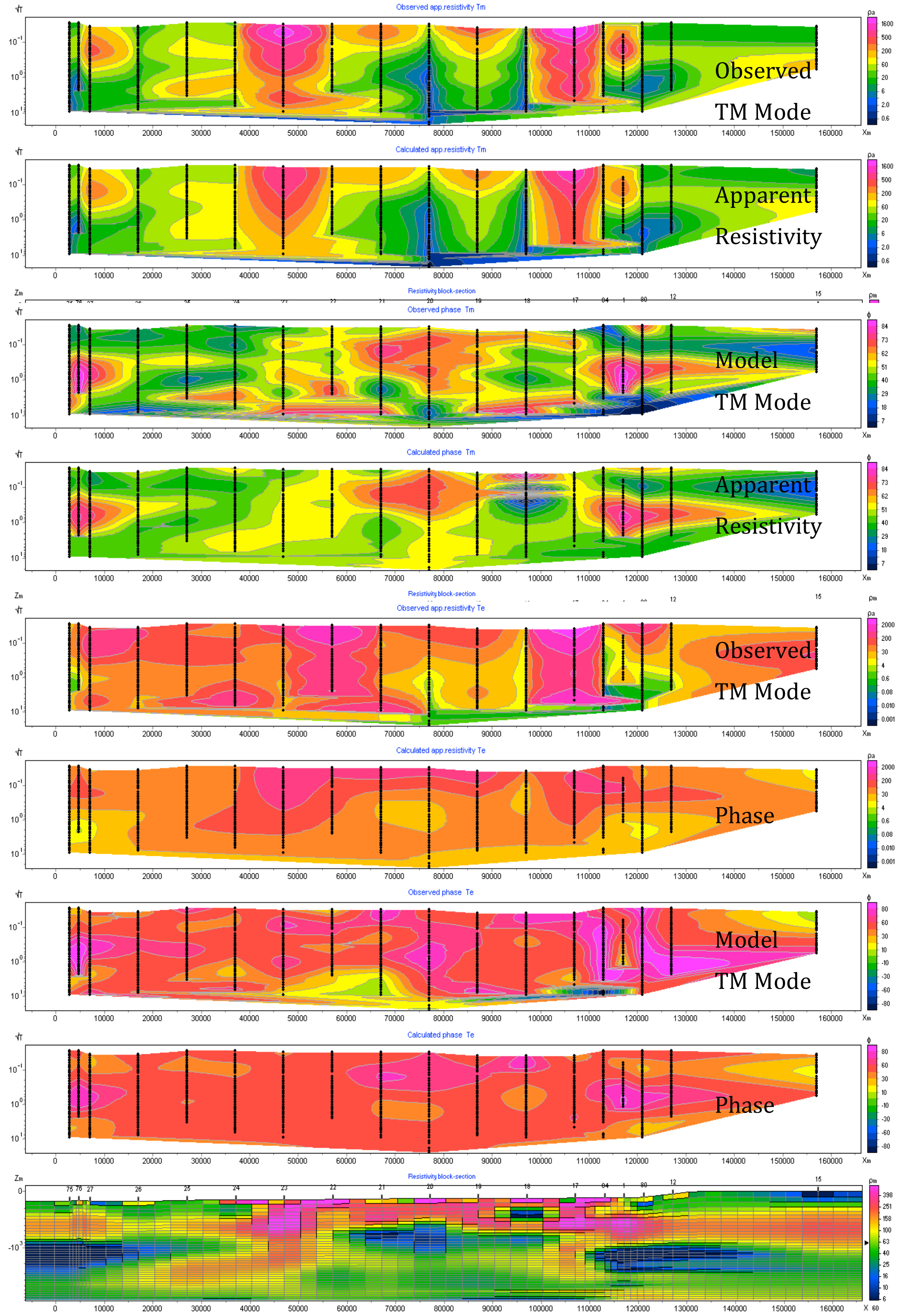

Figure 14. (bottom) 2D Inverse model constrained by half space prior model, and observed and model apparent resistivity and phase for TM and TM modes, as indicated, for profile from station 75 – 15 as seen previously in Figure 13.

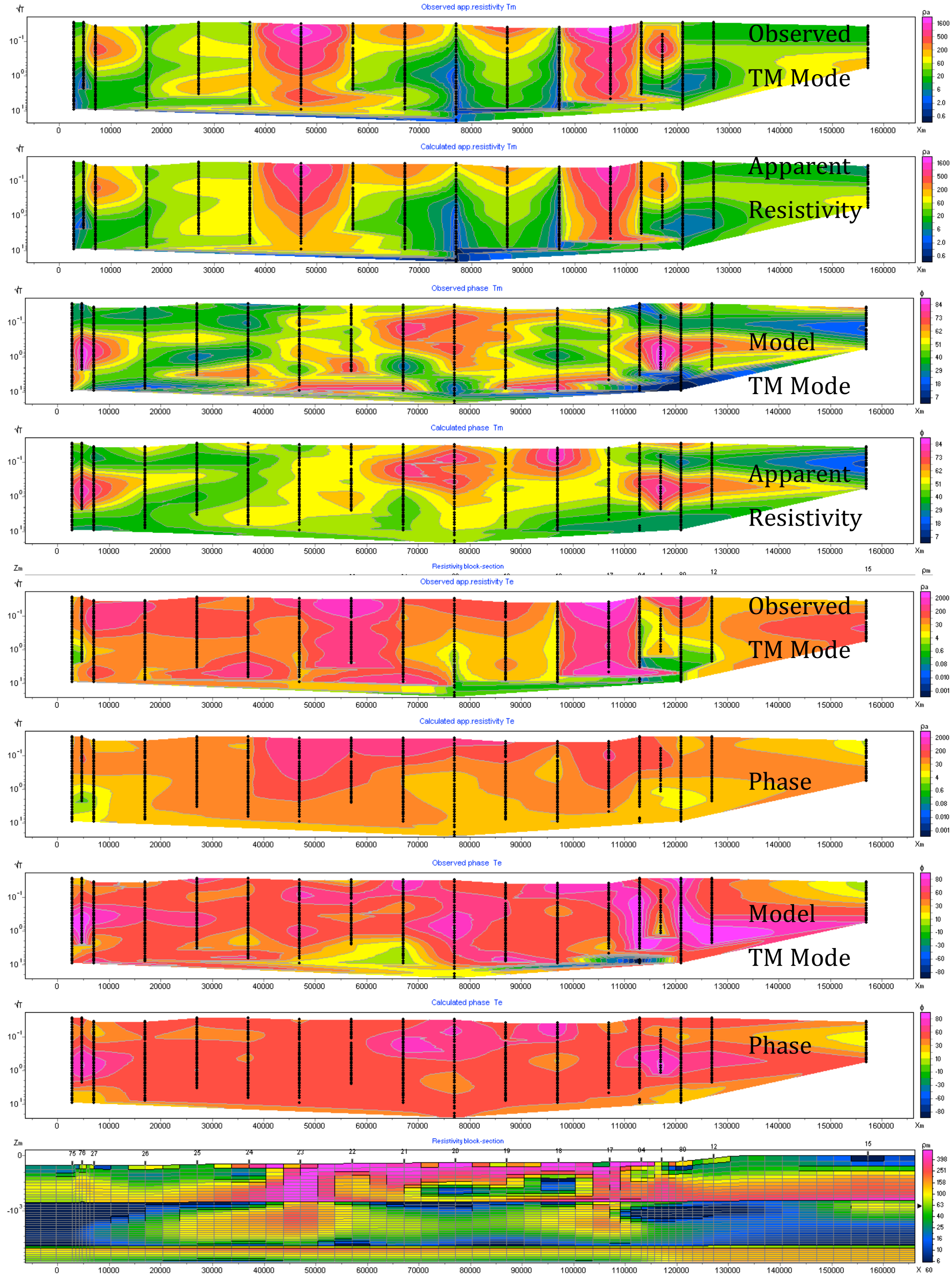

Figure 15. (bottom) 2D Inverse model constrained by lithologically constrained 1d prior model, and observed and model apparent resistivity and phase for TM and TM modes, as indicated, for profile from station 75 – 15 as seen previously in Figure 13.

Figures 14 and 15 reveal the fit of the 2D models constrained by a half space prior model, and by the 1D prior model, respectively. As indicated previously, our strategy was to fit the TM mode apparent resistivity and phase preferentially (which in all cases we have done to approximately 20% RMS misfit) to the TM mode, and to fit TE mode secondarily (which typically exhibits twice the misfit as TM mode).

The AMT station locations, labeled by station number, are shown as numbered marks at the top of the bottom most panel of Figures 14 and 15. The black symbols superimposed on the observed and calculated apparent resistivities and phases represent the frequencies (frequency scale on the left-hand axes) at which observed apparent resistivities and phases were determined during the RAK AMT survey. AMT stations associated with lower frequencies will generally provide resolving power to greater depths than those stations where only higher frequency data are available.

Summary of findings from Northwest-Southeast Long Profile from Stations 75 to 16

1. The fit to both apparent resistivity and phase for TM modes is excellent, with TE mode misfits approximately twice as large as for TM mode. This is to be expected given our inversion stabilization strategy of fitting TM mode first, and then using the resulting model as a prior model for the joint TM + TE mode inversion. The adoption of this approach was necessary to achieve stable 2D inversion results for a data set with significant 3D characteristics.

2. We have identified a strongly conductive zone beneath stations close to WBA-06 in the northern part of this profile, and also beneath stations near the center of the profile. The depth to the top of this feature appears to be well constrained, making it coincident with the top of the Aruma formation. The thickness of this conductive zone is not well constrained by this data set, although it is highly conductive and likely thick. A shallower conductive feature is found somewhat to the north of the center of the profile that might be coincident with the Umm er Radhuma formation, of with shallower overburden.
3. In this environment, highly conductive regions are likely associated with ionic conductors, either in the form of mobilized salts, or permeable rock formations saturated with saline or high total dissolved solids aqueous fluids. It is a reasonable supposition that the identified conductive regions may represent aquifers.
4. Thin aquitards interspersed within aquifer zones would be unresolvable with this data set.

2) Southwest-Northeast Long Profile 2D TM Mode Inversion from Stations 50 to 87

This profile extends from RAK-04 in the southwest crossing the center point (Station 1) and extending into the northeast (see Figure 16).

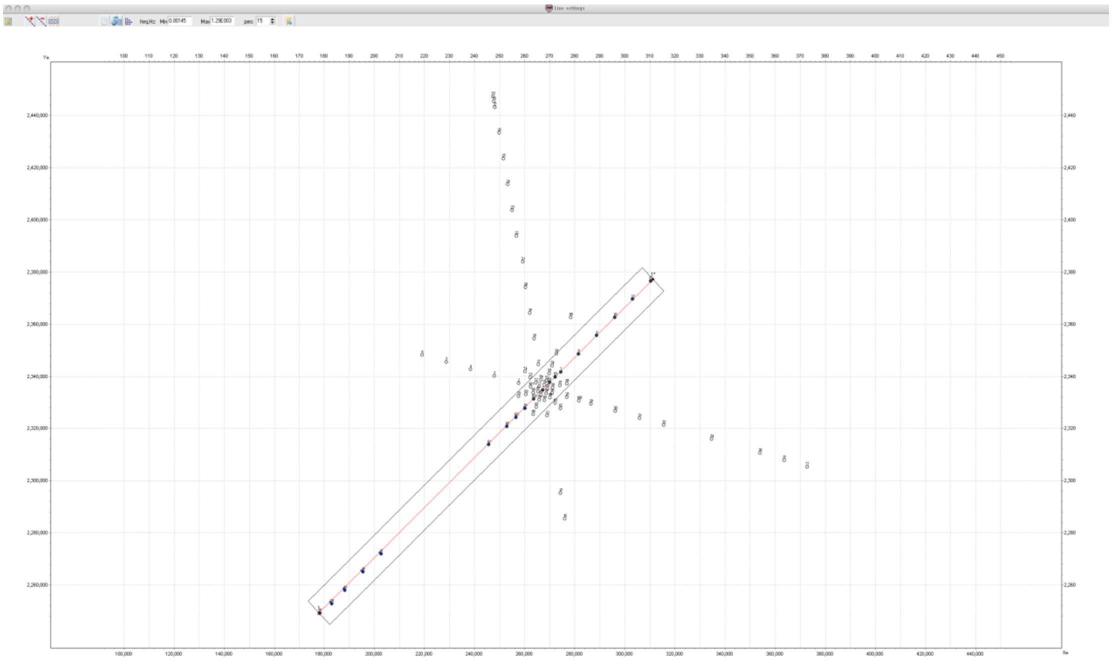

Figure 16. The orientation of long profile from stations 50 to 87. Station 1 is the central point shared by all profiles.

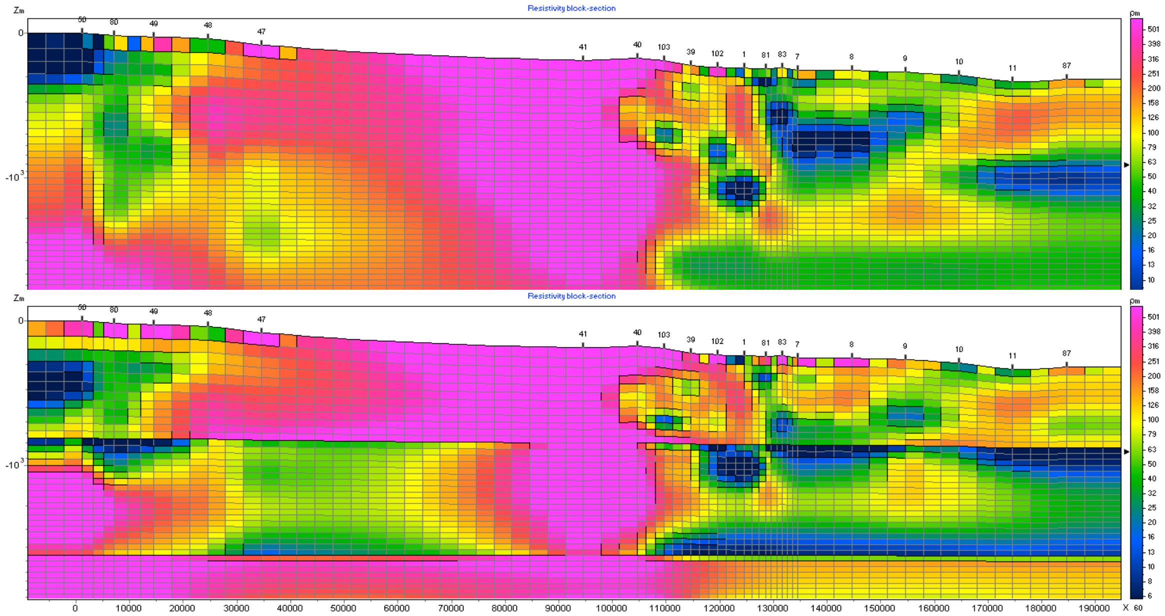

Figure 17. (top) 2D MT profile from station 50 in the southwest (left hand side) to station 87 in the northeast (right hand side). A uniform half space of 60 Ohm-m was used as the prior model. Note – the depth scale is logarithmic (Log_{10}), so the depths shown range from 1 m to just over 9000 m. (bottom) Same as above, but 1D prior model was used.

The 2D models with half space and 1D prior model constrains are shown in Figure 17 above. As with the previously discussed profile, several conductive zones appear to be robust features. The location of station 50 (RAK-04) appears to be associated with a shallow conductive feature whose depth is somewhat sensitive to selection of prior model. It is expressed as a surface feature in the half space prior, or starting at 80-100 m in the 1d prior result. It is probably impossible to resolve the difference between these two scenarios, given residual uncertainties in distortion removal and residual 3D effects in general. In both cases the conductor does appear to deepen and persist, albeit at somewhat higher resistivities, to the northeast, extending to depths as great as 3 km by distances of 40 km to the northeast of RAK-04.

As in the previous profile, a prominent but geographically limited in extent (from the azimuth of the current profile) conductor is found beneath the center of the array near station 1. A conductor starting at ~500 m and extending to ~800 m is found immediately northeast of the array center, extending for ~20 km, and a conductor at depths of 700 m and of at least 400 m thickness appears in the extreme northeast of this profile.

The next series of figures illustrates the fit of the models to the data. As for the previous profile, the model fits to the TM mode apparent resistivity and phase are excellent, and the relative fits of TM and TE mode are equivalent to that seen previously.

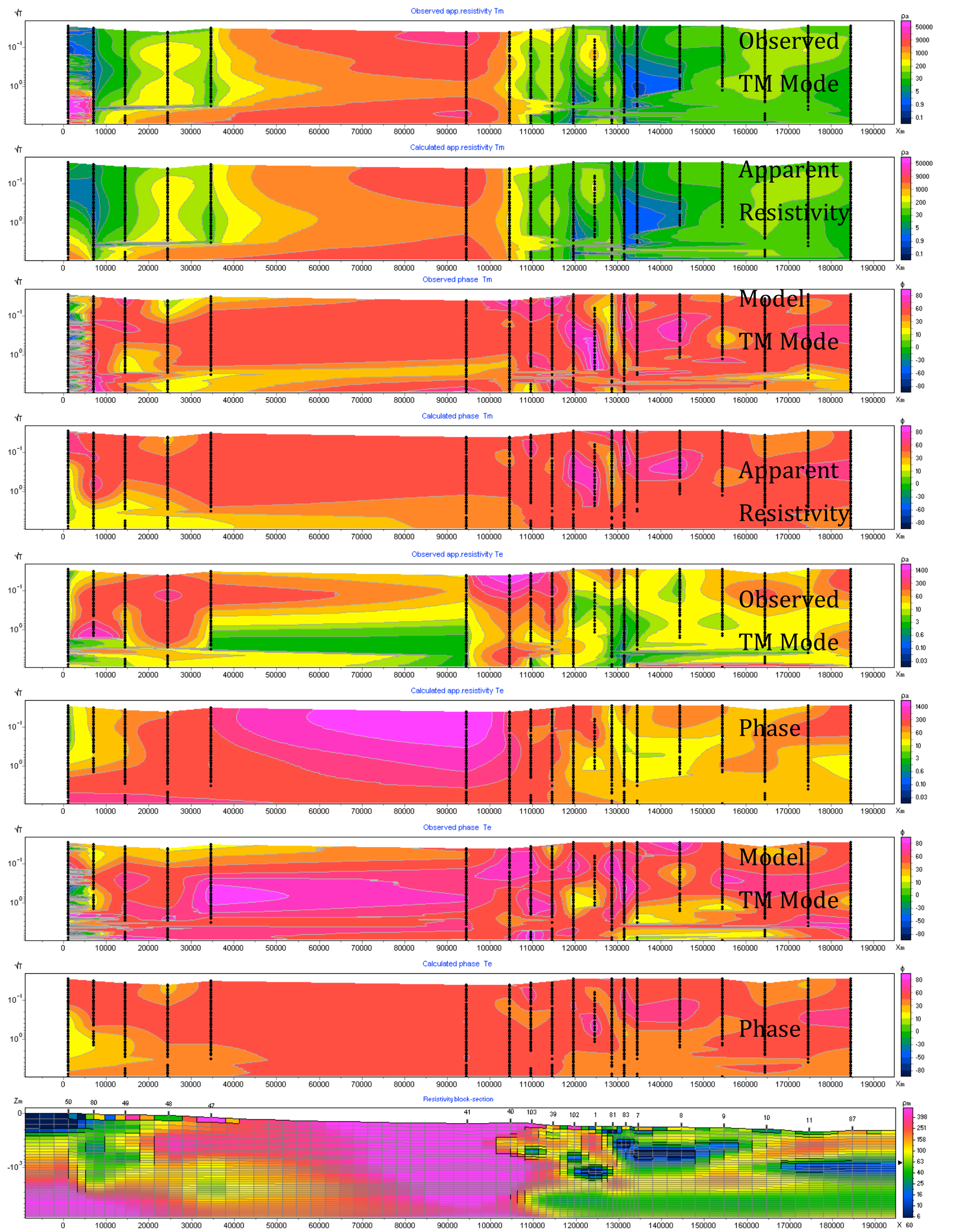

Figure 18.(bottom) 2D Inverse model constrained by uniform half space constrained 1d prior model, and observed and model apparent resistivity and phase for TM and TE modes, as indicated, for profile from station 50 – 87 as seen previously in Figure 8. Note – we have not provided an equivalent plot showing the misfits to the 1d prior model constrained inversion. On the scale

shown here, the misfits are essentially indistinguishable from those shown for the half space prior model results.

Summary of findings from Southwest-Northeast Long Profile 2D TM Mode Inversion from Stations 50 to 87

1. RAK-04 is located immediately over a shallow conductive feature that can reasonably be associated with the aquifers beneath that well. These may be contiguous with layers that deepen to the northeast, but given the more elevated resistivities, those formations may be less permeable or fluid saturated than directly beneath RAK-04.
2. The strongly conductive zone beneath stations close to the center of the profile is common with the conductive zone found in the previous set of profiles. The depth to the top of this feature appears to be well constrained, making it coincident with the top of the Aruma formation. The thickness of this conductive zone does appear better constrained along the azimuth of this profile than previously, with a best estimate of approximately 400 m. A conductive feature is found to the northeast of the center of the profile that might be coincident with the Aruma and possibly the top section of the Wasiya formations.
3. In this environment, highly conductive regions are likely associated with ionic conductors, either in the form of mobilized salts, or permeable rock formations saturated with saline or high total dissolved

solids aqueous fluids. It is a reasonable supposition that the identified conductive regions may represent aquifers.

4. Thin aquitards interspersed within aquifer zones would be unresolvable with this data set.

3) West-Northwest to East-Southeast Long Profile 2D TM Mode Inversion from Stations 6 to 77

This profile extends from the western part of the array east to RAK-03 after passing through the center point (Station 1) of the array (see Figure 19).

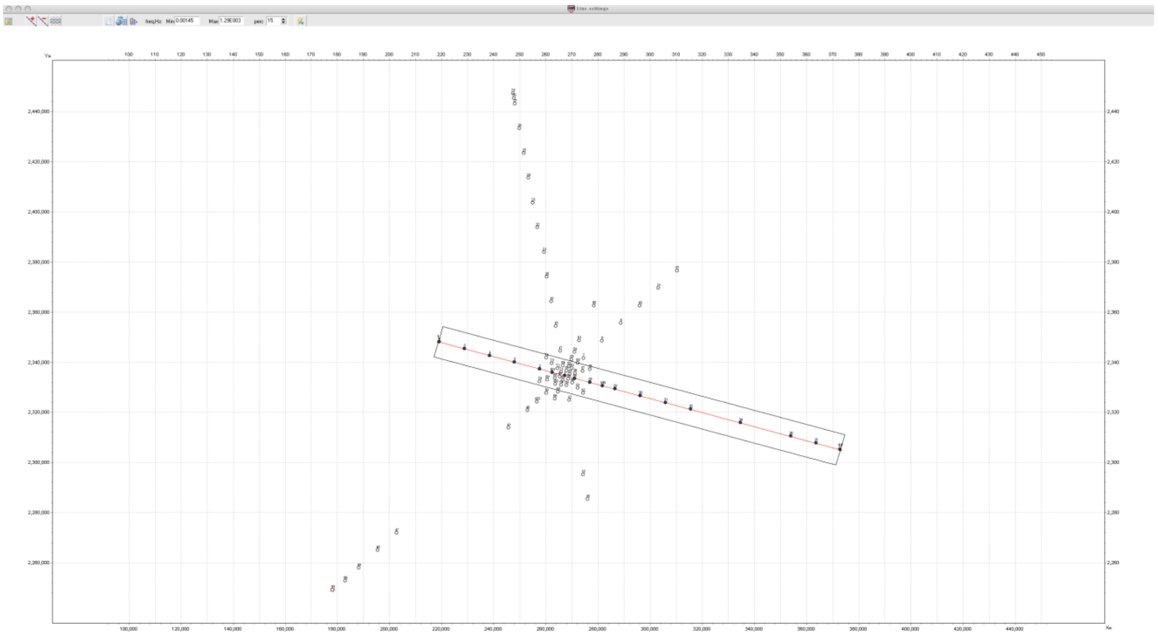

Figure 19. The orientation of long profile from stations 6 to 77. Station 1 is the central point shared by all profiles.

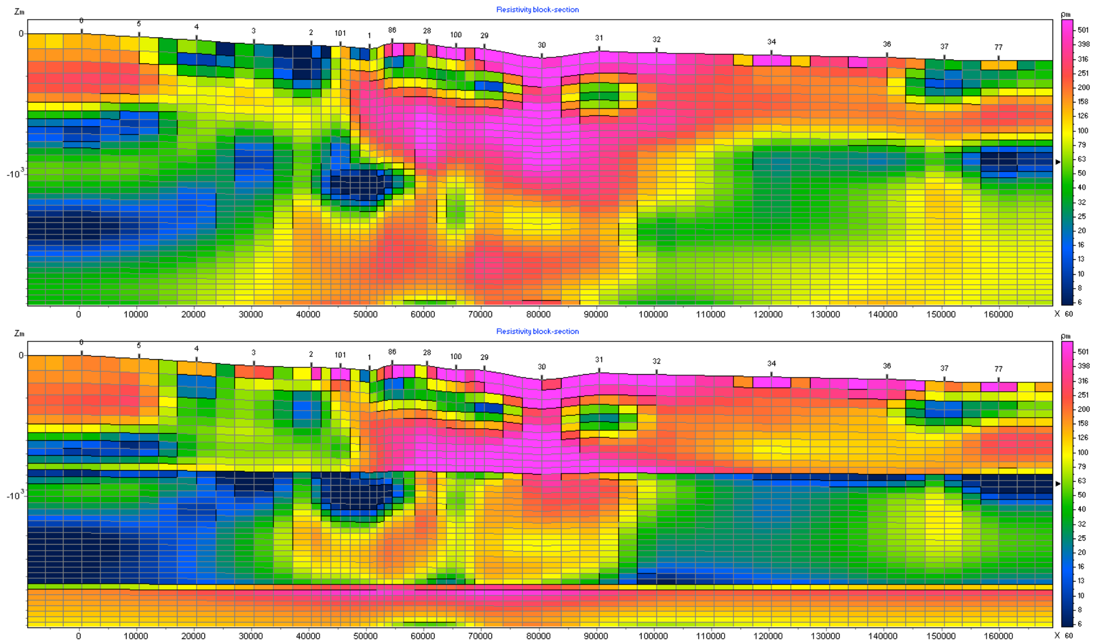

Figure 20.(top) 2D MT profile from station 6 in the west-northwest (left hand side) to station 77 in the east-southeast (right hand side). A uniform half space of 60 Ohm-m was used as the prior model. Note – the depth scale is logarithmic (Log_{10}), so the depths shown range from 1 m to just over 9000 m. (bottom) Same as above, but 1D prior model was used.

The 2D models with half space and 1D prior model constrains are shown in Figure 21 below. As with the previously discussed profiles, several conductive zones appear to be robust features. The location of station 77 (RAK-03) appears to be associated with a conductive feature whose depth is reasonably well constrained to ~400-700 m. In this location, near RAK-03, these depths are associated with the Neogene, Dammam and RUS formations rather than the underlying Umm er Radhuma.

As in the previous profiles, a prominent but geographically limited in extent (from the azimuth of the current profile) conductor is found beneath the center of the array near station 1, and is interpreted as the same feature.

Two distinct bedded conductors beneath stations 5 and 6 in the west-northwest of the survey array are found at depths of ~400-600 m and ~1800-4500 m. It is necessary to extrapolate from the known stratigraphy at RAK-04 and WBA-06 given the regional dip orientation, but these depths could reasonably be associated with Umm Er Radhuma and Biyadh formations. A number of surficial, localized conductive zones are also noted.

Figure 21 illustrates the fit of the models to the data. As for the previous profile, the model fits to the TM mode apparent resistivity are excellent, there is a good fit to the observed TM mode phase, and the relative fits of TM and TE mode are equivalent to that seen previously.

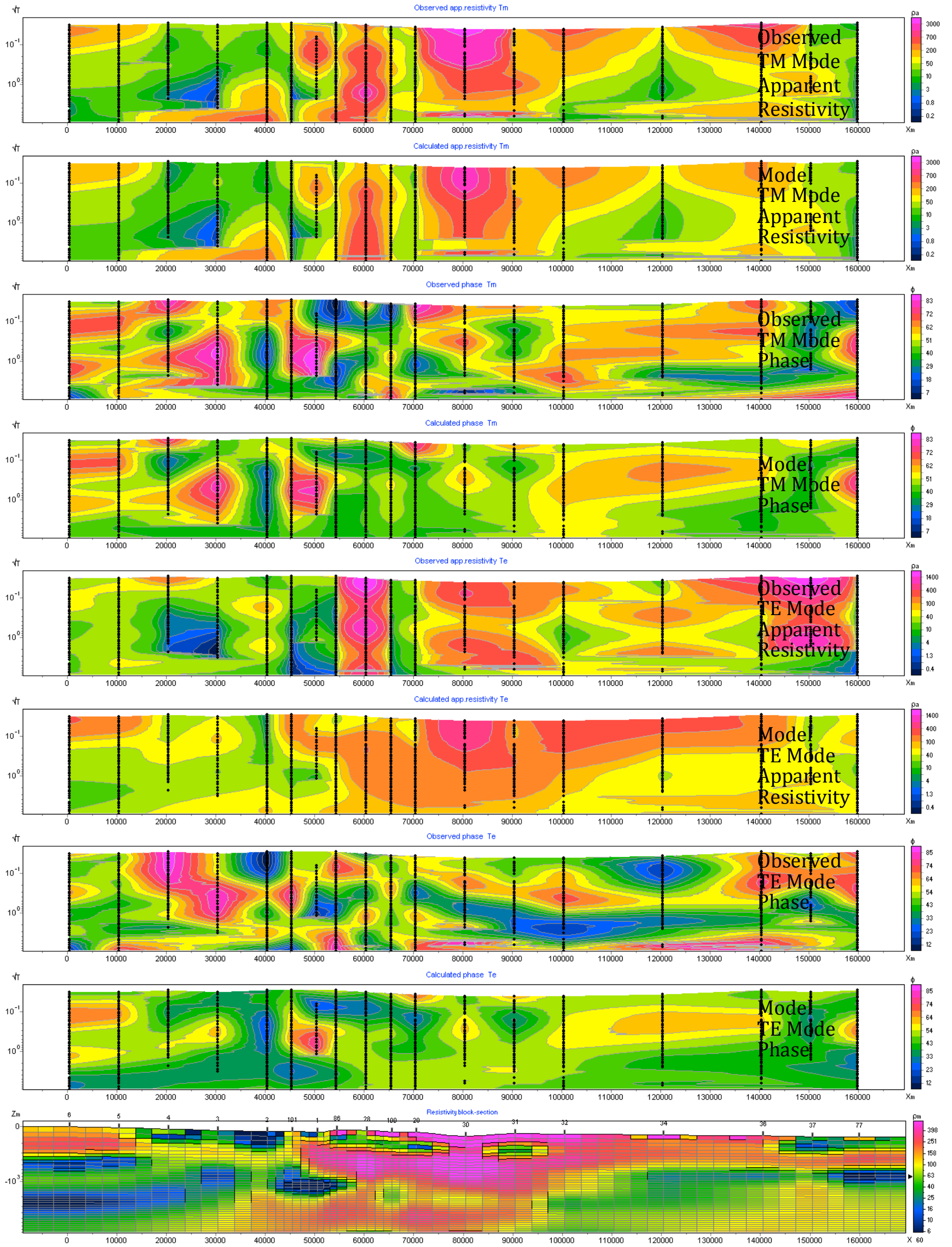

Figure 21.(bottom) 2D Inverse model constrained by uniform half space constrained 1d prior model, and observed and model apparent resistivity and phase for TM and TE modes, as indicated, for profile from station 6 – 77 as seen previously in Figure 19. Note – we have not provided an equivalent plot showing the misfits to the 1d prior model constrained inversion. On the scale

shown here, the misfits are essentially indistinguishable from those shown for the half space prior model results.

Summary of findings from West-Northwest to East-Southeast Long Profile 2D TM Mode Inversion from Stations 6 to 77

1. The location of station 77 (RAK-03) overlies a conductive feature from ~400-700 m depth, which is associated with the Neogene, Dammam and RUS formations rather than the underlying Umm er Radhuma.
2. As in the previous profiles, a prominent but geographically limited in extent (from the azimuth of the current profile) conductor is found beneath the center of the array near station 1, and is interpreted as the same feature.
3. Two distinct bedded conductors beneath stations 5 and 6 in the west-northwest of the survey array are found at depths of ~400-600 m and ~1800-4500 m. It is necessary to extrapolate from the known stratigraphy at RAK-04 and WBA-06 given the regional dip orientation, but these depths could reasonably be associated with Umm Er Radhuma and Biyadh formations. A number of other surficial, localized conductive zones are also noted.
4. In this environment, highly conductive regions are likely associated with ionic conductors, either in the form of mobilized salts, or permeable rock formations saturated with saline or high total dissolved

solids aqueous fluids. It is a reasonable supposition that the identified conductive regions may represent aquifers.

5. Thin aquitards interspersed within aquifer zones would be unresolvable with this data set.

4) The three short profiles near the center of the array – between stations 74 – 62, 70 – 58, 66 – 88

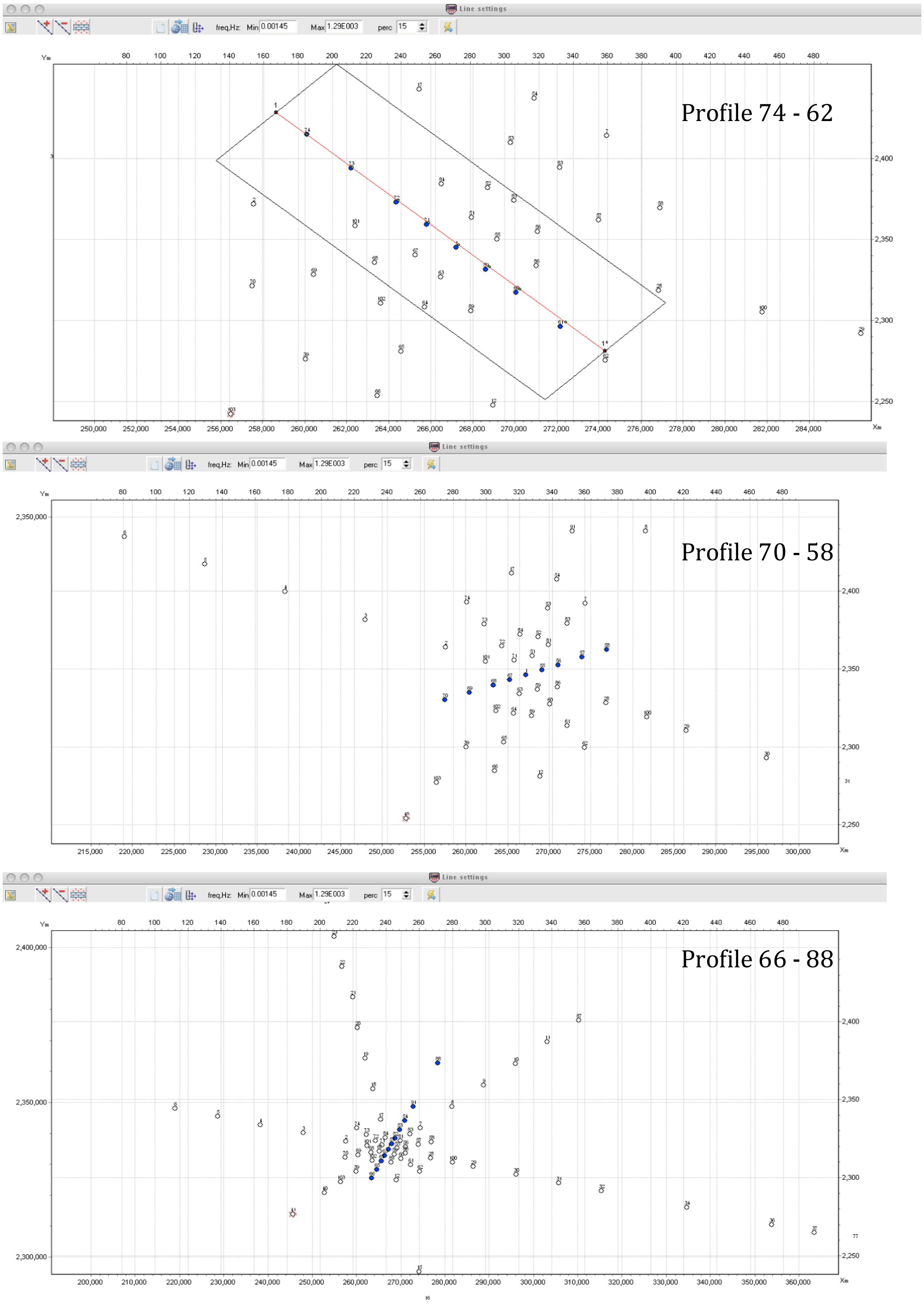

Figure 22. The orientations of the three short profiles. Station 1 is the central point shared by all profiles.

In contrast to the long profiles described above, three short profiles were installed with 2-3 km station spacing. These stations provide higher resolution in the center of the array, which is located adjacent to the most prominent topographic offset in the survey area. It is evident that the array center has some of the most pronounced 3D resistivity characteristics of any area within the survey footprint. Figures 23, 24 and 25 display the 2D resistivity model for each of these three profiles, for models constrained by half space and 1D priors respectively. The TM mode apparent resistivity and phase fits are also displayed.

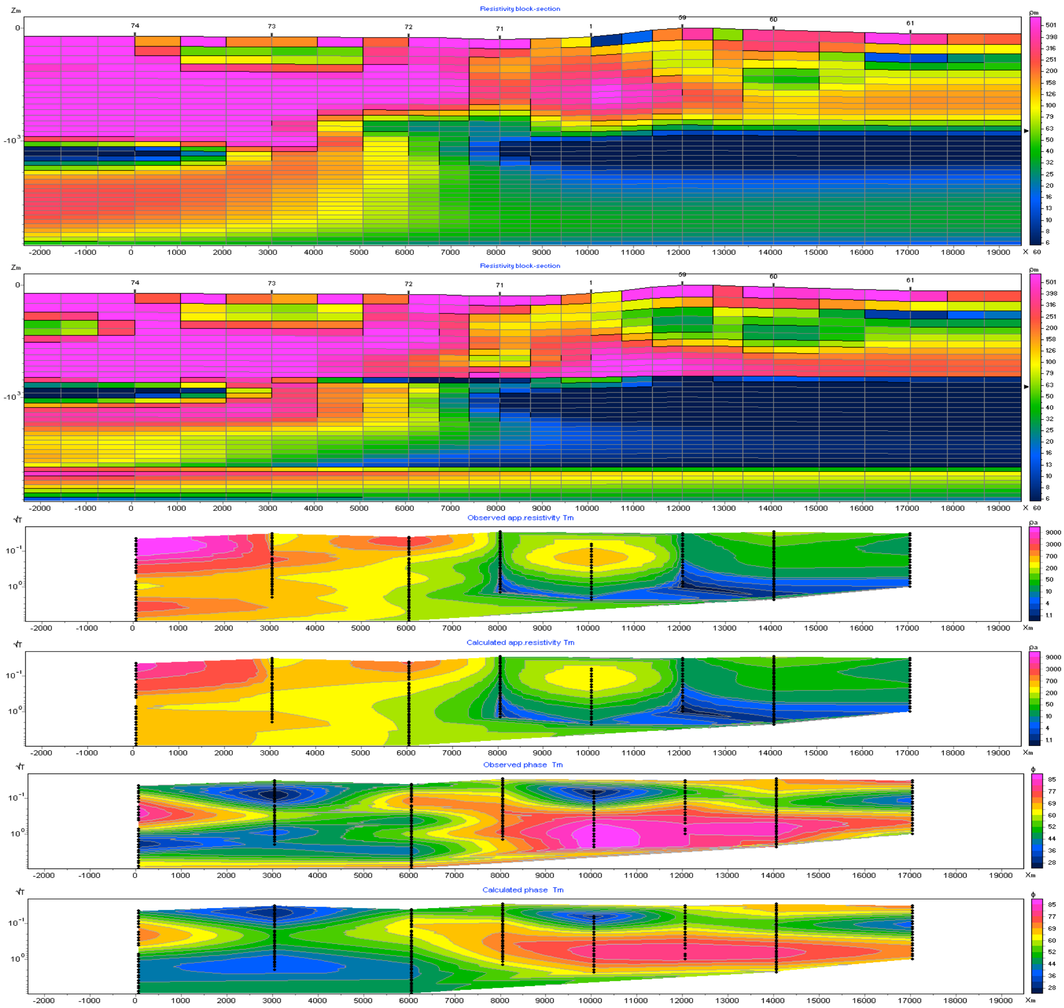

Figure 23.(top) 2D MT profile from station 74 in the northwest (left hand side) to station 62 in the southeast (right hand side). A uniform half space of 60 Ohm-m was used as the prior model. (bottom) Same as above, but 1D prior model was used. Observed and calculated apparent resistivities and phases are shown for TM mode.

Summary of findings from Short Profile from Stations 74 to 62

1. The fit to both apparent resistivity and phase for TM modes is excellent, with TE mode misfits approximately twice as large as for TM mode.
2. We have identified a strongly conductive zone beneath station 74, 8 km NW of the center of the array (station 1), which appears to be a discontinuous spur of the same conductor beneath station 1, which here extends to the southeast, at least 10 km to station 61, at which point the array ends. The depth to the top of this feature appears to be well constrained, making it coincident with the top of the Aruma formation. The thickness of this conductive zone is not well constrained by this data set, although it is highly conductive and likely thick.
3. In this environment, highly conductive regions are likely associated with ionic conductors, either in the form of mobilized salts, or permeable rock formations saturated with saline or high total dissolved solids aqueous fluids. It is a reasonable supposition that the identified conductive regions may represent aquifers.
4. Thin aquitards interspersed within aquifer zones would be unresolvable with this data set.

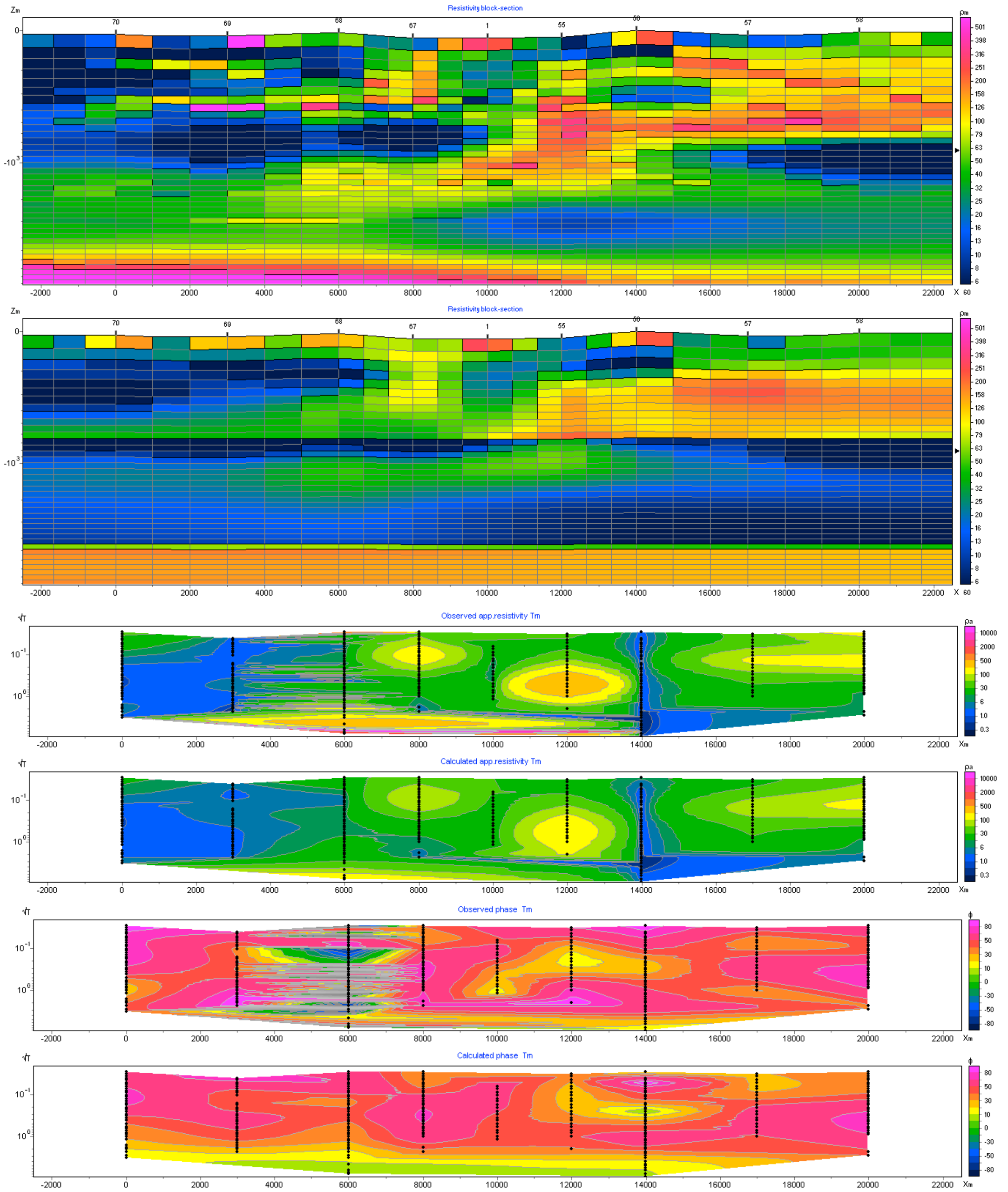

Figure 24. (top) 2D MT profile from station 70 in the west-southwest (left hand side) to station 58 in the east-northeast (right hand side). A uniform half space of 60 Ohm-m was used as the prior model. (bottom) Same as above, but 1D prior model was used. Observed and calculated apparent resistivities and phases are shown for TM mode.

Summary of findings from Short Profile from Stations 70 to 58

1. The fit to both apparent resistivity and phase for TM modes is adequate-to-good, with TE mode misfits approximately twice as large as for TM mode.
2. There are strong 3D effects in this profile, and the relative shortness of the profile in relation to its depth of penetration has made it difficult to achieve a stable 2D high, particularly given high noise levels that are evident in the apparent resistivities and phases in Figure 24.
3. No conclusions of a geological nature are drawn; 2D interpretation is inadequate in this case, and future efforts to obtain a 3D image near the array center are warranted.

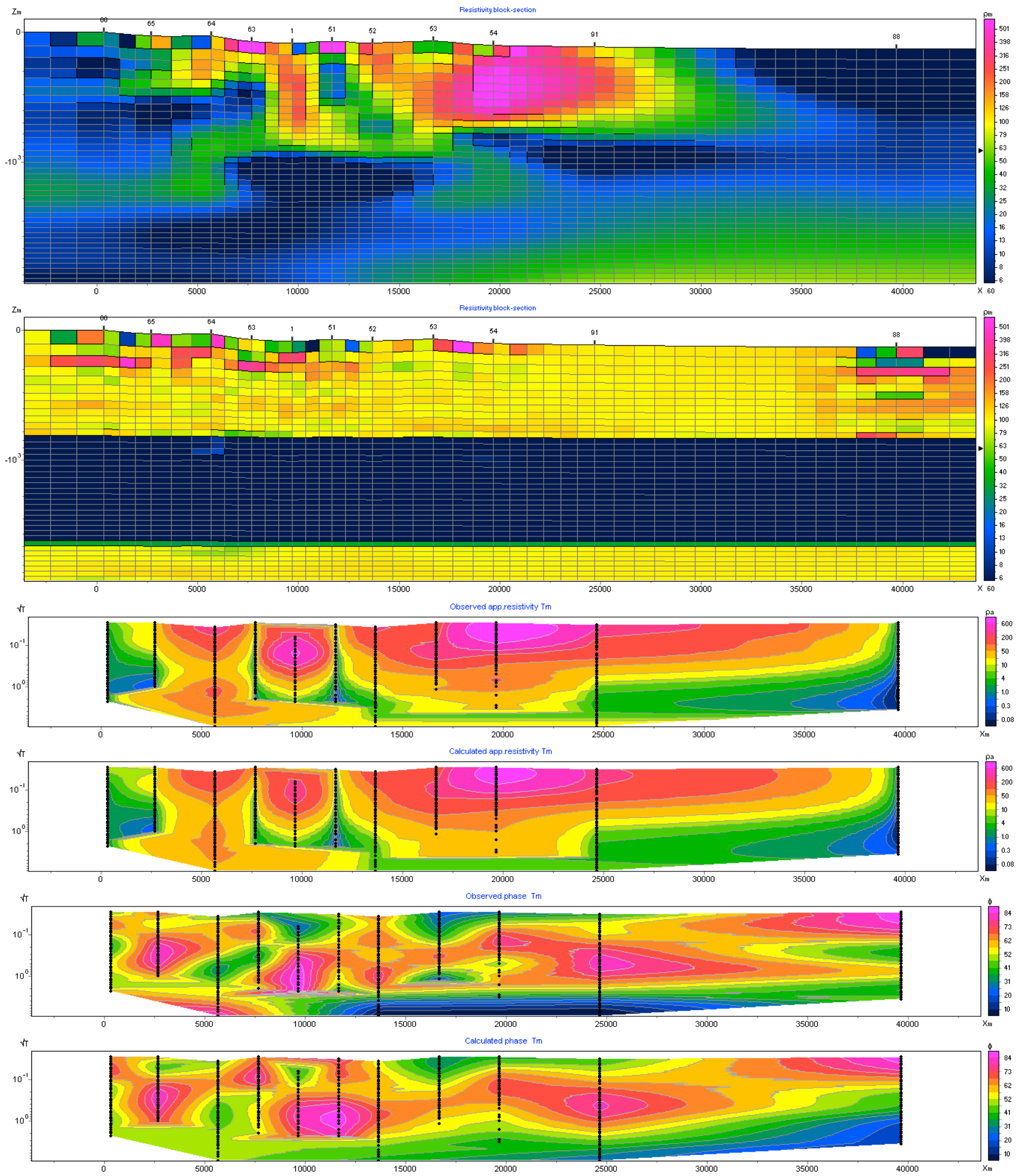

Figure 25.(top) 2D MT profile from station 66 in the southwest (left hand side) to station 88 in the northeast (right hand side). A uniform half space of 60 Ohm-m was used as the prior model. (bottom) Same as above, but 1D prior model was used. Observed and calculated apparent resistivities and phases are shown for TM mode.

Summary of findings from Short Profile from Stations 66 to 88

1. The fit to both apparent resistivity is excellent for TM mode, and the fit to phase is very good except at the lowest frequencies. The misfit to TE mode is approximately twice as large as for TM mode.
2. There are strong 3D effects in this profile, and the relative shortness of the profile in relation to its depth of penetration has made it difficult to achieve a stable 2D high, particularly given high noise levels that are evident in the apparent resistivities and phases in Figure 25.
3. It was not possible to obtain a stable, converged 2D model from the 1D prior in this case, consequently there is a great discrepancy between the two models. No conclusions of a geological nature are drawn; 2D interpretation is inadequate in this case, and future efforts to obtain a 3D image near the array center are warranted.

Pseudo-3D Section Views and Consistency of Results Between the Different 2D Profiles

One hallmark of the effectiveness of the removal of static distortion terms, and the use of appropriate regularization levels would be the alignment of electrical resistivity structures between intersecting 2D profiles. We assemble a set of intersecting profiles to test the alignment of key features, and we provide a series of interpolated layer resistivity maps vs. depth to show the geographic extent of highly conductive features that have been shown in the profiles presented previously.

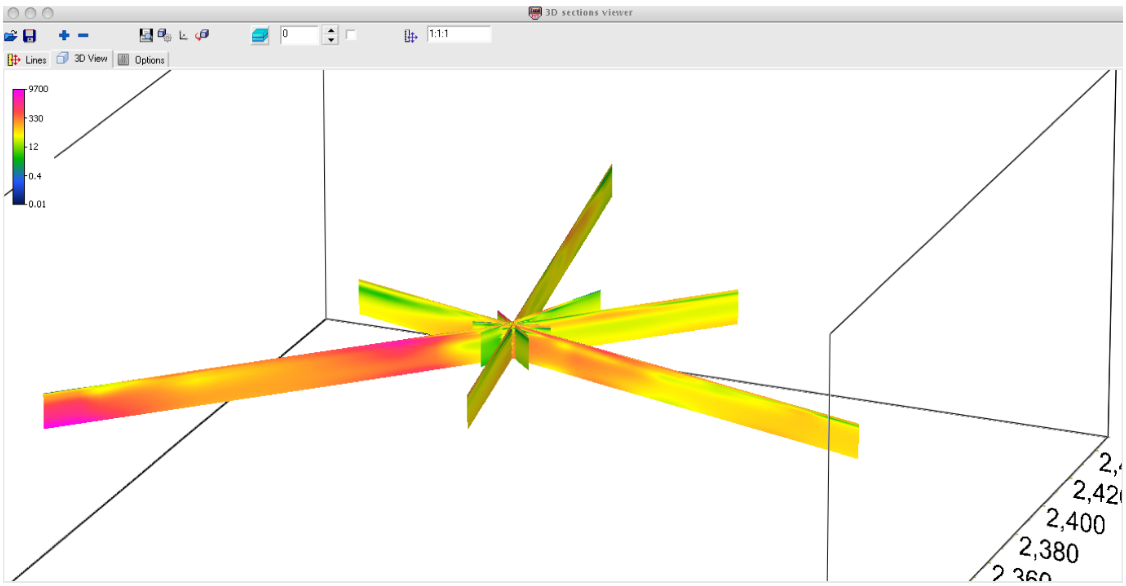

Figure 26. All six 2D profiles displayed in a 3D perspective. The vertical to horizontal aspect ratio is 1:1.

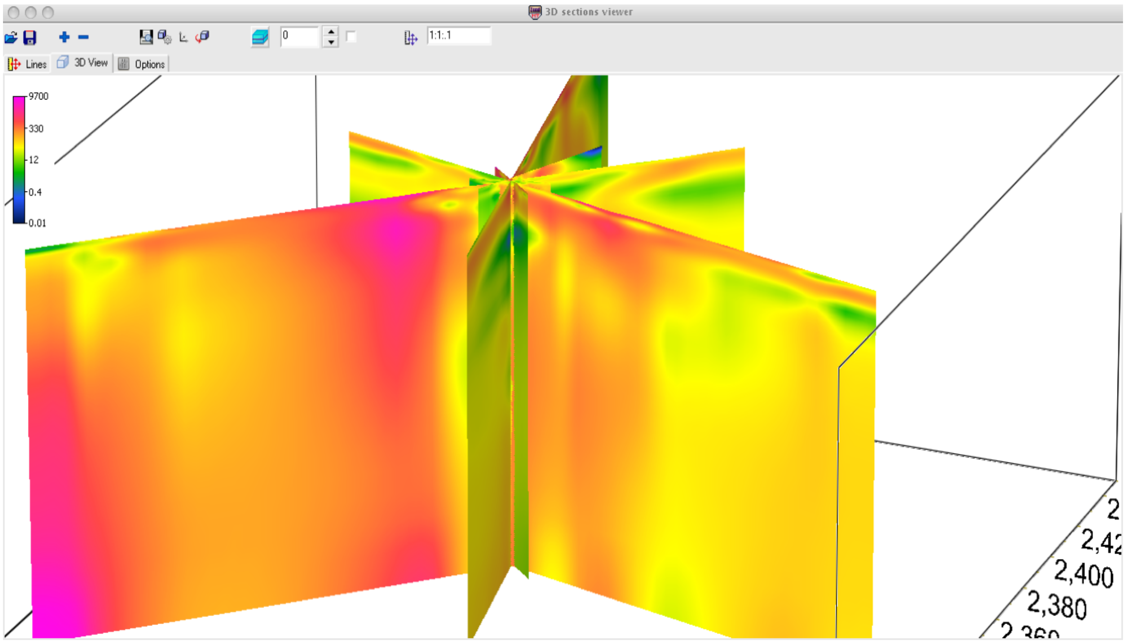

Figure 27. As above, but with a 10:1 vertical to horizontal aspect ratio. Note how the green (conductive) and orange (resistive) features near the top of the three intersecting planes in the foreground intersect and align.

Figures 26 and 27 display all six resistivity profiles in correct geographic orientation. These models were constrained by the uniform half space prior model. A visually more perfect alignment between structural elements on each of the profiles arises were we to display the models resulting from use of the 1d prior model, but much of this visual alignment would be an artifact of unresolvable structural elements in the original prior model that were not removed during the inversion. Rather we prefer to display the profiles that developed from the featureless half space prior model, since all model features here are required by the MT data. The foreground in Figure 27 shows the intersection of three different profiles (two long and one short), and the green and orange features align from one intersecting profile to the next. This is illustrated more clearly in Figures 28 and 29 below.

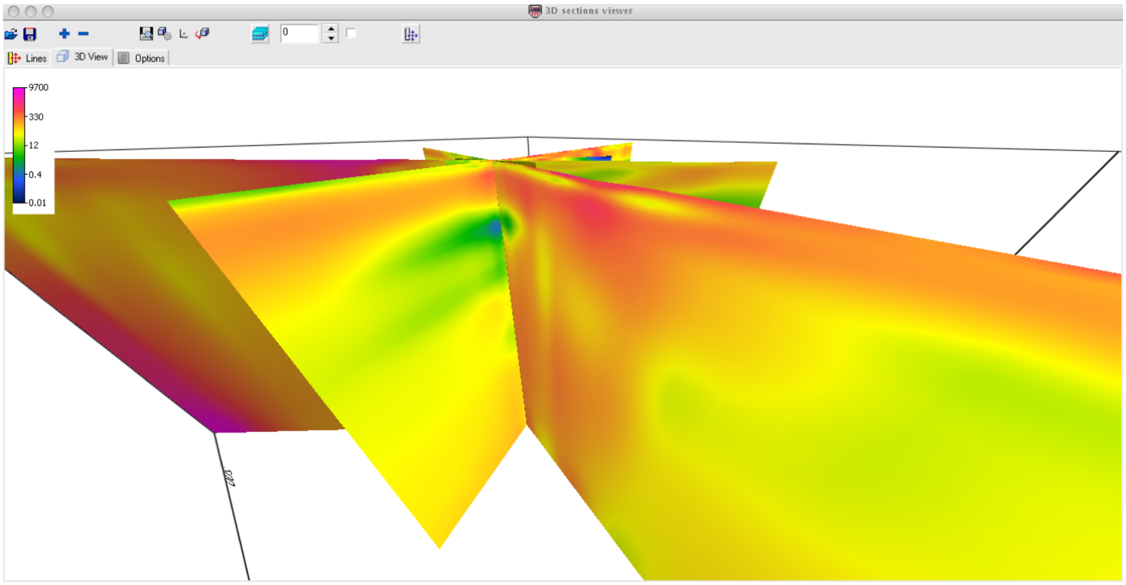

Figure 28. As above, but with the perspective distorted to show the intersection between two long profiles more clearly. Note how the green (conductive) and orange (resistive) features near the top of the three intersecting planes in the foreground intersect and align.

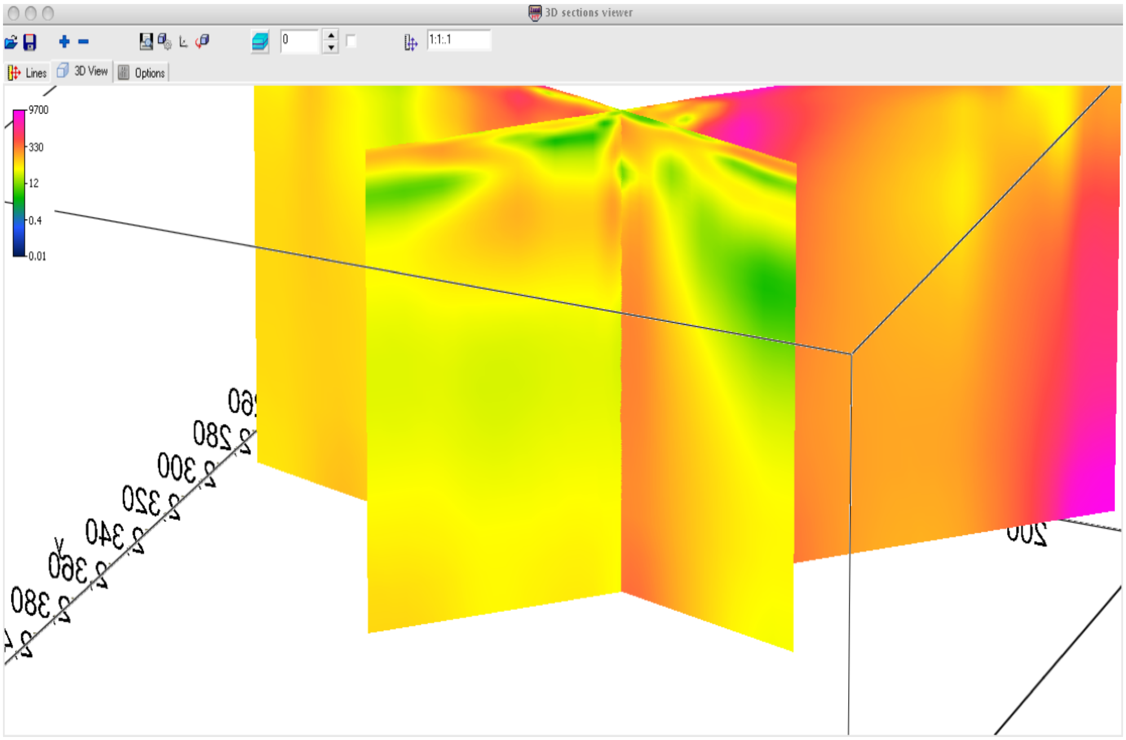

Figure 29. As above, but with the field of view rotated to provide another view of two long intersecting profiles. Note how the green (conductive) and orange (resistive) features near the top of the three intersecting planes in the foreground intersect and align.

Petrophysical & Seismic Processing

We obtained well-log data and 4 seismic refraction profiles from the Deputy Ministry of Petroleum and Mineral in Dhahran for Shuwahin-1 Well which has been drilled by LUKSAR. The LUKSAR Contract Area is situated in the southern part of the Eastern Province of Saudi Arabia. It consists of northern part of Rub Al-Khali, southern Summan, and southern Dahna area.

Seismic operations are being planned for selected parts of Contract Areas 1 and 2, however, the precise areas as well as the size of the operations may change is located in the transition zone between the Trade Wind deserts to the north and the tropical regions to the south.

We evaluated the petrophysical characteristics as well seismic data of this well. We concluded that :

- Only four zones encountered good sand with different salinity range from 1200 ppm of Minjur Formation @ 4925 ft, to 26200 ppm of Jilh Formation @ 5516 ft.
- Two interpreted surfaces (Surface 2 & 3) represent the interested zone, show regional up dip to the west direction.
- Petrophysical evaluation considered all zones are wet.

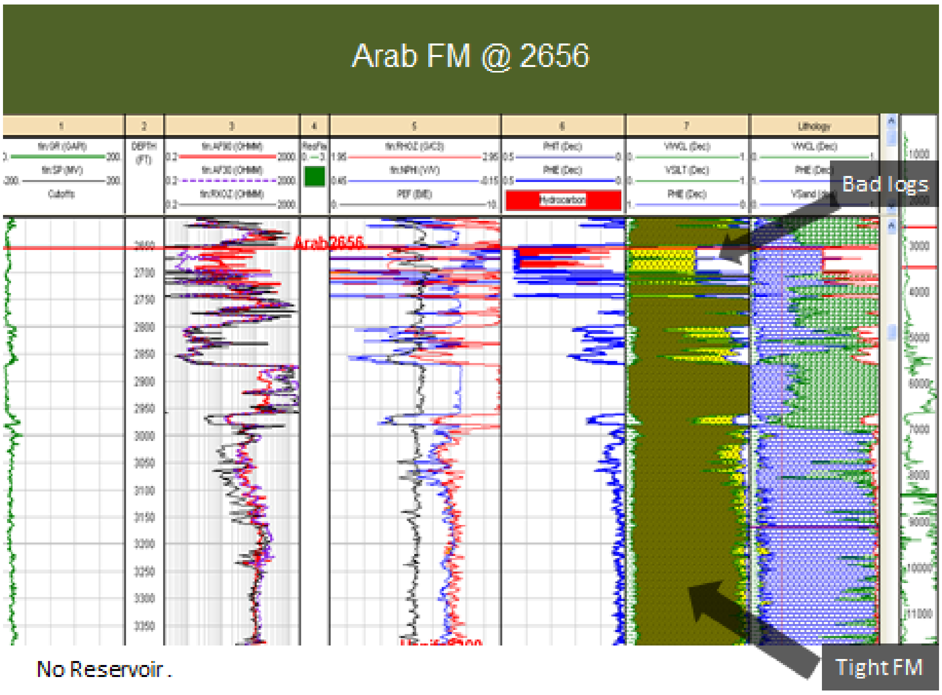
Arab FM @ 2656
Arab2656
Bad logs
Tight FM
No Reservoir.

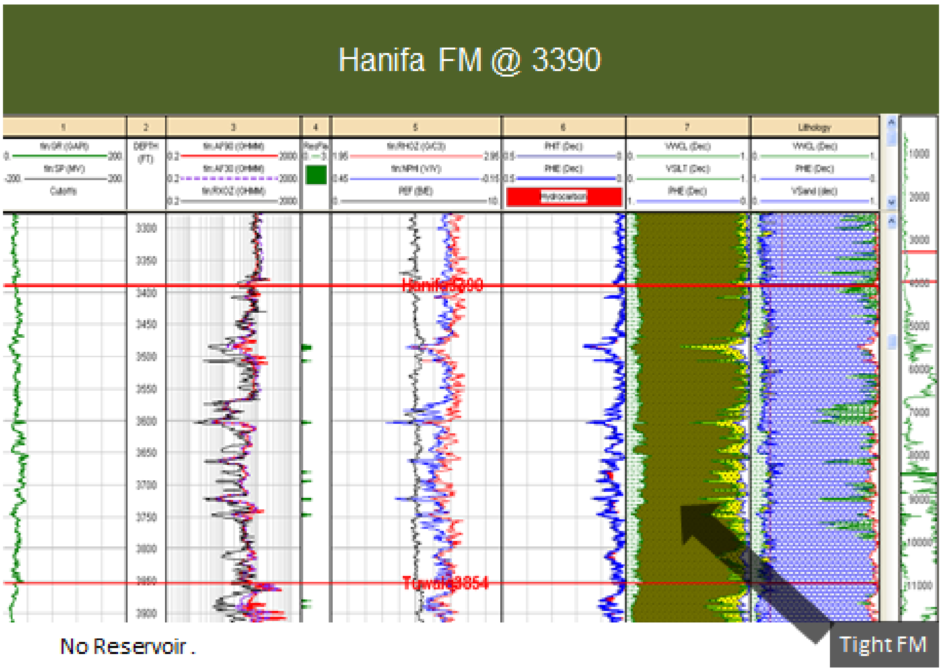
Hanifa FM @ 3390
Tight FM
No Reservoir.

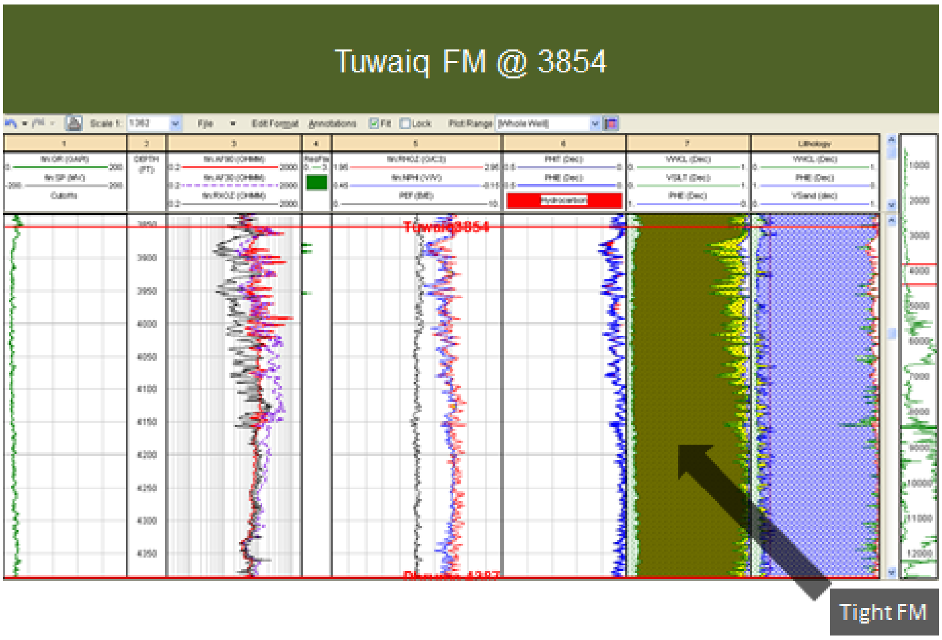

No Reservoir .

Minjur FM @ 4925

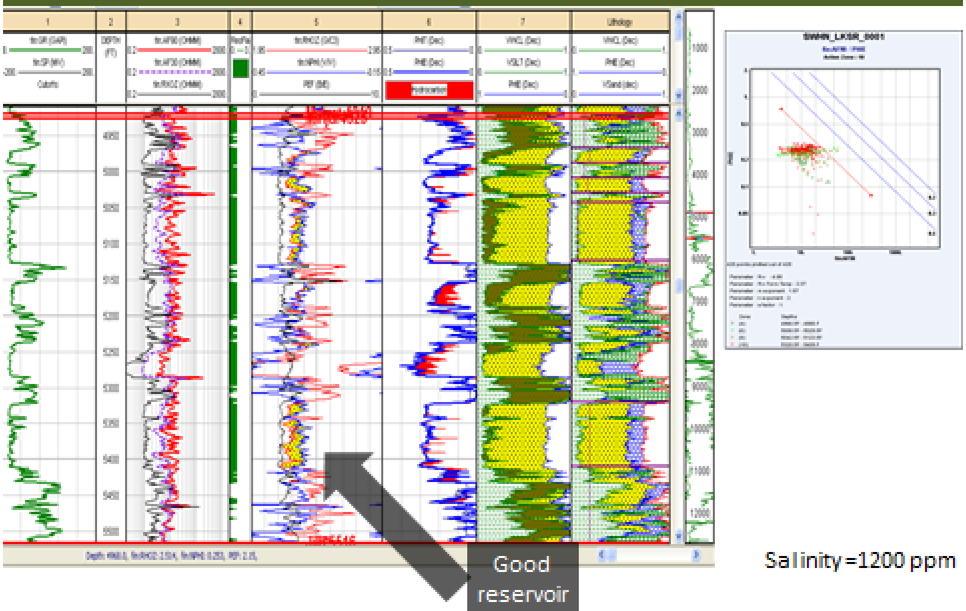

Salinity =1200 ppm

Dhruma FM @ 4387

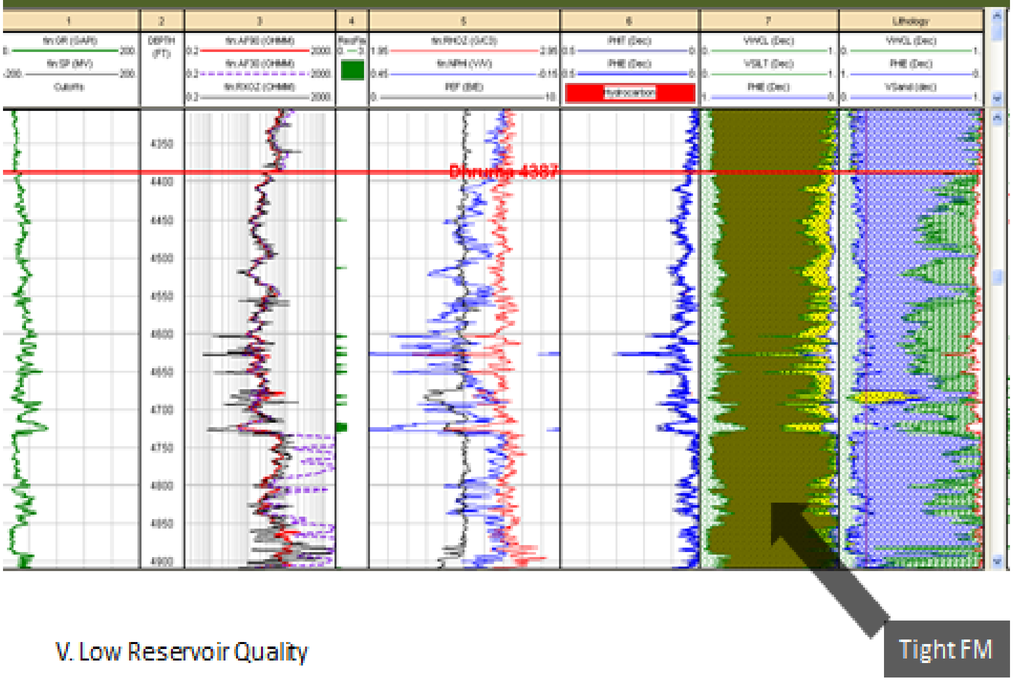

V. Low Reservoir Quality

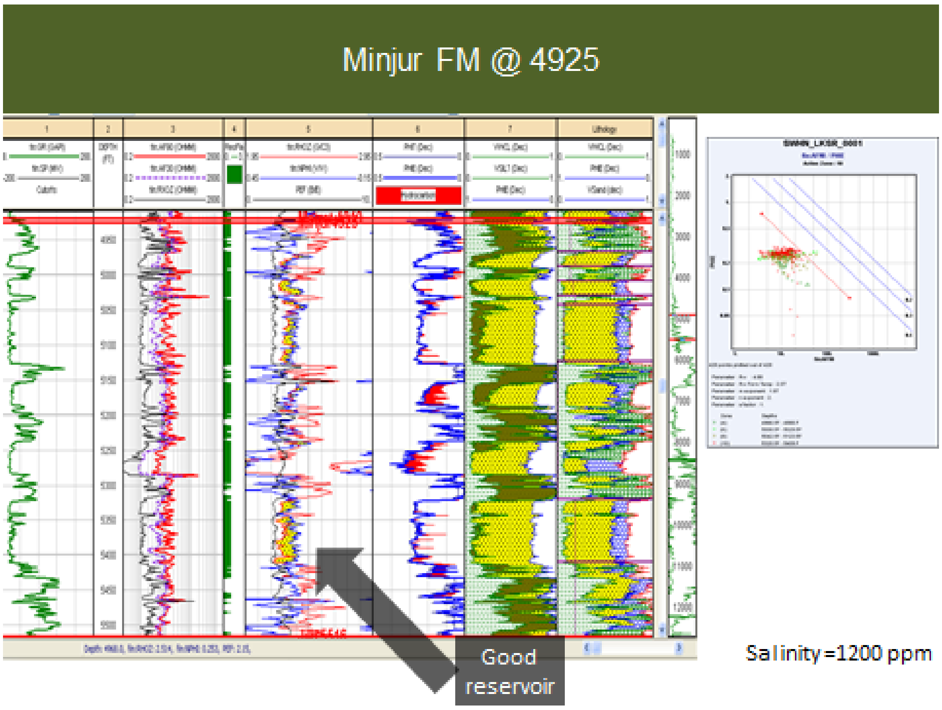
Minjur FM @ 4925
Good reservoir
Salinity =1200 ppm

Jilh Fm @ 5516

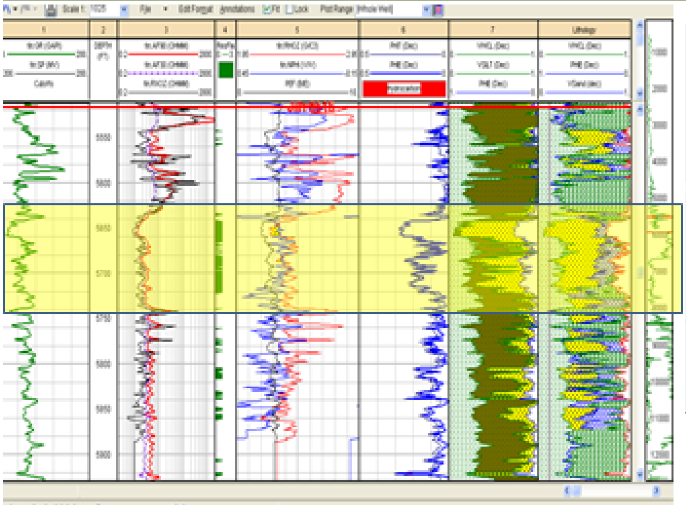

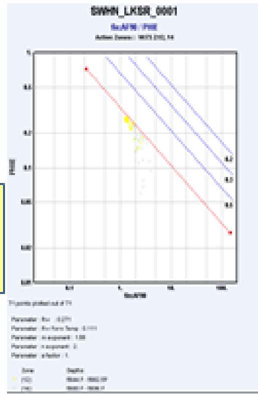

Salinity =26200 ppm

Sudair FM @ 5949

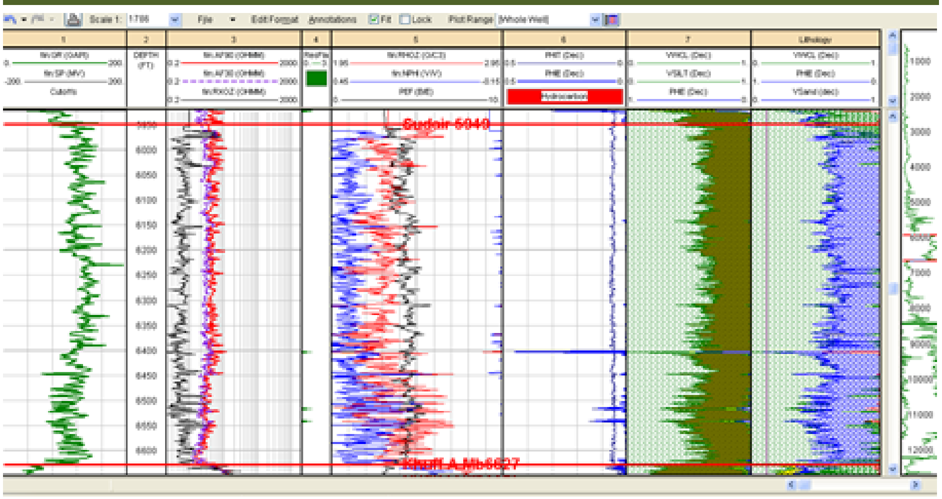

NO Reservoir

Khuff FM @ 6627

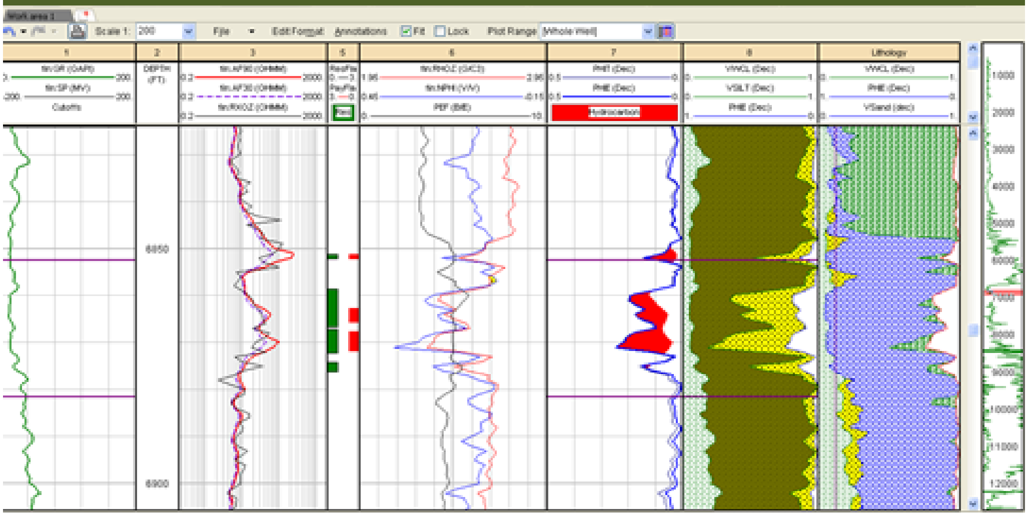

NP= 7 ft , Avg Porosity =19%, Avg SW =30
Assuming RW equivalent Salinity 10 k ppm

Sudair FM @ 5949

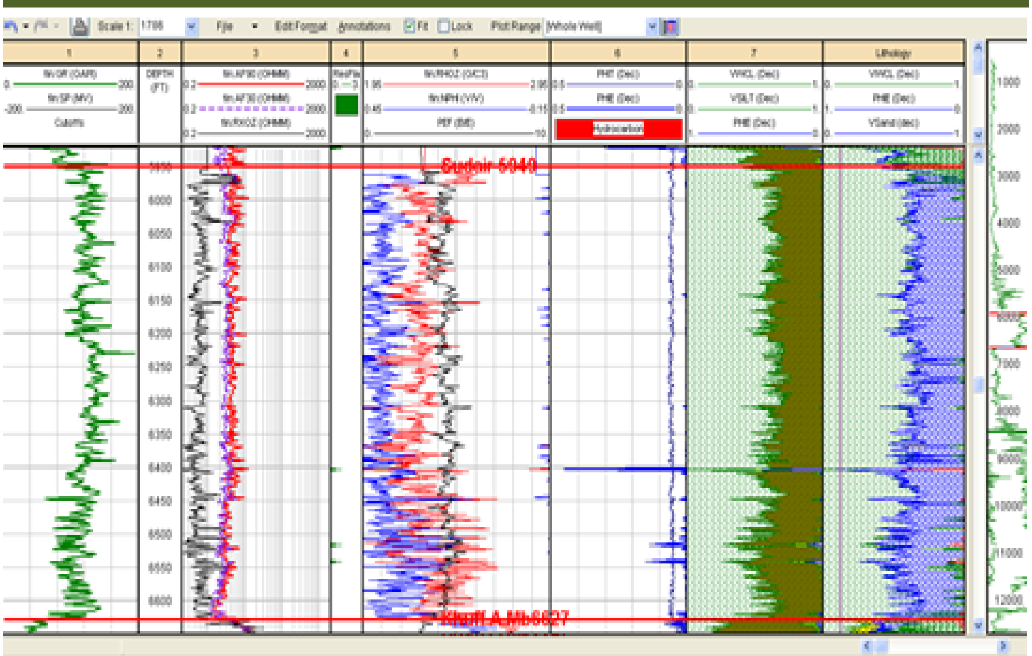

NO Reservoir

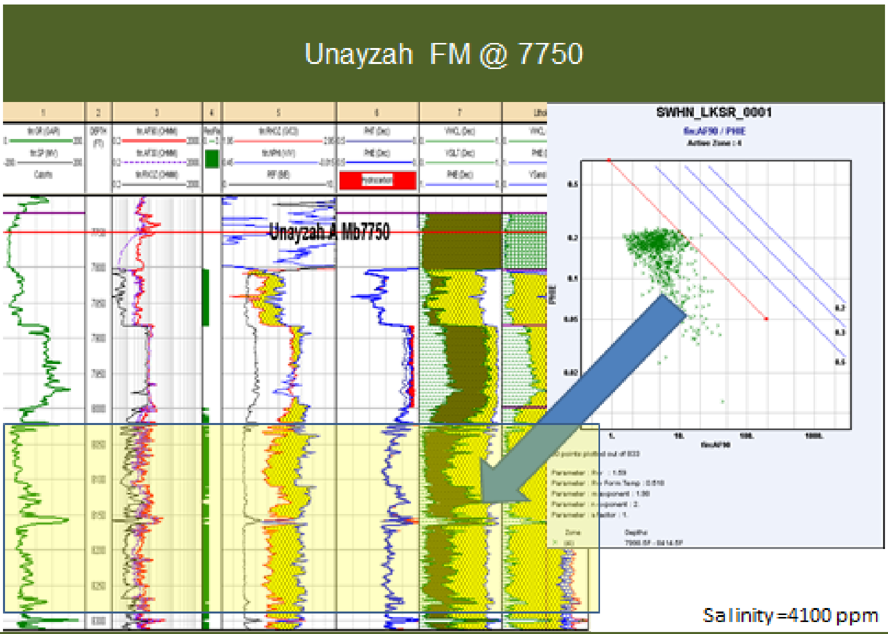

Salinity =4100 ppm

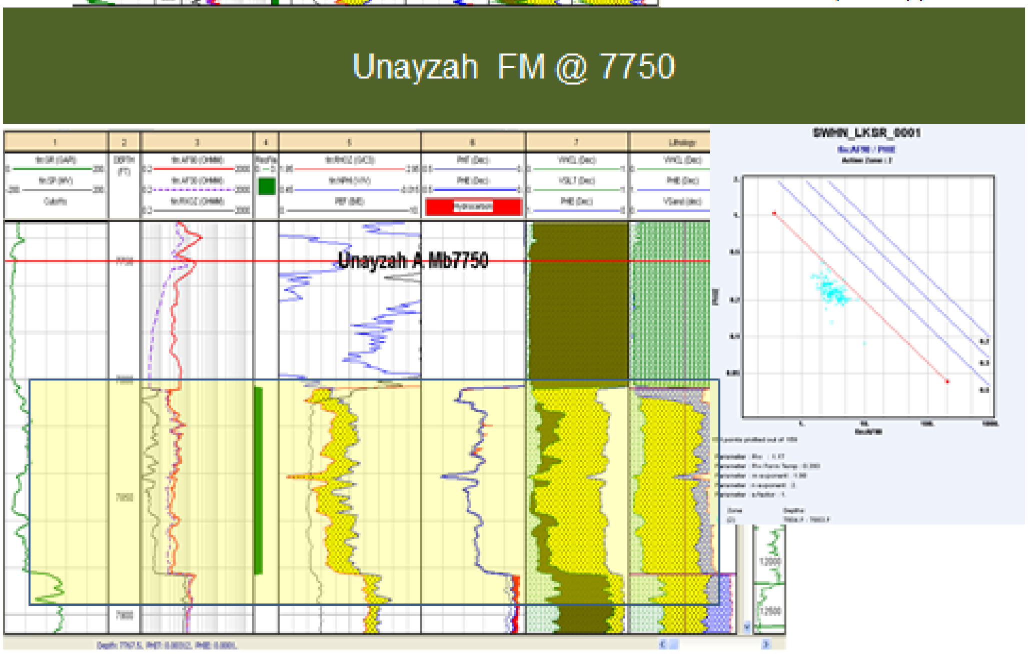

Salinity =5708 ppm

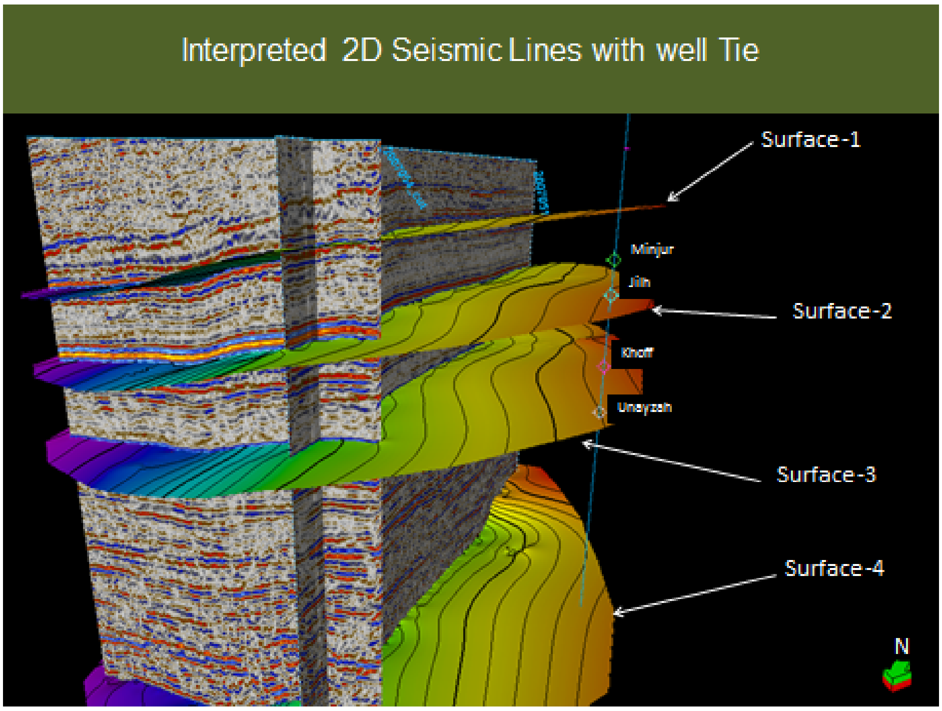
Interpreted 2D Seismic Lines with well Tie
Surface-1
Minjur
Jilh
Surface-2
Khoff
Unayzah
Surface-3
Surface-4
N

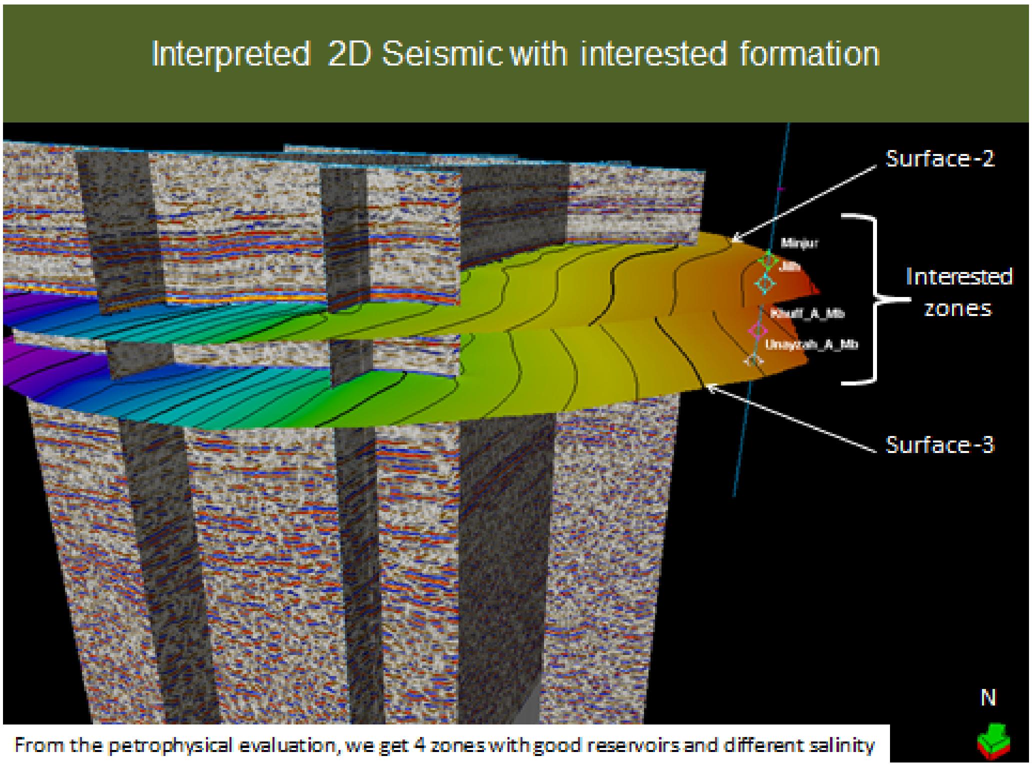
Interpreted 2D Seismic with interested formation
Surface-2
Minjur
Khuff_A_Mb
Unayzah_A_Mb
Interested zones
Surface-3
N
From the petrophysical evaluation, we get 4 zones with good reservoirs and different salinity

Summary & Conclusions

We have provided a 2D inverse modeling analysis of audio frequency MT data acquired. We have analyzed the data returned from the three long profiles that extend out to the existing wells that define the apexes of the triangular RAK survey area, and we have also analyzed the MT data from the three short, high resolution profiles near the center of the array. Our findings are that:

- The AMT data show strong 3D effects at all sites and over wide frequency bands
- We have been able to apply an Occam's inversion strategy to the best estimate of the TM mode, making use of Tikhonov regularization, to find the minimum structure 2D models that most closely match two sets of prior models. The first prior model is a uniform half space of 60 Ohm-m resistivity. The second is a 1d prior model based on bulk averaged resistivity anticipated to arise from saturated aquifers commencing 600 mbsl. The model fits to the TM mode data are extremely good in all cases. Our attempts to invert for 2D structure close in to the array center point were partially successful. Along two profile azimuths, strong 3D effects encountered require subsequent 3D interpretation, otherwise we have obtained robust 2D profiles that are based on a weighted contribution from TM mode (most strongly) and TE mode (only weakly).
- The resistivity of the conductive zones may be as low as 1 Ohm-m, which is consistent with values expected for saline groundwater. The ubiquity of high conductivity zones within the survey area is consistent with considerable

quantities of electrically continuous volumes of high TDS groundwater, localized into discrete water bearing layers. At each site, specific formations were associated with enhanced conductivity features in the subsurface.

- The location of station 77 (RAK-03) overlies a conductive feature from ~400-700 m depth, which is associated with the Neogene, Dammam and RUS formations rather than the underlying Umm er Radhuma.
- Two distinct bedded conductors beneath stations 5 and 6 in the west-northwest of the survey array are found at depths of ~400-600 m and ~1800-4500 m. It is necessary to extrapolate from the known stratigraphy at RAK-04 and WBA-06 given the regional dip orientation, but these depths could reasonably be associated with Umm Er Radhuma and Biyadh formations. A number of other surficial, localized conductive zones are also noted.
- We have identified a strongly conductive zone beneath stations close to WBA-06 in the northern part of the profile NW-SE, and also beneath stations near the center of the profile. The depth to the top of this feature appears to be well constrained, making it coincident with the top of the Aruma formation. A shallower conductive feature is found somewhat to the north of the center of the profile that might be coincident with the Umm er Radhuma formation, of with shallower overburden.

Station locations which represent the most promising sites of ground water potentiality for future drilling

Station	LATITUDE (N)	LONGITUDE (E)	DIST. FROM CENTER (km)
WBA-06	22 07 45.4	48 32 48.2	
1	21 05 54.6	48 45 32.7	0
5	21 11 24.5	48 23 11.6	40
6	21 12 46.4	48 17 36.1	50
9	21 17 23.2	48 57 49.3	30
10	21 21 12.6	49 01 55.3	40
24	21 48 28.9	48 36 47.6	80
28	21 04 31.7	48 51 07.7	10
100	21 03 49.5	48 53 58.2	15
29	21 03 08.7	48 56 42.6	20
77	20 50 36.9	49 46 35.2	2
12	21 00 35.3	48 46 37.9	10
89	21 03 46.3	48 45 59.3	4

References

Al-Alawi and M. Abdulrazzak. (1994). Water in Arabian Peninsula: Problems, in Water in the Arab World – Perspectives and Prognosis, ed. P.Rogers and P.Lyndon. Harward University: Division of Applied Sciences, 1994 ch. 7, pp. 171-202.

Al-Amri, M., and A. Al-Amri (1999).Configuration of the seismographic networks in Saudi Arabia, *Seism. Res. Lett.*, **70**, 322-331.

Al-Amri, A.M. (1998). The crustal structure of the western Arabian Platform from the spectral analysis of long-period P-wave amplitude ratios, Tectonophysics, **290**, 271-283.

Al-Amri, A.M. (1999). The crustal and upper-mantle structure of the interior Arabian platform, Geophysical Journal International, **136**,421-430.

Al-Amri, A. L., R. Mellors, and F. L. Vernon (1999). Broadband Seismic Noise Characteristics of the Arabian Shield, Arabian Journal of Science and Engineering, King Fahd University of Petroleum and Minerals, 24, 99-113.

Al-Amri, A. M., Davis, P., Al-Amri, M., Gharib, A. and Berger, J. (1999). Seismic characteristics of RAYN/ GSN station, Saudi Arabia ''. J. of King Saud University : Science (2) , V. 11, pp. 81 – 92.

Al-Damegh, K., Sandvol, E., Al-Lazki, A. and Barazangi, M. (2004). Regional wave propagation (Sn and Lg) and Pn attenuation in the Arabian plate and surrounding regions, *Geophys. J. Int.*, **157**, 775-795.

Al-Dulaijan et al, 2008), Magnetotellurics in the Rub al'Khali, Saudi Arabia; A. Al-Dulaijan (South Rub al-Khali Co. Ltd.), M.D. Watts (Geosystem, a Schlumberger Company) & P. van Mastrigt (South Rub al-Khali Co. Ltd.)

Al-Husseini M I (2000) Origin of the Arabian plate structures: Amar collision and Najd rift, GeoArabia, 5(4), 527-542

Alsharhan, A.S., Z. A. Rizk, A. E. M. Nairn, D. W. Bakhit, and, S. A. Alhajari (2001). Hydrogeology of an arid region: The Arabian Gulf and Adjoining Areas, Elsevier, Amsterdam-London-New York- Oxford-Paris-Tokyo.

AlSharhan, A.S., 2003, Petroleum geology and potential hydrocarbon plays in the Gulf of Suez rift basin, Egypt: AAPG Bulletin, v. 87, p. 143-180.

Badri, M. (1991). Crustal structure of central Saudi Arabia determined from seismic refraction profiling, *Tectonophysics*, **185**, 357-374.

Bauer, P., Burose, D. and Schulz, J., 2002. Rain detection over land surfaces using passive microwave satellite data. Meteorologische Zeitschrift, 11(1): 37-48.

Benoit, M., A. Nyblade, J. VanDecar, H. Gurrola (2003). Upper mantle P wave velocity structure and transition zone thickness beneath the Arabian Shield, *Geophys. Res. Lett.* 30, 1-4.

Debayle, E., J. Leveque, M. Cara, Seismic evidence for a deeply rooted low-velocity anomaly in the upper mantle beneath the northeastern Afro/Arabian continent (2001). *Earth Planet. Sci. Lett.* 193, 423-436.

Edgell, H. (1997). Aquifers of Saudi Arabia and their geological framework. The Arabian Journal of Science and Engineering, volume 22, Number 1C, June 1997.

Edgell, H.C. (1989). Evolution of Rub'al Khali Desert. Journal of King Abdul Aziz

University, Earth Sciences, 34, Special Issue, 1st Saudi Arabia Symposium on Earth Sciences, Jeddah (1989): 109-126.

Flower, T and Abu Nasser K. (2004). Environmental and Social Impact Assessment of Seismic Operations in SRAK Ltd Contract Areas: Rub alKhali Desert, Saudi Arabia.

Gettings, M., H. Blank, W. Mooney and J. Healey (1986). Crustal structure of southwestern Saudi Arabia*, J. Geophys.Res.,* 91, 6491- 6512.

Foster, S., Nanni, M., Kemper, K., Garduno, H., Tuinhof, A. (2003). Utilization of Non-Renewable Groundwater a socially-sustainable approach to resource management. GW-Mate Briefing Series Note 11, 2003, Published by World Bank, Washington D.C., USA.

Looseveld R J H, Bell A, Terken J J M (1996) The tectonic evolution of interior Oman, GeoArabia, 1 (1), 28-51

McClure, M.A. (1984). Late Quaternary Paleoenvironment of Rub'al Khali. Ph. D dissertation (unpublished), University College, London.

Mellors, R., Vernon, F., Camp, V., Al-Amri, A.M and Gharib, A. (1999). Regional waveform propagation in the Saudi Arabian Peninsula and evidence for a hot upper mantle under western Arabia.*J. Geophys. Res*., 104, 20,221–20,235

Mooney, M. Gettings, H. Blank, J. Healy, Saudi Arabian seismic refraction profile: A travel time interpretation of crustal and upper mantle structure (1985). *Tectonophysics* 111, 173-246.

Otkun, G., 1971, Paleozoic sandstone aquifers in Saudi Arabia, International Association of hydrogeologists: Tokyo Congress.

Pasyanos, M., E. Matzel, W..Walter, and A. Rodgers (2009a). Broad-band Lg attenuation modeling in the Middle East, *Geophys. J. Int., 177*, 1166-1176.

Powers R W, Ramirez L F, Redmond C D, Elberg E L (1966). Geology of the Arabian Peninsula, Sedimentary geology of Saudi Arabia: U. S. Geological Survey professional paper 560-D D1-D147

Rodgers, A., W. Walter, R. Mellors, A. M. S. Al-Amri and Y. S. Zhang (1999).Lithospheric structure of the Arabian Shield and Platform from complete regional waveform modeling and surface wave group velocities, *Geophys. J. Int*., 138, 871-878.

Sandvol, E., D. Seber, M. Barazangi, F. Vernon, R. Mellors and A. Al-Amri (1998). Lithospheric discontinuities beneath the Arabian Shield, *Geophys. Res. Lett*., 25, 2873-2877.

Stewart,et al, 1996), Stratigraphic Interpretation of Magnetotelluric Data in Central Saudi Arabia, Stewart, I. et al, p52-63, GeoArabia, Vo.1, No.1, 1996.

Stodt, J. (2005). Model HZB_01 / PWR_01 Buffer Amplifier.Operating Manual. Rev 1.1

Sultan, M., Sturchio, N.C., Gheith, H., Hady, Y.A. and El Anbeawy, M., 2000. Chemical and Isotopic Constraints on the Origin of Wadi El-Tarfa Ground Water, Eastern Desert, Egypt. Ground Water, 38(5): 743-751.

Sultan, M., Yan, E., Sturchio, N., Wagdy, A., Abdel Gelil, K., Becker, R., Manocha, M. and Milewski, A., 2007. Natural Discharge: A Key to Sustainable Utilization of Fossil Groundwater. Journal of Hydrology, 335: 25-36.

Sultan, M., Sturchio, N., El Sefry, S., Milewski, A., Becker, R., Nasr, I., 2008, Geochemical, Isotopic, and Modeling Constraints on the Origin and Evolution of the Rub Al Khali Groundwater Aquifer System, Arabian Peninsula, Journal of Hydrology, v. 356, p. 70– 83.

Tkalčić, H., M. Pasyanos, A. Rodgers, R. Gok and A. Al-Amri (2006). A multi-step approach for joint modeling of surface wave dispersion and teleseismic receiver functions: Implications for lithospheric structure of the Arabian Peninsula. *J. Geophys. Res.*, 111, B113111, doi:10.1029/2005JB004130.

Vernon, F., and J. Berger (1998).Broadband seismic characterization of the Arabian Shield, Final Scientific Technical Report, Department of Energy Contract No.F 19628-95-K-0015, 36 pp.

Water Atlas of Saudi Arabia. (1984).

Appendix A

WALDIM dimensional analysis summary for each station and frequency, arranged by survey line. Only results from the three long survey lines (see Figure 9) are shown here. Dimensional analysis from the three short survey lines is consistent with the long lines.

The reader is referred to the column marked "DIM" in the tables below. "DIM" refers to the dimensionality associated with the given site number and period (seconds), i.e. the reciprocal of frequency. A separate dimensional indicator appears for each period and site. The rows highlighted in yellow are those combinations of site locations and periods for which the dimensional analysis has been able to estimate a geoelectric strike direction. For a subset of those (site, period) combinations, the **WALDIM** analysis has been able to generate a principal TE, TM impedance pair, in the principal geoelectric strike and cross-strike directions, and it has been able to estimate and remove galvanic distortion effects from those estimates.

For all survey lines, **WALDIM** analysis has revealed that there are no consistent site groups or sufficiently wide frequency bands for which regional strike direction can be ascertained. For many (site, period) combinations, dimensionality cannot be determined, or alternatively, strong 3D effects are seen. To reiterate, there is no clear regional strike direction for the RAK AMT survey data. Any analysis based on 2D inversion must be interpreted with care, particularly to identify and localize the sites associated with the strongest 3D effects.

1. North-South long survey line.

Site	Per(s)	DIM	STRIKE(∫)	twist(∫)	shear(∫)	I7	skew	ph_s_skew
75	7.81E-04	UNDETERM.	---	------	-----	--------	0.159	0.259
75	9.77E-04	UNDETERM.	---	------	-----	--------	0.167	0.246
75	1.30E-03	UNDETERM.	---	------	-----	--------	0.175	0.228
75	1.56E-03	UNDETERM.	---	------	-----	--------	0.179	0.216
75	1.95E-03	UNDETERM.	---	------	-----	--------	0.183	0.202
75	2.60E-03	UNDETERM.	---	------	-----	--------	0.187	0.183
75	3.13E-03	3D/1D2D	---	------	-----	--------	0.189	0.172
75	3.91E-03	3D/1D2D	---	------	-----	--------	0.19	0.158
75	5.21E-03	3D/1D2D	---	------	-----	--------	0.19	0.142
75	6.25E-03	3D/1D2D	---	------	-----	--------	0.19	0.133
75	7.81E-03	3D/1D2D	---	------	-----	--------	0.189	0.125
75	1.04E-02	3D/1D2D	---	------	-----	--------	0.188	0.123
75	1.25E-02	UNDETERM.	---	------	-----	--------	0.186	0.128
75	1.56E-02	UNDETERM.	---	------	-----	--------	0.185	0.141
75	2.08E-02	3D/1D2D	---	------	-----	--------	0.185	0.167
75	2.50E-02	UNDETERM.	---	------	-----	--------	0.186	0.186
75	3.12E-02	3D	---	------	-----	0.748	0.19	0.21
75	4.17E-02	3D	---	------	-----	0.765	0.199	0.24
75	5.00E-02	3D	---	------	-----	0.794	0.207	0.258
75	6.25E-02	3D	---	------	-----	0.833	0.22	0.279
75	8.33E-02	3D	---	------	-----	0.869	0.241	0.301
75	1.00E-01	3D	---	------	-----	0.877	0.255	0.313
75	1.25E-01	3D	---	------	-----	0.87	0.273	0.323
75	1.67E-01	3D	---	------	-----	0.846	0.294	0.33
75	2.00E-01	3D	---	------	-----	0.833	0.305	0.332
75	2.50E-01	3D	---	------	-----	0.833	0.317	0.336
75	3.33E-01	3D	---	------	-----	0.87	0.332	0.346

75	4.00E-01	3D	---	------	-----	0.914	0.344	0.358
75	5.00E-01	3D	---	------	-----	0.979	0.362	0.377
75	6.67E-01	UNDETERM.	---	------	-----	--------	0.398	0.409
75	8.00E-01	UNDETERM.	---	------	-----	--------	0.428	0.432
75	1.00E+00	UNDETERM.	---	------	-----	--------	0.476	0.462
75	1.33E+00	UNDETERM.	---	------	-----	--------	0.553	0.498
75	1.60E+00	UNDETERM.	---	------	-----	--------	0.609	0.516
75	2.00E+00	UNDETERM.	---	------	-----	--------	0.683	0.531
75	2.67E+00	UNDETERM.	---	------	-----	--------	0.782	0.535
75	3.20E+00	UNDETERM.	---	------	-----	--------	0.845	0.527
75	4.00E+00	UNDETERM.	---	------	-----	--------	0.923	0.507
75	5.33E+00	UNDETERM.	---	------	-----	--------	1.02	0.456
75	6.40E+00	UNDETERM.	---	------	-----	--------	1.08	0.402
75	8.00E+00	UNDETERM.	---	------	-----	--------	1.14	0.298
75	1.07E+01	UNDETERM.	---	------	-----	--------	1.2	0.146
75	1.28E+01	UNDETERM.	---	------	-----	--------	1.21	0.296
75	1.60E+01	UNDETERM.	---	------	-----	--------	1.2	0.385
75	2.13E+01	UNDETERM.	---	------	-----	--------	1.16	0.41
75	2.56E+01	UNDETERM.	---	------	-----	--------	1.13	0.376
75	3.20E+01	UNDETERM.	---	------	-----	--------	1.09	0.262
75	4.27E+01	UNDETERM.	---	------	-----	--------	1.07	0.279
75	5.12E+01	UNDETERM.	---	------	-----	--------	1.08	0.442
75	6.40E+01	UNDETERM.	---	------	-----	--------	1.12	0.601
75	8.53E+01	UNDETERM.	---	------	-----	--------	1.22	0.783
76	7.81E-04	UNDETERM.	---	------	-----	--------	4.75E-02	4.63E-03
76	9.77E-04	UNDETERM.	---	------	-----	--------	4.74E-02	5.85E-02
76	1.30E-03	3D/1D2D	---	------	-----	--------	4.69E-02	9.00E-02
76	1.56E-03	3D/1D2D	---	------	-----	--------	4.65E-02	0.106
76	1.95E-03	3D/1D2D	---	------	-----	--------	4.59E-02	0.125
76	2.60E-03	3D/1D2D	---	------	-----	--------	4.52E-02	0.148
76	3.13E-03	3D	---	------	-----	0.53	4.48E-02	0.162

76	3.91E-03	3D	---	------	-----	0.511	4.43E-02	0.179
76	5.21E-03	3D	---	------	-----	0.514	4.34E-02	0.198
76	6.25E-03	3D	---	------	-----	0.523	4.27E-02	0.209
76	7.81E-03	3D	---	------	-----	0.533	4.15E-02	0.22
76	1.04E-02	3D	---	------	-----	0.537	3.99E-02	0.233
76	1.25E-02	3D	---	------	-----	0.534	3.91E-02	0.24
76	1.56E-02	3D	---	------	-----	0.531	3.86E-02	0.247
76	2.08E-02	3D	---	------	-----	0.535	3.88E-02	0.253
76	2.50E-02	UNDETERM.	---	------	-----	--------	3.95E-02	0.255
76	3.12E-02	3D	---	------	-----	0.567	4.11E-02	0.255
76	4.17E-02	3D	---	------	-----	0.613	4.43E-02	0.253
76	5.00E-02	3D	---	------	-----	0.652	4.71E-02	0.251
76	6.25E-02	3D	---	------	-----	0.702	5.11E-02	0.249
76	8.33E-02	3D	---	------	-----	0.758	5.71E-02	0.247
76	1.00E-01	3D	---	------	-----	0.779	6.11E-02	0.244
76	1.25E-01	3D	---	------	-----	0.783	6.58E-02	0.241
76	1.67E-01	3D	---	------	-----	0.755	7.12E-02	0.236
76	2.00E-01	3D	---	------	-----	0.722	7.43E-02	0.234
76	2.50E-01	3D	---	------	-----	0.672	7.78E-02	0.234
76	3.33E-01	3D	---	------	-----	0.607	8.25E-02	0.239
76	4.00E-01	3D	---	------	-----	0.572	8.60E-02	0.246
76	5.00E-01	UNDETERM.	---	------	-----	--------	9.15E-02	0.26
76	6.67E-01	UNDETERM.	---	------	-----	--------	0.102	0.287
76	8.00E-01	UNDETERM.	---	------	-----	--------	0.111	0.309
76	1.00E+00	UNDETERM.	---	------	-----	--------	0.126	0.342
76	1.33E+00	UNDETERM.	---	------	-----	--------	0.153	0.393
76	1.60E+00	UNDETERM.	---	------	-----	--------	0.175	0.43
76	2.00E+00	UNDETERM.	---	------	-----	--------	0.211	0.481
76	2.67E+00	UNDETERM.	---	------	-----	--------	0.273	0.556
76	3.20E+00	UNDETERM.	---	------	-----	--------	0.323	0.61
76	4.00E+00	UNDETERM.	---	------	-----	--------	0.399	0.682

76	5.33E+00	UNDETERM.	---	------	-----	--------		0.528	0.788
27	1.30E-03	2D	84.73	+	548.8607	i)		(	-540.5569
27	1.56E-03	2D	84.69	+	478.2258	i)		(	-537.6819
27	1.95E-03	2D	84.58	+	411.9645	i)		(	-532.5704
27	2.60E-03	3D/2D	66.31	2.6411	1.99	--------		4.02E-02	0.112
27	3.13E-03	1D	---	------	-----	--------		4.06E-02	0.102
27	3.91E-03	1D	---	------	-----	--------		4.05E-02	9.18E-02
27	5.21E-03	1D	---	------	-----	--------		3.97E-02	8.23E-02
27	6.25E-03	1D	---	------	-----	--------		3.90E-02	8.03E-02
27	7.81E-03	3D/2D	67.09	2.2138	3.6593	--------		3.81E-02	8.26E-02
27	1.04E-02	3D/2D	76	2.3143	2.4901	--------		3.73E-02	9.19E-02
27	1.25E-02	3D	---	------	-----		0.153	3.72E-02	9.99E-02
27	1.56E-02	3D/2D	80.83	2.6855	1.636	--------		3.76E-02	0.111
27	2.08E-02	UNDETERM.	---	------	-----	--------		3.90E-02	0.125
27	2.50E-02	3D	---	------	-----		0.159	4.03E-02	0.134
27	3.12E-02	3D	---	------	-----		0.181	4.25E-02	0.145
27	4.17E-02	3D	---	------	-----		0.229	4.62E-02	0.161
27	5.00E-02	3D	---	------	-----		0.275	4.93E-02	0.171
27	6.25E-02	3D	---	------	-----		0.355	5.40E-02	0.186
27	8.33E-02	3D	---	------	-----		0.505	6.24E-02	0.207
27	1.00E-01	UNDETERM.	---	------	-----	--------		6.95E-02	0.223
27	1.25E-01	3D	---	------	-----		0.799	8.05E-02	0.245
27	1.67E-01	3D	---	------	-----		0.978	9.99E-02	0.277
27	2.00E-01	UNDETERM.	---	------	-----	--------		0.116	0.301
27	2.50E-01	UNDETERM.	---	------	-----	--------		0.14	0.332
27	3.33E-01	UNDETERM.	---	------	-----	--------		0.181	0.378
27	4.00E-01	3D	---	------	-----		0.981	0.214	0.41
27	5.00E-01	3D	---	------	-----		0.956	0.262	0.453
27	6.67E-01	3D	---	------	-----		0.933	0.34	0.511
27	8.00E-01	3D	---	------	-----		0.924	0.399	0.548
27	1.00E+00	UNDETERM.	---	------	-----	--------		0.481	0.592

27	1.33E+00	UNDETERM.	---	------	-----	--------	0.6	0.64
27	1.60E+00	UNDETERM.	---	------	-----	--------	0.68	0.661
27	2.00E+00	UNDETERM.	---	------	-----	--------	0.775	0.674
27	2.67E+00	UNDETERM.	---	------	-----	--------	0.886	0.665
27	3.20E+00	UNDETERM.	---	------	-----	--------	0.945	0.645
27	4.00E+00	UNDETERM.	---	------	-----	--------	1	0.609
27	5.33E+00	UNDETERM.	---	------	-----	--------	1.06	0.549
27	6.40E+00	UNDETERM.	---	------	-----	--------	1.08	0.506
27	8.00E+00	UNDETERM.	---	------	-----	--------	1.11	0.452
27	1.07E+01	UNDETERM.	---	------	-----	--------	1.12	0.384
27	1.28E+01	UNDETERM.	---	------	-----	--------	1.13	0.344
27	1.60E+01	UNDETERM.	---	------	-----	--------	1.13	0.306
27	2.13E+01	UNDETERM.	---	------	-----	--------	1.13	0.286
27	2.56E+01	UNDETERM.	---	------	-----	--------	1.12	0.296
27	3.20E+01	UNDETERM.	---	------	-----	--------	1.11	0.331
27	4.27E+01	UNDETERM.	---	------	-----	--------	1.1	0.398
27	5.12E+01	UNDETERM.	---	------	-----	--------	1.09	0.448
27	6.40E+01	UNDETERM.	---	------	-----	--------	1.09	0.512
27	8.53E+01	UNDETERM.	---	------	-----	--------	1.08	0.594
25	7.81E-04	UNDETERM.	---	------	-----	--------	0.388	0.387
25	9.77E-04	UNDETERM.	---	------	-----	--------	0.441	0.367
25	1.30E-03	UNDETERM.	---	------	-----	--------	0.496	0.29
25	1.56E-03	UNDETERM.	---	------	-----	--------	0.516	0.192
25	1.95E-03	UNDETERM.	---	------	-----	--------	0.521	0.164
25	2.60E-03	UNDETERM.	---	------	-----	--------	0.496	0.31
25	3.13E-03	3D	---	------	-----	0.743	0.468	0.353
25	3.91E-03	3D	---	------	-----	0.857	0.426	0.376
25	5.21E-03	3D	---	------	-----	0.91	0.37	0.375
25	6.25E-03	3D	---	------	-----	0.905	0.336	0.363
25	7.81E-03	3D	---	------	-----	0.875	0.298	0.343
25	1.04E-02	3D	---	------	-----	0.815	0.255	0.312

25	1.25E-02	3D	---	------	-----	0.767	0.232	0.289
25	1.56E-02	3D	---	------	-----	0.689	0.208	0.258
25	2.08E-02	UNDETERM.	---	------	-----	--------	0.183	0.211
25	2.50E-02	3D	---	------	-----	0.412	0.172	0.174
25	3.12E-02	3D	---	------	-----	0.212	0.162	0.116
25	4.17E-02	UNDETERM.	---	------	-----	--------	0.157	8.90E-02
25	5.00E-02	UNDETERM.	---	------	-----	--------	0.159	0.146
25	6.25E-02	UNDETERM.	---	------	-----	--------	0.166	0.194
25	8.33E-02	UNDETERM.	---	------	-----	--------	0.184	0.242
25	1.00E-01	UNDETERM.	---	------	-----	--------	0.201	0.266
25	1.25E-01	3D	---	------	-----	0.874	0.227	0.289
25	1.67E-01	UNDETERM.	---	------	-----	--------	0.265	0.304
25	2.00E-01	UNDETERM.	---	------	-----	--------	0.29	0.301
25	2.50E-01	UNDETERM.	---	------	-----	--------	0.319	0.28
25	3.33E-01	UNDETERM.	---	------	-----	--------	0.348	0.21
25	4.00E-01	UNDETERM.	---	------	-----	--------	0.359	0.116
25	5.00E-01	UNDETERM.	---	------	-----	--------	0.36	0.166
25	6.67E-01	UNDETERM.	---	------	-----	--------	0.344	0.273
25	8.00E-01	UNDETERM.	---	------	-----	--------	0.325	0.307
25	1.00E+00	UNDETERM.	---	------	-----	--------	0.295	0.326
25	1.33E+00	UNDETERM.	---	------	-----	--------	0.254	0.32
25	1.60E+00	UNDETERM.	---	------	-----	--------	0.23	0.303
25	2.00E+00	UNDETERM.	---	------	-----	--------	0.204	0.274
25	2.67E+00	UNDETERM.	---	------	-----	--------	0.179	0.225
25	3.20E+00	UNDETERM.	---	------	-----	--------	0.169	0.186
25	4.00E+00	UNDETERM.	---	------	-----	--------	0.16	0.123
25	5.33E+00	UNDETERM.	---	------	-----	--------	0.156	9.58E-02
25	6.40E+00	UNDETERM.	---	------	-----	--------	0.157	0.157
25	8.00E+00	UNDETERM.	---	------	-----	--------	0.161	0.209
25	1.07E+01	UNDETERM.	---	------	-----	--------	0.171	0.262
24	7.81E-04	UNDETERM.	---	------	-----	--------	0.147	2.76E-02

24	1.30E-03	UNDETERM.	---	------	-----	--------		0.134	0.127
24	1.56E-03	3D	---	------	-----	0.33		0.13	0.136
24	1.95E-03	UNDETERM.	---	------	-----	--------		0.126	0.144
24	2.60E-03	UNDETERM.	---	------	-----	--------		0.121	0.152
24	3.13E-03	3D/1D2D	---	------	-----	--------		0.117	0.157
24	3.91E-03	3D/1D2D	---	------	-----	--------		0.111	0.159
24	5.21E-03	3D/1D2D	---	------	-----	--------		0.103	0.155
24	6.25E-03	3D	---	------	-----	0.333		9.70E-02	0.147
24	7.81E-03	3D	---	------	-----	0.192		9.09E-02	0.132
24	1.04E-02	3D/2Dtw	88.78	4.7192	-1.5666	--------		8.53E-02	0.101
24	1.25E-02	3D/2Dtw	88.67	4.7805	-1.4822	--------		8.34E-02	7.10E-02
24	1.56E-02	UNDETERM.	---	------	-----	--------		8.28E-02	4.24E-02
24	2.50E-02	UNDETERM.	---	------	-----	--------		8.75E-02	0.133
24	3.12E-02	UNDETERM.	---	------	-----	--------		9.22E-02	0.16
24	4.17E-02	UNDETERM.	---	------	-----	--------		0.101	0.19
24	5.00E-02	UNDETERM.	---	------	-----	--------		0.107	0.207
24	6.25E-02	UNDETERM.	---	------	-----	--------		0.116	0.225
24	8.33E-02	UNDETERM.	---	------	-----	--------		0.13	0.245
24	1.00E-01	UNDETERM.	---	------	-----	--------		0.139	0.256
24	1.25E-01	UNDETERM.	---	------	-----	--------		0.152	0.27
24	1.67E-01	UNDETERM.	---	------	-----	--------		0.171	0.286
24	2.00E-01	UNDETERM.	---	------	-----	--------		0.184	0.296
24	2.50E-01	UNDETERM.	---	------	-----	--------		0.2	0.307
24	3.33E-01	UNDETERM.	---	------	-----	--------		0.221	0.32
24	4.00E-01	UNDETERM.	---	------	-----	--------		0.234	0.329
24	5.00E-01	UNDETERM.	---	------	-----	--------		0.249	0.341
24	6.67E-01	UNDETERM.	---	------	-----	--------		0.269	0.362
24	8.00E-01	UNDETERM.	---	------	-----	--------		0.283	0.38
24	1.00E+00	UNDETERM.	---	------	-----	--------		0.302	0.405
24	1.33E+00	UNDETERM.	---	------	-----	--------		0.334	0.444
24	1.60E+00	UNDETERM.	---	------	-----	--------		0.359	0.471

24	2.00E+00	UNDETERM.	---	------	-----	--------		0.397	0.505
24	2.67E+00	UNDETERM.	---	------	-----	--------		0.456	0.545
24	3.20E+00	UNDETERM.	---	------	-----	--------		0.499	0.566
24	4.00E+00	UNDETERM.	---	------	-----	--------		0.553	0.582
24	5.33E+00	UNDETERM.	---	------	-----	--------		0.623	0.587
24	6.40E+00	UNDETERM.	---	------	-----	--------		0.664	0.58
24	8.00E+00	UNDETERM.	---	------	-----	--------		0.711	0.564
24	1.07E+01	UNDETERM.	---	------	-----	--------		0.769	0.537
24	1.28E+01	UNDETERM.	---	------	-----	--------		0.807	0.519
24	1.60E+01	UNDETERM.	---	------	-----	--------		0.859	0.496
24	2.13E+01	UNDETERM.	---	------	-----	--------		0.943	0.464
24	2.56E+01	UNDETERM.	---	------	-----	--------		1.01	0.437
24	3.20E+01	3D	---	------	-----		0.462	1.1	0.387
24	4.27E+01	UNDETERM.	---	------	-----	--------		1.24	0.246
23	9.77E-04	UNDETERM.	---	------	-----	--------		3.65E-03	2.65E-02
23	1.56E-03	3D/2D	86.52	-0.4158	-1.5884	--------		4.72E-03	1.13E-02
23	1.95E-03	3D/2D	86.6	-0.5635	-1.7933	--------		5.38E-03	1.47E-02
23	2.60E-03	3D/2D	86.14	-1.2385	-2.8466	--------		6.34E-03	3.71E-02
23	3.13E-03	2D	88.28	+	1341.8907	i)	(		-234.8043
23	3.91E-03	2D	88.06	+	1235.3297	i)	(		-170.6644
23	5.21E-03	2D	87.68	+	1060.8935	i)	(		-116.9925
23	6.25E-03	2D	87.4	+	941.904	i)	(		-94.946
23	7.81E-03	2D	87.09	+	800.2596	i)	(		-76.5401
23	1.04E-02	2D	86.8	+	637.6926	i)	(		-62.0919
23	1.25E-02	2D	86.71	+	550.0986	i)	(		-56.4501
23	1.56E-02	2D	86.71	+	459.986	i)	(		-51.8597
23	2.50E-02	2D	87	+	325.8949	i)	(		-46.7287
23	3.12E-02	2D	87.19	+	283.7581	i)	(		-45.3171
23	4.17E-02	2D	87.43	+	243.8128	i)	(		-43.7817
23	5.00E-02	3D/2D	4.31	7.9914	13.1383	--------		7.48E-03	6.36E-02
23	6.25E-02	3D/2D	4.08	6.9341	11.8901	--------		6.72E-03	8.17E-02

23	8.33E-02	3D	---	------	-----		0.184	5.85E-03	0.103
23	1.00E-01	3D	---	------	-----		0.19	5.37E-03	0.115
23	1.25E-01	3D	---	------	-----		0.205	4.85E-03	0.128
23	1.67E-01	UNDETERM.	---	------	-----	--------		4.27E-03	0.142
23	2.00E-01	UNDETERM.	---	------	-----	--------		3.94E-03	0.149
23	2.50E-01	UNDETERM.	---	------	-----	--------		3.60E-03	0.159
23	3.33E-01	UNDETERM.	---	------	-----	--------		3.25E-03	0.173
23	4.00E-01	UNDETERM.	---	------	-----	--------		3.12E-03	0.183
23	5.00E-01	UNDETERM.	---	------	-----	--------		3.07E-03	0.198
23	6.67E-01	UNDETERM.	---	------	-----	--------		3.39E-03	0.22
23	8.00E-01	UNDETERM.	---	------	-----	--------		3.95E-03	0.235
23	1.00E+00	UNDETERM.	---	------	-----	--------		5.15E-03	0.255
23	1.33E+00	UNDETERM.	---	------	-----	--------		7.64E-03	0.279
23	1.60E+00	UNDETERM.	---	------	-----	--------		9.74E-03	0.293
23	2.00E+00	UNDETERM.	---	------	-----	--------		1.27E-02	0.308
23	2.67E+00	UNDETERM.	---	------	-----	--------		1.68E-02	0.324
23	3.20E+00	UNDETERM.	---	------	-----	--------		1.94E-02	0.334
23	4.00E+00	UNDETERM.	---	------	-----	--------		2.25E-02	0.346
23	5.33E+00	UNDETERM.	---	------	-----	--------		2.69E-02	0.365
23	6.40E+00	UNDETERM.	---	------	-----	--------		3.05E-02	0.381
23	8.00E+00	UNDETERM.	---	------	-----	--------		3.66E-02	0.404
23	1.07E+01	UNDETERM.	---	------	-----	--------		4.92E-02	0.442
23	1.60E+01	UNDETERM.	---	------	-----	--------		8.28E-02	0.507
23	2.13E+01	UNDETERM.	---	------	-----	--------		0.126	0.555
23	3.20E+01	UNDETERM.	---	------	-----	--------		0.235	0.609
23	4.27E+01	UNDETERM.	---	------	-----	--------		0.364	0.622
23	8.53E+01	UNDETERM.	---	------	-----	--------		0.918	0.486
22	9.77E-04	3D/2D	89.95	-3.5281	5.6135	--------		1.19E-02	8.62E-02
22	1.30E-03	2D	4.66	+	846.5588	i)	(		-358.628
22	1.56E-03	2D	3.34	+	937.1393	i)	(		-329.4693
22	1.95E-03	2D	2.59	+	1027.799	i)	(		-298.6751

22	2.60E-03	3D	---	------	-----	0.177	1.18E-02	0.105
22	3.13E-03	2D	2.21	+	1076.9816	i)	(	-234.836
22	3.91E-03	2D	2.39	+	1022.097	i)	(	-203.9549
22	5.21E-03	2D	2.96	+	897.5952	i)	(	-166.7458
22	6.25E-03	3D	---	------	-----	0.619	1.79E-02	0.178
22	7.81E-03	3D	---	------	-----	0.526	2.04E-02	0.192
22	1.04E-02	3D	---	------	-----	0.447	2.37E-02	0.205
22	1.25E-02	UNDETERM.	---	------	-----	--------	2.56E-02	0.209
22	2.50E-02	UNDETERM.	---	------	-----	--------	2.75E-02	0.19
22	3.12E-02	UNDETERM.	---	------	-----	--------	2.55E-02	0.175
22	4.17E-02	UNDETERM.	---	------	-----	--------	2.11E-02	0.152
22	5.00E-02	UNDETERM.	---	------	-----	--------	1.74E-02	0.137
22	6.25E-02	UNDETERM.	---	------	-----	--------	1.18E-02	0.124
22	8.33E-02	UNDETERM.	---	------	-----	--------	3.05E-03	0.121
22	1.00E-01	UNDETERM.	---	------	-----	--------	3.51E-03	0.13
22	1.25E-01	UNDETERM.	---	------	-----	--------	1.22E-02	0.151
22	1.67E-01	UNDETERM.	---	------	-----	--------	2.45E-02	0.187
22	2.00E-01	UNDETERM.	---	------	-----	--------	3.27E-02	0.211
22	2.50E-01	UNDETERM.	---	------	-----	--------	4.29E-02	0.24
22	3.33E-01	UNDETERM.	---	------	-----	--------	5.66E-02	0.275
22	4.00E-01	UNDETERM.	---	------	-----	--------	6.59E-02	0.294
22	5.00E-01	UNDETERM.	---	------	-----	--------	7.85E-02	0.314
22	6.67E-01	UNDETERM.	---	------	-----	--------	9.69E-02	0.329
22	8.00E-01	UNDETERM.	---	------	-----	--------	0.11	0.329
22	1.00E+00	UNDETERM.	---	------	-----	--------	0.126	0.315
22	1.33E+00	UNDETERM.	---	------	-----	--------	0.146	0.256
22	1.60E+00	UNDETERM.	---	------	-----	--------	0.157	0.174
22	2.00E+00	UNDETERM.	---	------	-----	--------	0.165	0.158
22	2.67E+00	UNDETERM.	---	------	-----	--------	0.167	0.318
22	3.20E+00	UNDETERM.	---	------	-----	--------	0.162	0.376
22	4.00E+00	UNDETERM.	---	------	-----	--------	0.151	0.416

22	5.33E+00	UNDETERM.	---	------	-----	--------	0.132	0.429
22	6.40E+00	UNDETERM.	---	------	-----	--------	0.12	0.421
21	9.77E-04	3D/2D	88.62	11.5552	12.5903	--------	3.57E-02	0.215
21	1.30E-03	3D/2D	88.07	11.426	12.1826	--------	3.25E-02	0.205
21	1.56E-03	2D	82.45	+	691.2143	i)	(	-89.1906
21	1.95E-03	2D	84.46	+	655.0559	i)	(	-81.0261
21	2.60E-03	2D	84.94	+	607.7726	i)	(	-74.4248
21	3.13E-03	2D	84.64	+	572.27	i)	(	-71.2184
21	3.91E-03	2D	83.69	+	521.1207	i)	(	-67.7446
21	5.21E-03	3D/2D	53.54	-4.8232	-23.4224	--------	3.62E-02	7.51E-02
21	6.25E-03	3D/2D	38.69	-0.8345	25.3832	--------	4.02E-02	0.117
21	7.81E-03	3D	---	------	-----	0.184	4.64E-02	0.157
21	1.04E-02	3D	---	------	-----	0.203	5.67E-02	0.202
21	1.25E-02	3D	---	------	-----	0.213	6.43E-02	0.23
21	1.56E-02	3D	---	------	-----	0.23	7.41E-02	0.265
21	2.08E-02	3D	---	------	-----	0.259	8.63E-02	0.309
21	2.50E-02	3D	---	------	-----	0.281	9.25E-02	0.333
21	3.12E-02	3D	---	------	-----	0.309	9.76E-02	0.357
21	4.17E-02	3D	---	------	-----	0.339	9.95E-02	0.371
21	5.00E-02	UNDETERM.	---	------	-----	--------	9.87E-02	0.368
21	6.25E-02	UNDETERM.	---	------	-----	--------	9.68E-02	0.353
21	8.33E-02	UNDETERM.	---	------	-----	--------	9.45E-02	0.32
21	1.00E-01	3D	---	------	-----	0.358	9.37E-02	0.294
21	1.25E-01	3D	---	------	-----	0.356	9.35E-02	0.259
21	1.67E-01	3D	---	------	-----	0.361	9.41E-02	0.214
21	2.00E-01	UNDETERM.	---	------	-----	--------	9.47E-02	0.185
21	2.50E-01	UNDETERM.	---	------	-----	--------	9.54E-02	0.151
21	3.33E-01	UNDETERM.	---	------	-----	--------	9.60E-02	0.106
21	4.00E-01	UNDETERM.	---	------	-----	--------	9.61E-02	7.62E-02
21	5.00E-01	UNDETERM.	---	------	-----	--------	9.58E-02	3.19E-02
21	6.67E-01	UNDETERM.	---	------	-----	--------	9.43E-02	3.71E-02

21	8.00E-01	UNDETERM.	---	------	-----	--------		9.25E-02	1.63E-02
21	1.00E+00	UNDETERM.	---	------	-----	--------		8.89E-02	6.36E-02
21	1.33E+00	UNDETERM.	---	------	-----	--------		8.16E-02	0.115
21	1.60E+00	UNDETERM.	---	------	-----	--------		7.55E-02	0.142
21	2.00E+00	UNDETERM.	---	------	-----	--------		6.68E-02	0.168
21	2.67E+00	UNDETERM.	---	------	-----	--------		5.48E-02	0.192
21	3.20E+00	UNDETERM.	---	------	-----	--------		4.75E-02	0.205
21	4.00E+00	UNDETERM.	---	------	-----	--------		3.94E-02	0.219
21	5.33E+00	UNDETERM.	---	------	-----	--------		3.12E-02	0.24
21	6.40E+00	UNDETERM.	---	------	-----	--------		2.78E-02	0.255
21	8.00E+00	UNDETERM.	---	------	-----	--------		2.61E-02	0.276
21	1.07E+01	UNDETERM.	---	------	-----	--------		2.87E-02	0.308
21	1.28E+01	UNDETERM.	---	------	-----	--------		3.28E-02	0.331
21	1.60E+01	UNDETERM.	---	------	-----	--------		3.98E-02	0.36
21	2.13E+01	UNDETERM.	---	------	-----	--------		5.10E-02	0.395
21	2.56E+01	UNDETERM.	---	------	-----	--------		5.87E-02	0.414
21	3.20E+01	UNDETERM.	---	------	-----	--------		6.79E-02	0.431
21	4.27E+01	UNDETERM.	---	------	-----	--------		7.81E-02	0.436
21	6.40E+01	UNDETERM.	---	------	-----	--------		8.82E-02	0.411
21	8.53E+01	UNDETERM.	---	------	-----	--------		9.26E-02	0.379
20	9.77E-04	3D/1D2D	---	------	-----	--------		4.83E-02	3.83E-02
20	1.30E-03	2D	46.42	+	460.323	i)		(	-342.593
20	1.95E-03	3D/2Dtw	81.37	3.599	3.4859	--------		5.74E-02	0.12
20	2.60E-03	3D	---	------	-----		0.19	6.51E-02	0.147
20	3.91E-03	3D	---	------	-----		0.319	8.07E-02	0.182
20	5.21E-03	3D	---	------	-----		0.494	9.56E-02	0.204
20	7.81E-03	3D	---	------	-----		0.956	0.122	0.23
20	1.04E-02	UNDETERM.	---	------	-----	--------		0.144	0.24
20	1.56E-02	UNDETERM.	---	------	-----	--------		0.174	0.238
20	2.08E-02	UNDETERM.	---	------	-----	--------		0.19	0.22
20	3.12E-02	UNDETERM.	---	------	-----	--------		0.199	0.178

20	4.17E-02	3D	---	------	-----	0.569	0.196	0.148
20	6.25E-02	UNDETERM.	---	------	-----	--------	0.186	0.136
20	8.33E-02	UNDETERM.	---	------	-----	--------	0.179	0.157
20	1.25E-01	UNDETERM.	---	------	-----	--------	0.175	0.209
20	1.67E-01	UNDETERM.	---	------	-----	--------	0.179	0.252
20	2.50E-01	UNDETERM.	---	------	-----	--------	0.199	0.316
20	3.33E-01	UNDETERM.	---	------	-----	--------	0.224	0.364
20	5.00E-01	UNDETERM.	---	------	-----	--------	0.278	0.433
20	6.67E-01	UNDETERM.	---	------	-----	--------	0.33	0.485
20	1.00E+00	UNDETERM.	---	------	-----	--------	0.427	0.56
20	1.33E+00	UNDETERM.	---	------	-----	--------	0.513	0.617
20	2.00E+00	UNDETERM.	---	------	-----	--------	0.659	0.699
20	2.67E+00	UNDETERM.	---	------	-----	--------	0.782	0.759
20	4.00E+00	UNDETERM.	---	------	-----	--------	0.986	0.845
20	5.33E+00	UNDETERM.	---	------	-----	--------	1.16	0.904
20	8.00E+00	UNDETERM.	---	------	-----	--------	1.44	0.972
20	1.07E+01	UNDETERM.	---	------	-----	--------	1.66	0.998
20	1.60E+01	UNDETERM.	---	------	-----	--------	1.96	0.976
20	2.13E+01	UNDETERM.	---	------	-----	--------	2.13	0.91
20	3.20E+01	UNDETERM.	---	------	-----	--------	2.25	0.772
20	4.27E+01	UNDETERM.	---	------	-----	--------	2.26	0.673
20	6.40E+01	UNDETERM.	---	------	-----	--------	2.23	0.602
20	8.53E+01	UNDETERM.	---	------	-----	--------	2.19	0.627
20	1.28E+02	UNDETERM.	---	------	-----	--------	2.18	0.749
20	1.71E+02	UNDETERM.	---	------	-----	--------	2.22	0.871
20	5.12E+02	3D/2Ddiag	---	------	-----	--------	6.37E+32	1.16E+16
19	1.56E-03	3D/1D2D	---	------	-----	--------	5.13E-02	0.133
19	1.95E-03	3D/1D2D	---	------	-----	--------	5.45E-02	0.141
19	2.60E-03	3D	---	------	-----	0.306	5.95E-02	0.151
19	3.13E-03	3D	---	------	-----	0.282	6.29E-02	0.156
19	3.91E-03	3D	---	------	-----	0.282	6.69E-02	0.162

19	5.21E-03	3D	---	------	-----	0.333	7.19E-02	0.169
19	6.25E-03	3D	---	------	-----	0.412	7.51E-02	0.174
19	7.81E-03	3D	---	------	-----	0.596	7.93E-02	0.181
19	1.04E-02	UNDETERM.	---	------	-----	--------	8.56E-02	0.191
19	1.25E-02	UNDETERM.	---	------	-----	--------	9.02E-02	0.197
19	2.50E-02	UNDETERM.	---	------	-----	--------	0.109	0.211
19	3.12E-02	UNDETERM.	---	------	-----	--------	0.114	0.212
19	4.17E-02	UNDETERM.	---	------	-----	--------	0.12	0.215
19	5.00E-02	UNDETERM.	---	------	-----	--------	0.124	0.219
19	6.25E-02	UNDETERM.	---	------	-----	--------	0.13	0.225
19	8.33E-02	UNDETERM.	---	------	-----	--------	0.138	0.239
19	1.00E-01	UNDETERM.	---	------	-----	--------	0.145	0.249
19	1.25E-01	UNDETERM.	---	------	-----	--------	0.156	0.264
19	1.67E-01	UNDETERM.	---	------	-----	--------	0.173	0.284
19	2.00E-01	UNDETERM.	---	------	-----	--------	0.185	0.296
19	2.50E-01	UNDETERM.	---	------	-----	--------	0.201	0.309
19	3.33E-01	UNDETERM.	---	------	-----	--------	0.221	0.326
19	4.00E-01	UNDETERM.	---	------	-----	--------	0.233	0.338
19	5.00E-01	UNDETERM.	---	------	-----	--------	0.249	0.354
19	6.67E-01	UNDETERM.	---	------	-----	--------	0.272	0.38
19	8.00E-01	UNDETERM.	---	------	-----	--------	0.289	0.401
19	1.00E+00	UNDETERM.	---	------	-----	--------	0.315	0.43
19	1.33E+00	UNDETERM.	---	------	-----	--------	0.358	0.472
19	1.60E+00	UNDETERM.	---	------	-----	--------	0.393	0.5
19	2.00E+00	UNDETERM.	---	------	-----	--------	0.441	0.534
19	2.67E+00	UNDETERM.	---	------	-----	--------	0.513	0.573
19	3.20E+00	UNDETERM.	---	------	-----	--------	0.562	0.595
19	4.00E+00	UNDETERM.	---	------	-----	--------	0.625	0.619
19	5.33E+00	UNDETERM.	---	------	-----	--------	0.71	0.646
19	6.40E+00	UNDETERM.	---	------	-----	--------	0.767	0.661
19	8.00E+00	UNDETERM.	---	------	-----	--------	0.84	0.677

19	1.07E+01	UNDETERM.	---	------	-----	--------	0.939	0.692
19	1.28E+01	UNDETERM.	---	------	-----	--------	1	0.697
19	1.60E+01	UNDETERM.	---	------	-----	--------	1.08	0.697
19	2.13E+01	UNDETERM.	---	------	-----	--------	1.16	0.689
19	2.56E+01	UNDETERM.	---	------	-----	--------	1.21	0.681
19	3.20E+01	UNDETERM.	---	------	-----	--------	1.27	0.668
19	4.27E+01	UNDETERM.	---	------	-----	--------	1.33	0.65
19	5.12E+01	UNDETERM.	---	------	-----	--------	1.37	0.639
19	6.40E+01	UNDETERM.	---	------	-----	--------	1.4	0.63
18	1.56E-03	UNDETERM.	---	------	-----	--------	0.722	0.727
18	1.95E-03	UNDETERM.	---	------	-----	--------	0.78	0.732
18	2.60E-03	UNDETERM.	---	------	-----	--------	0.864	0.749
18	3.13E-03	3D	---	------	-----	0.64	0.925	0.771
18	3.91E-03	3D	---	------	-----	0.63	1.01	0.816
18	5.21E-03	3D	---	------	-----	0.639	1.15	0.901
18	6.25E-03	3D	---	------	-----	0.654	1.26	0.97
18	7.81E-03	3D	---	------	-----	0.676	1.42	1.06
18	1.04E-02	3D	---	------	-----	0.697	1.68	1.17
18	1.25E-02	UNDETERM.	---	------	-----	--------	1.87	1.22
18	2.08E-02	UNDETERM.	---	------	-----	--------	2.5	1.02
18	2.50E-02	UNDETERM.	---	------	-----	--------	2.67	0.638
18	3.12E-02	UNDETERM.	---	------	-----	--------	2.76	0.79
18	4.17E-02	UNDETERM.	---	------	-----	--------	2.62	1.34
18	5.00E-02	UNDETERM.	---	------	-----	--------	2.42	1.48
18	6.25E-02	UNDETERM.	---	------	-----	--------	2.15	1.51
18	8.33E-02	UNDETERM.	---	------	-----	--------	1.83	1.43
18	1.00E-01	UNDETERM.	---	------	-----	--------	1.68	1.34
18	1.25E-01	UNDETERM.	---	------	-----	--------	1.55	1.22
18	1.67E-01	UNDETERM.	---	------	-----	--------	1.46	1.06
18	2.00E-01	UNDETERM.	---	------	-----	--------	1.44	0.952
18	2.50E-01	UNDETERM.	---	------	-----	--------	1.44	0.806

18	3.33E-01	UNDETERM.	---	------	-----	--------		1.47	0.557
18	4.00E-01	UNDETERM.	---	------	-----	--------		1.49	0.292
18	5.00E-01	UNDETERM.	---	------	-----	--------		1.52	0.452
18	6.67E-01	UNDETERM.	---	------	-----	--------		1.54	0.775
18	8.00E-01	UNDETERM.	---	------	-----	--------		1.55	0.928
18	1.00E+00	UNDETERM.	---	------	-----	--------		1.57	1.09
18	1.33E+00	UNDETERM.	---	------	-----	--------		1.61	1.28
18	1.60E+00	UNDETERM.	---	------	-----	--------		1.66	1.4
18	2.00E+00	UNDETERM.	---	------	-----	--------		1.76	1.55
18	2.67E+00	UNDETERM.	---	------	-----	--------		2	1.75
18	3.20E+00	UNDETERM.	---	------	-----	--------		2.2	1.87
18	4.00E+00	UNDETERM.	---	------	-----	--------		2.49	1.98
18	5.33E+00	UNDETERM.	---	------	-----	--------		2.81	2
18	6.40E+00	UNDETERM.	---	------	-----	--------		2.93	1.91
18	8.00E+00	UNDETERM.	---	------	-----	--------		2.97	1.74
18	1.07E+01	UNDETERM.	---	------	-----	--------		2.87	1.47
18	1.28E+01	UNDETERM.	---	------	-----	--------		2.77	1.33
18	1.60E+01	UNDETERM.	---	------	-----	--------		2.67	1.21
18	2.13E+01	UNDETERM.	---	------	-----	--------		2.62	1.17
18	2.56E+01	UNDETERM.	---	------	-----	--------		2.64	1.19
18	3.20E+01	UNDETERM.	---	------	-----	--------		2.75	1.25
18	4.27E+01	UNDETERM.	---	------	-----	--------		3.03	1.36
18	5.12E+01	UNDETERM.	---	------	-----	--------		3.3	1.43
18	6.40E+01	UNDETERM.	---	------	-----	--------		3.73	1.5
18	8.53E+01	UNDETERM.	---	------	-----	--------		4.43	1.53
17	1.56E-03	3D/2D	0.11	2.2448	0.5061	--------		1.72E-02	0.104
17	1.95E-03	3D/2D	0.31	2.5086	0.5417	--------		1.94E-02	0.114
17	2.60E-03	3D/2D	0.8	2.9168	0.4905	--------		2.28E-02	0.126
17	3.13E-03	2D	1.33	+	1971.743	i)		(- 1193.5314	-
17	3.91E-03	3D	---	------	-----		0.192	2.88E-02	0.144

17	5.21E-03	3D	---	------	-----	0.434	3.40E-02	0.156
17	6.25E-03	1D	---	------	-----	--------	3.76E-02	0.163
17	7.81E-03	1D	---	------	-----	--------	4.23E-02	0.172
17	1.04E-02	1D	---	------	-----	--------	4.91E-02	0.183
17	1.25E-02	3D	---	------	-----	0.777	5.40E-02	0.191
17	1.56E-02	UNDETERM.	---	------	-----	--------	6.11E-02	0.202
17	2.50E-02	UNDETERM.	---	------	-----	--------	8.05E-02	0.227
17	3.12E-02	3D	---	------	-----	0.395	9.16E-02	0.238
17	4.17E-02	3D	---	------	-----	0.408	0.107	0.25
17	5.00E-02	UNDETERM.	---	------	-----	--------	0.116	0.255
17	6.25E-02	UNDETERM.	---	------	-----	--------	0.128	0.26
17	8.33E-02	UNDETERM.	---	------	-----	--------	0.141	0.263
17	1.00E-01	UNDETERM.	---	------	-----	--------	0.149	0.264
17	1.25E-01	UNDETERM.	---	------	-----	--------	0.159	0.264
17	1.67E-01	UNDETERM.	---	------	-----	--------	0.172	0.262
17	2.00E-01	UNDETERM.	---	------	-----	--------	0.179	0.259
17	2.50E-01	UNDETERM.	---	------	-----	--------	0.186	0.253
17	3.33E-01	UNDETERM.	---	------	-----	--------	0.194	0.244
17	4.00E-01	UNDETERM.	---	------	-----	--------	0.197	0.241
17	5.00E-01	UNDETERM.	---	------	-----	--------	0.202	0.241
17	6.67E-01	UNDETERM.	---	------	-----	--------	0.21	0.248
17	8.00E-01	UNDETERM.	---	------	-----	--------	0.218	0.254
17	1.00E+00	UNDETERM.	---	------	-----	--------	0.23	0.26
17	1.33E+00	UNDETERM.	---	------	-----	--------	0.249	0.26
17	1.60E+00	UNDETERM.	---	------	-----	--------	0.263	0.252
17	2.00E+00	UNDETERM.	---	------	-----	--------	0.279	0.23
17	2.67E+00	UNDETERM.	---	------	-----	--------	0.298	0.173
17	3.20E+00	UNDETERM.	---	------	-----	--------	0.307	9.74E-02
17	4.00E+00	UNDETERM.	---	------	-----	--------	0.313	0.142
17	5.33E+00	UNDETERM.	---	------	-----	--------	0.312	0.245
17	6.40E+00	UNDETERM.	---	------	-----	--------	0.305	0.286

17	8.00E+00	UNDETERM.	---	------	-----	--------	0.291	0.319
17	1.07E+01	UNDETERM.	---	------	-----	--------	0.269	0.337
17	2.13E+01	UNDETERM.	---	------	-----	--------	0.219	0.317
84	7.81E-04	UNDETERM.	---	------	-----	--------	0.903	0.914
84	9.77E-04	3D	---	------	-----	0.382	0.872	0.874
84	1.30E-03	3D	---	------	-----	0.388	0.829	0.809
84	1.56E-03	3D	---	------	-----	0.387	0.802	0.765
84	1.95E-03	3D	---	------	-----	0.383	0.773	0.711
84	2.60E-03	3D	---	------	-----	0.373	0.745	0.646
84	3.13E-03	3D	---	------	-----	0.366	0.733	0.608
84	3.91E-03	3D	---	------	-----	0.355	0.725	0.564
84	5.21E-03	3D	---	------	-----	0.337	0.72	0.507
84	6.25E-03	3D	---	------	-----	0.322	0.716	0.468
84	7.81E-03	3D	---	------	-----	0.295	0.705	0.414
84	1.04E-02	3D	---	------	-----	0.239	0.679	0.33
84	1.25E-02	3D	---	------	-----	0.184	0.655	0.267
84	1.56E-02	3D/2D	70.6	45.5383	19.6147	--------	0.621	0.167
84	2.08E-02	3D/2D	67.5	-3.9869	-33.5977	--------	0.576	0.144
84	2.50E-02	3D	---	------	-----	0.219	0.551	0.218
84	3.12E-02	3D	---	------	-----	0.387	0.53	0.277
84	4.17E-02	UNDETERM.	---	------	-----	--------	0.52	0.33
84	5.00E-02	UNDETERM.	---	------	-----	--------	0.524	0.353
84	6.25E-02	UNDETERM.	---	------	-----	--------	0.539	0.371
84	8.33E-02	UNDETERM.	---	------	-----	--------	0.572	0.375
84	1.00E-01	3D	---	------	-----	0.648	0.597	0.366
84	1.25E-01	3D	---	------	-----	0.594	0.63	0.342
84	1.67E-01	3D	---	------	-----	0.481	0.672	0.295
84	2.00E-01	3D	---	------	-----	0.388	0.697	0.259
84	2.50E-01	3D	---	------	-----	0.27	0.723	0.21
84	3.33E-01	3D/2D	64.46	-24.109	-61.7229	--------	0.751	0.154
84	4.00E-01	3D/2D	65.5	-23.5775	-59.8121	--------	0.766	0.133

84	5.00E-01	3D/2D	65.27	-22.9567	-59.1039	--------	0.787	0.139
84	6.67E-01	3D	---	------	-----	0.196	0.828	0.189
84	8.00E-01	3D	---	------	-----	0.272	0.866	0.232
84	1.00E+00	3D	---	------	-----	0.368	0.933	0.286
84	1.33E+00	UNDETERM.	---	------	-----	--------	1.05	0.352
84	1.60E+00	UNDETERM.	---	------	-----	--------	1.14	0.39
84	2.00E+00	UNDETERM.	---	------	-----	--------	1.25	0.428
84	2.67E+00	UNDETERM.	---	------	-----	--------	1.38	0.456
84	3.20E+00	UNDETERM.	---	------	-----	--------	1.43	0.456
84	4.00E+00	UNDETERM.	---	------	-----	--------	1.45	0.428
84	5.33E+00	UNDETERM.	---	------	-----	--------	1.39	0.329
84	6.40E+00	UNDETERM.	---	------	-----	--------	1.32	0.202
84	8.00E+00	UNDETERM.	---	------	-----	--------	1.21	0.229
84	1.07E+01	UNDETERM.	---	------	-----	--------	1.05	0.407
84	1.28E+01	3D/2Ddiag	---	------	-----	--------	#NAME?	NaN
84	2.13E+01	3D/2Ddiag	---	------	-----	--------	#NAME?	NaN
84	5.12E+01	UNDETERM.	---	------	-----	--------	0.397	0.395
84	6.40E+01	UNDETERM.	---	------	-----	--------	0.363	0.349
84	8.53E+01	UNDETERM.	---	------	-----	--------	0.335	0.292
1	3.91E-03	3D	---	------	-----	0.239	0.204	0.163
1	5.21E-03	3D	---	------	-----	0.183	0.205	0.141
1	7.81E-03	3D/2Dtw	89.36	23.8834	-16.491	--------	0.201	0.112
1	1.04E-02	3D/2Dtw	89.99	25.0764	-18.318	--------	0.194	9.66E-02
1	1.56E-02	3D/2Dtw	2.38	29.0473	-24.5088	--------	0.182	9.31E-02
1	2.08E-02	3D/1D2D	---	------	-----	--------	0.174	0.108
1	3.12E-02	UNDETERM.	---	------	-----	--------	0.169	0.145
1	4.17E-02	3D	---	------	-----	0.546	0.169	0.178
1	6.25E-02	UNDETERM.	---	------	-----	--------	0.179	0.226
1	8.33E-02	UNDETERM.	---	------	-----	--------	0.194	0.259
1	1.25E-01	UNDETERM.	---	------	-----	--------	0.224	0.298
1	1.67E-01	UNDETERM.	---	------	-----	--------	0.251	0.317

1	2.50E-01	UNDETERM.	---	------	-----	--------	0.29	0.325
1	3.33E-01	UNDETERM.	---	------	-----	--------	0.316	0.319
1	5.00E-01	UNDETERM.	---	------	-----	--------	0.353	0.302
1	6.67E-01	UNDETERM.	---	------	-----	--------	0.383	0.291
1	1.00E+00	UNDETERM.	---	------	-----	--------	0.435	0.286
1	2.00E+00	UNDETERM.	---	------	-----	--------	2	0
1	4.00E+00	UNDETERM.	---	------	-----	--------	2	0
89	7.81E-04	UNDETERM.	---	------	-----	--------	3.10E-02	0.416
89	9.77E-04	UNDETERM.	---	------	-----	--------	3.22E-02	0.443
89	1.30E-03	UNDETERM.	---	------	-----	--------	3.32E-02	0.473
89	1.56E-03	UNDETERM.	---	------	-----	--------	3.34E-02	0.488
89	1.95E-03	3D	---	------	-----	0.76	3.29E-02	0.504
89	2.60E-03	3D	---	------	-----	0.662	3.16E-02	0.523
89	3.13E-03	3D	---	------	-----	0.603	3.07E-02	0.536
89	3.91E-03	3D	---	------	-----	0.54	3.05E-02	0.554
89	5.21E-03	3D	---	------	-----	0.471	3.30E-02	0.582
89	6.25E-03	3D	---	------	-----	0.435	3.70E-02	0.603
89	7.81E-03	3D	---	------	-----	0.394	4.49E-02	0.629
89	1.04E-02	3D	---	------	-----	0.348	6.12E-02	0.664
89	1.25E-02	3D	---	------	-----	0.321	7.58E-02	0.687
89	1.56E-02	3D	---	------	-----	0.292	9.90E-02	0.715
89	2.08E-02	UNDETERM.	---	------	-----	--------	0.14	0.758
89	2.50E-02	UNDETERM.	---	------	-----	--------	0.173	0.798
89	3.12E-02	UNDETERM.	---	------	-----	--------	0.223	0.869
89	4.17E-02	UNDETERM.	---	------	-----	--------	0.306	1.01
89	5.00E-02	UNDETERM.	---	------	-----	--------	0.372	1.13
89	6.25E-02	UNDETERM.	---	------	-----	--------	0.466	1.3
89	8.33E-02	UNDETERM.	---	------	-----	--------	0.61	1.54
89	1.00E-01	UNDETERM.	---	------	-----	--------	0.712	1.7
89	1.25E-01	UNDETERM.	---	------	-----	--------	0.845	1.89
89	1.67E-01	UNDETERM.	---	------	-----	--------	1.02	2.12

89	2.00E-01	UNDETERM.	---	------	-----	--------	1.13	2.25
89	2.50E-01	UNDETERM.	---	------	-----	--------	1.26	2.42
89	3.33E-01	UNDETERM.	---	------	-----	--------	1.41	2.63
89	4.00E-01	UNDETERM.	---	------	-----	--------	1.49	2.77
89	5.00E-01	UNDETERM.	---	------	-----	--------	1.57	2.94
89	6.67E-01	UNDETERM.	---	------	-----	--------	1.64	3.17
89	8.00E-01	UNDETERM.	---	------	-----	--------	1.66	3.31
89	1.00E+00	UNDETERM.	---	------	-----	--------	1.63	3.46
89	1.33E+00	UNDETERM.	---	------	-----	--------	1.52	3.55
89	1.60E+00	UNDETERM.	---	------	-----	--------	1.41	3.52
89	2.00E+00	UNDETERM.	---	------	-----	--------	1.24	3.38
89	2.67E+00	UNDETERM.	---	------	-----	--------	1.01	3.04
89	3.20E+00	UNDETERM.	---	------	-----	--------	0.867	2.78
89	4.00E+00	UNDETERM.	---	------	-----	--------	0.722	2.44
89	5.33E+00	UNDETERM.	---	------	-----	--------	0.58	2.01
89	6.40E+00	UNDETERM.	---	------	-----	--------	0.514	1.74
89	8.00E+00	UNDETERM.	---	------	-----	--------	0.456	1.41
89	1.07E+01	UNDETERM.	---	------	-----	--------	0.406	0.929
89	1.28E+01	UNDETERM.	---	------	-----	--------	0.386	0.492
89	1.60E+01	UNDETERM.	---	------	-----	--------	0.371	0.653
89	2.13E+01	UNDETERM.	---	------	-----	--------	0.361	1.06
89	2.56E+01	UNDETERM.	---	------	-----	--------	0.359	1.21
89	3.20E+01	UNDETERM.	---	------	-----	--------	0.359	1.31
89	4.27E+01	UNDETERM.	---	------	-----	--------	0.361	1.34
89	5.12E+01	UNDETERM.	---	------	-----	--------	0.362	1.31
89	6.40E+01	UNDETERM.	---	------	-----	--------	0.362	1.25
89	8.53E+01	UNDETERM.	---	------	-----	--------	0.363	1.13
12	7.81E-04	UNDETERM.	---	------	-----	--------	3.11E-02	9.84E-02
12	9.77E-04	UNDETERM.	---	------	-----	--------	3.24E-02	0.13
12	1.30E-03	UNDETERM.	---	------	-----	--------	3.58E-02	0.16
12	1.56E-03	UNDETERM.	---	------	-----	--------	3.93E-02	0.175

12	1.95E-03	UNDETERM.	---	------	-----	--------		4.53E-02	0.189
12	2.60E-03	UNDETERM.	---	------	-----	--------		5.60E-02	0.201
12	3.13E-03	3D	---	------	-----		0.354	6.46E-02	0.206
12	3.91E-03	3D	---	------	-----		0.326	7.66E-02	0.209
12	5.21E-03	3D	---	------	-----		0.293	9.34E-02	0.209
12	6.25E-03	3D	---	------	-----		0.275	0.104	0.206
12	7.81E-03	3D	---	------	-----		0.256	0.116	0.198
12	1.04E-02	3D	---	------	-----		0.233	0.128	0.182
12	1.25E-02	3D	---	------	-----		0.221	0.134	0.17
12	1.56E-02	3D	---	------	-----		0.216	0.14	0.157
12	2.08E-02	UNDETERM.	---	------	-----	--------		0.147	0.149
12	2.50E-02	UNDETERM.	---	------	-----	--------		0.15	0.152
12	3.12E-02	3D	---	------	-----		0.485	0.155	0.163
12	4.17E-02	UNDETERM.	---	------	-----	--------		0.162	0.179
12	5.00E-02	UNDETERM.	---	------	-----	--------		0.167	0.185
12	6.25E-02	UNDETERM.	---	------	-----	--------		0.172	0.18
12	8.33E-02	UNDETERM.	---	------	-----	--------		0.178	0.143
12	1.00E-01	UNDETERM.	---	------	-----	--------		0.18	8.48E-02
12	1.25E-01	UNDETERM.	---	------	-----	--------		0.181	0.122
12	1.67E-01	UNDETERM.	---	------	-----	--------		0.183	0.227
12	2.00E-01	UNDETERM.	---	------	-----	--------		0.186	0.281
12	2.50E-01	UNDETERM.	---	------	-----	--------		0.192	0.342
12	4.00E-01	UNDETERM.	---	------	-----	--------		0.217	0.463
12	5.00E-01	UNDETERM.	---	------	-----	--------		0.238	0.518
12	6.67E-01	UNDETERM.	---	------	-----	--------		0.275	0.585
12	8.00E-01	UNDETERM.	---	------	-----	--------		0.305	0.622
12	1.00E+00	UNDETERM.	---	------	-----	--------		0.348	0.658
12	1.60E+00	1D	---	------	-----	--------		4.09E+31	3.39E+15
12	2.67E+00	1D	---	------	-----	--------		5.45E+31	3.63E+15
12	4.00E+00	1D	---	------	-----	--------		6.86E+31	4.29E+15
15	1.30E-03	UNDETERM.	---	------	-----	--------		0.491	0.238

15	1.56E-03	3D/2D	5.3	14.209	10.9221	--------	0.533	0.104
15	1.95E-03	3D/2D	7	9.5866	12.5743	--------	0.576	0.353
15	2.60E-03	UNDETERM.	---	------	-----	--------	0.609	0.552
15	3.13E-03	3D	---	------	-----	0.281	0.616	0.647
15	3.91E-03	3D	---	------	-----	0.415	0.611	0.735
15	5.21E-03	3D	---	------	-----	0.602	0.587	0.801
15	6.25E-03	3D	---	------	-----	0.718	0.565	0.818
15	7.81E-03	3D	---	------	-----	0.837	0.535	0.817
15	1.04E-02	3D	---	------	-----	0.903	0.493	0.786
15	1.25E-02	3D	---	------	-----	0.851	0.466	0.748
15	1.56E-02	UNDETERM.	---	------	-----	--------	0.432	0.678
15	2.50E-02	UNDETERM.	---	------	-----	--------	0.363	0.359
15	3.12E-02	UNDETERM.	---	------	-----	--------	0.333	0.325
15	4.17E-02	UNDETERM.	---	------	-----	--------	0.298	0.716
15	5.00E-02	UNDETERM.	---	------	-----	--------	0.281	0.923
15	6.25E-02	UNDETERM.	---	------	-----	--------	0.265	1.18
15	8.33E-02	UNDETERM.	---	------	-----	--------	0.256	1.55
15	1.00E-01	UNDETERM.	---	------	-----	--------	0.257	1.82
15	1.25E-01	UNDETERM.	---	------	-----	--------	0.268	2.22
15	1.67E-01	UNDETERM.	---	------	-----	--------	0.3	2.92
15	2.00E-01	UNDETERM.	---	------	-----	--------	0.336	3.51
15	2.50E-01	UNDETERM.	---	------	-----	--------	0.403	4.46
15	3.33E-01	UNDETERM.	---	------	-----	--------	0.541	6.19
16	7.81E-04	3D	---	------	-----	0.249	2.72E-02	0.211
16	9.77E-04	UNDETERM.	---	------	-----	--------	2.67E-02	0.219
16	1.30E-03	UNDETERM.	---	------	-----	--------	2.56E-02	0.22
16	1.56E-03	UNDETERM.	---	------	-----	--------	2.47E-02	0.215
16	1.95E-03	UNDETERM.	---	------	-----	--------	2.33E-02	0.203
16	2.60E-03	3D/2D	88.15	-1.7444	6.2296	--------	2.13E-02	0.182
16	3.13E-03	2D	2.58	+	1684.3936	i)	(	-569.9615
16	3.91E-03	2D	2.5	+	1514.2636	i)	(	-568.6737

16	5.21E-03	2D	2.41	+	1382.2515	i)	(	-565.4144
16	6.25E-03	2D	2.38	+	1335.4188	i)	(	-561.9849
16	7.81E-03	2D	2.43	+	1299.9653	i)	(	-555.7101
16	1.04E-02	2D	2.74	+	1258.2257	i)	(	-542.8162
16	2.50E-02	3D/2D	87.01	1.5685	4.5156	--------	1.45E-02	0.183
16	3.12E-02	UNDETERM.	---	------	-----	--------	1.57E-02	0.191
16	4.17E-02	3D/2D	85.64	3.8553	5.6638	--------	1.77E-02	0.196
16	5.00E-02	UNDETERM.	---	------	-----	--------	1.94E-02	0.197
16	6.25E-02	UNDETERM.	---	------	-----	--------	2.16E-02	0.194
16	8.33E-02	UNDETERM.	---	------	-----	--------	2.50E-02	0.187
16	1.00E-01	UNDETERM.	---	------	-----	--------	2.73E-02	0.18
16	1.25E-01	UNDETERM.	---	------	-----	--------	3.01E-02	0.168
16	1.67E-01	UNDETERM.	---	------	-----	--------	3.31E-02	0.146
16	4.00E-01	UNDETERM.	---	------	-----	--------	2.71E-02	0.117
16	5.00E-01	UNDETERM.	---	------	-----	--------	1.87E-02	0.157
16	6.67E-01	UNDETERM.	---	------	-----	--------	1.90E-04	0.195
16	8.00E-01	UNDETERM.	---	------	-----	--------	1.87E-02	0.21
16	1.00E+00	UNDETERM.	---	------	-----	--------	5.16E-02	0.213
16	1.33E+00	UNDETERM.	---	------	-----	--------	0.118	0.163
16	1.60E+00	UNDETERM.	---	------	-----	--------	0.178	7.70E-02

2. Northwest-Southeast long survey line.

Site	Per(s)	DIM	STRIKE(∫)	twist(∫)	shear(∫)	I7	skew	ph_s_skew
6	9.77E-04	3D/2D	80.05	-2.7575	-6.0832	--------	7.01E-03	8.90E-02
6	1.30E-03	3D/2D	75.17	-4.7079	-10.8944	--------	7.68E-03	9.63E-02
6	1.56E-03	3D	---	------	-----	0.153	9.26E-03	0.1
6	1.95E-03	3D/2D	48.18	-2.8964	-23.345	--------	1.24E-02	0.103
6	2.60E-03	3D/2D	22.39	4.253	20.4945	--------	1.84E-02	0.101

6	3.13E-03	3D/2D	15.76	4.7552	17.389	--------	2.33E-02	9.49E-02
6	3.91E-03	3D/2D	11.88	4.6049	14.9959	--------	3.04E-02	8.13E-02
6	5.21E-03	3D/2D	9.55	4.535	13.3767	--------	4.09E-02	4.90E-02
6	6.25E-03	3D/2D	8.8	4.6295	12.7904	--------	4.83E-02	2.02E-02
6	7.81E-03	3D/2D	8.33	4.8258	12.2883	--------	5.75E-02	5.95E-02
6	1.04E-02	3D/2Dtw	8.3	5.1155	11.7664	--------	6.92E-02	8.32E-02
6	1.25E-02	3D/2D	8.67	5.3193	11.4309	--------	7.65E-02	9.50E-02
6	1.56E-02	3D/2D	9.68	5.6559	10.9309	--------	8.51E-02	0.11
6	2.08E-02	UNDETERM.	---	------	-----	--------	9.65E-02	0.133
6	2.50E-02	3D/2D	15.13	7.2064	8.8583	--------	0.104	0.149
6	3.12E-02	3D	---	------	-----	0.178	0.115	0.164
6	4.17E-02	UNDETERM.	---	------	-----	--------	0.129	0.171
6	5.00E-02	UNDETERM.	---	------	-----	--------	0.139	0.163
6	6.25E-02	UNDETERM.	---	------	-----	--------	0.149	0.133
6	8.33E-02	UNDETERM.	---	------	-----	--------	0.157	5.55E-02
6	1.00E-01	UNDETERM.	---	------	-----	--------	0.158	0.141
6	1.25E-01	3D	---	------	-----	0.359	0.155	0.204
6	1.67E-01	3D	---	------	-----	0.622	0.146	0.259
6	2.00E-01	UNDETERM.	---	------	-----	--------	0.137	0.285
6	2.50E-01	UNDETERM.	---	------	-----	--------	0.127	0.312
6	3.33E-01	UNDETERM.	---	------	-----	--------	0.115	0.345
6	4.00E-01	UNDETERM.	---	------	-----	--------	0.111	0.367
6	5.00E-01	UNDETERM.	---	------	-----	--------	0.108	0.396
6	6.67E-01	UNDETERM.	---	------	-----	--------	0.11	0.436
6	8.00E-01	UNDETERM.	---	------	-----	--------	0.115	0.461
6	1.00E+00	UNDETERM.	---	------	-----	--------	0.125	0.487
6	1.33E+00	UNDETERM.	---	------	-----	--------	0.141	0.509
6	1.60E+00	UNDETERM.	---	------	-----	--------	0.154	0.513
6	2.00E+00	UNDETERM.	---	------	-----	--------	0.173	0.508
6	2.67E+00	UNDETERM.	---	------	-----	--------	0.201	0.486
6	3.20E+00	UNDETERM.	---	------	-----	--------	0.222	0.464

6	4.00E+00	UNDETERM.	---	------	-----	--------	0.253	0.433
6	5.33E+00	UNDETERM.	---	------	-----	--------	0.3	0.384
6	6.40E+00	UNDETERM.	---	------	-----	--------	0.334	0.349
6	8.00E+00	UNDETERM.	---	------	-----	--------	0.377	0.298
6	1.07E+01	UNDETERM.	---	------	-----	--------	0.429	0.221
6	1.28E+01	UNDETERM.	---	------	-----	--------	0.456	0.173
6	2.13E+01	UNDETERM.	---	------	-----	--------	0.511	0.174
6	2.56E+01	UNDETERM.	---	------	-----	--------	0.528	0.194
6	3.20E+01	UNDETERM.	---	------	-----	--------	0.546	0.173
6	4.27E+01	UNDETERM.	---	------	-----	--------	0.553	0.139
6	5.12E+01	UNDETERM.	---	------	-----	--------	0.543	0.257
6	6.40E+01	UNDETERM.	---	------	-----	--------	0.513	0.35
6	8.53E+01	UNDETERM.	---	------	-----	--------	0.454	0.414
5	9.77E-04	3D/2Dtw	89.11	7.8381	4.7584	--------	9.66E-02	9.09E-02
5	1.30E-03	3D/1D2D	---	------	-----	--------	9.31E-02	0.102
5	1.56E-03	3D/1D2D	---	------	-----	--------	9.16E-02	0.114
5	1.95E-03	3D	---	------	-----	0.278	9.12E-02	0.133
5	2.60E-03	3D	---	------	-----	0.271	9.36E-02	0.159
5	3.13E-03	3D	---	------	-----	0.292	9.68E-02	0.176
5	3.91E-03	3D	---	------	-----	0.331	0.103	0.195
5	5.21E-03	3D	---	------	-----	0.389	0.113	0.217
5	6.25E-03	3D	---	------	-----	0.421	0.12	0.23
5	7.81E-03	3D	---	------	-----	0.447	0.131	0.244
5	1.04E-02	3D	---	------	-----	0.454	0.145	0.259
5	1.25E-02	3D	---	------	-----	0.449	0.154	0.268
5	1.56E-02	3D	---	------	-----	0.44	0.166	0.278
5	2.08E-02	3D	---	------	-----	0.444	0.181	0.29
5	2.50E-02	UNDETERM.	---	------	-----	--------	0.192	0.298
5	3.12E-02	3D	---	------	-----	0.519	0.206	0.308
5	4.17E-02	UNDETERM.	---	------	-----	--------	0.228	0.321
5	5.00E-02	UNDETERM.	---	------	-----	--------	0.244	0.328

5	6.25E-02	UNDETERM.	---	------	-----	--------	0.265	0.332
5	8.33E-02	UNDETERM.	---	------	-----	--------	0.292	0.326
5	1.00E-01	UNDETERM.	---	------	-----	--------	0.307	0.314
5	1.25E-01	UNDETERM.	---	------	-----	--------	0.319	0.289
5	1.67E-01	UNDETERM.	---	------	-----	--------	0.324	0.248
5	2.00E-01	UNDETERM.	---	------	-----	--------	0.32	0.225
5	2.50E-01	UNDETERM.	---	------	-----	--------	0.311	0.211
5	3.33E-01	UNDETERM.	---	------	-----	--------	0.298	0.227
5	4.00E-01	UNDETERM.	---	------	-----	--------	0.293	0.253
5	5.00E-01	UNDETERM.	---	------	-----	--------	0.292	0.295
5	6.67E-01	UNDETERM.	---	------	-----	--------	0.306	0.358
5	8.00E-01	UNDETERM.	---	------	-----	--------	0.323	0.4
5	1.00E+00	UNDETERM.	---	------	-----	--------	0.356	0.453
5	1.33E+00	UNDETERM.	---	------	-----	--------	0.416	0.52
5	1.60E+00	UNDETERM.	---	------	-----	--------	0.463	0.561
5	2.00E+00	UNDETERM.	---	------	-----	--------	0.531	0.606
5	2.67E+00	UNDETERM.	---	------	-----	--------	0.626	0.654
5	3.20E+00	UNDETERM.	---	------	-----	--------	0.688	0.676
5	4.00E+00	UNDETERM.	---	------	-----	--------	0.76	0.695
5	5.33E+00	UNDETERM.	---	------	-----	--------	0.843	0.711
5	6.40E+00	UNDETERM.	---	------	-----	--------	0.892	0.721
5	8.00E+00	UNDETERM.	---	------	-----	--------	0.949	0.738
5	1.07E+01	UNDETERM.	---	------	-----	--------	1.03	0.774
5	1.28E+01	UNDETERM.	---	------	-----	--------	1.08	0.807
5	1.60E+01	UNDETERM.	---	------	-----	--------	1.17	0.858
5	2.13E+01	UNDETERM.	---	------	-----	--------	1.31	0.94
5	2.56E+01	UNDETERM.	---	------	-----	--------	1.42	0.999
5	3.20E+01	UNDETERM.	---	------	-----	--------	1.57	1.07
5	4.27E+01	UNDETERM.	---	------	-----	--------	1.8	1.17
5	6.40E+01	UNDETERM.	---	------	-----	--------	2.17	1.31
5	8.53E+01	UNDETERM.	---	------	-----	--------	2.46	1.41

4	7.81E-04	UNDETERM.	---	------	-----	--------	5.73E-02	0.274
4	9.77E-04	UNDETERM.	---	------	-----	--------	6.07E-02	0.304
4	1.30E-03	3D	---	------	-----	0.737	6.73E-02	0.347
4	1.56E-03	3D	---	------	-----	0.734	7.31E-02	0.376
4	1.95E-03	3D	---	------	-----	0.727	8.20E-02	0.412
4	2.60E-03	3D	---	------	-----	0.715	9.67E-02	0.457
4	3.13E-03	3D	---	------	-----	0.703	0.108	0.482
4	3.91E-03	3D	---	------	-----	0.683	0.122	0.506
4	5.21E-03	3D	---	------	-----	0.647	0.14	0.523
4	6.25E-03	3D	---	------	-----	0.62	0.15	0.524
4	7.81E-03	UNDETERM.	---	------	-----	--------	0.16	0.515
4	1.04E-02	UNDETERM.	---	------	-----	--------	0.166	0.493
4	1.25E-02	UNDETERM.	---	------	-----	--------	0.165	0.477
4	1.56E-02	UNDETERM.	---	------	-----	--------	0.16	0.463
4	2.08E-02	UNDETERM.	---	------	-----	--------	0.144	0.461
4	2.50E-02	UNDETERM.	---	------	-----	--------	0.13	0.469
4	3.12E-02	UNDETERM.	---	------	-----	--------	0.112	0.479
4	4.17E-02	UNDETERM.	---	------	-----	--------	8.91E-02	0.479
4	5.00E-02	UNDETERM.	---	------	-----	--------	7.65E-02	0.466
4	6.25E-02	UNDETERM.	---	------	-----	--------	6.39E-02	0.438
4	8.33E-02	UNDETERM.	---	------	-----	--------	5.20E-02	0.385
4	1.00E-01	UNDETERM.	---	------	-----	--------	4.69E-02	0.342
4	1.25E-01	UNDETERM.	---	------	-----	--------	4.26E-02	0.281
4	1.67E-01	UNDETERM.	---	------	-----	--------	4.00E-02	0.179
4	2.00E-01	UNDETERM.	---	------	-----	--------	3.98E-02	6.86E-02
4	2.50E-01	UNDETERM.	---	------	-----	--------	4.12E-02	0.159
4	3.33E-01	UNDETERM.	---	------	-----	--------	4.59E-02	0.237
4	4.00E-01	UNDETERM.	---	------	-----	--------	5.08E-02	0.264
4	5.00E-01	UNDETERM.	---	------	-----	--------	5.98E-02	0.281
4	6.67E-01	UNDETERM.	---	------	-----	--------	7.76E-02	0.281
4	8.00E-01	UNDETERM.	---	------	-----	--------	9.40E-02	0.267

4	1.00E+00	UNDETERM.	---	------	-----	--------	0.121	0.232
4	1.33E+00	UNDETERM.	---	------	-----	--------	0.171	0.127
4	1.60E+00	UNDETERM.	---	------	-----	--------	0.212	0.128
4	2.00E+00	UNDETERM.	---	------	-----	--------	0.271	0.252
4	3.20E+00	3D/1D2D	---	------	-----	--------	1	0
4	5.33E+00	UNDETERM.	---	------	-----	--------	0.54	0.373
4	6.40E+00	3D/2Ddiag	---	------	-----	--------	#NAME?	NaN
4	1.07E+01	3D/2Ddiag	---	------	-----	--------	#NAME?	NaN
4	1.60E+01	3D/2Ddiag	---	------	-----	--------	#NAME?	NaN
4	2.56E+01	3D/2Ddiag	---	------	-----	--------	#NAME?	NaN
4	4.27E+01	3D/2Ddiag	---	------	-----	--------	#NAME?	NaN
4	6.40E+01	3D/2Ddiag	---	------	-----	--------	#NAME?	NaN
3	9.77E-04	3D	---	------	-----	0.592	5.43E-02	0.203
3	1.30E-03	3D	---	------	-----	0.439	5.59E-02	0.193
3	1.95E-03	3D	---	------	-----	0.269	5.98E-02	0.169
3	2.60E-03	3D	---	------	-----	0.19	6.33E-02	0.146
3	3.91E-03	3D/2Dtw	23.51	3.4385	-7.6494	--------	6.74E-02	9.93E-02
3	5.21E-03	3D/2Dtw	27.71	2.7475	-6.8277	--------	6.82E-02	1.28E-02
3	7.81E-03	3D	---	------	-----	0.186	6.48E-02	0.125
3	1.04E-02	3D	---	------	-----	0.305	5.96E-02	0.16
3	1.56E-02	3D	---	------	-----	0.387	5.08E-02	0.188
3	2.08E-02	3D	---	------	-----	0.397	4.46E-02	0.197
3	3.12E-02	3D	---	------	-----	0.392	3.61E-02	0.196
3	4.17E-02	3D	---	------	-----	0.386	3.01E-02	0.186
3	6.25E-02	UNDETERM.	---	------	-----	--------	2.19E-02	0.165
3	8.33E-02	UNDETERM.	---	------	-----	--------	1.66E-02	0.145
3	1.25E-01	UNDETERM.	---	------	-----	--------	1.04E-02	0.115
3	1.67E-01	UNDETERM.	---	------	-----	--------	6.89E-03	9.03E-02
3	2.50E-01	UNDETERM.	---	------	-----	--------	3.39E-03	4.23E-02
3	3.33E-01	UNDETERM.	---	------	-----	--------	3.58E-03	5.15E-02
3	5.00E-01	UNDETERM.	---	------	-----	--------	7.41E-03	9.78E-02

3	6.67E-01	UNDETERM.	---	------	-----	--------	1.12E-02	0.125
3	1.00E+00	UNDETERM.	---	------	-----	--------	1.82E-02	0.164
3	1.33E+00	UNDETERM.	---	------	-----	--------	2.46E-02	0.197
3	2.00E+00	UNDETERM.	---	------	-----	--------	3.65E-02	0.253
3	2.67E+00	UNDETERM.	---	------	-----	--------	4.73E-02	0.299
3	4.00E+00	UNDETERM.	---	------	-----	--------	6.68E-02	0.37
3	5.33E+00	UNDETERM.	---	------	-----	--------	8.40E-02	0.417
3	8.00E+00	UNDETERM.	---	------	-----	--------	0.113	0.461
3	1.07E+01	UNDETERM.	---	------	-----	--------	0.135	0.463
3	1.60E+01	3D/1D2D	---	------	-----	--------	1	0
3	6.40E+01	3D/2Ddiag	---	------	-----	--------	#NAME?	NaN
2	7.81E-04	UNDETERM.	---	------	-----	--------	0.241	0.138
2	9.77E-04	3D/2D	1.32	10.3972	29.2172	--------	0.239	0.214
2	1.30E-03	3D	---	------	-----	0.219	0.241	0.298
2	1.56E-03	3D	---	------	-----	0.279	0.244	0.347
2	1.95E-03	3D	---	------	-----	0.35	0.25	0.403
2	2.60E-03	3D	---	------	-----	0.437	0.257	0.466
2	3.13E-03	3D	---	------	-----	0.49	0.261	0.499
2	3.91E-03	3D	---	------	-----	0.554	0.261	0.531
2	5.21E-03	UNDETERM.	---	------	-----	--------	0.254	0.555
2	6.25E-03	3D	---	------	-----	0.684	0.245	0.561
2	7.81E-03	3D	---	------	-----	0.742	0.23	0.557
2	1.04E-02	3D	---	------	-----	0.812	0.205	0.536
2	1.25E-02	3D	---	------	-----	0.855	0.187	0.515
2	1.56E-02	3D	---	------	-----	0.909	0.166	0.482
2	2.08E-02	UNDETERM.	---	------	-----	--------	0.14	0.432
2	2.50E-02	UNDETERM.	---	------	-----	--------	0.125	0.396
2	3.12E-02	3D	---	------	-----	0.787	0.108	0.349
2	4.17E-02	UNDETERM.	---	------	-----	--------	8.84E-02	0.281
2	5.00E-02	UNDETERM.	---	------	-----	--------	7.67E-02	0.231
2	6.25E-02	UNDETERM.	---	------	-----	--------	6.38E-02	0.159

2	8.33E-02	UNDETERM.	---	------	-----	--------	5.00E-02	6.76E-02
2	1.00E-01	UNDETERM.	---	------	-----	--------	4.33E-02	0.137
2	1.25E-01	3D/2D	9.97	-1.3877	10.3666	--------	3.76E-02	0.174
2	1.67E-01	3D/2D	9.89	-0.3863	10.488	--------	3.35E-02	0.192
2	2.00E-01	UNDETERM.	---	------	-----	--------	3.22E-02	0.193
2	2.50E-01	UNDETERM.	---	------	-----	--------	3.12E-02	0.186
2	3.33E-01	UNDETERM.	---	------	-----	--------	3.02E-02	0.169
2	4.00E-01	3D/2D	9.68	0.4938	10.099	--------	2.97E-02	0.156
2	5.00E-01	UNDETERM.	---	------	-----	--------	2.93E-02	0.139
2	6.67E-01	3D/2D	8.03	0.5006	9.4065	--------	2.90E-02	0.115
2	8.00E-01	UNDETERM.	---	------	-----	--------	2.90E-02	9.87E-02
2	1.00E+00	UNDETERM.	---	------	-----	--------	2.93E-02	7.51E-02
2	1.33E+00	UNDETERM.	---	------	-----	--------	3.01E-02	2.32E-02
2	1.60E+00	UNDETERM.	---	------	-----	--------	3.09E-02	5.30E-02
2	2.00E+00	UNDETERM.	---	------	-----	--------	3.25E-02	8.50E-02
2	2.67E+00	UNDETERM.	---	------	-----	--------	3.58E-02	0.118
2	3.20E+00	UNDETERM.	---	------	-----	--------	3.86E-02	0.137
2	4.00E+00	UNDETERM.	---	------	-----	--------	4.32E-02	0.159
2	5.33E+00	UNDETERM.	---	------	-----	--------	5.11E-02	0.186
2	6.40E+00	UNDETERM.	---	------	-----	--------	5.72E-02	0.201
2	8.00E+00	UNDETERM.	---	------	-----	--------	6.56E-02	0.216
2	1.07E+01	UNDETERM.	---	------	-----	--------	7.73E-02	0.226
2	1.28E+01	UNDETERM.	---	------	-----	--------	8.46E-02	0.226
2	1.60E+01	UNDETERM.	---	------	-----	--------	9.25E-02	0.217
2	2.13E+01	UNDETERM.	---	------	-----	--------	0.1	0.192
2	2.56E+01	UNDETERM.	---	------	-----	--------	0.103	0.167
2	3.20E+01	UNDETERM.	---	------	-----	--------	0.105	0.128
2	4.27E+01	UNDETERM.	---	------	-----	--------	0.104	5.61E-02
2	5.12E+01	UNDETERM.	---	------	-----	--------	0.101	5.23E-02
2	6.40E+01	UNDETERM.	---	------	-----	--------	9.60E-02	7.79E-02
2	8.53E+01	UNDETERM.	---	------	-----	--------	8.75E-02	5.29E-02

101	7.81E-04	3D/2D	8.8	10.4153	6.1242	--------	0.148	0.107
101	9.77E-04	3D	---	------	-----	0.168	0.151	0.123
101	1.30E-03	3D	---	------	-----	0.298	0.155	0.143
101	1.56E-03	3D	---	------	-----	0.382	0.159	0.157
101	1.95E-03	3D	---	------	-----	0.465	0.165	0.173
101	2.60E-03	3D	---	------	-----	0.549	0.174	0.194
101	3.13E-03	3D	---	------	-----	0.6	0.181	0.206
101	3.91E-03	3D	---	------	-----	0.667	0.191	0.219
101	5.21E-03	3D	---	------	-----	0.74	0.204	0.234
101	6.25E-03	3D	---	------	-----	0.768	0.213	0.244
101	7.81E-03	3D	---	------	-----	0.79	0.225	0.257
101	1.04E-02	3D	---	------	-----	0.821	0.241	0.276
101	1.25E-02	3D	---	------	-----	0.86	0.253	0.291
101	1.56E-02	3D	---	------	-----	0.942	0.27	0.313
101	2.08E-02	UNDETERM.	---	------	-----	--------	0.296	0.348
101	2.50E-02	UNDETERM.	---	------	-----	--------	0.316	0.374
101	3.12E-02	UNDETERM.	---	------	-----	--------	0.346	0.407
101	4.17E-02	UNDETERM.	---	------	-----	--------	0.395	0.452
101	5.00E-02	UNDETERM.	---	------	-----	--------	0.43	0.479
101	6.25E-02	UNDETERM.	---	------	-----	--------	0.477	0.508
101	8.33E-02	UNDETERM.	---	------	-----	--------	0.537	0.538
101	1.00E-01	UNDETERM.	---	------	-----	--------	0.572	0.552
101	1.25E-01	UNDETERM.	---	------	-----	--------	0.612	0.569
101	1.67E-01	UNDETERM.	---	------	-----	--------	0.66	0.593
101	2.00E-01	UNDETERM.	---	------	-----	--------	0.692	0.613
101	2.50E-01	UNDETERM.	---	------	-----	--------	0.739	0.646
101	3.33E-01	UNDETERM.	---	------	-----	--------	0.822	0.701
101	4.00E-01	UNDETERM.	---	------	-----	--------	0.894	0.745
101	5.00E-01	UNDETERM.	---	------	-----	--------	1.01	0.807
101	6.67E-01	UNDETERM.	---	------	-----	--------	1.21	0.896
101	8.00E-01	UNDETERM.	---	------	-----	--------	1.37	0.956

101	1.00E+00	UNDETERM.	---	------	-----	--------	1.61	1.03
101	1.33E+00	UNDETERM.	---	------	-----	--------	1.96	1.11
101	1.60E+00	UNDETERM.	---	------	-----	--------	2.2	1.15
101	2.00E+00	UNDETERM.	---	------	-----	--------	2.51	1.18
101	2.67E+00	UNDETERM.	---	------	-----	--------	2.88	1.19
101	3.20E+00	UNDETERM.	---	------	-----	--------	3.11	1.18
101	4.00E+00	UNDETERM.	---	------	-----	--------	3.37	1.16
101	5.33E+00	UNDETERM.	---	------	-----	--------	3.7	1.1
101	6.40E+00	UNDETERM.	---	------	-----	--------	3.89	1.03
101	8.00E+00	UNDETERM.	---	------	-----	--------	4.07	0.898
101	1.07E+01	UNDETERM.	---	------	-----	--------	4.18	0.573
101	1.28E+01	UNDETERM.	---	------	-----	--------	4.13	8.87E-02
101	1.60E+01	UNDETERM.	---	------	-----	--------	3.96	0.619
101	2.13E+01	UNDETERM.	---	------	-----	--------	3.6	0.845
101	2.56E+01	UNDETERM.	---	------	-----	--------	3.34	0.905
101	3.20E+01	UNDETERM.	---	------	-----	--------	3.01	0.926
101	4.27E+01	UNDETERM.	---	------	-----	--------	2.65	0.904
101	5.12E+01	UNDETERM.	---	------	-----	--------	2.46	0.876
101	6.40E+01	UNDETERM.	---	------	-----	--------	2.27	0.835
101	8.53E+01	UNDETERM.	---	------	-----	--------	2.08	0.779
1	3.91E-03	3D	---	------	-----	0.239	0.204	0.163
1	5.21E-03	3D	---	------	-----	0.183	0.205	0.141
1	7.81E-03	3D/2Dtw	89.36	23.8834	-16.491	--------	0.201	0.112
1	1.04E-02	3D/2Dtw	89.99	25.0764	-18.318	--------	0.194	9.66E-02
1	1.56E-02	3D/2Dtw	2.38	29.0473	-24.5088	--------	0.182	9.31E-02
1	2.08E-02	3D/1D2D	---	------	-----	--------	0.174	0.108
1	3.12E-02	UNDETERM.	---	------	-----	--------	0.169	0.145
1	4.17E-02	3D	---	------	-----	0.546	0.169	0.178
1	6.25E-02	UNDETERM.	---	------	-----	--------	0.179	0.226
1	8.33E-02	UNDETERM.	---	------	-----	--------	0.194	0.259
1	1.25E-01	UNDETERM.	---	------	-----	--------	0.224	0.298

1	1.67E-01	UNDETERM.	---	------	-----	--------	0.251	0.317
1	2.50E-01	UNDETERM.	---	------	-----	--------	0.29	0.325
1	3.33E-01	UNDETERM.	---	------	-----	--------	0.316	0.319
1	5.00E-01	UNDETERM.	---	------	-----	--------	0.353	0.302
1	6.67E-01	UNDETERM.	---	------	-----	--------	0.383	0.291
1	1.00E+00	UNDETERM.	---	------	-----	--------	0.435	0.286
1	2.00E+00	UNDETERM.	---	------	-----	--------	2	0
1	4.00E+00	UNDETERM.	---	------	-----	--------	2	0
86	7.81E-04	UNDETERM.	---	------	-----	--------	1.86E-02	0.452
86	9.77E-04	UNDETERM.	---	------	-----	--------	2.48E-02	0.499
86	1.30E-03	3D	---	------	-----	0.549	3.66E-02	0.561
86	1.56E-03	UNDETERM.	---	------	-----	--------	4.64E-02	0.597
86	1.95E-03	3D	---	------	-----	0.573	6.05E-02	0.636
86	2.60E-03	3D	---	------	-----	0.59	7.94E-02	0.665
86	3.13E-03	3D	---	------	-----	0.599	8.97E-02	0.667
86	3.91E-03	3D	---	------	-----	0.607	9.80E-02	0.652
86	5.21E-03	3D	---	------	-----	0.612	9.94E-02	0.607
86	6.25E-03	3D	---	------	-----	0.614	9.45E-02	0.569
86	7.81E-03	3D	---	------	-----	0.62	8.40E-02	0.521
86	1.04E-02	3D	---	------	-----	0.64	6.79E-02	0.463
86	1.25E-02	3D	---	------	-----	0.664	6.05E-02	0.431
86	1.56E-02	3D	---	------	-----	0.712	5.89E-02	0.398
86	2.08E-02	UNDETERM.	---	------	-----	--------	7.06E-02	0.36
86	2.50E-02	UNDETERM.	---	------	-----	--------	8.36E-02	0.339
86	3.12E-02	UNDETERM.	---	------	-----	--------	0.103	0.314
86	4.17E-02	UNDETERM.	---	------	-----	--------	0.132	0.284
86	5.00E-02	UNDETERM.	---	------	-----	--------	0.152	0.267
86	6.25E-02	UNDETERM.	---	------	-----	--------	0.179	0.247
86	8.33E-02	UNDETERM.	---	------	-----	--------	0.216	0.218
86	1.00E-01	3D	---	------	-----	0.582	0.238	0.192
86	1.25E-01	3D	---	------	-----	0.238	0.261	0.144

86	1.67E-01	3D/2D	71.84	31.0841	29.5344	--------	0.283	6.27E-02
86	2.00E-01	UNDETERM.	---	------	-----	--------	0.291	0.141
86	2.50E-01	UNDETERM.	---	------	-----	--------	0.293	0.191
86	3.33E-01	UNDETERM.	---	------	-----	--------	0.287	0.218
86	4.00E-01	3D	---	------	-----	0.275	0.28	0.218
86	5.00E-01	3D	---	------	-----	0.268	0.27	0.199
86	6.67E-01	3D	---	------	-----	0.199	0.259	0.139
86	8.00E-01	UNDETERM.	---	------	-----	--------	0.254	5.28E-02
86	1.00E+00	UNDETERM.	---	------	-----	--------	0.25	0.142
86	1.33E+00	UNDETERM.	---	------	-----	--------	0.249	0.227
86	1.60E+00	UNDETERM.	---	------	-----	--------	0.251	0.267
86	2.00E+00	UNDETERM.	---	------	-----	--------	0.256	0.307
86	2.67E+00	UNDETERM.	---	------	-----	--------	0.263	0.344
86	3.20E+00	UNDETERM.	---	------	-----	--------	0.267	0.359
86	4.00E+00	UNDETERM.	---	------	-----	--------	0.271	0.368
86	5.33E+00	UNDETERM.	---	------	-----	--------	0.271	0.367
86	6.40E+00	UNDETERM.	---	------	-----	--------	0.267	0.361
86	8.00E+00	UNDETERM.	---	------	-----	--------	0.26	0.349
86	1.07E+01	UNDETERM.	---	------	-----	--------	0.245	0.329
86	1.28E+01	UNDETERM.	---	------	-----	--------	0.234	0.314
86	1.60E+01	UNDETERM.	---	------	-----	--------	0.218	0.293
86	2.13E+01	UNDETERM.	---	------	-----	--------	0.196	0.263
86	2.56E+01	UNDETERM.	---	------	-----	--------	0.182	0.241
86	3.20E+01	UNDETERM.	---	------	-----	--------	0.165	0.209
86	4.27E+01	UNDETERM.	---	------	-----	--------	0.147	0.155
86	5.12E+01	UNDETERM.	---	------	-----	--------	0.137	0.102
86	6.40E+01	UNDETERM.	---	------	-----	--------	0.127	8.41E-02
86	8.53E+01	UNDETERM.	---	------	-----	--------	0.116	0.178
28	9.77E-04	UNDETERM.	---	------	-----	--------	3.33E-02	0.15
28	1.30E-03	3D/2D	0.85	-6.2516	4.471	--------	2.96E-02	0.154
28	1.56E-03	2D	89.34	-	829.9497	i)	(-	-

							2119.6927	
28	1.95E-03	2D	89.34	-	669.4754	i)	(- 1710.0451	-
28	2.60E-03	3D	---	------	-----	0.805	2.44E-02	0.206
28	3.13E-03	3D	---	------	-----	0.242	2.41E-02	0.224
28	3.91E-03	2D	89.16	-	3.58E+02	i)	(	-738.6541
28	5.21E-03	3D/2D	86.52	4.5306	-1.7555	--------	2.51E-02	0.28
28	6.25E-03	3D/2D	86.94	3.2729	-1.304	--------	2.63E-02	0.303
28	7.81E-03	3D/2D	87.28	2.2908	-1.0408	--------	2.86E-02	0.337
28	1.04E-02	3D/2D	87.53	1.5285	-0.9091	--------	3.32E-02	0.394
28	1.25E-02	3D/2D	87.62	1.2442	-0.8768	--------	3.78E-02	0.446
28	1.56E-02	3D/2D	87.64	1.0693	-0.8568	--------	4.62E-02	0.539
28	2.50E-02	UNDETERM.	---	------	-----	--------	8.73E-02	0.99
28	3.12E-02	UNDETERM.	---	------	-----	--------	0.137	1.52
28	4.17E-02	UNDETERM.	---	------	-----	--------	0.25	2.7
28	5.00E-02	UNDETERM.	---	------	-----	--------	0.244	2.56
28	6.25E-02	UNDETERM.	---	------	-----	--------	0.18	1.81
28	8.33E-02	UNDETERM.	---	------	-----	--------	0.135	1.27
28	1.00E-01	UNDETERM.	---	------	-----	--------	0.12	1.1
28	1.25E-01	UNDETERM.	---	------	-----	--------	0.11	0.965
28	1.67E-01	UNDETERM.	---	------	-----	--------	0.104	0.874
28	2.00E-01	UNDETERM.	---	------	-----	--------	0.103	0.847
28	2.50E-01	UNDETERM.	---	------	-----	--------	0.102	0.834
28	3.33E-01	UNDETERM.	---	------	-----	--------	0.104	0.84
28	4.00E-01	UNDETERM.	---	------	-----	--------	0.106	0.85
28	5.00E-01	UNDETERM.	---	------	-----	--------	0.11	0.861
28	6.67E-01	UNDETERM.	---	------	-----	--------	0.116	0.865
28	8.00E-01	UNDETERM.	---	------	-----	--------	0.121	0.858
28	1.00E+00	UNDETERM.	---	------	-----	--------	0.126	0.843
28	1.33E+00	UNDETERM.	---	------	-----	--------	0.13	0.825
28	1.60E+00	UNDETERM.	---	------	-----	--------	0.133	0.824

28	2.00E+00	UNDETERM.	---	------	-----	--------	0.135	0.843
28	2.67E+00	UNDETERM.	---	------	-----	--------	0.141	0.904
28	3.20E+00	UNDETERM.	---	------	-----	--------	0.148	0.961
28	4.00E+00	UNDETERM.	---	------	-----	--------	0.162	1.05
28	5.33E+00	UNDETERM.	---	------	-----	--------	0.191	1.18
28	6.40E+00	UNDETERM.	---	------	-----	--------	0.219	1.26
28	8.00E+00	UNDETERM.	---	------	-----	--------	0.263	1.37
28	1.07E+01	UNDETERM.	---	------	-----	--------	0.344	1.49
28	1.28E+01	UNDETERM.	---	------	-----	--------	0.41	1.53
28	1.60E+01	UNDETERM.	---	------	-----	--------	0.507	1.53
28	2.13E+01	UNDETERM.	---	------	-----	--------	0.65	1.37
28	2.56E+01	UNDETERM.	---	------	-----	--------	0.738	1.08
28	3.20E+01	UNDETERM.	---	------	-----	--------	0.815	0.364
28	4.27E+01	UNDETERM.	---	------	-----	--------	0.805	1.35
28	6.40E+01	UNDETERM.	---	------	-----	--------	0.568	1.46
28	8.53E+01	UNDETERM.	---	------	-----	--------	0.374	1.21
100	1.30E-03	3D	---	------	-----	0.642	1.04	1.21
100	1.56E-03	3D	---	------	-----	0.629	1.12	1.21
100	1.95E-03	3D	---	------	-----	0.608	1.19	1.17
100	2.60E-03	UNDETERM.	---	------	-----	--------	1.22	1.09
100	3.13E-03	3D	---	------	-----	0.555	1.22	1.03
100	3.91E-03	3D	---	------	-----	0.533	1.18	0.96
100	5.21E-03	3D	---	------	-----	0.515	1.11	0.876
100	6.25E-03	3D	---	------	-----	0.508	1.06	0.829
100	7.81E-03	3D	---	------	-----	0.502	1.01	0.774
100	1.04E-02	3D	---	------	-----	0.494	0.95	0.711
100	1.25E-02	3D	---	------	-----	0.486	0.92	0.675
100	1.56E-02	3D	---	------	-----	0.474	0.886	0.639
100	2.08E-02	3D	---	------	-----	0.457	0.839	0.602
100	2.50E-02	3D	---	------	-----	0.447	0.803	0.583
100	3.12E-02	3D	---	------	-----	0.436	0.75	0.56

100	4.17E-02	3D	---	------	-----	0.426	0.669	0.527
100	5.00E-02	3D	---	------	-----	0.422	0.615	0.501
100	6.25E-02	3D	---	------	-----	0.417	0.55	0.463
100	8.33E-02	3D	---	------	-----	0.412	0.475	0.407
100	1.00E-01	3D	---	------	-----	0.41	0.436	0.368
100	1.25E-01	3D	---	------	-----	0.408	0.398	0.318
100	1.67E-01	3D	---	------	-----	0.413	0.364	0.248
100	2.00E-01	UNDETERM.	---	------	-----	--------	0.35	0.198
100	2.50E-01	UNDETERM.	---	------	-----	--------	0.343	0.123
100	3.33E-01	UNDETERM.	---	------	-----	--------	0.348	0.103
100	4.00E-01	3D	---	------	-----	0.227	0.361	0.153
100	5.00E-01	3D	---	------	-----	0.224	0.388	0.188
100	6.67E-01	3D	---	------	-----	0.193	0.441	0.207
100	8.00E-01	3D	---	------	-----	0.165	0.487	0.208
100	1.00E+00	3D/2D	21.41	-54.8809	-32.5496	--------	0.555	0.199
100	1.33E+00	UNDETERM.	---	------	-----	--------	0.661	0.176
100	1.60E+00	UNDETERM.	---	------	-----	--------	0.736	0.158
100	2.00E+00	UNDETERM.	---	------	-----	--------	0.826	0.141
100	2.67E+00	UNDETERM.	---	------	-----	--------	0.931	0.149
100	3.20E+00	UNDETERM.	---	------	-----	--------	0.982	0.18
100	4.00E+00	UNDETERM.	---	------	-----	--------	1.03	0.241
100	5.33E+00	UNDETERM.	---	------	-----	--------	1.05	0.345
100	6.40E+00	UNDETERM.	---	------	-----	--------	1.06	0.418
100	8.00E+00	UNDETERM.	---	------	-----	--------	1.06	0.511
100	1.07E+01	UNDETERM.	---	------	-----	--------	1.05	0.633
100	1.28E+01	UNDETERM.	---	------	-----	--------	1.05	0.71
100	1.60E+01	UNDETERM.	---	------	-----	--------	1.05	0.805
100	2.13E+01	UNDETERM.	---	------	-----	--------	1.05	0.927
100	2.56E+01	UNDETERM.	---	------	-----	--------	1.07	1.01
100	3.20E+01	UNDETERM.	---	------	-----	--------	1.1	1.11
100	4.27E+01	UNDETERM.	---	------	-----	--------	1.19	1.25

100	5.12E+01	UNDETERM.	---	------	-----	--------	1.28	1.35
100	6.40E+01	UNDETERM.	---	------	-----	--------	1.41	1.47
100	8.53E+01	UNDETERM.	---	------	-----	--------	1.64	1.65
29	1.30E-03	UNDETERM.	---	------	-----	--------	0.102	0.151
29	1.56E-03	UNDETERM.	---	------	-----	--------	0.104	0.167
29	1.95E-03	3D	---	------	-----	0.157	0.107	0.19
29	2.60E-03	UNDETERM.	---	------	-----	--------	0.116	0.223
29	3.13E-03	3D	---	------	-----	0.283	0.123	0.246
29	3.91E-03	3D	---	------	-----	0.39	0.136	0.275
29	5.21E-03	3D	---	------	-----	0.581	0.16	0.313
29	6.25E-03	3D	---	------	-----	0.724	0.179	0.336
29	7.81E-03	3D	---	------	-----	0.896	0.206	0.359
29	1.04E-02	UNDETERM.	---	------	-----	--------	0.245	0.378
29	1.25E-02	UNDETERM.	---	------	-----	--------	0.27	0.379
29	1.56E-02	UNDETERM.	---	------	-----	--------	0.297	0.367
29	2.50E-02	UNDETERM.	---	------	-----	--------	0.33	0.284
29	3.12E-02	3D	---	------	-----	0.332	0.332	0.223
29	4.17E-02	3D/2Dtw	1.4	18.5375	-2.8659	--------	0.325	0.13
29	5.00E-02	UNDETERM.	---	------	-----	--------	0.318	3.71E-02
29	6.25E-02	UNDETERM.	---	------	-----	--------	0.308	0.113
29	8.33E-02	UNDETERM.	---	------	-----	--------	0.293	0.16
29	1.00E-01	3D/2D	1.29	14.3217	-0.9302	--------	0.283	0.176
29	1.25E-01	3D/2Dtw	0.89	13.3825	-0.614	--------	0.269	0.184
29	1.67E-01	3D	---	------	-----	0.168	0.248	0.173
29	2.00E-01	UNDETERM.	---	------	-----	--------	0.236	0.15
29	2.50E-01	UNDETERM.	---	------	-----	--------	0.222	9.24E-02
29	3.33E-01	UNDETERM.	---	------	-----	--------	0.212	0.126
29	4.00E-01	3D	---	------	-----	0.297	0.21	0.184
29	5.00E-01	3D	---	------	-----	0.303	0.214	0.241
29	6.67E-01	3D	---	------	-----	0.312	0.229	0.299
29	8.00E-01	UNDETERM.	---	------	-----	--------	0.244	0.33

29	1.00E+00	UNDETERM.	---		------		-----		--------		0.266	0.36
29	1.33E+00	UNDETERM.	---		------		-----		--------		0.297	0.387
29	1.60E+00	UNDETERM.	---		------		-----		--------		0.318	0.398
29	2.00E+00	UNDETERM.	---		------		-----		--------		0.341	0.405
29	2.67E+00	UNDETERM.	---		------		-----		--------		0.368	0.41
29	3.20E+00	UNDETERM.	---		------		-----		--------		0.385	0.414
29	4.00E+00	UNDETERM.	---		------		-----		--------		0.406	0.421
29	5.33E+00	UNDETERM.	---		------		-----		--------		0.437	0.437
29	6.40E+00	UNDETERM.	---		------		-----		--------		0.461	0.451
29	8.00E+00	UNDETERM.	---		------		-----		--------		0.496	0.472
29	1.07E+01	UNDETERM.	---		------		-----		--------		0.548	0.501
29	1.28E+01	UNDETERM.	---		------		-----		--------		0.586	0.519
29	1.60E+01	UNDETERM.	---		------		-----		--------		0.634	0.541
29	2.13E+01	UNDETERM.	---		------		-----		--------		0.699	0.565
29	2.56E+01	UNDETERM.	---		------		-----		--------		0.742	0.576
29	3.20E+01	UNDETERM.	---		------		-----		--------		0.8	0.582
29	4.27E+01	UNDETERM.	---		------		-----		--------		0.883	0.558
29	5.12E+01	UNDETERM.	---		------		-----		--------		0.937	0.509
29	6.40E+01	UNDETERM.	---		------		-----		--------		0.998	0.375
29	8.53E+01	UNDETERM.	---		------		-----		--------		1.05	0.33
30	1.56E-03	3D/2D		62.54		-5.1912		-26.4505	--------		2.05E-02	0.138
30	1.95E-03	3D	---		------		-----			0.432	2.32E-02	0.148
30	2.60E-03	3D	---		------		-----			0.329	2.74E-02	0.158
30	3.13E-03	3D	---		------		-----			0.32	3.03E-02	0.163
30	3.91E-03	3D	---		------		-----			0.352	3.37E-02	0.166
30	5.21E-03	3D	---		------		-----			0.528	3.78E-02	0.165
30	6.25E-03	2D		2.01	+			4.86E+02	i)		(	-776.3477
30	7.81E-03	3D/2D		22.2		9.358		18.1679	--------		4.26E-02	0.158
30	1.04E-02	3D	---		------		-----			0.348	4.55E-02	0.155
30	1.25E-02	3D	---		------		-----			0.271	4.73E-02	0.154
30	2.50E-02	3D	---		------		-----			0.336	5.45E-02	0.168

30	3.12E-02	3D	---	------	-----	0.487	5.75E-02	0.178
30	4.17E-02	3D	---	------	-----	0.953	6.28E-02	0.197
30	5.00E-02	UNDETERM.	---	------	-----	--------	6.73E-02	0.211
30	6.25E-02	UNDETERM.	---	------	-----	--------	7.45E-02	0.231
30	8.33E-02	UNDETERM.	---	------	-----	--------	8.75E-02	0.26
30	1.00E-01	UNDETERM.	---	------	-----	--------	9.83E-02	0.28
30	1.25E-01	UNDETERM.	---	------	-----	--------	0.114	0.306
30	1.67E-01	UNDETERM.	---	------	-----	--------	0.14	0.339
30	2.00E-01	UNDETERM.	---	------	-----	--------	0.158	0.358
30	2.50E-01	UNDETERM.	---	------	-----	--------	0.183	0.379
30	3.33E-01	UNDETERM.	---	------	-----	--------	0.214	0.398
30	4.00E-01	UNDETERM.	---	------	-----	--------	0.233	0.405
30	5.00E-01	UNDETERM.	---	------	-----	--------	0.254	0.411
30	6.67E-01	UNDETERM.	---	------	-----	--------	0.278	0.414
30	8.00E-01	UNDETERM.	---	------	-----	--------	0.292	0.416
30	1.00E+00	UNDETERM.	---	------	-----	--------	0.307	0.418
30	1.33E+00	UNDETERM.	---	------	-----	--------	0.327	0.424
30	1.60E+00	UNDETERM.	---	------	-----	--------	0.341	0.429
30	2.00E+00	UNDETERM.	---	------	-----	--------	0.361	0.439
30	2.67E+00	UNDETERM.	---	------	-----	--------	0.396	0.456
30	4.00E+00	UNDETERM.	---	------	-----	--------	0.473	0.485
30	5.33E+00	UNDETERM.	---	------	-----	--------	0.548	0.497
30	3.20E+01	UNDETERM.	---	------	-----	--------	0.834	0.229
30	4.27E+01	UNDETERM.	---	------	-----	--------	0.831	0.237
31	1.56E-03	3D/2D	81.21	4.4772	0.5469	--------	6.70E-02	8.75E-02
31	2.60E-03	UNDETERM.	---	------	-----	--------	7.17E-02	0.13
31	3.13E-03	3D	---	------	-----	0.161	7.53E-02	0.143
31	3.91E-03	3D	---	------	-----	0.243	8.14E-02	0.158
31	5.21E-03	3D	---	------	-----	0.434	9.14E-02	0.174
31	6.25E-03	3D	---	------	-----	0.629	9.88E-02	0.181
31	7.81E-03	UNDETERM.	---	------	-----	--------	0.108	0.185

31	1.04E-02	3D	---	------	-----	0.577	0.12	0.183
31	2.50E-02	UNDETERM.	---	------	-----	--------	0.147	0.126
31	3.12E-02	UNDETERM.	---	------	-----	--------	0.152	9.53E-02
31	4.17E-02	UNDETERM.	---	------	-----	--------	0.155	1.40E-02
31	5.00E-02	UNDETERM.	---	------	-----	--------	0.156	7.66E-02
31	6.25E-02	UNDETERM.	---	------	-----	--------	0.157	0.11
31	8.33E-02	UNDETERM.	---	------	-----	--------	0.155	0.135
31	1.00E-01	UNDETERM.	---	------	-----	--------	0.154	0.145
31	1.25E-01	UNDETERM.	---	------	-----	--------	0.152	0.153
31	1.67E-01	UNDETERM.	---	------	-----	--------	0.15	0.157
31	2.00E-01	UNDETERM.	---	------	-----	--------	0.148	0.155
31	2.50E-01	UNDETERM.	---	------	-----	--------	0.147	0.149
31	3.33E-01	UNDETERM.	---	------	-----	--------	0.146	0.134
31	4.00E-01	UNDETERM.	---	------	-----	--------	0.146	0.12
31	5.00E-01	UNDETERM.	---	------	-----	--------	0.147	9.90E-02
31	6.67E-01	UNDETERM.	---	------	-----	--------	0.149	6.32E-02
31	8.00E-01	UNDETERM.	---	------	-----	--------	0.152	2.69E-02
31	1.00E+00	UNDETERM.	---	------	-----	--------	0.157	4.95E-02
31	1.33E+00	UNDETERM.	---	------	-----	--------	0.164	6.86E-02
31	1.60E+00	UNDETERM.	---	------	-----	--------	0.168	6.94E-02
31	2.00E+00	UNDETERM.	---	------	-----	--------	0.174	5.92E-02
31	2.67E+00	UNDETERM.	---	------	-----	--------	0.179	1.92E-02
31	3.20E+00	UNDETERM.	---	------	-----	--------	0.181	6.10E-02
31	4.00E+00	UNDETERM.	---	------	-----	--------	0.181	8.93E-02
31	5.33E+00	UNDETERM.	---	------	-----	--------	0.177	0.107
31	6.40E+00	UNDETERM.	---	------	-----	--------	0.172	0.106
31	8.00E+00	UNDETERM.	---	------	-----	--------	0.165	8.29E-02
31	1.07E+01	UNDETERM.	---	------	-----	--------	0.156	7.22E-02
31	2.13E+01	UNDETERM.	---	------	-----	--------	0.154	0.237
31	4.27E+01	UNDETERM.	---	------	-----	--------	0.193	0.34
32	1.56E-03	3D/2D	48.88	0.9276	-19.9415	--------	1.26E-02	0.129

32	1.95E-03	3D/2D	69.11	-1.188	-13.5773	--------	1.43E-02	0.14
32	2.60E-03	3D	---	------	-----	0.382	1.70E-02	0.15
32	3.13E-03	3D	---	------	-----	0.425	1.90E-02	0.156
32	3.91E-03	3D	---	------	-----	0.532	2.19E-02	0.161
32	5.21E-03	3D	---	------	-----	0.557	2.63E-02	0.169
32	6.25E-03	3D	---	------	-----	0.477	2.97E-02	0.174
32	7.81E-03	3D	---	------	-----	0.411	3.44E-02	0.182
32	1.04E-02	3D	---	------	-----	0.392	4.11E-02	0.193
32	1.25E-02	3D	---	------	-----	0.401	4.57E-02	0.198
32	1.56E-02	3D	---	------	-----	0.417	5.12E-02	0.201
32	2.08E-02	3D	---	------	-----	0.412	5.73E-02	0.195
32	2.50E-02	3D	---	------	-----	0.379	6.01E-02	0.185
32	3.12E-02	UNDETERM.	---	------	-----	--------	6.18E-02	0.165
32	4.17E-02	UNDETERM.	---	------	-----	--------	6.12E-02	0.131
32	5.00E-02	UNDETERM.	---	------	-----	--------	5.94E-02	0.11
32	6.25E-02	UNDETERM.	---	------	-----	--------	5.59E-02	9.35E-02
32	8.33E-02	UNDETERM.	---	------	-----	--------	5.02E-02	0.106
32	1.00E-01	UNDETERM.	---	------	-----	--------	4.63E-02	0.132
32	1.25E-01	3D	---	------	-----	0.177	4.12E-02	0.173
32	1.67E-01	UNDETERM.	---	------	-----	--------	3.44E-02	0.233
32	2.00E-01	UNDETERM.	---	------	-----	--------	3.00E-02	0.273
32	2.50E-01	UNDETERM.	---	------	-----	--------	2.45E-02	0.323
32	3.33E-01	UNDETERM.	---	------	-----	--------	2.12E-02	0.39
32	4.00E-01	UNDETERM.	---	------	-----	--------	2.63E-02	0.435
32	5.00E-01	UNDETERM.	---	------	-----	--------	4.18E-02	0.492
32	6.67E-01	UNDETERM.	---	------	-----	--------	7.35E-02	0.569
32	8.00E-01	UNDETERM.	---	------	-----	--------	9.88E-02	0.619
32	1.00E+00	UNDETERM.	---	------	-----	--------	0.134	0.68
32	1.33E+00	UNDETERM.	---	------	-----	--------	0.183	0.758
32	1.60E+00	UNDETERM.	---	------	-----	--------	0.215	0.809
32	2.00E+00	UNDETERM.	---	------	-----	--------	0.258	0.873

32	2.67E+00	UNDETERM.	---	------	-----	--------	0.319	0.961
32	3.20E+00	UNDETERM.	---	------	-----	--------	0.364	1.02
32	4.00E+00	UNDETERM.	---	------	-----	--------	0.424	1.08
32	5.33E+00	UNDETERM.	---	------	-----	--------	0.509	1.16
32	6.40E+00	UNDETERM.	---	------	-----	--------	0.563	1.19
32	1.07E+01	UNDETERM.	---	------	-----	--------	0.683	1.17
32	2.13E+01	UNDETERM.	---	------	-----	--------	0.686	0.925
32	3.20E+01	UNDETERM.	---	------	-----	--------	0.634	0.747
32	4.27E+01	UNDETERM.	---	------	-----	--------	0.608	0.63
32	5.12E+01	UNDETERM.	---	------	-----	--------	0.604	0.564
32	6.40E+01	UNDETERM.	---	------	-----	--------	0.617	0.494
32	8.53E+01	UNDETERM.	---	------	-----	--------	0.666	0.436
34	1.30E-03	UNDETERM.	---	------	-----	--------	0.216	0.211
34	1.56E-03	3D	---	------	-----	0.466	0.228	0.217
34	1.95E-03	3D	---	------	-----	0.294	0.244	0.216
34	2.60E-03	3D	---	------	-----	0.173	0.265	0.199
34	3.13E-03	3D/2Dtw	74.89	17.0559	1.2856	--------	0.276	0.178
34	3.91E-03	3D/2Dtw	75.53	16.9847	1.6236	--------	0.285	0.14
34	5.21E-03	3D/2Dtw	76.29	16.4608	1.802	--------	0.289	5.88E-02
34	6.25E-03	3D/2Dtw	76.82	15.998	1.9192	--------	0.288	7.36E-02
34	7.81E-03	3D/2Dtw	77.44	15.3601	2.1499	--------	0.285	0.119
34	1.04E-02	3D/2Dtw	78.03	14.4202	2.6769	--------	0.28	0.151
34	1.25E-02	3D/2Dtw	78.21	13.7131	3.1929	--------	0.276	0.163
34	1.56E-02	3D/2Dtw	78.19	12.6875	4.049	--------	0.27	0.173
34	2.08E-02	UNDETERM.	---	------	-----	--------	0.261	0.176
34	2.50E-02	UNDETERM.	---	------	-----	--------	0.255	0.171
34	3.12E-02	UNDETERM.	---	------	-----	--------	0.249	0.154
34	4.17E-02	UNDETERM.	---	------	-----	--------	0.243	0.109
34	5.00E-02	UNDETERM.	---	------	-----	--------	0.242	4.50E-02
34	6.25E-02	UNDETERM.	---	------	-----	--------	0.244	0.111
34	8.33E-02	UNDETERM.	---	------	-----	--------	0.253	0.185

34	1.00E-01	UNDETERM.	---	------	-----	--------	0.263	0.222
34	1.25E-01	UNDETERM.	---	------	-----	--------	0.28	0.262
34	1.67E-01	UNDETERM.	---	------	-----	--------	0.309	0.308
34	2.00E-01	UNDETERM.	---	------	-----	--------	0.329	0.334
34	2.50E-01	UNDETERM.	---	------	-----	--------	0.355	0.361
34	3.33E-01	UNDETERM.	---	------	-----	--------	0.388	0.39
34	4.00E-01	UNDETERM.	---	------	-----	--------	0.409	0.404
34	5.00E-01	UNDETERM.	---	------	-----	--------	0.431	0.415
34	6.67E-01	UNDETERM.	---	------	-----	--------	0.458	0.416
34	8.00E-01	UNDETERM.	---	------	-----	--------	0.472	0.408
34	1.00E+00	UNDETERM.	---	------	-----	--------	0.486	0.387
34	1.33E+00	UNDETERM.	---	------	-----	--------	0.499	0.34
34	1.60E+00	UNDETERM.	---	------	-----	--------	0.503	0.297
34	2.00E+00	UNDETERM.	---	------	-----	--------	0.504	0.23
34	2.67E+00	UNDETERM.	---	------	-----	--------	0.499	8.29E-02
34	3.20E+00	UNDETERM.	---	------	-----	--------	0.492	0.141
34	4.00E+00	UNDETERM.	---	------	-----	--------	0.479	0.217
34	5.33E+00	UNDETERM.	---	------	-----	--------	0.458	0.263
34	6.40E+00	UNDETERM.	---	------	-----	--------	0.444	0.273
34	4.27E+01	UNDETERM.	---	------	-----	--------	0.713	0.341
34	5.12E+01	UNDETERM.	---	------	-----	--------	0.811	0.356
36	7.81E-04	UNDETERM.	---	------	-----	--------	4.12E-02	0.113
36	9.77E-04	UNDETERM.	---	------	-----	--------	4.66E-02	0.125
36	1.30E-03	UNDETERM.	---	------	-----	--------	5.41E-02	0.133
36	1.56E-03	UNDETERM.	---	------	-----	--------	5.85E-02	0.132
36	1.95E-03	UNDETERM.	---	------	-----	--------	6.30E-02	0.126
36	2.60E-03	UNDETERM.	---	------	-----	--------	6.65E-02	0.109
36	3.13E-03	3D/1D2D	---	------	-----	--------	6.72E-02	9.43E-02
36	3.91E-03	2D	82.07	+	6.54E+02	i)	(	-221.8693
36	5.21E-03	2D	83.8	+	5.41E+02	i)	(	-181.0853
36	6.25E-03	3D/2D	89.37	4.1174	1.9978	--------	6.16E-02	5.12E-02

36	7.81E-03	3D/2Dtw	89.65	4.1086	2.033	--------	5.91E-02	5.70E-02
36	1.04E-02	3D/2D	89.72	4.427	2.2021	--------	5.66E-02	7.49E-02
36	1.25E-02	3D/2Dtw	89.71	4.8587	2.4427	--------	5.58E-02	8.85E-02
36	1.56E-02	3D	---	------	-----	0.155	5.57E-02	0.106
36	2.50E-02	3D	---	------	-----	0.325	5.97E-02	0.142
36	3.12E-02	3D	---	------	-----	0.429	6.37E-02	0.159
36	4.17E-02	3D	---	------	-----	0.566	7.06E-02	0.18
36	5.00E-02	UNDETERM.	---	------	-----	--------	7.59E-02	0.193
36	6.25E-02	UNDETERM.	---	------	-----	--------	8.31E-02	0.207
36	8.33E-02	UNDETERM.	---	------	-----	--------	9.27E-02	0.225
36	1.00E-01	UNDETERM.	---	------	-----	--------	9.90E-02	0.235
36	1.25E-01	UNDETERM.	---	------	-----	--------	0.107	0.248
36	1.67E-01	UNDETERM.	---	------	-----	--------	0.118	0.265
36	2.00E-01	UNDETERM.	---	------	-----	--------	0.125	0.277
36	2.50E-01	UNDETERM.	---	------	-----	--------	0.137	0.294
36	3.33E-01	UNDETERM.	---	------	-----	--------	0.155	0.319
36	4.00E-01	UNDETERM.	---	------	-----	--------	0.17	0.338
36	5.00E-01	UNDETERM.	---	------	-----	--------	0.192	0.362
36	6.67E-01	UNDETERM.	---	------	-----	--------	0.228	0.392
36	8.00E-01	UNDETERM.	---	------	-----	--------	0.254	0.409
36	1.00E+00	UNDETERM.	---	------	-----	--------	0.289	0.424
36	1.33E+00	UNDETERM.	---	------	-----	--------	0.335	0.428
36	1.60E+00	UNDETERM.	---	------	-----	--------	0.362	0.42
36	2.00E+00	UNDETERM.	---	------	-----	--------	0.388	0.397
36	2.67E+00	UNDETERM.	---	------	-----	--------	0.41	0.35
36	3.20E+00	UNDETERM.	---	------	-----	--------	0.415	0.315
36	4.00E+00	UNDETERM.	---	------	-----	--------	0.415	0.276
36	5.33E+00	UNDETERM.	---	------	-----	--------	0.407	0.249
36	6.40E+00	UNDETERM.	---	------	-----	--------	0.402	0.251
36	8.00E+00	UNDETERM.	---	------	-----	--------	0.4	0.269
36	1.07E+01	UNDETERM.	---	------	-----	--------	0.406	0.305

36	1.28E+01	UNDETERM.	---	------	-----	--------	0.416	0.329
36	2.13E+01	UNDETERM.	---	------	-----	--------	0.473	0.392
36	2.56E+01	UNDETERM.	---	------	-----	--------	0.505	0.416
36	4.27E+01	UNDETERM.	---	------	-----	--------	0.651	0.495
36	8.53E+01	UNDETERM.	---	------	-----	--------	1.05	0.648
37	9.77E-04	2D	45.25	+	1.30E+03	i)	(- 1273.4086	-
37	1.30E-03	2D	45.41	+	1.17E+03	i)	(	-953.6102
37	1.56E-03	2D	45.53	+	1.07E+03	i)	(	-790.6383
37	1.95E-03	2D	0.69	+	1.76E+03	i)	(	-146.5429
37	2.60E-03	2D	0.9	+	1.46E+03	i)	(	-121.4033
37	3.13E-03	2D	1.01	+	1.30E+03	i)	(	-110.2602
37	3.91E-03	2D	1.13	+	1.12E+03	i)	(	-100.4644
37	5.21E-03	2D	1.23	+	9.26E+02	i)	(	-92.2045
37	6.25E-03	2D	1.28	+	8.19E+02	i)	(	-88.6034
37	7.81E-03	3D/2Dtw	2.3	-5.6682	2.8358	--------	4.74E-02	7.10E-02
37	1.04E-02	3D/2Dtw	2.51	-5.2989	2.1622	--------	4.92E-02	8.07E-02
37	2.50E-02	UNDETERM.	---	------	-----	--------	5.90E-02	9.97E-02
37	3.12E-02	UNDETERM.	---	------	-----	--------	6.24E-02	0.102
37	4.17E-02	UNDETERM.	---	------	-----	--------	6.72E-02	0.104
37	5.00E-02	UNDETERM.	---	------	-----	--------	7.04E-02	0.106
37	6.25E-02	UNDETERM.	---	------	-----	--------	7.42E-02	0.11
37	8.33E-02	UNDETERM.	---	------	-----	--------	7.87E-02	0.116
37	1.00E-01	UNDETERM.	---	------	-----	--------	8.13E-02	0.121
37	1.25E-01	UNDETERM.	---	------	-----	--------	8.42E-02	0.128
37	1.67E-01	UNDETERM.	---	------	-----	--------	8.77E-02	0.139
37	4.00E-01	UNDETERM.	---	------	-----	--------	0.101	0.172
37	5.00E-01	UNDETERM.	---	------	-----	--------	0.105	0.178
37	6.67E-01	UNDETERM.	---	------	-----	--------	0.112	0.183
37	8.00E-01	UNDETERM.	---	------	-----	--------	0.116	0.187
37	1.00E+00	UNDETERM.	---	------	-----	--------	0.123	0.193

37	1.33E+00	UNDETERM.	---	------	-----	--------	0.134	0.203
37	1.60E+00	UNDETERM.	---	------	-----	--------	0.144	0.211
37	2.00E+00	UNDETERM.	---	------	-----	--------	0.158	0.222
37	2.67E+00	UNDETERM.	---	------	-----	--------	0.184	0.238
77	7.81E-04	UNDETERM.	---	------	-----	--------	0.441	0.751
77	9.77E-04	3D	---	------	-----	0.595	0.5	0.803
77	1.30E-03	3D	---	------	-----	0.554	0.58	0.869
77	1.56E-03	3D	---	------	-----	0.53	0.632	0.911
77	1.95E-03	3D	---	------	-----	0.505	0.692	0.962
77	2.60E-03	3D	---	------	-----	0.481	0.755	1.02
77	3.13E-03	3D	---	------	-----	0.47	0.782	1.05
77	3.91E-03	3D	---	------	-----	0.459	0.796	1.08
77	5.21E-03	3D	---	------	-----	0.449	0.784	1.07
77	6.25E-03	3D	---	------	-----	0.445	0.763	1.04
77	7.81E-03	3D	---	------	-----	0.444	0.735	0.998
77	1.04E-02	3D	---	------	-----	0.451	0.706	0.919
77	1.25E-02	3D	---	------	-----	0.46	0.699	0.862
77	1.56E-02	3D	---	------	-----	0.473	0.705	0.789
77	2.08E-02	UNDETERM.	---	------	-----	--------	0.739	0.687
77	2.50E-02	UNDETERM.	---	------	-----	--------	0.773	0.614
77	3.12E-02	UNDETERM.	---	------	-----	--------	0.828	0.504
77	4.17E-02	UNDETERM.	---	------	-----	--------	0.915	0.277
77	5.00E-02	UNDETERM.	---	------	-----	--------	0.979	0.232
77	6.25E-02	UNDETERM.	---	------	-----	--------	1.07	0.49
77	8.33E-02	UNDETERM.	---	------	-----	--------	1.2	0.732
77	1.00E-01	3D	---	------	-----	0.433	1.29	0.872
77	1.25E-01	3D	---	------	-----	0.523	1.41	1.03
77	1.67E-01	3D	---	------	-----	0.621	1.57	1.22
77	2.00E-01	UNDETERM.	---	------	-----	--------	1.68	1.32
77	2.50E-01	UNDETERM.	---	------	-----	--------	1.82	1.42
77	3.33E-01	UNDETERM.	---	------	-----	--------	1.98	1.51

77	4.00E-01	UNDETERM.	---	------	-----	--------	2.08	1.55
77	5.00E-01	UNDETERM.	---	------	-----	--------	2.2	1.6
77	6.67E-01	UNDETERM.	---	------	-----	--------	2.37	1.67
77	8.00E-01	UNDETERM.	---	------	-----	--------	2.52	1.74
77	1.00E+00	UNDETERM.	---	------	-----	--------	2.75	1.85
77	1.33E+00	UNDETERM.	---	------	-----	--------	3.16	2.02
77	1.60E+00	UNDETERM.	---	------	-----	--------	3.5	2.14
77	2.00E+00	UNDETERM.	---	------	-----	--------	4.02	2.29
77	2.67E+00	UNDETERM.	---	------	-----	--------	4.87	2.47
77	3.20E+00	UNDETERM.	---	------	-----	--------	5.56	2.58
77	4.00E+00	UNDETERM.	---	------	-----	--------	6.68	2.74
77	5.33E+00	UNDETERM.	---	------	-----	--------	8.99	3.17
77	6.40E+00	UNDETERM.	---	------	-----	--------	11.6	3.85
77	8.00E+00	UNDETERM.	---	------	-----	--------	17.9	5.95
77	1.07E+01	UNDETERM.	---	------	-----	--------	50.5	18.2
77	1.28E+01	UNDETERM.	---	------	-----	--------	55.9	21.3
77	1.60E+01	UNDETERM.	---	------	-----	--------	23.9	9.65
77	2.13E+01	UNDETERM.	---	------	-----	--------	13.7	5.66
77	2.56E+01	UNDETERM.	---	------	-----	--------	11	4.52
77	3.20E+01	UNDETERM.	---	------	-----	--------	9.13	3.59
77	4.27E+01	UNDETERM.	---	------	-----	--------	7.73	2.77
77	5.12E+01	UNDETERM.	---	------	-----	--------	7.15	2.37
77	6.40E+01	UNDETERM.	---	------	-----	--------	6.64	1.97
77	8.53E+01	UNDETERM.	---	------	-----	--------	6.2	1.56

3. Southwest – Northeast long survey line

Site	Per(s)	DIM	STRIKE(∫)	twist(∫)	shear(∫)	I7	skew	ph_s_skew
87	7.81E-04	3D/1D2D	---	------	-----	--------	0.108	0.111
87	9.77E-04	3D/1D2D	---	------	-----	--------	0.107	8.25E-02
87	1.30E-03	3D/1D2D	---	------	-----	--------	0.103	5.54E-02
87	1.56E-03	3D/1D2D	---	------	-----	--------	0.101	5.42E-02
87	1.95E-03	3D/1D2D	---	------	-----	--------	9.83E-02	6.96E-02
87	2.60E-03	3D/1D2D	---	------	-----	--------	9.74E-02	9.84E-02
87	3.13E-03	3D/1D2D	---	------	-----	--------	9.86E-02	0.116
87	3.91E-03	3D/1D2D	---	------	-----	--------	0.102	0.135
87	5.21E-03	3D/1D2D	---	------	-----	--------	0.109	0.151
87	6.25E-03	3D	---	------	-----	5.01E-01	0.115	0.155
87	7.81E-03	3D	---	------	-----	4.58E-01	0.121	0.154
87	1.04E-02	3D	---	------	-----	3.43E-01	0.127	0.142
87	1.25E-02	3D	---	------	-----	0.266	0.129	0.131
87	1.56E-02	3D	---	------	-----	0.197	0.129	0.118
87	2.08E-02	UNDETERM.	---	------	-----	--------	0.128	0.111
87	2.50E-02	UNDETERM.	---	------	-----	--------	0.126	0.114
87	3.12E-02	3D	---	------	-----	0.253	0.125	0.126
87	4.17E-02	UNDETERM.	---	------	-----	--------	0.125	0.149
87	5.00E-02	UNDETERM.	---	------	-----	--------	0.126	0.166
87	6.25E-02	UNDETERM.	---	------	-----	--------	0.13	0.187
87	8.33E-02	UNDETERM.	---	------	-----	--------	0.139	0.213
87	1.00E-01	UNDETERM.	---	------	-----	--------	0.146	0.229
87	1.25E-01	UNDETERM.	---	------	-----	--------	0.157	0.247
87	1.67E-01	UNDETERM.	---	------	-----	--------	0.174	0.267
87	2.00E-01	UNDETERM.	---	------	-----	--------	0.186	0.278

87	2.50E-01	UNDETERM.	---	------	-----	--------	0.201	0.288
87	3.33E-01	UNDETERM.	---	------	-----	--------	0.22	0.298
87	4.00E-01	UNDETERM.	---	------	-----	--------	0.231	0.304
87	5.00E-01	UNDETERM.	---	------	-----	--------	0.244	0.312
87	6.67E-01	UNDETERM.	---	------	-----	--------	0.26	0.326
87	8.00E-01	UNDETERM.	---	------	-----	--------	0.27	0.338
87	1.00E+00	UNDETERM.	---	------	-----	--------	0.283	0.358
87	1.33E+00	UNDETERM.	---	------	-----	--------	0.302	0.391
87	1.60E+00	UNDETERM.	---	------	-----	--------	0.316	0.418
87	2.00E+00	UNDETERM.	---	------	-----	--------	0.337	0.457
87	2.67E+00	UNDETERM.	---	------	-----	--------	0.375	0.518
87	3.20E+00	UNDETERM.	---	------	-----	--------	0.407	0.561
87	4.00E+00	UNDETERM.	---	------	-----	--------	0.458	0.619
87	5.33E+00	UNDETERM.	---	------	-----	--------	0.546	0.701
87	6.40E+00	UNDETERM.	---	------	-----	--------	0.616	0.755
87	8.00E+00	UNDETERM.	---	------	-----	--------	0.719	0.82
87	1.07E+01	UNDETERM.	---	------	-----	--------	0.875	0.893
87	1.28E+01	UNDETERM.	---	------	-----	--------	0.982	0.928
87	1.60E+01	UNDETERM.	---	------	-----	--------	1.11	0.951
87	2.13E+01	UNDETERM.	---	------	-----	--------	1.26	0.937
87	2.56E+01	UNDETERM.	---	------	-----	--------	1.33	0.901
87	3.20E+01	UNDETERM.	---	------	-----	--------	1.38	0.833
87	4.27E+01	UNDETERM.	---	------	-----	--------	1.41	0.716
87	5.12E+01	UNDETERM.	---	------	-----	--------	1.42	0.632
87	6.40E+01	UNDETERM.	---	------	-----	--------	1.41	0.524
87	8.53E+01	UNDETERM.	---	------	-----	--------	1.4	0.367
11	7.81E-04	3D/1D2D	---	------	-----	--------	0.111	0.163
11	9.77E-04	3D/1D2D	---	------	-----	--------	0.106	0.14
11	1.30E-03	3D/1D2D	---	------	-----	--------	0.101	0.111
11	1.56E-03	3D/1D2D	---	------	-----	--------	9.89E-02	9.31E-02
11	1.95E-03	3D/1D2D	---	------	-----	--------	9.73E-02	6.97E-02

11	2.60E-03	3D/1D2D	---	------	-----	--------	9.69E-02	2.58E-02
11	3.13E-03	3D/1D2D	---	------	-----	--------	9.75E-02	4.15E-02
11	3.91E-03	3D/1D2D	---	------	-----	--------	9.92E-02	6.67E-02
11	5.21E-03	3D/1D2D	---	------	-----	--------	0.103	8.67E-02
11	6.25E-03	3D/1D2D	---	------	-----	--------	0.106	9.50E-02
11	7.81E-03	3D/1D2D	---	------	-----	--------	0.11	0.101
11	1.04E-02	3D/1D2D	---	------	-----	--------	0.114	0.1
11	1.25E-02	3D/1D2D	---	------	-----	--------	0.116	9.65E-02
11	1.56E-02	3D/1D2D	---	------	-----	--------	0.118	9.17E-02
11	2.08E-02	UNDETERM.	---	------	-----	--------	0.119	9.28E-02
11	2.50E-02	3D	---	------	-----	0.181	0.12	0.102
11	3.12E-02	3D	---	------	-----	0.217	0.122	0.121
11	4.17E-02	3D	---	------	-----	0.282	0.129	0.155
11	5.00E-02	UNDETERM.	---	------	-----	--------	0.136	0.178
11	6.25E-02	UNDETERM.	---	------	-----	--------	0.15	0.209
11	8.33E-02	UNDETERM.	---	------	-----	--------	0.175	0.249
11	1.00E-01	3D	---	------	-----	0.411	0.196	0.274
11	1.25E-01	UNDETERM.	---	------	-----	--------	0.229	0.305
11	1.67E-01	UNDETERM.	---	------	-----	--------	0.28	0.341
11	2.00E-01	UNDETERM.	---	------	-----	--------	0.317	0.362
11	2.50E-01	UNDETERM.	---	------	-----	--------	0.366	0.383
11	3.33E-01	UNDETERM.	---	------	-----	--------	0.431	0.402
11	4.00E-01	UNDETERM.	---	------	-----	--------	0.472	0.411
11	5.00E-01	UNDETERM.	---	------	-----	--------	0.523	0.423
11	6.67E-01	UNDETERM.	---	------	-----	--------	0.592	0.446
11	8.00E-01	UNDETERM.	---	------	-----	--------	0.641	0.47
11	1.00E+00	UNDETERM.	---	------	-----	--------	0.71	0.513
11	1.33E+00	UNDETERM.	---	------	-----	--------	0.819	0.594
11	1.60E+00	UNDETERM.	---	------	-----	--------	0.903	0.657
11	2.00E+00	UNDETERM.	---	------	-----	--------	1.02	0.745
11	2.67E+00	UNDETERM.	---	------	-----	--------	1.21	0.867

11	3.20E+00	UNDETERM.	---	------	-----	--------	1.35	0.946
11	4.00E+00	UNDETERM.	---	------	-----	--------	1.55	1.04
11	5.33E+00	UNDETERM.	---	------	-----	--------	1.83	1.13
11	6.40E+00	UNDETERM.	---	------	-----	--------	2.01	1.18
11	1.07E+01	UNDETERM.	---	------	-----	--------	2.5	1.2
11	1.60E+01	UNDETERM.	---	------	-----	--------	2.78	1.11
10	1.30E-03	UNDETERM.	---	------	-----	--------	4.21E-02	0.349
10	1.56E-03	3D	---	------	-----	0.397	4.70E-02	0.356
10	1.95E-03	3D	---	------	-----	0.394	5.27E-02	0.357
10	2.60E-03	UNDETERM.	---	------	-----	--------	5.90E-02	0.343
10	3.13E-03	3D	---	------	-----	0.402	6.24E-02	0.326
10	3.91E-03	3D	---	------	-----	0.416	6.60E-02	0.298
10	5.21E-03	3D	---	------	-----	0.456	7.06E-02	0.254
10	6.25E-03	3D	---	------	-----	0.508	7.38E-02	0.223
10	7.81E-03	3D/1D2D	---	------	-----	--------	7.79E-02	0.178
10	1.04E-02	3D/1D2D	---	------	-----	--------	8.24E-02	9.92E-02
10	1.25E-02	3D/1D2D	---	------	-----	--------	8.42E-02	5.44E-02
10	1.56E-02	3D	---	------	-----	0.322	8.49E-02	0.13
10	2.08E-02	UNDETERM.	---	------	-----	--------	8.37E-02	0.177
10	2.50E-02	3D	---	------	-----	0.47	8.23E-02	0.197
10	3.12E-02	3D	---	------	-----	0.5	8.01E-02	0.216
10	4.17E-02	UNDETERM.	---	------	-----	--------	7.73E-02	0.237
10	5.00E-02	UNDETERM.	---	------	-----	--------	7.54E-02	0.249
10	6.25E-02	UNDETERM.	---	------	-----	--------	7.30E-02	0.264
10	8.33E-02	UNDETERM.	---	------	-----	--------	6.99E-02	0.279
10	1.00E-01	UNDETERM.	---	------	-----	--------	6.78E-02	0.287
10	1.25E-01	UNDETERM.	---	------	-----	--------	6.55E-02	0.291
10	1.67E-01	UNDETERM.	---	------	-----	--------	6.34E-02	0.286
10	2.00E-01	UNDETERM.	---	------	-----	--------	6.29E-02	0.277
10	2.50E-01	UNDETERM.	---	------	-----	--------	6.35E-02	0.26
10	3.33E-01	UNDETERM.	---	------	-----	--------	6.67E-02	0.226

10	4.00E-01	UNDETERM.	---	------	-----	--------	7.02E-02	0.198
10	5.00E-01	UNDETERM.	---	------	-----	--------	7.59E-02	0.153
10	6.67E-01	UNDETERM.	---	------	-----	--------	8.51E-02	4.05E-02
10	8.00E-01	UNDETERM.	---	------	-----	--------	9.15E-02	0.116
10	1.00E+00	UNDETERM.	---	------	-----	--------	9.97E-02	0.184
10	1.33E+00	UNDETERM.	---	------	-----	--------	0.11	0.252
10	1.60E+00	UNDETERM.	---	------	-----	--------	0.118	0.291
10	2.00E+00	UNDETERM.	---	------	-----	--------	0.127	0.337
10	2.67E+00	UNDETERM.	---	------	-----	--------	0.142	0.396
10	3.20E+00	UNDETERM.	---	------	-----	--------	0.153	0.434
10	4.00E+00	UNDETERM.	---	------	-----	--------	0.169	0.483
10	5.33E+00	UNDETERM.	---	------	-----	--------	0.193	0.55
10	6.40E+00	UNDETERM.	---	------	-----	--------	0.211	0.594
10	2.56E+01	UNDETERM.	---	------	-----	--------	0.302	0.755
10	3.20E+01	UNDETERM.	---	------	-----	--------	0.285	0.699
10	4.27E+01	UNDETERM.	---	------	-----	--------	0.253	0.594
10	5.12E+01	UNDETERM.	---	------	-----	--------	0.23	0.523
9	7.81E-04	3D	---	------	-----	0.999	0.219	0.328
9	9.77E-04	UNDETERM.	---	------	-----	--------	0.232	0.331
9	1.30E-03	UNDETERM.	---	------	-----	--------	0.249	0.333
9	1.56E-03	UNDETERM.	---	------	-----	--------	0.261	0.333
9	1.95E-03	UNDETERM.	---	------	-----	--------	0.276	0.335
9	2.60E-03	UNDETERM.	---	------	-----	--------	0.298	0.339
9	3.13E-03	UNDETERM.	---	------	-----	--------	0.314	0.343
9	3.91E-03	UNDETERM.	---	------	-----	--------	0.335	0.348
9	5.21E-03	UNDETERM.	---	------	-----	--------	0.365	0.356
9	6.25E-03	UNDETERM.	---	------	-----	--------	0.385	0.361
9	7.81E-03	UNDETERM.	---	------	-----	--------	0.411	0.368
9	1.04E-02	UNDETERM.	---	------	-----	--------	0.445	0.376
9	1.25E-02	UNDETERM.	---	------	-----	--------	0.467	0.378
9	1.56E-02	UNDETERM.	---	------	-----	--------	0.494	0.374

9	2.08E-02	3D	---	------	-----	0.674	0.523	0.353
9	2.50E-02	UNDETERM.	---	------	-----	--------	0.537	0.331
9	3.12E-02	UNDETERM.	---	------	-----	--------	0.546	0.292
9	4.17E-02	UNDETERM.	---	------	-----	--------	0.543	0.226
9	5.00E-02	UNDETERM.	---	------	-----	--------	0.532	0.174
9	6.25E-02	UNDETERM.	---	------	-----	--------	0.511	9.23E-02
9	8.33E-02	UNDETERM.	---	------	-----	--------	0.475	0.103
9	1.00E-01	UNDETERM.	---	------	-----	--------	0.449	0.131
9	1.25E-01	3D/2D	7.37	-24.0451	-9.34E+00	--------	0.419	0.142
9	1.67E-01	UNDETERM.	---	------	-----	--------	0.386	0.135
9	2.00E-01	UNDETERM.	---	------	-----	--------	0.37	0.122
9	2.50E-01	UNDETERM.	---	------	-----	--------	0.356	9.89E-02
9	3.33E-01	UNDETERM.	---	------	-----	--------	0.346	5.46E-02
9	4.00E-01	UNDETERM.	---	------	-----	--------	0.344	2.75E-02
9	5.00E-01	UNDETERM.	---	------	-----	--------	0.345	6.37E-02
9	6.67E-01	UNDETERM.	---	------	-----	--------	0.35	7.08E-02
9	8.00E-01	UNDETERM.	---	------	-----	--------	0.355	5.61E-02
9	1.00E+00	UNDETERM.	---	------	-----	--------	0.361	4.61E-02
9	1.60E+00	UNDETERM.	---	------	-----	--------	0.368	0.15
9	2.00E+00	3D/1D2D	---	------	-----	--------	1	0
9	3.20E+00	3D/2Ddiag	---	------	-----	--------	#NAME?	NaN
9	5.33E+00	3D/2Ddiag	---	------	-----	--------	#NAME?	NaN
9	8.00E+00	3D/2Ddiag	---	------	-----	--------	#NAME?	NaN
9	2.13E+01	3D/2Ddiag	---	------	-----	--------	#NAME?	NaN
9	6.40E+01	3D/2Ddiag	---	------	-----	--------	#NAME?	NaN
8	7.81E-04	UNDETERM.	---	------	-----	--------	0.207	0.233
8	9.77E-04	UNDETERM.	---	------	-----	--------	0.216	0.244
8	1.30E-03	3D	---	------	-----	0.24	0.229	0.264
8	1.56E-03	3D	---	------	-----	0.305	0.238	0.28
8	1.95E-03	3D	---	------	-----	0.431	0.25	0.302
8	2.60E-03	UNDETERM.	---	------	-----	--------	0.267	0.333

8	3.13E-03	3D	---	------	-----	0.97	0.279	0.354
8	3.91E-03	UNDETERM.	---	------	-----	--------	0.295	0.382
8	5.21E-03	UNDETERM.	---	------	-----	--------	0.32	0.421
8	6.25E-03	3D	---	------	-----	0.976	0.339	0.448
8	7.81E-03	3D	---	------	-----	0.858	0.368	0.481
8	1.04E-02	3D	---	------	-----	0.75	0.417	0.52
8	1.25E-02	3D	---	------	-----	0.692	0.453	0.539
8	1.56E-02	3D	---	------	-----	0.621	0.5	0.549
8	2.08E-02	UNDETERM.	---	------	-----	--------	0.554	0.531
8	2.50E-02	UNDETERM.	---	------	-----	--------	0.579	0.498
8	3.12E-02	UNDETERM.	---	------	-----	--------	0.593	0.433
8	4.17E-02	UNDETERM.	---	------	-----	--------	0.583	0.317
8	5.00E-02	UNDETERM.	---	------	-----	--------	0.562	0.231
8	6.25E-02	UNDETERM.	---	------	-----	--------	0.528	0.106
8	8.33E-02	UNDETERM.	---	------	-----	--------	0.48	0.127
8	1.00E-01	UNDETERM.	---	------	-----	--------	0.453	0.144
8	1.25E-01	UNDETERM.	---	------	-----	--------	0.424	0.13
8	1.67E-01	UNDETERM.	---	------	-----	--------	0.399	5.58E-02
8	2.00E-01	UNDETERM.	---	------	-----	--------	0.39	9.09E-02
8	2.50E-01	3D/2Ddiag	---	------	-----	--------	#NAME?	NaN
8	4.00E-01	UNDETERM.	---	------	-----	--------	0.397	0.22
8	5.00E-01	UNDETERM.	---	------	-----	--------	0.409	0.231
8	6.67E-01	UNDETERM.	---	------	-----	--------	0.427	0.226
8	8.00E-01	UNDETERM.	---	------	-----	--------	0.437	0.21
8	1.00E+00	UNDETERM.	---	------	-----	--------	0.446	0.173
8	1.33E+00	UNDETERM.	---	------	-----	--------	0.453	8.64E-02
8	1.60E+00	3D/2Ddiag	---	------	-----	--------	#NAME?	NaN
8	2.67E+00	3D/1D2D	---	------	-----	--------	1	0
8	4.00E+00	3D/2Ddiag	---	------	-----	--------	#NAME?	NaN
8	6.40E+00	3D/2Ddiag	---	------	-----	--------	#NAME?	NaN
8	1.07E+01	3D/2Ddiag	---	------	-----	--------	#NAME?	NaN

7	7.81E-04	UNDETERM.	---	------	-----	--------	7.36E-02	0.243
7	9.77E-04	3D	---	------	-----	0.626	6.08E-02	0.215
7	1.30E-03	3D	---	------	-----	0.251	4.59E-02	0.158
7	1.56E-03	UNDETERM.	---	------	-----	--------	3.84E-02	0.101
7	1.95E-03	UNDETERM.	---	------	-----	--------	3.15E-02	8.79E-02
7	2.60E-03	UNDETERM.	---	------	-----	--------	2.65E-02	0.172
7	3.13E-03	3D	---	------	-----	0.225	2.52E-02	0.205
7	3.91E-03	3D	---	------	-----	2.71E-01	2.54E-02	0.234
7	5.21E-03	3D	---	------	-----	3.20E-01	2.74E-02	0.257
7	6.25E-03	3D	---	------	-----	3.54E-01	2.94E-02	0.264
7	7.81E-03	3D	---	------	-----	4.08E-01	3.25E-02	0.265
7	1.04E-02	3D	---	------	-----	0.525	3.73E-02	0.255
7	1.25E-02	3D	---	------	-----	0.646	4.06E-02	0.244
7	1.56E-02	3D	---	------	-----	0.805	4.49E-02	0.227
7	2.08E-02	3D	---	------	-----	0.686	5.03E-02	0.203
7	2.50E-02	3D	---	------	-----	0.537	5.31E-02	0.188
7	3.12E-02	3D	---	------	-----	0.447	5.59E-02	0.177
7	4.17E-02	3D	---	------	-----	0.486	5.84E-02	0.177
7	5.00E-02	UNDETERM.	---	------	-----	--------	5.97E-02	0.186
7	6.25E-02	UNDETERM.	---	------	-----	--------	6.15E-02	0.206
7	8.33E-02	UNDETERM.	---	------	-----	--------	6.50E-02	0.235
7	1.00E-01	3D	---	------	-----	0.742	6.83E-02	0.255
7	1.25E-01	3D	---	------	-----	0.705	7.37E-02	0.278
7	1.67E-01	UNDETERM.	---	------	-----	--------	8.37E-02	0.306
7	2.00E-01	UNDETERM.	---	------	-----	--------	9.21E-02	0.324
7	2.50E-01	UNDETERM.	---	------	-----	--------	0.105	0.346
7	3.33E-01	UNDETERM.	---	------	-----	--------	0.125	0.377
7	4.00E-01	UNDETERM.	---	------	-----	--------	0.141	0.397
7	5.00E-01	UNDETERM.	---	------	-----	--------	0.163	0.42
7	6.67E-01	UNDETERM.	---	------	-----	--------	0.195	0.445
7	8.00E-01	UNDETERM.	---	------	-----	--------	0.217	0.458

7	1.00E+00	UNDETERM.	---	------	-----	--------	0.245	0.468
7	1.33E+00	UNDETERM.	---	------	-----	--------	0.282	0.476
7	1.60E+00	UNDETERM.	---	------	-----	--------	0.306	0.479
7	2.00E+00	UNDETERM.	---	------	-----	--------	0.339	0.481
7	2.67E+00	UNDETERM.	---	------	-----	--------	0.386	0.48
7	3.20E+00	UNDETERM.	---	------	-----	--------	0.419	0.478
7	4.00E+00	3D/1D2D	---	------	-----	--------	1	0
7	6.40E+00	3D/1D2D	---	------	-----	--------	1	0
7	1.07E+01	UNDETERM.	---	------	-----	--------	0.629	0.387
7	2.13E+01	3D/2Ddiag	---	------	-----	--------	#NAME?	NaN
7	4.27E+01	3D/2Ddiag	---	------	-----	--------	#NAME?	NaN
7	6.40E+01	3D/1D2D	---	------	-----	--------	1	0
83	7.81E-04	3D	---	------	-----	0.266	0.236	0.199
83	9.77E-04	3D	---	------	-----	0.211	0.23	0.157
83	1.30E-03	3D/2Dtw	70.64	12.1249	-0.0726	--------	0.229	8.68E-02
83	1.56E-03	3D/2Dtw	69.3	13.1844	-0.5334	--------	0.232	4.01E-02
83	1.95E-03	UNDETERM.	---	------	-----	--------	0.237	0.104
83	2.60E-03	3D	---	------	-----	0.214	0.246	0.138
83	3.13E-03	3D	---	------	-----	0.218	0.252	0.148
83	3.91E-03	3D	---	------	-----	0.196	0.26	0.151
83	5.21E-03	3D/2Dtw	74.16	18.3705	-2.3233	--------	0.269	0.143
83	6.25E-03	3D/2Dtw	75.43	18.2617	-2.4967	--------	0.272	0.13
83	7.81E-03	3D/2Dtw	77.01	17.6938	-2.5116	--------	0.274	0.108
83	1.04E-02	3D/2Dtw	79.03	16.5158	-2.2582	--------	0.272	7.25E-02
83	1.25E-02	3D/2Dtw	80.28	15.8261	-2.1318	--------	0.269	5.10E-02
83	1.56E-02	3D/2Dtw	81.85	15.4529	-2.3373	--------	0.263	4.42E-02
83	2.08E-02	UNDETERM.	---	------	-----	--------	0.254	7.99E-02
83	2.50E-02	UNDETERM.	---	------	-----	--------	0.249	0.111
83	3.12E-02	UNDETERM.	---	------	-----	--------	0.244	0.151
83	4.17E-02	UNDETERM.	---	------	-----	--------	0.244	0.202
83	5.00E-02	UNDETERM.	---	------	-----	--------	0.248	0.232

83	6.25E-02	UNDETERM.	---	------	-----	--------	0.257	0.268
83	8.33E-02	UNDETERM.	---	------	-----	--------	0.277	0.311
83	1.00E-01	3D	---	------	-----	0.616	0.295	0.336
83	1.25E-01	3D	---	------	-----	5.76E-01	0.32	0.361
83	1.67E-01	3D	---	------	-----	5.36E-01	0.358	0.386
83	2.00E-01	3D	---	------	-----	0.512	0.382	0.396
83	2.50E-01	3D	---	------	-----	0.479	0.413	0.402
83	3.33E-01	UNDETERM.	---	------	-----	--------	0.449	0.401
83	4.00E-01	UNDETERM.	---	------	-----	--------	0.47	0.397
83	5.00E-01	UNDETERM.	---	------	-----	--------	0.494	0.388
83	6.67E-01	UNDETERM.	---	------	-----	--------	0.52	0.373
83	8.00E-01	UNDETERM.	---	------	-----	--------	0.534	0.362
83	1.00E+00	UNDETERM.	---	------	-----	--------	0.549	0.347
83	1.33E+00	UNDETERM.	---	------	-----	--------	0.566	0.326
83	1.60E+00	UNDETERM.	---	------	-----	--------	0.575	0.311
83	2.00E+00	UNDETERM.	---	------	-----	--------	0.585	0.293
83	2.67E+00	UNDETERM.	---	------	-----	--------	0.597	0.271
83	3.20E+00	UNDETERM.	---	------	-----	--------	0.605	0.259
83	4.00E+00	UNDETERM.	---	------	-----	--------	0.617	0.246
83	5.33E+00	UNDETERM.	---	------	-----	--------	0.637	0.232
83	6.40E+00	UNDETERM.	---	------	-----	--------	0.654	0.224
83	8.00E+00	UNDETERM.	---	------	-----	--------	0.683	0.213
83	1.07E+01	UNDETERM.	---	------	-----	--------	0.735	0.183
83	1.28E+01	3D/2Ddiag	---	------	-----	--------	#NAME?	NaN
83	2.13E+01	UNDETERM.	---	------	-----	--------	0.91	0.262
83	2.56E+01	3D/1D2D	---	------	-----	--------	1	0
83	4.27E+01	UNDETERM.	---	------	-----	--------	0.982	0.567
83	5.12E+01	UNDETERM.	---	------	-----	--------	0.953	0.62
83	6.40E+01	UNDETERM.	---	------	-----	--------	0.888	0.661
83	8.53E+01	UNDETERM.	---	------	-----	--------	0.772	0.676
81	7.81E-04	3D	---	------	-----	0.61	0.141	0.262

81	9.77E-04	3D	---	------	-----	0.704	0.122	0.305
81	1.30E-03	3D	---	------	-----	0.749	0.103	0.36
81	1.56E-03	UNDETERM.	---	------	-----	--------	9.46E-02	0.395
81	1.95E-03	UNDETERM.	---	------	-----	--------	8.57E-02	0.438
81	2.60E-03	UNDETERM.	---	------	-----	--------	7.55E-02	0.494
81	3.13E-03	3D	---	------	-----	0.7	6.92E-02	0.529
81	3.91E-03	3D	---	------	-----	0.664	6.11E-02	0.569
81	5.21E-03	3D	---	------	-----	0.602	5.13E-02	0.612
81	6.25E-03	3D	---	------	-----	0.551	4.80E-02	0.631
81	7.81E-03	UNDETERM.	---	------	-----	--------	5.24E-02	0.643
81	1.04E-02	UNDETERM.	---	------	-----	--------	7.53E-02	0.635
81	1.25E-02	UNDETERM.	---	------	-----	--------	9.73E-02	0.613
81	1.56E-02	UNDETERM.	---	------	-----	--------	0.129	0.561
81	2.08E-02	UNDETERM.	---	------	-----	--------	0.171	0.417
81	2.50E-02	UNDETERM.	---	------	-----	--------	0.194	0.198
81	3.12E-02	UNDETERM.	---	------	-----	--------	0.214	0.415
81	4.17E-02	UNDETERM.	---	------	-----	--------	0.221	0.693
81	5.00E-02	UNDETERM.	---	------	-----	--------	0.213	0.81
81	6.25E-02	UNDETERM.	---	------	-----	--------	0.192	0.901
81	8.33E-02	UNDETERM.	---	------	-----	--------	0.154	0.946
81	1.00E-01	UNDETERM.	---	------	-----	--------	0.128	0.94
81	1.25E-01	UNDETERM.	---	------	-----	--------	9.80E-02	0.905
81	1.67E-01	UNDETERM.	---	------	-----	--------	6.76E-02	0.829
81	2.00E-01	UNDETERM.	---	------	-----	--------	5.41E-02	0.767
81	2.50E-01	UNDETERM.	---	------	-----	--------	4.34E-02	0.681
81	3.33E-01	UNDETERM.	---	------	-----	--------	3.72E-02	0.56
81	4.00E-01	UNDETERM.	---	------	-----	--------	3.59E-02	0.478
81	5.00E-01	UNDETERM.	---	------	-----	--------	3.58E-02	0.373
81	6.67E-01	UNDETERM.	---	------	-----	--------	3.69E-02	0.207
81	8.00E-01	UNDETERM.	---	------	-----	--------	3.83E-02	9.72E-02
81	1.00E+00	UNDETERM.	---	------	-----	--------	4.09E-02	0.258

81	1.33E+00	UNDETERM.	---	------	-----	--------	4.62E-02	0.365
81	1.60E+00	UNDETERM.	---	------	-----	--------	5.12E-02	0.416
81	2.00E+00	UNDETERM.	---	------	-----	--------	5.96E-02	0.467
81	2.67E+00	UNDETERM.	---	------	-----	--------	7.52E-02	0.518
81	3.20E+00	UNDETERM.	---	------	-----	--------	8.84E-02	0.541
81	4.00E+00	UNDETERM.	---	------	-----	--------	0.108	0.559
81	5.33E+00	UNDETERM.	---	------	-----	--------	0.139	0.561
81	8.00E+00	UNDETERM.	---	------	-----	--------	0.188	0.507
81	1.07E+01	UNDETERM.	---	------	-----	--------	0.219	0.396
81	1.28E+01	3D/2Ddiag	---	------	-----	--------	#NAME?	NaN
81	2.13E+01	UNDETERM.	---	------	-----	--------	0.238	0.44
81	2.56E+01	UNDETERM.	---	------	-----	--------	0.228	0.509
81	4.27E+01	3D/2Ddiag	---	------	-----	--------	#NAME?	NaN
81	6.40E+01	UNDETERM.	---	------	-----	--------	0.147	0.502
81	8.53E+01	UNDETERM.	---	------	-----	--------	0.128	0.446
1	3.91E-03	3D	---	------	-----	0.239	0.204	0.163
1	5.21E-03	3D	---	------	-----	0.183	0.205	0.141
1	7.81E-03	3D/2Dtw	89.36	23.8834	-1.65E+01	--------	0.201	0.112
1	1.04E-02	3D/2Dtw	89.99	25.0764	-1.83E+01	--------	0.194	9.66E-02
1	1.56E-02	3D/2Dtw	2.38	29.0473	-2.45E+01	--------	0.182	9.31E-02
1	2.08E-02	3D/1D2D	---	------	-----	--------	0.174	0.108
1	3.12E-02	UNDETERM.	---	------	-----	--------	0.169	0.145
1	4.17E-02	3D	---	------	-----	0.546	0.169	0.178
1	6.25E-02	UNDETERM.	---	------	-----	--------	0.179	0.226
1	8.33E-02	UNDETERM.	---	------	-----	--------	0.194	0.259
1	1.25E-01	UNDETERM.	---	------	-----	--------	0.224	0.298
1	1.67E-01	UNDETERM.	---	------	-----	--------	0.251	0.317
1	2.50E-01	UNDETERM.	---	------	-----	--------	0.29	0.325
1	3.33E-01	UNDETERM.	---	------	-----	--------	0.316	0.319
1	5.00E-01	UNDETERM.	---	------	-----	--------	0.353	0.302
1	6.67E-01	UNDETERM.	---	------	-----	--------	0.383	0.291

1	1.00E+00	UNDETERM.	---	------	-----	--------	0.435	0.286
1	2.00E+00	UNDETERM.	---	------	-----	--------	2	0
1	4.00E+00	UNDETERM.	---	------	-----	--------	2	0
102	7.81E-04	UNDETERM.	---	------	-----	--------	0.441	3.42
102	9.77E-04	UNDETERM.	---	------	-----	--------	0.538	4.06
102	1.30E-03	UNDETERM.	---	------	-----	--------	0.678	5.01
102	1.56E-03	UNDETERM.	---	------	-----	--------	0.685	5.04
102	1.95E-03	UNDETERM.	---	------	-----	--------	0.563	4.16
102	2.60E-03	3D	---	------	-----	0.949	0.402	3
102	3.13E-03	UNDETERM.	---	------	-----	--------	0.34	2.54
102	3.91E-03	3D	---	------	-----	0.854	0.298	2.18
102	5.21E-03	3D	---	------	-----	0.941	0.281	1.94
102	6.25E-03	UNDETERM.	---	------	-----	--------	0.287	1.88
102	7.81E-03	UNDETERM.	---	------	-----	--------	0.307	1.85
102	1.04E-02	UNDETERM.	---	------	-----	--------	0.354	1.88
102	1.25E-02	UNDETERM.	---	------	-----	--------	0.394	1.93
102	1.56E-02	UNDETERM.	---	------	-----	--------	0.452	2.01
102	2.08E-02	UNDETERM.	---	------	-----	--------	0.54	2.12
102	2.50E-02	UNDETERM.	---	------	-----	--------	0.598	2.17
102	3.12E-02	UNDETERM.	---	------	-----	--------	0.666	2.22
102	4.17E-02	UNDETERM.	---	------	-----	--------	0.737	2.23
102	5.00E-02	UNDETERM.	---	------	-----	--------	0.769	2.2
102	6.25E-02	UNDETERM.	---	------	-----	--------	0.791	2.12
102	8.33E-02	UNDETERM.	---	------	-----	--------	0.789	1.92
102	1.00E-01	3D	---	------	-----	0.683	0.771	1.75
102	1.25E-01	3D	---	------	-----	0.492	0.735	1.47
102	1.67E-01	3D	---	------	-----	0.255	0.671	0.999
102	2.00E-01	UNDETERM.	---	------	-----	--------	0.622	0.587
102	2.50E-01	UNDETERM.	---	------	-----	--------	0.557	0.551
102	3.33E-01	UNDETERM.	---	------	-----	--------	0.469	0.92
102	4.00E-01	UNDETERM.	---	------	-----	--------	0.412	1.01

102	5.00E-01	UNDETERM.	---	------	-----	--------	0.343	1.04
102	6.67E-01	UNDETERM.	---	------	-----	--------	0.26	0.995
102	8.00E-01	UNDETERM.	---	------	-----	--------	0.212	0.937
102	1.00E+00	UNDETERM.	---	------	-----	--------	0.16	0.85
102	1.33E+00	UNDETERM.	---	------	-----	--------	0.105	0.726
102	1.60E+00	UNDETERM.	---	------	-----	--------	7.86E-02	0.645
102	2.00E+00	UNDETERM.	---	------	-----	--------	6.12E-02	0.545
102	2.67E+00	UNDETERM.	---	------	-----	--------	7.28E-02	0.407
102	3.20E+00	UNDETERM.	---	------	-----	--------	9.36E-02	0.3
102	4.00E+00	UNDETERM.	---	------	-----	--------	0.125	3.72E-02
102	5.33E+00	UNDETERM.	---	------	-----	--------	0.172	0.341
102	8.00E+00	UNDETERM.	---	------	-----	--------	0.253	0.554
102	1.07E+01	3D/1D2D	---	------	-----	--------	1	0
102	1.60E+01	UNDETERM.	---	------	-----	--------	0.473	0.888
102	2.13E+01	UNDETERM.	---	------	-----	--------	0.618	1.04
102	2.56E+01	UNDETERM.	---	------	-----	--------	0.73	1.13
102	3.20E+01	UNDETERM.	---	------	-----	--------	0.886	1.24
102	4.27E+01	UNDETERM.	---	------	-----	--------	1.09	1.31
102	5.12E+01	UNDETERM.	---	------	-----	--------	1.19	1.28
102	6.40E+01	UNDETERM.	---	------	-----	--------	1.24	1.15
102	8.53E+01	UNDETERM.	---	------	-----	--------	1.18	0.87
39	1.30E-03	UNDETERM.	---	------	-----	--------	9.75E-02	0.267
39	1.56E-03	3D/2D	89.33	0.8753	6.0275	--------	0.11	0.296
39	1.95E-03	UNDETERM.	---	------	-----	--------	0.125	0.331
39	2.60E-03	UNDETERM.	---	------	-----	--------	0.146	0.378
39	3.13E-03	3D/2D	0.38	-1.4963	5.1008	--------	0.16	0.407
39	3.91E-03	3D/2D	0.65	-2.006	4.8191	--------	0.178	0.443
39	5.21E-03	3D/2D	0.88	-2.3771	4.4646	--------	0.204	0.486
39	6.25E-03	3D/2D	0.93	-2.37	4.2202	--------	0.223	0.508
39	7.81E-03	3D/2D	0.78	-1.892	3.8536	--------	0.249	0.522
39	1.04E-02	3D/2D	89.53	0.9743	3.0399	--------	0.289	0.506

39	1.25E-02	UNDETERM.	---	------	-----	--------	0.32	0.465
39	1.56E-02	UNDETERM.	---	------	-----	--------	0.366	0.369
39	2.50E-02	UNDETERM.	---	------	-----	--------	0.506	0.326
39	3.12E-02	3D/2D	10.49	-19.9496	4.1424	--------	0.596	0.47
39	4.17E-02	UNDETERM.	---	------	-----	--------	0.728	0.577
39	5.00E-02	UNDETERM.	---	------	-----	--------	0.814	0.611
39	6.25E-02	UNDETERM.	---	------	-----	--------	0.913	0.627
39	8.33E-02	UNDETERM.	---	------	-----	--------	1.02	0.615
39	1.00E-01	UNDETERM.	---	------	-----	--------	1.07	0.594
39	1.25E-01	UNDETERM.	---	------	-----	--------	1.12	0.562
39	1.67E-01	UNDETERM.	---	------	-----	--------	1.16	0.509
39	2.00E-01	UNDETERM.	---	------	-----	--------	1.18	0.467
39	2.50E-01	UNDETERM.	---	------	-----	--------	1.21	0.402
39	3.33E-01	UNDETERM.	---	------	-----	--------	1.26	0.267
39	4.00E-01	UNDETERM.	---	------	-----	--------	1.3	6.10E-02
39	5.00E-01	UNDETERM.	---	------	-----	--------	1.38	0.301
39	6.67E-01	UNDETERM.	---	------	-----	--------	1.53	0.477
39	8.00E-01	UNDETERM.	---	------	-----	--------	1.64	0.566
39	1.00E+00	UNDETERM.	---	------	-----	--------	1.81	0.663
39	1.33E+00	UNDETERM.	---	------	-----	--------	2.03	0.775
39	1.60E+00	UNDETERM.	---	------	-----	--------	2.18	0.844
39	2.00E+00	UNDETERM.	---	------	-----	--------	2.36	0.929
39	2.67E+00	UNDETERM.	---	------	-----	--------	2.62	1.05
39	3.20E+00	UNDETERM.	---	------	-----	--------	2.81	1.13
39	4.00E+00	UNDETERM.	---	------	-----	--------	3.11	1.24
39	5.33E+00	UNDETERM.	---	------	-----	--------	3.62	1.38
39	1.07E+01	UNDETERM.	---	------	-----	--------	5.89	1.73
39	2.13E+01	UNDETERM.	---	------	-----	--------	10.8	2.03
39	2.56E+01	UNDETERM.	---	------	-----	--------	12.9	2.17
39	3.20E+01	UNDETERM.	---	------	-----	--------	16.1	2.46
39	4.27E+01	UNDETERM.	---	------	-----	--------	21.8	3.16

39	5.12E+01	UNDETERM.	---	------	-----	--------	26.6	3.89
39	6.40E+01	UNDETERM.	---	------	-----	--------	34	5.16
39	8.53E+01	UNDETERM.	---	------	-----	--------	45	7.31
103	1.30E-03	UNDETERM.	---	------	-----	--------	1.79E-02	0.313
103	1.56E-03	UNDETERM.	---	------	-----	--------	1.76E-02	0.357
103	1.95E-03	UNDETERM.	---	------	-----	--------	1.67E-02	0.419
103	2.60E-03	UNDETERM.	---	------	-----	--------	1.40E-02	0.506
103	3.13E-03	UNDETERM.	---	------	-----	--------	1.11E-02	0.564
103	3.91E-03	UNDETERM.	---	------	-----	--------	5.96E-03	0.636
103	5.21E-03	UNDETERM.	---	------	-----	--------	5.14E-03	0.728
103	6.25E-03	UNDETERM.	---	------	-----	--------	1.37E-02	0.786
103	7.81E-03	UNDETERM.	---	------	-----	--------	2.72E-02	0.856
103	1.04E-02	UNDETERM.	---	------	-----	--------	5.00E-02	0.942
103	1.25E-02	UNDETERM.	---	------	-----	--------	6.79E-02	0.993
103	1.56E-02	UNDETERM.	---	------	-----	--------	9.37E-02	1.05
103	2.50E-02	UNDETERM.	---	------	-----	--------	0.159	1.14
103	3.12E-02	UNDETERM.	---	------	-----	--------	0.193	1.16
103	4.17E-02	UNDETERM.	---	------	-----	--------	0.235	1.18
103	5.00E-02	UNDETERM.	---	------	-----	--------	0.259	1.21
103	6.25E-02	UNDETERM.	---	------	-----	--------	0.286	1.28
103	8.33E-02	UNDETERM.	---	------	-----	--------	0.319	1.5
103	1.00E-01	UNDETERM.	---	------	-----	--------	0.34	1.74
103	1.25E-01	UNDETERM.	---	------	-----	--------	0.366	2.15
103	1.67E-01	UNDETERM.	---	------	-----	--------	0.402	2.82
103	2.00E-01	UNDETERM.	---	------	-----	--------	0.425	3.26
103	2.50E-01	UNDETERM.	---	------	-----	--------	0.451	3.74
103	3.33E-01	UNDETERM.	---	------	-----	--------	0.482	4.17
103	4.00E-01	UNDETERM.	---	------	-----	--------	0.504	4.35
103	5.00E-01	UNDETERM.	---	------	-----	--------	0.537	4.51
103	6.67E-01	UNDETERM.	---	------	-----	--------	0.601	4.73
103	8.00E-01	UNDETERM.	---	------	-----	--------	0.659	4.92

103	1.00E+00	UNDETERM.	---	------	-----	--------	0.759	5.26
103	1.33E+00	UNDETERM.	---	------	-----	--------	0.947	5.91
103	1.60E+00	UNDETERM.	---	------	-----	--------	1.11	6.48
103	2.00E+00	UNDETERM.	---	------	-----	--------	1.38	7.36
103	2.67E+00	UNDETERM.	---	------	-----	--------	1.81	8.6
103	3.20E+00	UNDETERM.	---	------	-----	--------	2.05	9.08
103	4.00E+00	UNDETERM.	---	------	-----	--------	2.12	8.72
103	3.20E+01	UNDETERM.	---	------	-----	--------	0.248	1.43
103	4.27E+01	UNDETERM.	---	------	-----	--------	0.289	1.45
103	5.12E+01	UNDETERM.	---	------	-----	--------	0.316	1.41
103	6.40E+01	UNDETERM.	---	------	-----	--------	0.34	1.32
103	8.53E+01	UNDETERM.	---	------	-----	--------	0.357	1.19
40	1.56E-03	2D	45.4	+	2.22E+03	i)	(	-815.5706
40	1.95E-03	3D/2Dtw	88.21	4.1851	-1.03E+00	--------	2.77E-02	0.104
40	2.60E-03	3D/1D2D	---	------	-----	--------	3.21E-02	0.116
40	3.13E-03	2D	44.5	+	1243.9553	i)	(	-425.9626
40	3.91E-03	3D	---	------	-----	0.27	3.84E-02	0.127
40	5.21E-03	3D/2D	89.24	5.1191	-0.9308	--------	4.29E-02	0.131
40	6.25E-03	2D	1.91	+	922.6949	i)	(	-298.9106
40	7.81E-03	3D/2Dtw	88.93	5.1502	-0.0599	--------	4.91E-02	0.131
40	1.04E-02	3D/2D	88.88	5.1559	0.426	--------	5.30E-02	0.126
40	1.25E-02	3D/2Dtw	88.88	5.1026	0.6451	--------	5.50E-02	0.12
40	1.56E-02	3D/2Dtw	88.9	4.9449	0.7869	--------	5.67E-02	0.109
40	2.50E-02	3D/2Dtw	88.95	4.3909	0.7281	--------	5.68E-02	8.37E-02
40	3.12E-02	3D/2Dtw	88.99	4.2189	0.7293	--------	5.55E-02	7.74E-02
40	4.17E-02	3D/2Dtw	89.09	4.3578	1.0495	--------	5.35E-02	8.27E-02
40	5.00E-02	3D/2Dtw	89.25	4.7392	1.5364	--------	5.25E-02	9.32E-02
40	6.25E-02	3D/2Dtw	89.61	5.5454	2.4984	--------	5.20E-02	0.111
40	8.33E-02	3D	---	------	-----	0.154	5.35E-02	0.137
40	1.00E-01	3D	---	------	-----	0.292	5.58E-02	0.155
40	1.25E-01	UNDETERM.	---	------	-----	--------	6.05E-02	0.176

40	1.67E-01	UNDETERM.	---	------	-----	--------	6.95E-02	0.205
40	2.00E-01	UNDETERM.	---	------	-----	--------	7.72E-02	0.223
40	2.50E-01	UNDETERM.	---	------	-----	--------	8.85E-02	0.245
40	3.33E-01	UNDETERM.	---	------	-----	--------	0.107	0.273
40	4.00E-01	UNDETERM.	---	------	-----	--------	0.12	0.289
40	5.00E-01	UNDETERM.	---	------	-----	--------	0.138	0.308
40	6.67E-01	UNDETERM.	---	------	-----	--------	0.163	0.327
40	8.00E-01	UNDETERM.	---	------	-----	--------	0.18	0.336
40	1.00E+00	UNDETERM.	---	------	-----	--------	0.2	0.342
40	1.33E+00	UNDETERM.	---	------	-----	--------	0.223	0.344
40	1.60E+00	UNDETERM.	---	------	-----	--------	0.237	0.343
40	2.00E+00	UNDETERM.	---	------	-----	--------	0.252	0.339
40	2.67E+00	UNDETERM.	---	------	-----	--------	0.269	0.334
40	3.20E+00	UNDETERM.	---	------	-----	--------	0.278	0.332
40	4.00E+00	UNDETERM.	---	------	-----	--------	0.29	0.331
40	5.33E+00	UNDETERM.	---	------	-----	--------	0.307	0.334
40	6.40E+00	UNDETERM.	---	------	-----	--------	0.319	0.336
40	8.00E+00	UNDETERM.	---	------	-----	--------	0.334	0.336
40	1.07E+01	UNDETERM.	---	------	-----	--------	0.353	0.329
40	1.28E+01	UNDETERM.	---	------	-----	--------	0.363	0.318
40	1.60E+01	UNDETERM.	---	------	-----	--------	0.372	0.297
40	2.13E+01	UNDETERM.	---	------	-----	--------	0.377	0.261
40	2.56E+01	UNDETERM.	---	------	-----	--------	0.376	0.237
40	3.20E+01	UNDETERM.	---	------	-----	--------	0.373	0.214
40	4.27E+01	UNDETERM.	---	------	-----	--------	0.368	0.207
40	5.12E+01	UNDETERM.	---	------	-----	--------	0.367	0.219
40	6.40E+01	UNDETERM.	---	------	-----	--------	0.369	0.247
40	8.53E+01	UNDETERM.	---	------	-----	--------	0.383	0.293
41	1.56E-03	3D/2D	88.06	-6.7492	-8.6456	--------	1.38E-02	3.00E-02
41	1.95E-03	3D/2D	88.46	-3.1992	-4.7164	--------	1.40E-02	3.02E-02
41	2.60E-03	2D	89.58	+	3823.7035	i)	(	-193.142

41	3.13E-03	2D		89.56	+	3540.0702	i)	(	-187.8167
41	3.91E-03	2D		89.54	+	3182.4492	i)	(	-178.7812
41	5.21E-03	2D		89.52	+	2709.9159	i)	(	-162.078
41	6.25E-03	2D		89.52	+	2419.0883	i)	(	-148.3187
41	7.81E-03	2D		89.52	+	2087.855	i)	(	-128.5911
41	1.04E-02	2D		89.55	+	1715.3384	i)	(	-100.6585
41	1.56E-02	3D/2D		27.95	14.4171	39.658	--------	1.62E-02	5.84E-02
41	2.08E-02	3D/2D		6.56	25.6603	31.4593	--------	1.65E-02	6.41E-02
41	2.50E-02	2D		89.62	+	9.24E+02	i)	(	-35.5057
41	3.12E-02	2D		89.63	+	7.86E+02	i)	(	-27.118
41	4.17E-02	2D		89.64	+	6.43E+02	i)	(	-19.9241
41	5.00E-02	UNDETERM.	---		------	-----	--------	1.95E-02	6.80E-02
41	6.25E-02	2D		89.64	+	5.02E+02	i)	(	-14.1673
41	8.33E-02	UNDETERM.	---		------	-----	--------	2.13E-02	5.57E-02
41	1.00E-01	3D/2D		0.71	23.7977	2.41E+01	--------	2.17E-02	5.07E-02
41	1.25E-01	3D/2D		0.25	21.5685	2.15E+01	--------	2.22E-02	4.61E-02
41	1.67E-01	3D/2D		89.89	20.169	1.97E+01	--------	2.31E-02	4.43E-02
41	2.00E-01	UNDETERM.	---		------	-----	--------	2.39E-02	4.57E-02
41	2.50E-01	UNDETERM.	---		------	-----	--------	2.53E-02	4.95E-02
41	3.33E-01	UNDETERM.	---		------	-----	--------	2.81E-02	5.67E-02
41	4.00E-01	3D/1D2D	---		------	-----	--------	3.06E-02	6.18E-02
41	5.00E-01	3D/1D2D	---		------	-----	--------	3.44E-02	6.84E-02
41	6.67E-01	UNDETERM.	---		------	-----	--------	4.07E-02	7.67E-02
41	8.00E-01	UNDETERM.	---		------	-----	--------	4.55E-02	8.13E-02
41	1.00E+00	UNDETERM.	---		------	-----	--------	5.17E-02	8.61E-02
41	1.33E+00	UNDETERM.	---		------	-----	--------	6.01E-02	8.99E-02
41	1.60E+00	UNDETERM.	---		------	-----	--------	6.51E-02	9.08E-02
41	2.00E+00	UNDETERM.	---		------	-----	--------	7.06E-02	9.06E-02
41	2.67E+00	UNDETERM.	---		------	-----	--------	7.66E-02	8.85E-02
41	3.20E+00	UNDETERM.	---		------	-----	--------	7.97E-02	8.65E-02
41	4.00E+00	UNDETERM.	---		------	-----	--------	8.30E-02	8.37E-02

41	5.33E+00	UNDETERM.	---	------	-----	--------	8.63E-02	8.00E-02
41	6.40E+00	UNDETERM.	---	------	-----	--------	8.81E-02	7.76E-02
41	8.00E+00	UNDETERM.	---	------	-----	--------	9.01E-02	7.48E-02
41	1.07E+01	UNDETERM.	---	------	-----	--------	9.27E-02	7.18E-02
41	1.28E+01	UNDETERM.	---	------	-----	--------	9.45E-02	7.04E-02
41	2.13E+01	UNDETERM.	---	------	-----	--------	0.101	6.80E-02
41	2.56E+01	UNDETERM.	---	------	-----	--------	0.105	6.75E-02
41	3.20E+01	UNDETERM.	---	------	-----	--------	0.109	6.64E-02
41	4.27E+01	UNDETERM.	---	------	-----	--------	0.115	6.36E-02
41	5.12E+01	UNDETERM.	---	------	-----	--------	0.119	6.05E-02
41	6.40E+01	UNDETERM.	---	------	-----	--------	0.123	5.51E-02
41	8.53E+01	UNDETERM.	---	------	-----	--------	0.128	4.44E-02
47	9.77E-04	UNDETERM.	---	------	-----	--------	2.75	1.28
47	1.30E-03	UNDETERM.	---	------	-----	--------	2.93	1.55
47	1.56E-03	UNDETERM.	---	------	-----	--------	3.05	1.7
47	1.95E-03	UNDETERM.	---	------	-----	--------	3.21	1.83
47	2.60E-03	3D	---	------	-----	0.702	3.39	1.89
47	3.13E-03	3D	---	------	-----	0.591	3.46	1.84
47	3.91E-03	3D	---	------	-----	0.415	3.47	1.65
47	5.21E-03	3D	---	------	-----	0.19	3.37	1.22
47	6.25E-03	3D/2D	2.84	4.388	16.9975	--------	3.29	0.833
47	7.81E-03	3D/2D	89.95	9.3426	16.753	--------	3.21	0.363
47	1.04E-02	UNDETERM.	---	------	-----	--------	3.13	0.921
47	1.25E-02	UNDETERM.	---	------	-----	--------	3.09	1.03
47	1.56E-02	3D/2D	78.43	30.0718	13.2977	--------	3.02	1.03
47	2.08E-02	UNDETERM.	---	------	-----	--------	2.87	0.842
47	2.50E-02	UNDETERM.	---	------	-----	--------	2.73	0.623
47	3.12E-02	UNDETERM.	---	------	-----	--------	2.51	0.173
47	4.17E-02	UNDETERM.	---	------	-----	--------	2.22	0.49
47	5.00E-02	UNDETERM.	---	------	-----	--------	2.05	0.532
47	6.25E-02	UNDETERM.	---	------	-----	--------	1.87	0.472

47	8.33E-02	UNDETERM.	---	------	-----	--------		1.71	0.139
47	1.00E-01	UNDETERM.	---	------	-----	--------		1.66	0.397
47	1.25E-01	UNDETERM.	---	------	-----	--------		1.64	0.64
47	1.67E-01	UNDETERM.	---	------	-----	--------		1.69	0.888
47	2.00E-01	UNDETERM.	---	------	-----	--------		1.77	1.03
47	2.50E-01	UNDETERM.	---	------	-----	--------		1.89	1.2
47	3.33E-01	UNDETERM.	---	------	-----	--------		2.11	1.42
47	4.00E-01	UNDETERM.	---	------	-----	--------		2.27	1.56
47	5.00E-01	UNDETERM.	---	------	-----	--------		2.48	1.75
47	6.67E-01	UNDETERM.	---	------	-----	--------		2.77	2
47	8.00E-01	UNDETERM.	---	------	-----	--------		2.96	2.16
47	1.00E+00	UNDETERM.	---	------	-----	--------		3.23	2.37
47	1.33E+00	UNDETERM.	---	------	-----	--------		3.64	2.64
47	1.60E+00	UNDETERM.	---	------	-----	--------		3.94	2.79
47	2.00E+00	UNDETERM.	---	------	-----	--------		4.35	2.94
47	2.67E+00	UNDETERM.	---	------	-----	--------		4.89	3.04
47	3.20E+00	UNDETERM.	---	------	-----	--------		5.21	3.04
47	4.00E+00	UNDETERM.	---	------	-----	--------		5.57	2.97
47	5.33E+00	UNDETERM.	---	------	-----	--------		5.93	2.79
47	6.40E+00	UNDETERM.	---	------	-----	--------		6.11	2.64
47	1.07E+01	UNDETERM.	---	------	-----	--------		6.4	2.17
48	1.56E-03	UNDETERM.	---	------	-----	--------		1.22	0.802
48	1.95E-03	UNDETERM.	---	------	-----	--------		1.34	0.795
48	2.60E-03	UNDETERM.	---	------	-----	--------		1.53	0.662
48	3.13E-03	3D/2D	0.72	3.9427	13.106	--------		1.65	0.398
48	3.91E-03	3D/2D	88.34	8.3038	12.7454	--------		1.8	0.614
48	5.21E-03	3D	---	------	-----		0.159	1.94	1.12
48	6.25E-03	3D	---	------	-----		0.206	1.96	1.32
48	7.81E-03	3D	---	------	-----		0.232	1.93	1.43
48	1.04E-02	3D	---	------	-----		0.213	1.8	1.34
48	1.25E-02	UNDETERM.	---	------	-----	--------		1.69	1.19

48	1.56E-02	UNDETERM.	---	------	-----	--------	1.55	0.925
48	2.08E-02	UNDETERM.	---	------	-----	--------	1.43	0.515
48	2.50E-02	UNDETERM.	---	------	-----	--------	1.38	7.27E-02
48	3.12E-02	UNDETERM.	---	------	-----	--------	1.37	0.453
48	4.17E-02	UNDETERM.	---	------	-----	--------	1.44	0.579
48	5.00E-02	UNDETERM.	---	------	-----	--------	1.54	0.582
48	6.25E-02	UNDETERM.	---	------	-----	--------	1.75	0.469
48	8.33E-02	UNDETERM.	---	------	-----	--------	2.23	0.633
48	1.00E-01	UNDETERM.	---	------	-----	--------	2.74	1.24
48	1.25E-01	UNDETERM.	---	------	-----	--------	3.86	2.36
48	1.67E-01	UNDETERM.	---	------	-----	--------	8.5	6.65
48	2.00E-01	UNDETERM.	---	------	-----	--------	32	28.1
48	2.50E-01	UNDETERM.	---	------	-----	--------	8.75	8.6
48	3.33E-01	UNDETERM.	---	------	-----	--------	3.33	3.66
48	4.00E-01	UNDETERM.	---	------	-----	--------	2.33	2.7
48	5.00E-01	UNDETERM.	---	------	-----	--------	1.69	2.08
48	6.67E-01	UNDETERM.	---	------	-----	--------	1.28	1.66
48	8.00E-01	UNDETERM.	---	------	-----	--------	1.14	1.51
48	1.00E+00	UNDETERM.	---	------	-----	--------	1.04	1.42
48	1.33E+00	UNDETERM.	---	------	-----	--------	0.995	1.38
48	1.60E+00	UNDETERM.	---	------	-----	--------	1	1.38
48	2.00E+00	UNDETERM.	---	------	-----	--------	1.03	1.39
48	2.67E+00	UNDETERM.	---	------	-----	--------	1.1	1.39
48	3.20E+00	UNDETERM.	---	------	-----	--------	1.15	1.36
48	4.00E+00	UNDETERM.	---	------	-----	--------	1.2	1.28
48	5.33E+00	UNDETERM.	---	------	-----	--------	1.25	1.1
48	6.40E+00	UNDETERM.	---	------	-----	--------	1.27	0.941
48	8.00E+00	UNDETERM.	---	------	-----	--------	1.26	0.68
48	2.13E+01	UNDETERM.	---	------	-----	--------	1.01	0.985
48	2.56E+01	UNDETERM.	---	------	-----	--------	0.916	1.03
48	3.20E+01	UNDETERM.	---	------	-----	--------	0.799	1.03

48	4.27E+01	UNDETERM.	---	------	-----	--------		0.649	0.986
48	5.12E+01	UNDETERM.	---	------	-----	--------		0.562	0.937
48	6.40E+01	UNDETERM.	---	------	-----	--------		0.467	0.866
48	8.53E+01	UNDETERM.	---	------	-----	--------		0.366	0.768
49	1.30E-03	UNDETERM.	---	------	-----	--------		5.75E-03	0.196
49	1.56E-03	2D	40.76	+	315.6646	i)		(	-295.8482
49	1.95E-03	3D/2D	84.97	3.4224	-6.5804	--------		9.86E-03	0.201
49	2.60E-03	3D/2D	84.78	3.6945	-6.6266	--------		1.38E-02	0.2
49	3.13E-03	3D/2D	84.57	3.8784	-6.6133	--------		1.67E-02	0.198
49	3.91E-03	3D	---	------	-----		0.154	2.06E-02	0.195
49	5.21E-03	3D	---	------	-----		0.199	2.63E-02	0.191
49	6.25E-03	3D	---	------	-----		0.238	3.01E-02	0.188
49	7.81E-03	3D	---	------	-----		0.295	3.48E-02	0.184
49	1.04E-02	3D	---	------	-----		0.366	4.04E-02	0.176
49	1.25E-02	3D	---	------	-----		0.394	4.36E-02	0.167
49	1.56E-02	3D	---	------	-----		0.395	4.68E-02	0.152
49	2.08E-02	3D	---	------	-----		0.314	4.98E-02	0.122
49	2.50E-02	3D	---	------	-----		0.195	5.12E-02	9.27E-02
49	3.12E-02	UNDETERM.	---	------	-----	--------		5.23E-02	1.48E-02
49	4.17E-02	UNDETERM.	---	------	-----	--------		5.30E-02	0.108
49	5.00E-02	UNDETERM.	---	------	-----	--------		5.32E-02	0.141
49	6.25E-02	UNDETERM.	---	------	-----	--------		5.31E-02	0.174
49	8.33E-02	UNDETERM.	---	------	-----	--------		5.26E-02	0.212
49	1.00E-01	UNDETERM.	---	------	-----	--------		5.20E-02	0.234
49	1.25E-01	UNDETERM.	---	------	-----	--------		5.10E-02	0.258
49	1.67E-01	UNDETERM.	---	------	-----	--------		4.93E-02	0.284
49	2.00E-01	UNDETERM.	---	------	-----	--------		4.81E-02	0.298
49	2.50E-01	UNDETERM.	---	------	-----	--------		4.67E-02	0.312
49	3.33E-01	UNDETERM.	---	------	-----	--------		4.56E-02	0.33
49	4.00E-01	UNDETERM.	---	------	-----	--------		4.55E-02	0.343
49	5.00E-01	UNDETERM.	---	------	-----	--------		4.63E-02	0.362

49	6.67E-01	UNDETERM.	---	------	-----	--------	4.89E-02	0.394
49	8.00E-01	UNDETERM.	---	------	-----	--------	5.15E-02	0.418
49	1.00E+00	UNDETERM.	---	------	-----	--------	5.54E-02	0.449
49	1.33E+00	UNDETERM.	---	------	-----	--------	6.13E-02	0.487
49	1.60E+00	UNDETERM.	---	------	-----	--------	6.51E-02	0.508
49	2.00E+00	UNDETERM.	---	------	-----	--------	6.96E-02	0.527
49	2.67E+00	UNDETERM.	---	------	-----	--------	7.53E-02	0.539
49	3.20E+00	UNDETERM.	---	------	-----	--------	7.93E-02	0.54
49	4.00E+00	UNDETERM.	---	------	-----	--------	8.50E-02	0.536
49	5.33E+00	UNDETERM.	---	------	-----	--------	9.44E-02	0.524
49	6.40E+00	UNDETERM.	---	------	-----	--------	0.102	0.512
49	8.00E+00	UNDETERM.	---	------	-----	--------	0.112	0.489
49	3.20E+01	UNDETERM.	---	------	-----	--------	0.242	0.32
49	4.27E+01	UNDETERM.	---	------	-----	--------	0.295	0.47
49	5.12E+01	UNDETERM.	---	------	-----	--------	0.334	0.555
49	6.40E+01	UNDETERM.	---	------	-----	--------	0.388	0.656
49	8.53E+01	UNDETERM.	---	------	-----	--------	0.471	0.789
80	9.77E-04	UNDETERM.	---	------	-----	--------	0.309	0.284
80	1.30E-03	UNDETERM.	---	------	-----	--------	0.314	0.281
80	1.56E-03	UNDETERM.	---	------	-----	--------	0.314	0.283
80	1.95E-03	UNDETERM.	---	------	-----	--------	0.312	0.291
80	2.60E-03	UNDETERM.	---	------	-----	--------	0.31	0.305
80	3.13E-03	3D	---	------	-----	0.741	0.311	0.315
80	3.91E-03	3D	---	------	-----	0.706	0.313	0.325
80	5.21E-03	3D	---	------	-----	0.669	0.318	0.33
80	6.25E-03	3D	---	------	-----	0.649	0.321	0.326
80	7.81E-03	UNDETERM.	---	------	-----	--------	0.325	0.315
80	1.04E-02	3D	---	------	-----	0.6	0.326	0.29
80	1.25E-02	UNDETERM.	---	------	-----	--------	0.326	0.27
80	1.56E-02	UNDETERM.	---	------	-----	--------	0.324	0.241
80	2.08E-02	UNDETERM.	---	------	-----	--------	0.319	0.202

80	2.50E-02	UNDETERM.	---	------	-----	--------	0.314	0.176
80	3.12E-02	UNDETERM.	---	------	-----	--------	0.307	0.145
80	4.17E-02	UNDETERM.	---	------	-----	--------	0.295	0.11
80	5.00E-02	UNDETERM.	---	------	-----	--------	0.285	9.64E-02
80	6.25E-02	UNDETERM.	---	------	-----	--------	0.271	9.33E-02
80	8.33E-02	UNDETERM.	---	------	-----	--------	0.247	0.109
80	1.00E-01	3D	---	------	-----	0.271	0.229	0.123
80	1.25E-01	3D	---	------	-----	0.31	0.206	0.14
80	1.67E-01	3D	---	------	-----	0.338	0.174	0.156
80	2.00E-01	UNDETERM.	---	------	-----	--------	0.154	0.162
80	2.50E-01	3D/1D2D	---	------	-----	--------	1	0
80	4.00E-01	3D	---	------	-----	0.293	9.32E-02	0.159
80	5.00E-01	3D	---	------	-----	0.282	7.91E-02	0.151
80	6.67E-01	3D	---	------	-----	0.273	6.49E-02	0.138
80	8.00E-01	UNDETERM.	---	------	-----	--------	5.80E-02	0.129
80	1.00E+00	UNDETERM.	---	------	-----	--------	5.16E-02	0.118
80	1.33E+00	3D	---	------	-----	0.263	4.59E-02	0.103
80	1.60E+00	UNDETERM.	---	------	-----	--------	4.36E-02	9.46E-02
80	2.00E+00	UNDETERM.	---	------	-----	--------	4.19E-02	8.47E-02
80	2.67E+00	3D/1D2D	---	------	-----	--------	1	0
80	4.00E+00	3D/1D2D	---	------	-----	--------	1	0
80	6.40E+00	3D/1D2D	---	------	-----	--------	1	0
80	1.07E+01	3D/1D2D	---	------	-----	--------	1	0
80	1.60E+01	3D/1D2D	---	------	-----	--------	1	0
80	2.56E+01	3D/1D2D	---	------	-----	--------	1	0
80	4.27E+01	3D/1D2D	---	------	-----	--------	1	0
80	6.40E+01	3D/1D2D	---	------	-----	--------	1	0
50	7.81E-04	UNDETERM.	---	------	-----	--------	1.29	0.579
50	9.77E-04	UNDETERM.	---	------	-----	--------	0.973	0.825
50	1.30E-03	UNDETERM.	---	------	-----	--------	4.8	1.49
50	1.56E-03	UNDETERM.	---	------	-----	--------	2.31	1.24

50	1.95E-03	UNDETERM.	---	------	-----	--------		5.55	1.37
50	2.60E-03	3D	---	------	-----		0.892	3.97	1.42
50	3.13E-03	UNDETERM.	---	------	-----	--------		7.87	2.37
50	3.91E-03	UNDETERM.	---	------	-----	--------		8.69	2.59
50	5.21E-03	UNDETERM.	---	------	-----	--------		9.81	3.02
50	6.25E-03	UNDETERM.	---	------	-----	--------		10.5	3.21
50	7.81E-03	3D	---	------	-----		0.979	7.74	2.41
50	1.04E-02	UNDETERM.	---	------	-----	--------		8.48	2.58
50	1.25E-02	3D	---	------	-----		0.988	8.93	2.66
50	1.56E-02	UNDETERM.	---	------	-----	--------		7.96	2.33
50	2.08E-02	UNDETERM.	---	------	-----	--------		5.64	2.89
50	2.50E-02	3D	---	------	-----		0.884	3.28	1.09
50	3.12E-02	3D	---	------	-----		0.999	3.17	0.807
50	4.17E-02	UNDETERM.	---	------	-----	--------		1.86	0.464
50	5.00E-02	UNDETERM.	---	------	-----	--------		2.65	0.372
50	6.25E-02	UNDETERM.	---	------	-----	--------		1.59	0.454
50	8.33E-02	3D	---	------	-----		0.842	2.16	0.438
50	1.00E-01	3D	---	------	-----		0.27	0.968	0.144
50	1.25E-01	UNDETERM.	---	------	-----	--------		1.28	0.139
50	1.67E-01	UNDETERM.	---	------	-----	--------		2.07	0.32
50	2.00E-01	UNDETERM.	---	------	-----	--------		0.934	0.391
50	2.50E-01	UNDETERM.	---	------	-----	--------		0.876	0.366
50	3.33E-01	UNDETERM.	---	------	-----	--------		0.143	0.295
50	4.00E-01	UNDETERM.	---	------	-----	--------		1.65	0.409
50	5.00E-01	UNDETERM.	---	------	-----	--------		0.359	6.09E-02
50	6.67E-01	UNDETERM.	---	------	-----	--------		1.06	0.113
50	8.00E-01	UNDETERM.	---	------	-----	--------		4.42	0.354
50	1.00E+00	UNDETERM.	---	------	-----	--------		0.479	0.227
50	1.33E+00	UNDETERM.	---	------	-----	--------		2.48	0.432
50	1.60E+00	UNDETERM.	---	------	-----	--------		0.309	5.08E-02
50	2.00E+00	UNDETERM.	---	------	-----	--------		0.604	5.12E-02

50	2.67E+00	UNDETERM.	---	------	-----	--------	0.885	0.192
50	3.20E+00	UNDETERM.	---	------	-----	--------	0.617	0.115
50	4.00E+00	UNDETERM.	---	------	-----	--------	0.653	8.63E-02
50	5.33E+00	UNDETERM.	---	------	-----	--------	0.357	7.21E-02
50	6.40E+00	UNDETERM.	---	------	-----	--------	1.72	0.106
50	8.00E+00	UNDETERM.	---	------	-----	--------	0.529	0.135
50	1.07E+01	UNDETERM.	---	------	-----	--------	0.73	9.70E-02
50	1.28E+01	UNDETERM.	---	------	-----	--------	1.9	0.325
50	1.60E+01	UNDETERM.	---	------	-----	--------	1.69	0.209
50	2.13E+01	UNDETERM.	---	------	-----	--------	0.305	3.75E-02
50	2.56E+01	UNDETERM.	---	------	-----	--------	1.05	0.183
50	3.20E+01	UNDETERM.	---	------	-----	--------	0.355	7.56E-02
50	4.27E+01	UNDETERM.	---	------	-----	--------	0.246	0.188
50	6.40E+01	UNDETERM.	---	------	-----	--------	1.2	0.738
50	8.53E+01	UNDETERM.	---	------	-----	--------	0.68	0.4